A Robust Fault Detection and Diagnosis Strategy for Centrifugal Chillers

CUI Jingtan

A thesis submitted in partial fulfillment of the requirements

for the Degree of Doctor of Philosophy

Department of Building Services Engineering

The Hong Kong Polytechnic University

April, 2005

All our science, measured against reality,

is primitive and childlike - and yet it is

the most precious thing we have.

Albert Einstein (1879-1955)

CERTIFICATE OF ORIGINALITY

I hereby declare that this submission is my own work and to the best of my knowledge and belief, it contains no materials previously published or written by another person, nor material which to a substantial extent has been accepted for the award of any other degree or diploma at any educational institution, except where due acknowledgement is made in the thesis. Any contribution made to the research by others, with whom I have worked at The Hong Kong Polytechnic University or elsewhere, is explicitly acknowledged in the thesis.

I also declare that the intellectual content of this thesis is the product of my own work, except to the extent that assistance from others in the project's design and conception or in style, presentation and linguistic expression is acknowledged.

CUI Jingtan

Department of Building Services Engineering

The Hong Kong Polytechnic University

Hong Kong SAR, China

April, 2005

ABSTRACT

Abstract of thesis entitled: A Robust Fault Detection and Diagnosis Strategy for Centrifugal Chillers

submitted by : CUI Jingtan

for the degree of : Doctor of Philosophy

at The Hong Kong Polytechnic University in April, 2005

Building Heating, Ventilating, Air-conditioning and Refrigerating (HVAC&R) systems usually fail to satisfy performance expectations envisioned at design stage for a variety of reasons. FDD (Fault Detection and Diagnosis) methods are needed to identify the faults and help put the systems back into normal operation. However, the performance of FDD methods applied to HVAC&R systems require sensor measurements, which are also susceptible to various faults. Although a great deal of FDD research has been carried out on component faults or sensor faults in HVAC&R systems, not much research has tackled these two different kinds of faults when they occur simultaneously in HVAC&R systems.

This thesis presents a robust FDD strategy for centrifugal chillers, which are the core of building HVAC&R systems. The strategy consists of a basic chiller FDD scheme and a PCA-based sensor FDD&E (Fault Detection, Diagnosis and Estimation) scheme, which target chiller component faults (called chiller faults hereafter for conciseness) and sensor faults, respectively. In implementing the strategy, it is important that the measurements

of the sensors crucial to the chiller FDD are validated by the sensor FDD&E scheme before the chiller FDD scheme is carried out to detect and diagnose chiller faults.

The basic chiller FDD scheme employs six performance indexes which have strong thermophysical meaning to depict the health status of a typical centrifugal chiller. The residual for each performance index is generated by comparing the measured value with its benchmark predicted by a simple reference model. Once residuals of one or more performance indexes are outside the range defined by the corresponding fault detection thresholds, the chiller will be considered to be faulty. Particular faults are diagnosed by a fault diagnostic classifier, which is based on the deviation pattern of the performance indexes when a chiller fault occurs. Robustness of the scheme is achieved by the adoption of an adaptive estimator for the fault detection threshold. The estimator can set reasonable fault detection thresholds by taking account of essential influencing factors.

Because the performance of the basic chiller FDD scheme depends on the quality of sensor measurements, a sensor FDD&E scheme is developed to tackle sensor faults. The latter scheme uses a PCA method to capture correlations among key variables in centrifugal chillers. The *Q-statistic* is used to measure the variance of the correlations, and its upper limit usually defines the normal ranges of the variance. If the *Q-statistic* exceeds the normal ranges, it will indicate that the correlations among variables are invalid and the sensors are unreliable. Afterwards, the *Q-contribution* plot and an iterative approach are respectively used to diagnose and correct sensor faults. The PCA-based sensor FDD&E scheme can detect, diagnose and estimate sensor faults even in the presence of most typical chiller faults. The reason for this is that chiller faults are pertinent to performance degradations which are physically explainable and belong to the variance captured by the PCA model.

Each of the two schemes is validated using laboratory data provided by an ASHRAE research project as well as field data collected from the BMS of a real building in Hong Kong. In particular, it is the first time in the HVAC&R FDD field that a sensor FDD method has been verified while taking into consideration the possible effects of typical chiller faults. Moreover, validation results of the robust chiller FDD strategy using the laboratory data show that the strategy is capable of handling chiller faults and sensor faults that exist simultaneously.

The outcomes of the research reported in this thesis should provide an effective prototype for developing robust FDD strategies that can be applied in the HVAC&R industry. This will in turn help achieve better Indoor Environmental Quality (IEQ) for occupants and lower building energy consumption.

DEDICATION

To
my parents for giving me life and dream

ACKNOWLEDGEMETNS

The road to the accomplishment of this thesis has been a long, winding and challenging one. The lessons learned and the experiences gained during the entire process have been invaluable. However, all this would not have been possible without the help of many people during my study. It is with great pleasure that I thank them here.

Firstly, it is difficult to overstate my gratitude to my supervisor, Dr. Wang Shengwei. His enthusiasm, inspiration, encouragement, and belief in my capability have greatly helped make this thesis a success.

I owe a great deal to Prof. James Braun, of Purdue University, for providing detailed laboratory data in ASHRAE 1043-RP without reservation. The data are particularly important for the validation tests of the strategy developed in this thesis. For the same reason, my thanks go to engineers of Hong Kong Swire Properties for providing a great amount of the field chiller data used in this thesis.

I would like to thank all colleagues in the department. The long road to accomplishing this research is memorable because of their company and support.

Lastly, I also would like say a big “Thank-you” to my family members: my parents, my grandmother, my sister and brother-in-law for their unconditional trust and support in my life. Most importantly, to my wife, Li Hong: thank you for your love, endless patience, understanding, and all the other things that make it so worthwhile being married to you.

TABLE OF CONTENTS

Page

LIST OF FIGURES

Page

LIST OF TABLES

Page

NOMENCALTURE

a	Number of loading vectors retained in PCA model
$\mathbf{A}$	Original matrix with n samples of the variables included in the PCA model in Chapter 6
$b_0 \ldots b_7$	Regression coefficients in reference models
$\mathbf{b}$	Vector of regression coefficients
$\mathbf{b}_{OLS}$	OLS estimate of $\mathbf{b}$
$\mathbf{c}_i$	The ith row vector of $\mathbf{C}$
$\mathbf{C}$	Projection matrix for score subspace
COP	Coefficient of performance
C_{pw}	Water specific heat (kJ $\cdot kg^{-1} \cdot K^{-1}$)
$D(\cdot)$	Variance
e_i	The ith element of $\mathbf{e}$
$\mathbf{e}$	Residual vector
Eff_{motor}	Motor efficiency
$E(\cdot)$	Expectation
$g_i(\cdot)$	Formula for calculating the ith performance index
$f_i(\cdot)$	Polynomial regression model of the ith performance index
m	Number of variables
M	Flow rate ($kg \cdot s^{-1}$)
n	Number of observations
h	Specific enthalpy (kJ/kg)
$\mathbf{I}$	Unit matrix
$LMTD$	Logarithm mean temperature difference(^oC)
p	Number of coefficients estimated from the model development data
$\mathbf{P}$	Loading matrix consists of a retained loading vectors
P	Pressure (Pa)

Q	Heat transfer rate (kW)
r_i	Residual of the *i*th performance index
$\mathbf{S}$	Covariance matrix of $\mathbf{X}$
t	Student's distribution
T	Temperature (°C)
$U(\cdot)$	Uncertainty
$\mathbf{U}$	Matrix of eigenvectors
v	Specific volume ($m^3 \cdot kg^{-1}$)
V	Volume flow rate ($m^3 \cdot s^{-1}$)
W	Power consumption (kW)
$\mathbf{x}$	Normalized new observation (row) vector
$\hat{\mathbf{x}}$	Estimate of $\mathbf{x}$
$\mathbf{x}^*$	True value of $\mathbf{x}$
$\mathbf{X}$	Normalized sample matrix with *m* observations and *n* variables in Chapter 6
$\mathbf{X}_0$	Vector of regressors for the current prediction
$\mathbf{X}_{reg}$	Matrix of regressors associated with the model development data
$\mathbf{y}$	Projection of $\mathbf{x}$ into the lower-dimension (*a*-dimension) space
Y	Response variable of regression model
$\mathbf{Y}$	Vector of response variables
$\mathbf{Y}_{reg}$	Vector of response variables associated with the model development data
$\mathbf{z}$	Vector of variables used to calculate a performance index in Chapter 3
$\mathbf{Z}$	Sample matrix with *m* observations and *n* variables in Chapter 6

Greek

$\mathbf{\Lambda}$	Diagonal matrix of non-negative real eigenvalues with decreasing magnitude
γ	Mean isentropic coefficient

ε	Random error of regression model
σ	Standard deviation
δ	Gaussian noise of measured variable
λ_i	The *i*th eigenvalue of **S**

Subscripts

1,2,3, 4	State points in pressure-enthalpy graph
chw	Chilled water
cd	Condenser
chws	Chilled water supply
chwr	Chilled water return
cw	Condenser water
comp	Compressor
ecw	Entering condenser water
elec	Electrical
ev	Evaporator
dis	Hot gas discharge
lcw	Leaving condenser water
ref	Refrigerant
suc	Compressor suction

Superscripts

^	Estimated value in Chapter 6
^	Observed value in Appendix
~	Estimated value in Chapter 3 and Appendix
$^{-1}$	Matrix inversion
$^{-T}$	Matrix transpose

CHAPTER 1 INTRODUCTION

1.1 Motivation

According to the Collaborating Label and Appliance Standards Program of United Nations Foundation, energy use for appliances, lighting, and other in-building applications accounts for one third of total energy consumption worldwide. In large commercial buildings, it was estimated that 10%-20% of the total electricity consumption could be ascribed to HVAC&R (Heating, Ventilating, Air-conditioning and Refrigeration) systems alone (Huang et al. 1991) and this figure was typically 35-40% in Hong Kong (Chan and Yik 2002). From the standpoint of initial and operating costs, centrifugal chillers are the core of HVAC&R systems serving commercial, medical and residential buildings in hot climates. They also find wide applications in product cooling. As Menzer (1997) shows, in the commercial air conditioning sector, centrifugal chillers account for 70% of the global installed cooling capacity which has been estimated at 60×10^6 tons (211×10^6 kW). During operation, various faults may occur in centrifugal chillers due to abnormal physical changes or aging of components, improper installation and operation, as well as inadequate maintenance, which make the chillers fail to satisfy performance expectations envisioned at the design stage. Failure to identify these performance problems in time results in a great waste of energy, shortened equipment life, unscheduled equipment downtime, and a lot of occupant complaint due to degraded IEA (Indoor Environmental Quality).

Automated fault detection and diagnostics (FDD) for chillers can help remedy the faults and enhance chiller operation by automatically identifying performance problems and bringing them to the attention of building operators or engineers. Nevertheless, given the significance of chillers in building HVAC&R systems from a standpoint of energy consumption and occupant comfort, there has been a relatively small body of FDD studies directly aimed at chillers. Moreover, the performance of FDD methods for chillers depends heavily on the accuracy and reliability of sensors, which however may also suffer from various faults, including bias errors, drift errors and complete failure.

Therefore, it is necessary to develop a systematic chiller FDD strategy that can detect and diagnose faults that occur in both chiller components and sensors simultaneously.

1. 2 Background of FDD for Chillers

1.2.1 Fault Definitions

In the process and manufacturing industries, there has been a strong drive to produce quality products while reducing operating costs and satisfying ever-increasing requirements of safety and environment. Although modern controllers in the process can maintain satisfactory operation by compensating for the effects of disturbances and changes occurred there, there are process changes the controller can not handle adequately (Chiang et al. 2001). These changes are called faults. More specifically, a fault in the context of HVAC&R systems is defined as an unsatisfactory or unacceptable

condition in the operation of a system or subsystem (McIntosh 1999). In the following text, faults affecting the performance of subsystems or components of chillers, such as refrigerant leakage are called chiller faults, and those affecting the performance of sensors, such as a biased temperature measurement, are called sensor faults

Furthermore, faults in HVAC&R systems can also be grouped into two types in terms of fault severity level: soft faults and hard failures. Soft faults cause performance degradation in a system and hard failures cause the system to stop functioning.

Soft faults

Soft faults in components include process parameter changes and disturbance parameter changes (Gertler 1998), which happen unnoticeably at a slow rate but progressively worsen over a period of time. Overall system performance is not drastically changed until the degradation has deteriorated beyond a critical level. Typical examples of parameter changes are the fouling of the tubes of condensers and evaporators. The loss of refrigerant and the liquid line restriction are examples of disturbance parameter changes. These faults usually result in such adverse outcomes as pressure drops, reduced flow rates and heat transfer coefficient, etc.

Soft faults in sensors, i.e., noise and bias, are one of the typical faults found in chiller systems. Because a faulty sensor provides control systems with deceiving signals, it not only affects the energy consumption, efficiency monitoring and optimal control in chillers, but also misguides the implementation of FDD strategies for chillers (Dexter

and Pakanen 2001). Nowadays, sensors are playing a very important role in BMSs (Building Management Systems). Because of the complexity of BMS, the number of sensors is large and different sensors have different functions. The FDD system for sensors has never been more important than it is now. Great contributions in this field are made by Wang S.W. and Wang J.B. (1999, 2002a and 2002b).

In the case of soft faults, it is necessary to get a reference base, the benchmark, which defines the performances of system free of faults, and a threshold, below which the fault is considered insignificant and above which it is considered desirable to detect the fault. This threshold may not be easy to set, and usually it is set empirically. A low threshold can benefit the detection of smaller faults and the earlier detection of major faults but tends to produce false alarms.

Hard failures

Seized compressors, broken fan belts and malfunctioning electrical components are typical examples of hard component failure. Frozen and jumping readings are typical examples of hard sensor failure. An automated FDD system should be able to diagnose hard faults. These hard failures are easier to detect, since they occur abruptly and result in a sudden failure of some part of the plant (Haves 1999). Adverse impacts of hard failures are severe enough to justify the most immediate service.

Since hard failures are easier to identify than soft faults, soft faults in both chiller

component category and sensor category are the prime concern of FDD applications within HVAC&R systems. From now on, both chiller faults and sensor faults in this thesis, if not specifically stated, refer to the soft faults.

1.2.2 Basic Knowledge of FDD

Generally speaking, there are three procedures in a FDD system for industrial applications and these procedures include fault detection, fault diagnosis and fault evaluation (Haves 1999). Fault detection is the determination whether the operation of a system is incorrect or unacceptable in some respects. This can be done either by:

- assessing the performance of all or part of the system over a period of time (e.g. from electricity consumption) and then comparing that performance to what is expected;
- monitoring the temperatures, flow rates and electrical power consumptions and continuously checking for incorrect operation or unsatisfactory performance.

Faults may occur over the whole operating range or be confined to a limited region and hence only occur at certain times.

Fault diagnosis, as defined in Webster's New Collegiate Dictionary, is an investigation or analysis of the cause or nature of a condition, situation, or problem. It involves determining which of the possible causes of faulty behavior are consistent with the observed behavior. Automated fault diagnosis usually relies entirely on sensors and so

may not be able to identify the nature of the fault exactly. However it can help eliminate some of the possible causes and narrow the range of potential causes.

In addition to finding the physical cause of faulty operation (e.g. fouled heat exchanger, overridden control function), it is also desirable to estimate both the cost of fixing the fault and the cost of delaying fixing it, which is called fault evaluation. The fault evaluation then balances these two costs and provides appropriate recommendations, including: let it go, adjust the control to compensate for the fault, schedule service when it is convenient, or shut the unit down and repair it now. The basic procedures of FDD in HVAC&R applications are shown in Figure 1.1 (Braun 2003).

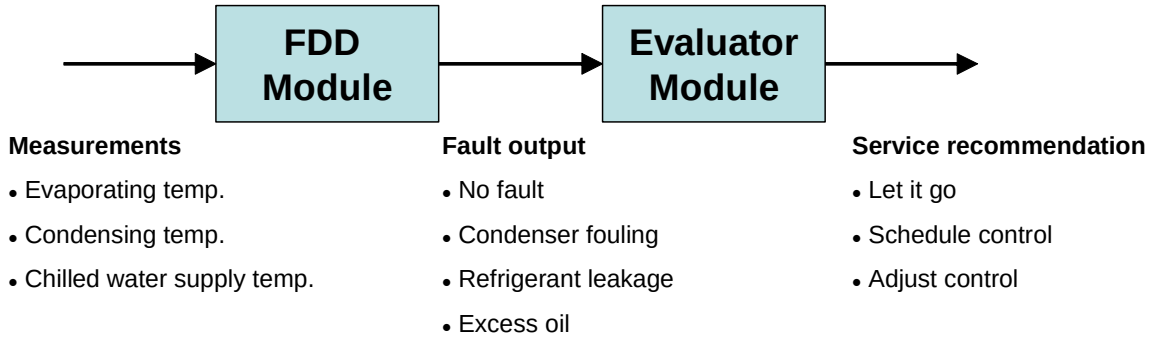

Figure 1.1 Procedures of a typical FDD system in HVAC&R applications

It is worth pointing out that it is not always necessary to implement all three procedures in a FDD system even though they may be. Actually, the fault evaluation procedure often involves much knowledge beyond the scope of HVAC&R engineering itself. More often than not, the goal of a FDD system in HVA&R applications is to consolidate the information into a clear picture of equipment status and incorporate the plant operators

and engineers into process monitoring efficiently, rather than only automate all the procedures. Therefore, the fault detection and diagnosis are virtually the two procedures of great concern in the application of FDD system to HVAC&R systems.

1.2.3 State of the Art of FDD in HVAC&R Systems

As early as the 1960s, engineers and scientists came to realize that faults, even a minor malfunction, of critical applications, e.g., nuclear power plants and air craft industries, could lead to severe consequences - loss of money, time or even life. These considerations led to increasing research into automated (even on-line) fault detection, diagnosis (FDD) systems. Automated FDD systems in critical applications have the potential to ensure safe operation, improve business productivity, reduce equipment down time, and reduce operating costs. For critical applications, safety is an overriding consideration and expensive sensors and electronics can be used within FDD system to achieve this goal. In chemical process plant, FDD systems can go a long way towards reducing downtime and improving production efficiencies (Braun 2003).

The primary difference between HVAC&R systems and critical applications for FDD is the cost-to-benefit ratio. In general, the benefits of FDD for HVAC&R systems are lower than for critical applications (Braun 1999). Traditionally, the benefits of FDD in HVAC&R systems are reduced operating costs. But now, the ever-rising awareness of the effects of IEQ on health, productivity and the quality of life has been greatly speeding up the development and deployment of FDD in HVAC&R systems.

On the other hand, one of the primary obstacles to the development and deployment of FDD in HVAC&R systems has been for a long time the lack of information of target systems, as it is not economical to apply many sophisticated electronics to such non-critical systems. Fortunately, the costs of sensors and control hardware have gone down. In addition, the recent advances in network technology and the compatibility of BMS network protocols allows the Direct Digital Control (DDC) panels of individual HVAC&R devices to be conveniently integrated into the BMS through gateway technologies (Hartman 2000). The integration between the individual devices and BMS have created the opportunity for the BMS to have rich information of individual devices and the whole HVAC&R system, while eliminating the need for duplicating sensing components and wiring. This has provided a necessary background and infrastructure for the use of quantifiable information for better performance analysis and decision making, especially for FDD in HVAC&R systems in buildings.

Furthermore, the initial, operating and maintenance costs for chillers, especially large-sized centrifugal chillers, are significantly greater than those for other devices in HVAC&R systems. These large components can absorb more added costs associated with FDD than others. Moreover, FDD systems for large-sized chillers can be integrated into DDC panels of individual chillers and BMS, reducing the added costs in these applications even further. Therefore, FDD systems for centrifugal chillers have a high benefit-cost ratio and are increasingly attractive for researchers.

Up to now, there are many FDD studies on HVAC&R systems. However, there have been relatively few studies targeting chillers, considering their importance to thermal comfort and energy use. Literature reviews of FDD studies on HVAC&R systems are presented in a source book by International Energy Agency (IEA Annex 25 1996), Comstock et al. (1999), Reddy et al. (2001), and Dexter and Pakanen (2001). Specific contributions made by a few researchers in the development of FDD for chillers will be presented in the following subsections.

Moreover, in the past several years ASHRAE (American Society of Heating, Refrigerating and Air-conditioning Engineers) has also been active in sponsoring research in the area of FDD for HVAC&R systems. The ASHRAE research specifically aimed at diagnostics includes:

- Small Scale On-Line Diagnostics for an HVAC System (883-RP)
- Demonstration of Fault Detection and Diagnostic Methods in a Real Building (1020-RP)
- Fault Detection and Diagnostic Requirements and Evaluation Tools for Chillers (1043-RP)
- Development and Comparison of On-Line Model Training Techniques for Model-Based FDD Methods Applied to Vapor Compression Equipment (1139-RP)

The cited efforts above have made significant contribution to enabling FDD applications within the HVAC&R industry.

1.2.4 Fault Survey in Chillers

One of the first steps in developing a FDD strategy is to identify the most important faults, both hard failures and soft faults, which are worth consideration. This section concludes with how and why the faults are selected for the development of the FDD strategy in this thesis.

The primary information sources used to determine the faults in chillers come from technicians who serve them. Comstock and Braun (1999) conducted a fault survey for chillers (screw and centrifugal) by gathering information from service technicians and design engineers. Their survey of centrifugal chillers is most pertinent to the study in this project. Figure 1.2 shows the normalized frequency results from the service records detailing the various kinds of faults that occur in centrifugal chillers. Obviously, the most common fault was a problem in the control box or starter. Although these kinds of faults are typically easy to detect and fix, they are a nuisance because of the downtime they cause. The high frequency of refrigerant leakage is surprising, but is relatively simple to correct. Nevertheless, environmental regulations warrant the detection of refrigerant leakage as soon as possible. Approximately 56% of the faults have the potential to affect the thermodynamic states of the chiller. The results are similar to those reported by Breuker (1997) for rooftop air-conditioners.

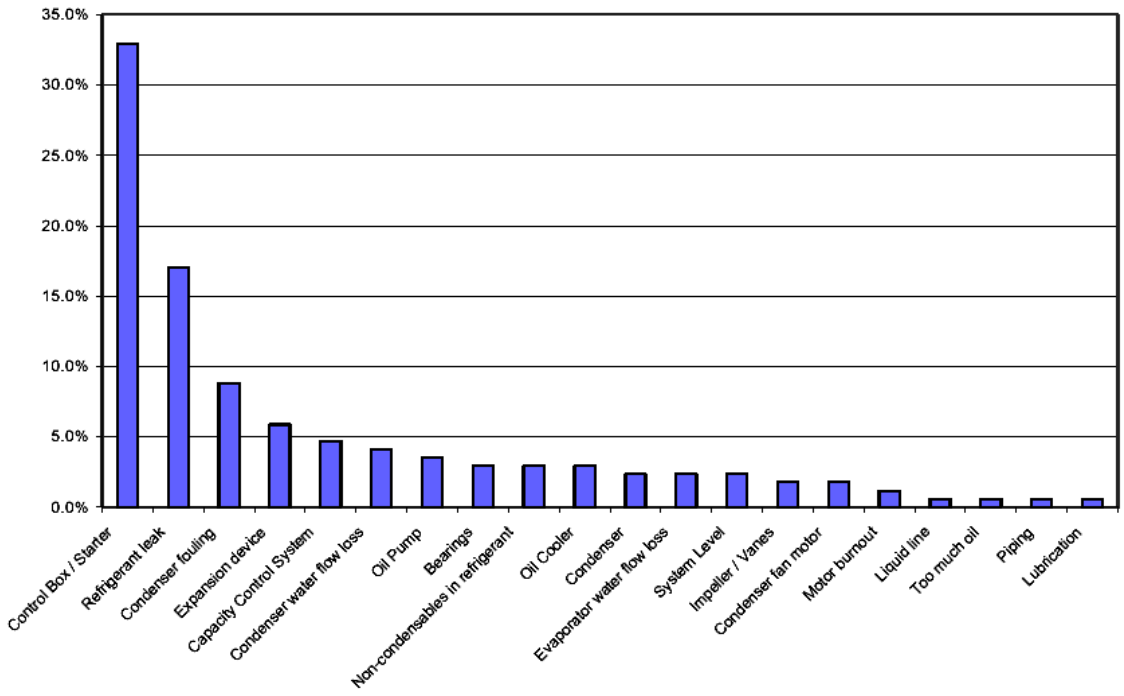

Figure 1.2 Centrifugal chiller detailed fault survey results normalized by frequency (Comstock and Braun 1999)

Although a large number of possible faults and failures in centrifugal chillers were identified by the survey of Comstock and Braun (1999), it is noteworthy that not all of them would be of practical significance for the study of FDD in chillers. For example, most electrical and compressor failures (e.g. motor burnout, control box/ starter failure, and condenser fan loss) do not need sophisticated detection methods, since their presence is obvious. In addition, some failures can be easily detected with simple sensors. For example, the reduced condenser and evaporator water flow rates can be easily detected by the mounted precise flow meters. As for faults associated with lubrication (e.g., faulty oil cooler and faulty oil pump), they are not practical for further investigation as part of FDD as they can easily detected by measuring oil temperature and oil pressure.

Soft faults generally lead to a loss of performance, but are otherwise not easily detected (since the chiller is often still operational) and cannot normally be detected with a single

sensor. For example, the frequency of refrigerant leakage is very high and unnoticeable for system operators. This fault needs to be detected as soon as possible due to environmental regulations.

Consequently, the chiller faults chosen for study in this thesis are:

- Evaporator fouling
- Refrigerant leakage
- Excess oil
- Condenser fouling
- Non-condensables in refrigerant
- Degradation of centrifugal compressor

It was known that some of these fault conditions do not occur very frequently. However, they cumulatively account for around 30% of the service calls made and the repair cost. It is worth pointing out here that evaporator fouling and compressor degradation - two faults are not included in the survey of Comstock and Braun (1999) - are added to the above list. The reason for it is that evaporator fouling can occur to a flooded evaporator when oil can not return to the compressor properly, and compression degradation actually takes faulty impeller/vanes into account.

It could be expected that the faults chosen for study could change the thermophysical states of centrifugal chillers and therefore could be detected by monitoring performance indexes that have great thermophysical meaning. The performance indexes indicative of soft chiller faults usually do not change abruptly but degrade gradually, which allows

operators to notice the degradations easily by tracing them. Moreover, according to Breuker's research (1997), it is possible that many of the detectable faults may serve as a warning sign for potential failures that can occur later if the fault is not handled well.

1.3 Literature Review

1.3.1 FDD Methods for HVAC&R Systems

Since a fault is actually an unsatisfactory deviation from a normal expectation, comparison is the essence of FDD, e.g., selection of parameters (qualitative or quantitative) for comparison, construction of benchmarks for comparison, and analysis of comparison results. As presented by Gertler (1998), the methods of fault detection and diagnosis may be classified into two major groups: model-free FDD methods, which do not use an explicit mathematical model of the target system (Figure 1.3), and model-based FDD methods, which however utilize the model (Figure 1.4). Nevertheless, it should be noted that there is no clear boundary between these two definitions and sometimes these two methods are used jointly.

Model-free methods do not need models of the target system. Actually the monitored parameters are fed into a fault diagnostic classifier, the outputs of which will indicate the presence or absence of a predefined fault. The classifier is usually constructed by rules that relate the monitored parameters to the corresponding faults. Although model-free methods have a simple structure and can detect and diagnose faults simultaneously, it is difficult to construct a series of robust rules for them and evaluate faults effectively.

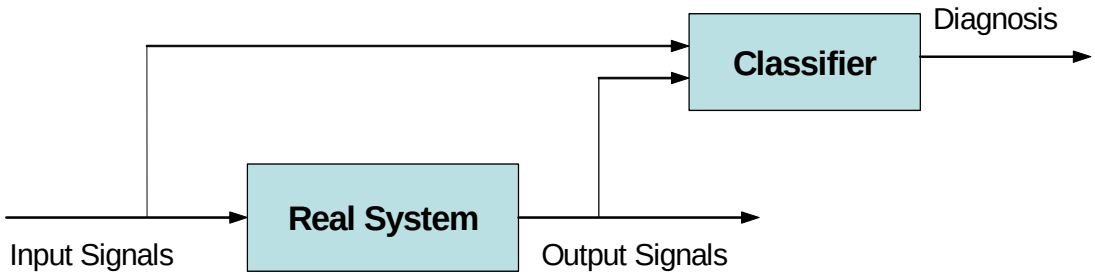

Figure 1.3 Schematic diagram of a model-free FDD method

The model-free FDD methods range from physical redundancy and special sensors through limit-checking to expert system. Of course there is also no strict demarcation between the various categories below, as some methods tend to overlap.

- *Physical redundancy* uses multiple sensors installed to measure the same physical quantity. Frank (1987) described how information redundancy was advisable for robust FDD to be achieved. In his study, multiple sensors and actuators were used to measure the same quantities. A voting procedure was used to compare performance, and faults were detected by a set of majority rules. Even though the method can often be effective in sensor FDD, its cost, and the complexity associated with installing redundant sensors and limitations in its capability make it unattractive in most engineering applications. However, the method is usually used in nuclear power plant where safety and reliability are overwhelming concerns.
- *Special sensors* may be installed explicitly for fault detection and diagnosis (Gertler 1998). Examples of special sensors are limit sensors performing limit checking (see below) in hardware by measuring temperature or pressure. Other special sensors

may measure some fault-indicating physical quantities to detect special faults in engineering applications, e.g., leakage of liquid or gas.

- *Limit checking* is widely used in engineering applications, where plant measurements are compared by computers to preset limits (Wagner and Shoureshi 1992). Exceeding the threshold indicates a fault condition. In many systems of this kind, there are two levels of limits, the first one serving for pre-warning while the second one triggers an emergency reaction.
- *An Expert system* generates links between observed behaviors and particular faults (Han et al. 1999). The development of an expert system, according to Tsutsui and Kamimura (1996) involves three main steps: the acquisition of knowledge from knowledgeable experts and case histories, the expression of this knowledge logically, e.g., using "*if-then-else*" statements, graphically or in decision table format and a method of reasoning, which deals with how to implement the fault diagnosis. Rule-based systems are considered to belong to expert systems.

Model-based methods utilize a mathematical model or physical model as the reference model to describe the system under fault-free operation. The monitored parameters are compared to the behavior predicted by the reference model to generate residuals, which are then used to indicate occurred faults.

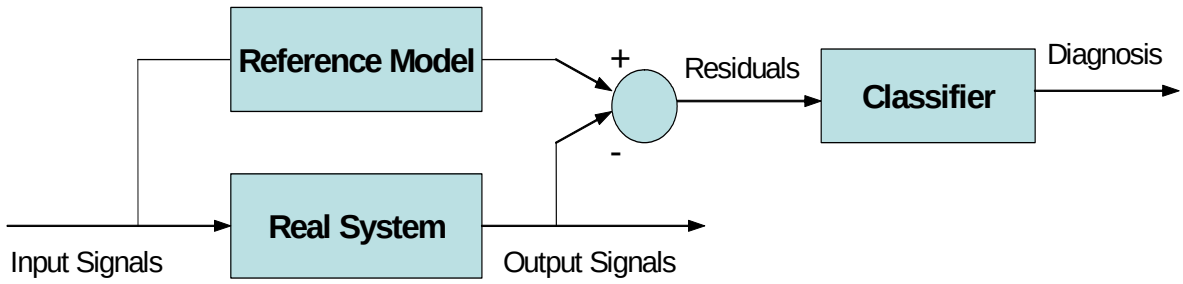

Figure 1.4 Schematic diagram of a model-based FDD method

Model-based FDD methods can be classified into three groups in terms of model construction:

- *Data driven models* do not incorporate any knowledge of the system. Examples of these models include artificial neural networks (ANN) (Peitsman and Bakker 1996, Bailey, 1998), polynomial regression models (Rossi and Braun 1997, Jia 2002), autoregressive (AR) models (Peitsman and Bakker 1996), multi-step fuzzy models (Dexter 2001), principal component analysis (PCA), etc. Transients are often neglected in data driven models used for FDD. An advantage of these models is that detailed physical knowledge of the system is not necessary. A disadvantage is that these models are reliable only for operating points that training data can take into account. In order to get proper models, training data containing much information are required.
- *Physical models* are largely based on fundamental thermophysical knowledge. Examples of physical models include ASHRAE Primary Toolkit Models (Bourdouxhe et al. 1997), Gordon-Ng universal chiller models (Gordon et al. 1995), component physical models (Mclntosh et al. 2000), etc. Physical models require less training data, but a deep understanding of the process, which is

usually difficult to obtain, is necessary for developing an accurate model. In addition, the more detailed the model, the less transportable.

- *Semi-physical models* may be partly data driven and partly based on fundamental thermophysical knowledge. Actually, these models are data driven models that are calibrated by experimental study, e.g., CoolTools/ DOE-2 Model (PG&E, 2001). Semi-physical models are more transportable than physical models and require less training data than data driven models.

It is noteworthy that all FDD methods, whether model-based or model-free they are, have their own advantages and disadvantages. In this regard, there is no single approach that is applicable to all engineering applications. Considering the strong robustness and high accuracy of the model-based methods, most investigators have recently shown great interest in them. Many efforts have been made to incorporate different FDD methods into a hybrid system for better fault detection, diagnosis and evaluation, e.g., data-driven models for sensor FDD and semi-physical models for chiller component FDD.

1.3.2 Applications of FDD Method for Chillers

Model-free FDD methods

The review of model-free FDD methods shows that those methods were widely employed in the early investigation of FDD for small or medium-sized chillers.

Stallard (1989) developed an expert system for automated FDD applied to refrigerators.

Different temperature measurements were used directly as classification features. Feature limit checking was used for both detection and diagnostic classification. Fault diagnoses were performed by evaluating the direction in which the classification features changed from benchmark values and then by matching these changes to expected directional changes related to each predefined fault.

Yoshimura and Ito (1989) used a combination of seven temperature and pressure measurements to perform rule-based FDD for packaged air conditioners. The rule-based method was used with the thresholds defined as fuzzy variables. They did not utilize any preprocessing or statistical rule evaluation.

A FDD method was developed by Inatsu et al. (1992) by measuring the amount of refrigerant in an automotive air-conditioning system. It was concluded that measuring the liquid-gas flow ratio could give desirable results and identify up to 40% loss of refrigerant charge under medium to high load conditions.

More recently, McIntosh (1999) made use of redundant physical measurements in parallel chillers to detect and diagnose measurement bias errors. This method requires another sensor of known accuracy as a reference base.

Model-based FDD methods

A prototype diagnostic system, which can be used under variable operation conditions, has been developed for compression refrigeration plants by Grimmelius el at. (1995).

Based on a combination of causal analysis, expert knowledge and simulated failure modes, a symptom matrix with many failure modes has been established. The accuracy and transplantable capability of the FDD system still need be improved.

Stylianou and Nikanpour (1996) used a thermodynamic model that was developed by Gordon and Ng (1995) as part of their FDD method for a reciprocating chiller. This model was used solely for fault detection but not for diagnosis during steady-state operation of the chiller. Similar to the approach of Grimmelius et al. (1995), fault diagnoses were implemented based on a fault pattern matrix which, as shown in Table 1.1, relates faults to corresponding changes in measured variables. Among the faults tested, it is not known whether the faults were tested at various levels of severity, except the liquid line restriction that was introduced at two levels and characterized as a pressure drop along the liquid line.

Table 1.1 Fault patterns used in Stylianou and Nikanpour's fault diagnostic module

Fault	**Discharge temp.**	**Discharge pressure**	**High pressure liquid line temp.**	**Low pressure liquid line temp.**	**Suction line temp.**	**Suction pressure**	**Condenser water temp. difference**	**Evaporator water temp. difference**
Liquid line restriction	▲	▼	▼	▼	▲	▼	▼	▲
Refrigerant leakage	▲	▼	▼	▼	▲	▼	▼	▲
Reduced condenser water flow rate	▲	▲	▲	▼	▼	▼	▲	▼
Reduced evaporator water flow rate	▲	▼	▼	▼	▼	▼	▼	▼

A '▲' signifies an increase in the variable, and a '▼' corresponds to a decrease.

Stylianou (1997) developed a FDD method for commercial reciprocating chillers using a Statistical Pattern Recognition Algorithm (SPRA). The SPRA requires little computational effort and can improve the diagnostic classifier. However, very limited evaluation of the FDD method was presented.

Rossi and Braun (1997) presented an FDD method for packaged air conditioners using nine key measurements to detect and diagnose five faults. The FDD technique uses a steady-state polynomial regression model to predict temperatures during normal operation in order to generate residuals for FDD. The magnitudes of the residuals are statistically evaluated to find faulty operation and then compared with a set of fault patterns based on directional changes in measured variables (as shown in Table 1.2) to perform fault diagnosis. This study did not consider the effect of modeling errors on the sensitivity of the FDD method.

Table 1.2 Fault patterns used in Rossi and Braun's fault diagnostic module

Fault	**Evaporating temp.**	**Suction line super heating**	**Condensing temp.**	**Liquid line subcooling**	**Hot gas discharge temp.**	**Air temp. rise across the condenser**	**Air temp. rise across the evaporator**
Refrigerant leakage	▼	▲	▼	▼	▲	▼	▼
Compressor valve leakage	▲	▼	▼	▼	▼	▼	▼
Liquid line restriction	▼	▲	▼	▲	▲	▼	▼
Condenser fouling	▲	▼	▲	▼	▲	▲	▼
Evaporator fouling	▼	▼	▼	▼	▼	▼	▲

A '▲' signifies an increase in the variable, and a '▼' corresponds to a decrease.

Peitsman and Bakker (1996) used black box models to generate residuals for a FDD method that was applied to a laboratory chiller. Models were used at the system level to detect a fault and at the component level to isolate the fault. Both AR models and neural network models were investigated. Only limited evaluation of the FDD method was presented.

Bailey (1998) trained an artificial neural network (NN) using normal and fault data from a screw chiller in order to provide direct classification of normal and faulty performance. The NN model used a large number of inputs to predict the output classes and therefore required a large data set. Although the data collection process appears to have been thorough, the sensitivity of the measured variables to the faults introduced was not given. Moreover, the ability of the neural network to classify the faults is difficult to deduce from the results.

McIntosh (1999) developed a robust model-based FDD methodology for a centrifugal chiller system and found the characteristic quantities that are most appropriate for identifying faults. Subsequently, the FDD methodology computed residual errors of characteristic quantities and determined their overall significance using the appropriate statistical analyses. Robustness of the methodology is obtained by accounting for the accuracy (noise errors) of the sensors used in obtaining measurement data. However, the accuracy of the sensors was considered independently from the component faults.

Jia (2002) characterized every primary component of the centrifugal chiller with at least one performance parameter, the magnitude of which is indicative of the health of that

component. Also, fault detection and fault diagnosis can often be done simultaneously. Mathematical models for these characteristic parameters are presented, and how well these models can be developed with field-monitored data is illustrated. The proposed FDD method was only partially validated using transient data from normal conditions but not the data indicative of fault conditions.

More recently, Li and Braun (2003) proposed an improved statistical rule-based (SRB) FDD method based upon the work of Rossi (1995) and Rossi and Braun (1997) for packaged air-conditioners. As compared with the original SRB method, the improved method does not require the covariance matrix for faulty operation or probability calculations but utilizes new fault detection and diagnostic classifiers that are simpler to implement and provide improved FDD sensitivity. The FDD method is capable of detecting and diagnosing individual faults and can be applied to packaged air-conditioners that incorporate a fixed expansion device with on/off control of the compressor and fixed-speed condenser and evaporator fans

To sum up, many advanced techniques and algorithms in mathematics, statistics, signal processing, process control and monitoring, etc., have been introduced to the investigation of FDD in chiller systems and other HVAC&R systems. Due to the complexity of FDD in these fields, sometimes different methods are used jointly.

1.3.3 Sensor FDD Methods in Engineering Systems

Sensor faults have been a major concern in engine performance monitoring (Ogaji et al. 2002) for a long time. Research on sensor FDD in engineering systems has been very active in recent years. In engineering systems, a sensor fault distinguishes itself from a chiller fault in that the latter affects the system performance in the physical while the former can't, if the sensor is not involved in any control of the system. Due to this difference, the FDD methods targeting chiller faults may not necessarily handle sensor faults and therefore need some modifications when applied to sensor FDD. Basically, there are four kinds of methods for sensor FDD: model-based, knowledge-based, measurement aberration detection, and physical redundancy, which are briefly described as follows.

- *Model-based methods* (Patton and Chen 1991, Usoro 1985, Stylianou and Nikanpour 1996, Wang S.W. and Wang J.B. 1999, Wang and Xiao 2004) examine the implicit analytical redundancy in the system. Residuals are generated by comparing monitored parameters with those predicted by the system model, and then analyzed by decision-making process, resulting in a report of identified faults.
- *Knowledge-based methods* use heuristic reasoning to build and manipulate qualitative models of the targeted process. Techniques used include an expert system (Tzafestas 1991), a neural network (Lee et al. 1997), and a fuzzy logic (Vachekov and Matsuyama 1992).
- *Measurement aberration detection method* analyzes the output of a single sensor

while assuming that the true measurement value has certain time and/or frequency domain properties and that a fault may occur randomly at any time (Yung and Clarke, 1989).

- *Physical redundancy methods* use several sensors to measure the same physical quantity. Any serious discrepancy among the measurements indicates a sensor fault (Dorr et al. 1997). Even though this method can often be effective, the cost and complexity of incorporating redundant sensors makes this approach less unattractive to in less critical applications, e.g., HVAC&R and chemical fields.

1.3.4 Conclusions

Research on FDD for chiller systems is becoming more and more active because FDD plays an important role in improving automatic monitoring and control for chillers, benefiting effective preventing maintenance, enhancing energy efficiency of buildings and maintaining agreeable IEQ.

The first and the most important issue to point out is that most recent investigations paid attention to only one of these two different types of fault, i.e., chiller faults or sensor faults, and have not considered the two simultaneously. However, sensor faults and chiller faults might occur simultaneously as components and sensors within a chiller are both susceptible to degradation. The existence of sensor faults has a great impact on the effective implementation of chiller FDD methods as the implementation depends on the reliability and accuracy of measurements from BMS or chiller control panels. Therefore,

it is essential to develop a chiller FDD strategy that is capable of handling both sensor faults and chiller faults. In order to achieve this goal, it is desirable that before the implementation of chiller FDD, sensor FDD should be carried out to validate all measurements used in chiller FDD.

Secondly, the traditional FDD methods for HVAC&R systems usually appointed a great number of measurements as fault indicators. The fault diagnostic classifiers of these methods use the statistically significant deviations of measurements to detect a fault and use their deviation patterns to diagnose the fault. However it is very difficult to determine how many and which measurements should be chosen to fulfill the duty as there are now a great number of sensors instrumented in a large-sized centrifugal chiller. A robust fault diagnostic classifier in FDD should make use of the impacts of faults, preferably, on performance indexes that have strong thermophysical meaning, rather than on purely numerical measurements from a great number of sensors.

Moreover, most model-free FDD methods have inevitable shortcomings in dealing with complicated large-sized systems as mentioned above, so they are not very popular in the engineering field. The performance of FDD methods based on physical models depends heavily on accuracy and completeness of the information database, which, however, is always difficult to acquire. Semi-physical models combining merits of data driven models and physical models are preferable to other models in FDD applications and therefore show great potential in engineering applications. However, it is rather difficult to determine a proper semi-physical model structure which is easy to identify, and which

is physically explainable and robust against measurement errors as well.

Another fundamental issue in FDD application for chillers is to set appropriate fault detection thresholds. The thresholds are usually determined empirically or experimentally. A lower threshold can benefit the earlier detection of faults but tends to produce false alarms. A higher threshold can effectively reduce the possibility of false alarms but tends to miss identifying faults. It is much preferable for a FDD strategy to set reasonable thresholds by taking into account as many influencing factors as possible.

1.4 Objectives

FDD for chillers, especially for large-sized centrifugal chillers, plays an important role in improving IEQ, enhancing building energy efficiency, prolonging equipment life and reducing maintenance costs and unscheduled equipment downtime. However, given the benefits of FDD for chillers mentioned above, current studies on FDD for chillers are not sufficient though research efforts in this field are growing continuously. The objectives of this thesis are listed as follows.

The primary objective of this thesis is to develop a robust strategy that is suitable for FDD application to centrifugal chillers, when both sensor faults and chiller faults exist simultaneously. Since the two kinds of faults have different characteristics, the robust FDD strategy will be developed by organically incorporating a sensor FDD&E (Fault Detection, Diagnosis and Estimation) scheme with a basic chiller FDD scheme. In the

sensor FDD&E scheme, the estimation is to estimate the magnitude of an identified sensor error. During implementation, the second scheme will rely on the results of the first scheme. More specifically, the sensor FDD&E scheme needs to be capable of detecting, diagnosing and estimating sensor faults even in the presence of chiller faults. With the aid of data validated by the sensor FDD&E scheme, the basic chiller FDD scheme will effectively and accurately identify chiller faults.

Besides developing this robust strategy, another objective of this thesis is to assess and evaluate the performance of the developed FDD strategy using real-life chiller data. The data will be representative of a wide variety of both chiller faults and sensor faults, under various chiller operating conditions.

1.5 Organization of this Thesis

The motivation of this research thesis is put forward at the beginning of this chapter and then followed by an introduction of the background of FDD for chillers and the comprehensive review of FDD applications to HVAC&R systems, especially to chillers. Many FDD methods were analyzed and compared with one another. Conclusions drawn from the review show that the studies on FDD for chillers are insufficient and thus further efforts in this field are needed. All this directs and shapes the research objective in this thesis and proves its practical significance. The subsequent chapters follow a logical sequence as follows.

Chapter 2 reviews the fundamentals of centrifugal chillers. The basic refrigeration cycle, primary components and sensors, basic control and typical operating conditions for centrifugal chillers are briefly introduced. Also, an overview of the robust FDD strategy for centrifugal chillers is outlined in this chapter.

Chapter 3 presents a basic chiller FDD scheme for centrifugal chillers using a model-based method. Some performance indexes that have strong thermophysical meaning are selected to indicate chiller performance. A set of rules used in the fault diagnostic classifier is derived from thermophysical analysis of faults and their impacts on performance indexes. In particular, an adaptive estimator for fault detection threshold is developed in this chapter on the basis of considering essential influencing factors, including measurement quality, model fitness and chiller operating conditions. The adaptive threshold estimator provides a quantitative approach to scientifically determining thresholds.

Chapter 4 briefly introduces two test facilities that are used to validate the two FDD schemes and the robust FDD strategy developed in this thesis. One facility is a laboratory centrifugal chiller in ASHRAE 1043-RP and the other is a chiller plant in a real building in Hong Kong.

Chapter 5 presents validation tests of the basic chiller FDD scheme using data from the two test facilities introduced in Chapter 4. The performance of the basic chiller FDD scheme in detecting and diagnosing several typical chiller faults is evaluated and

assessed. Problems associated with the implementation of the basic chiller FDD scheme are put forward.

Chapter 6 presents a sensor FDD&E scheme based on a PCA model, which is used to capture correlations among key variables and to realize automatic detection, diagnosis and estimation of sensor faults. The sensor FDD&E scheme aims at validating sensors whose measurements are crucial to chiller FDD, energy monitoring and control in centrifugal chillers,

Chapter 7 presents validation tests of the sensor FDD&E scheme using data from the two test facilities introduced in Chapter 4. The sensitivity of the PCA model to typical chiller faults is investigated using real-life chiller data. The performance of the sensor FDD&E in detecting, diagnosing and estimating sensor faults is also evaluated and assessed.

Based on the validated chiller FDD scheme and sensor FDD&E scheme, Chapter 8 presents the implementation structure of the robust FDD strategy that incorporates the above two schemes so as to achieve our ultimate goal, namely to tackle chiller faults and sensor faults simultaneously. The validation results of the robust strategy using chiller data from laboratory tests are provided. A software package of the robust strategy is developed in the MATLAB 6.1 environment and then its integration with an intelligent building management platform is proposed.

Chapter 9 summarizes the work reported in this thesis, and gives recommendations for future applications and research in related areas.

CHAPTER 2 CENTRIFUGAL CHILLER SYSTEMS AND AN OVERVIEW OF ROBUST FDD STRATEGY

Since the thesis is directly aimed at the FDD for centrifugal chillers, a general understanding of their fundamentals and operating characteristics is needed to assist in developing FDD methods and avoiding major pitfalls.

Section 2.1 briefly describes centrifugal chiller systems, including the basic refrigeration cycle, primary components and sensors, basic control and interlocks within centrifugal chillers, and their typical operating conditions. Section 2.2 briefly describes the FDD strategy for centrifugal chillers developed in this thesis. A summary of this chapter is given in Section 2.3.

2.1 Centrifugal Chiller Systems

2.1.1 Basic Refrigeration Cycle

Centrifugal chillers belong to the category of vapor compression chillers, which utilize a vapor compression cycle to remove heat from chilled water and reject the heat from the chilled water plus the heat from the centrifugal compressor to the environment. Figure 2.1 shows the basic refrigeration cycle with a centrifugal compressor. The whole refrigeration cycle can be thought to include four processes with appropriate assumptions:

- 1-2 Heat absorption in the evaporator under constant pressure;

- 2-3 Adiabatic compression in the compressor;
- 2-3 Heat rejection in the condenser under constant pressure;
- 3-4 Throttling across the expansion device under constant enthalpy;

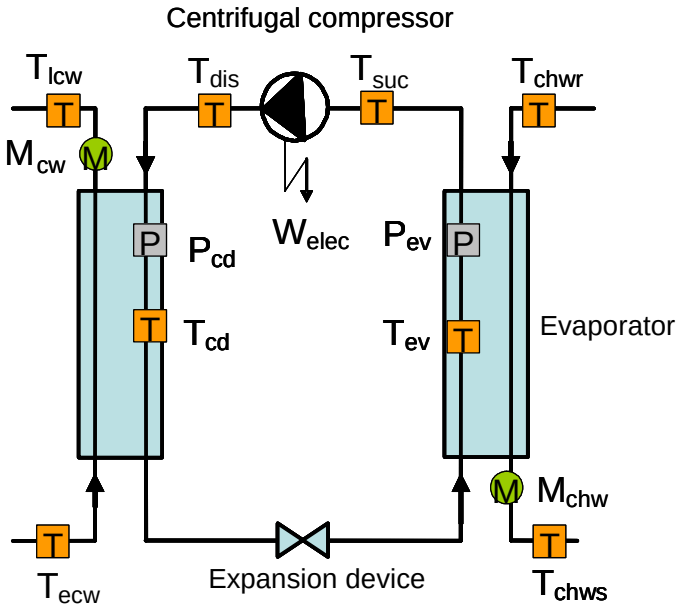

Figure 2.1 Schematic diagram of a typical centrifugal chiller refrigeration cycle

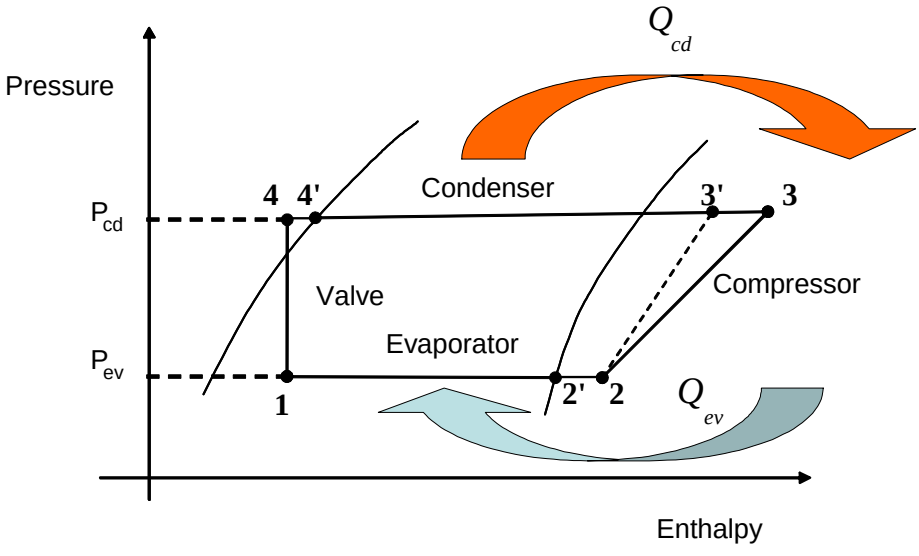

Figure 2.2 Basic refrigeration cycle shown on a pressure-enthalpy diagram with two isotonic and one adiabatic and one isentropic process

The Pressure-Enthalpy (P-H) diagram is another way of illustrating the refrigeration

cycle. Figure 2.2 shows the basic refrigeration cycle of the chiller on a pressure-enthalpy cycle, consisting of two isotonic processes (1-2 and 3-4) and one polytropic process (2-3) (where, 2-3′ is an ideal adiabatic process), and one isentropic process (4-1), for the same refrigeration circuit shown in Figure 2.1.

The process for each of the components is indicated. From state 1 to state 2, the refrigerant changes from a liquid state to a gaseous state and absorbs heat from the chilled water while its pressure stays constant. Superheating occurs before reaching state 2. The line from state 2 to 3 represents the compression process, where an amount of power is consumed and converted into heat in the refrigerant. Open drive motors reject their winding heat to the mechanical room. Since chiller motors are typically over 95% efficient, a little less than 5% of the motor power ends up as heat in the mechanical room. The next process takes place in the condenser, from state 3 to state 4. The first section (outside the refrigerant dome) is the de-superheating process. Once the refrigerant is saturated, condensation occurs and the refrigerant changes from a gas to a liquid. Like the evaporator, the line is horizontal indicating constant pressure (or temperature). Note the liquid subcooling portion of the condenser to the left of the dome， from state 4' to 4. It is easy to see on the P-H diagram that the subcooling improves the total cooling effect without an increase in power input. The final process take place in the expansion device, which is indicated by the vertical line from state 4 to state 1, indicating the pressure and temperature drop that occurs as the refrigerant passes through the thermal expansion valve.

2.1.2 System Mechanism

As a vapor compression refrigeration unit, a typical centrifugal chiller consists of the following four main components and many sensors.

Evaporator

The evaporator is a heat exchanger that removes the building heat from the chilled water lowering the water temperature in the process. The heat is used to boil the refrigerant, changing it from a liquid to a gas. Usually, centrifugal chillers use a flooded type evaporator, which is very energy efficient. Flooded evaporators have the chilled water in the tubes and the refrigerant in the shell. Large chillers can have over five miles of tubing in their heat exchangers.

Compressor

The centrifugal compressor works very much like a centrifugal fan, compressing the refrigerant vapor flowing through it by spinning it from the center of an impeller wheel radially outward and allowing centrifugal forces to compress the vapor. Therefore, the temperature and pressure of the vapor are increased through the compression. Some compressors use multiple impellers to compress the refrigerant in multiple stages. Centrifugal chillers can use liquid refrigerant to cool a hermetic compressor or water to cool an open one. The centrifugal compressor is a non-positive displacement type. It raises the pressure and temperature of the refrigerant by converting kinetic energy into pressure.

Condenser

Like the evaporator, the condenser is also a heat exchanger. It removes heat from the refrigerant causing it to condense from a gas to a liquid. The heat raises the water temperature. The condenser water then carries the heat to the cooling tower where the heat is rejected to atmosphere.

Expansion device

After the refrigerant condenses to a liquid, it passes through a pressure-reducing device. This can be as simple as an orifice plate or as complicated as an electronic modulating thermal expansion valve.

Sensors instrumentation

There are a great number of sensors installed in chiller systems and the sensor instrumentation is different for different applications. In this study, the sensors crucial to chiller efficiency monitoring and control systems are listed in Table 2.1. These sensors exist in most centrifugal chiller systems.

Table 2.1 Important sensors in a typical centrifugal chiller system

Measurement	Description	Unit
T_{chws}	Chilled-water supply temperature	^{o}C
T_{chwr}	Chilled-water return temperature	^{o}C
M_{chw}	Chilled-water flow rate	L/s
T_{ecw}	Entering condenser water temperature	^{o}C
T_{lcw}	Leaving condenser water temperature	^{o}C
M_{cw}	Condenser water flow rate	L/s
T_{ev}	Evaporating temperature	^{o}C
P_{ev}	Evaporating pressure	Pa
T_{cd}	Condensing temperature	^{o}C
P_{cd}	Condensing pressure	Pa
T_{suc}	Compressor suction temperature	^{o}C
T_{dis}	Compressor discharge temperature	^{o}C
W_{elec}	Motor electrical power input	kW

2.1.3 Basic Control

For minimizing chiller energy use, the entering condenser water set-point should be as low as can be provided by outdoor air conditions (i.e., wet bulb temperature). However, the control set-point should be at or above the lowest temperature attainable by cooling tower at certain air (wet-bulb) temperature to avoid the waste of fan energy trying to reach an unobtainable value.

The chilled water supply temperature control is achieved by inlet guide vane control as shown in Figure 2.3. Mounted on the inlet of a centrifugal compressor, the inlet guide vanes open or close to change the flow angle of the gas entering the impeller, and then

change both the power consumed by the impellor and the cooling effect produced. In this way, the chiller can operate down to a claimed 10% of its rated cooling capacity. The vane control motor opens or closes the inlet guide vanes by a feedback control module to maintain the preset chilled water supply temperature (Jia 2002).

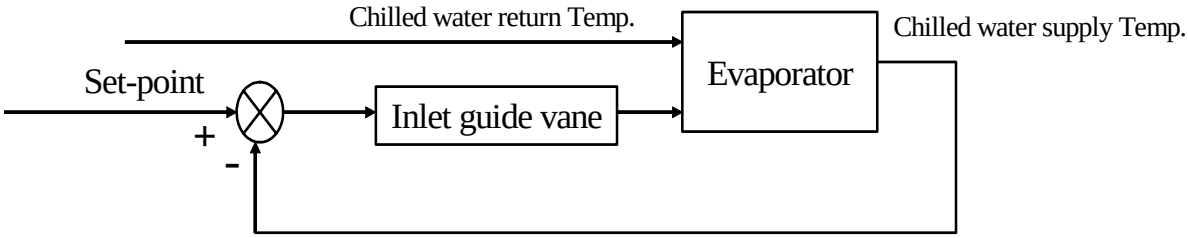

Figure 2.3 Control of chilled water supply temperature through inlet guide vane

2.1.4 Safety Interlocks

An interlock system aims to prevent the compressor motor from being started if any of the following conditions exist and stops the compressor if any except the first condition occurs:

- Open suction vane, detected by limit switch;
- Low water temperature leaving evaporator, near freezing point, sensed by low temperature switch;
- Low water flow rate, sensed by low flow switch;
- High compressor discharge pressure, sensed by high pressure switch;
- High motor bearing or winding temperature, detected by high temperature switch;
- Low oil pressure.

Another interlock system guarantees that the following are operating upon starting of the compressor: water pump, oil pump and water to oil cooler. The suction vane usually has an interlock to be sure it is completely closed when the compressor stops.

2.1.5 Typical Operating Conditions

The design conditions imposed by most water-cooled HVAC&R systems work very well for centrifugal chillers. The Air-Conditioning and Refrigeration Institute (ARI) provides test standards and certification for a wide range of HVAC products including centrifugal chillers.

The ARI standard 550/590-2003 (2003) is used to test and rate chillers. Additionally, chillers typically have a certification that provides engineers and owners with a third party validation that the chiller will meet the performance the manufacturer indicates. The ARI test criteria allow an "apples to apples" comparison of different chillers.

Standard rating conditions

The standard ARI rating conditions are:

- Leaving chilled water temperature 6.7 ^{o}C
- Chilled water flow rate 0.043L/s per kW
- Entering condenser water temperature 29.4 ^{o}C
- Condenser water flow rate 0.054L/s per kW
- 1.8×10^{-5} ($m^2\cdot{}^{o}C$)/W evaporator fouling factor and 4.4×10^{-5} ($m^2\cdot{}^{o}C$)/W condenser

fouling factor

Part-load rating conditions

Water-cooled centrifugal chillers capable of capacity reduction shall be rated at 100% and at each step of capacity reduction provided by the refrigeration systems as published by the manufacturer. Part-load ratings points are usually presented in the way of IPLV (Integrated Part Load Value). As provided by ARI Standard 550/590-2003 (2003), the IPLV can be calculated as follows: firstly determine the part-load energy efficiency at 100%, 75%, 50%, and 25% load points at the conditions specified in Table 2.2, and then use the following Equation 2.1 to calculate the IPLV.

$$IPLV = 0.01COP_{100\%} + 0.42COP_{75\%} + 0.45COP_{50\%} + 0.12COP_{25\%} \quad (2.1)$$

where $COP_{100\%}$ is the *COP* at 100% load, $COP_{75\%}$ is the *COP* at 75% load, and so on.

Table 2.2 Part-load conditions for rating water-cooled centrifugal chillers
(EWT – entering condenser water temperature)

100% load EWT	**75% load EWT**	**50% load EWT**	**25% load EWT**	**Condenser water flow rate**	**Fouling factor allowance**
29.4 ^{o}C	23.9 ^{o}C	18.3 ^{o}C	18.3 ^{o}C	0.054L/s per kW	4.4×10^{-5} ($m^2\cdot{}^{o}C$)/W

2.2 Overview of Robust FDD Strategy for Centrifugal Chillers

In the following part of this thesis, a robust FDD strategy for a typical centrifugal chiller will be developed and validated. The strategy mainly consists of two FDD schemes - a basic chiller FDD scheme and a PCA-based sensor FDD&E scheme, which respectively tackles chiller faults and sensor faults. The strategy could achieve the ultimate objective of this thesis, namely an overall and robust diagnosis for centrifugal chillers.

Figure 2.4 gives an overview of the robust FDD strategy. The inputs are measurements collected from the chiller system. The results of the strategy are the identified sensor faults and chiller faults. The robust strategy is conceptually different from and more advanced than those developed by previous researchers in that a sensor FDD&E scheme is integrated with a basic chiller FDD scheme. In this way, the quality of sensor measurements on which the effectiveness and robustness of the basic chiller FDD scheme depend can be ensured. The two schemes are implemented in series. The measurements crucial to the chiller FDD scheme are validated by proper approaches such as sensor fault estimation, or sensor recalibration/replacement, before the basic chiller FDD scheme is carried out to detect and diagnose degraded chiller performance.

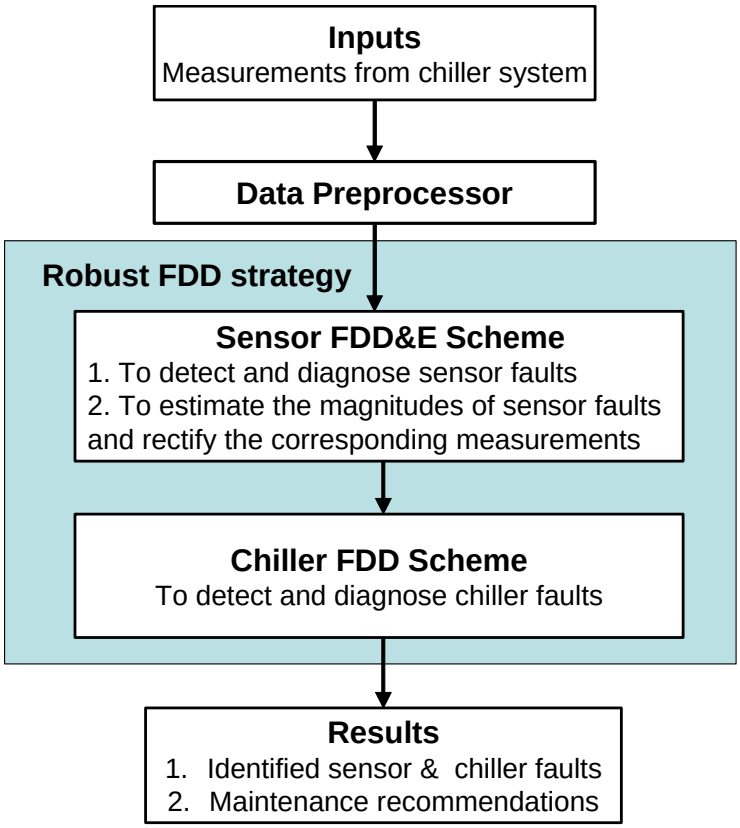

Figure 2.4 Overview of the robust FDD strategy for centrifugal chillers

2.3 Summary

This chapter first briefly introduces centrifugal chiller systems. It is clear how primary components operate and what variables are measured and involved in control systems within a typical centrifugal chiller. Subsequently, the overview of a robust FDD strategy for centrifugal chillers is presented to tackle two simultaneously existing fault types, i.e., sensor faults and chiller faults. In the following chapters, two important FDD schemes in the robust strategy will be respectively developed as well as validated using both laboratory and field data.

CHAPTER 3 BASIC CHILLER FDD SCHEME

As discussed in Chapter 1, model-based FDD methods are widely used in large-scale chillers, especially centrifugal chillers, and the FDD methods based on semi-physical chiller models have proved more favorable than those based on pure data-driven or physical models. A chiller FDD scheme is developed in this chapter as a basic approach to identify faults associated with centrifugal chiller system and components.

Based on the operation characteristics of centrifugal chillers, six performance indexes of strong physical meaning are selected to indicate chiller health conditions. The existence of a fault is detected when one or more monitored performance indexes significantly deviate from their benchmarks (i.e., what is normally expected) by corresponding thresholds. The reference models can be called semi-physical ones in that they contain some deterministic variables in chillers while needing model development data for model identification. Such thresholds for fault detection are not determined empirically but estimated by detailed uncertainty analysis. Subsequently, faults are diagnosed by a fault diagnostic classifier, which relates each fault to the change pattern of the performance indexes when the fault occurs.

Section 3.1 presents the formulation of the chiller FDD scheme, which includes the selection of six performance indexes indicative of various chiller characteristics, the construction of reference models of the performances indexes and the deduction of rules in the fault diagnostic classifier. Section 3.2 presents the online adaptive estimator of fault detection threshold. The threshold estimator takes into account factors that have strong influence on the accuracy of fault detection. Such an adaptive estimator can

effectively reduce false alarms and avoid missing timely detection. The implementation structure of the basic chiller FDD scheme is presented in Section 3.3. Finally, Section 3.4 summarizes this chapter.

3.1 Development of Basic Chiller FDD Scheme for Centrifugal Chillers

3.1.1 Performance Indexes of Centrifugal Chillers

As mentioned in Chapter 1, a fault in HVAC& R is actually an unsatisfactory deviation from a performance expectation envisioned at design. In order to produce the deviation, namely the residual in FDD applications, it is essential for chiller FDD methods to find a cluster of quantities that can describe the performance of chillers. In the early development of chiller FDD methods, measurements from sensors and transducers, e.g., temperatures, pressures, electric power, etc., are used to indicate chiller performance (Comstock and Braun 2001, Rossi and Braun 1997, etc). As shown in Table 1.1 and 1.2, rules are constructed to relate each fault to the set of directions that each measurement changes when the fault occurs. During FDD implementation, residuals are formed as the difference between the measurements and their benchmark values, which are predicted by corresponding steady-state models of the measurements. Significant residuals of the measurements are used to determine a binary "fault" or "no-fault" output. Subsequently, the fault diagnostic classifier that is usually constructed by experimental approaches can use the deviation patterns of the measurements to identify the most likely cause of the occurred faults (Comstock and Braun 2001). However, an occurred fault usually results in changes in many measurements as shown in Table 1.1 and Table 1.2. Moreover, the sensitivity of a set of measurements to a chiller fault might be affected by both chiller

operating condition and fault severity level. Beyond that, it is also difficult to determine how many and which measurements should be picked to construct a fault diagnostic classifier as there are a great number of sensors available on large centrifugal chiller systems.

More recently, parameters that can effectively characterize the chiller performance, called performance indexes in this thesis, are favored by many researchers in the field of chiller FDD (McIntosh et al. 2000 and Jia 2003). In this basic chiller FDD scheme, six performance indexes, as shown in Table 3.1, are selected with detailed explanation provided.

Table 3.1 Formulas for calculating the six performance indexes

Performance indexes	**Abbreviations**	**Formulations**
logarithmic mean temperature difference of evaporator	$LMTD_{ev}$	$LMTD_{ev} = \frac{T_{chwr} - T_{chws}}{\ln\left(\frac{T_{chwr} - T_{ev}}{T_{chws} - T_{ev}}\right)}$
logarithmic mean temperature difference of condenser	$LMTD_{cd}$	$LMTD_{cd} = \frac{T_{lcw} - T_{ecw}}{\ln\left(\frac{T_{lcw} - T_{cd}}{T_{ecw} - T_{cd}}\right)}$
mass flow rate of refrigerant	M_{ref}	$M_{ref} = \frac{C_{pw} M_{chw} (T_{chwr} - T_{chws})}{h_2 - h_1}$
compressor polytropic efficiency	Eff_{poly}	$Eff_{poly} = \frac{\left[\frac{P_{cd} v_3 - P_{ev} v_2}{\ln(P_{cd} v_3 / P_{ev} v_2)}\right] \ln(P_{cd} / P_{ev})}{(h_3 - h_2)}$
drive motor efficiency	Eff_{motor}	$Eff_{motor} = \frac{M_{ref}(h_3 - h_2)}{W_{elec}}$
coefficient of performance	COP	$COP = \frac{C_{pw} M_{chw} (T_{chwr} - T_{chws})}{W_{elec}}$

All the measurements used in the calculation of the performance indexes are available on the data acquisition system of laboratory chillers and also obtainable from the BMSs in modern buildings. The six performance indexes have strong physical meaning and therefore are able to depict health conditions of a centrifugal chiller system. By comparing the performance indexes with their benchmarks predicted by the reference models presented in the following section, the existence of particular faults can be detected.

The advantages of using performance indexes are listed as follows:

- Since performance indexes have specific physical meaning and can describe chiller performance straightforward, one of them might be sensitive to a particular fault but insensitive to other faults. For example, $LMTD_{cd}$ is sensitive to condenser fouling but not to such faults as evaporator fouling, excess oil, etc. Also, the sensitivity can be explained by basic physical principles, e.g., the laws of mass, energy and momentum conservation. This characteristic enables performance indexes to effectively isolate different chiller faults.
- Since performance indexes have strong physical meaning, it is both understandable and straightforward to use the performance indexes to quantify the severity level of an occurred fault. This can benefit preventative maintenance and timely repairs when necessary.
- Performance indexes have the capability of synthesizing the information provided by a large number of sensor measurements. Therefore it is easier to construct and implement a fault diagnostic classifier based on the deviation patterns of a relatively small number of performance indexes than that based on the deviation patterns of a large number of sensor measurements.

The mathematical formulations of the performance indexes (see Table 3.1) are deduced on the basis of the thermodynamic cycle of a standard centrifugal chiller shown in Figure 2.2 with the assumptions stated as follows:

- Adiabatic compression in the centrifugal compressor (from state 2 to 3);
- Heat rejection at constant refrigerant pressure in the flood type condenser (P_3=P_4);
- Heat absorption at constant refrigerant pressure in the flood type evaporator (P_1=P_2);
- Isenthalpic throttling through the expansion device (h_1=h_4).

Logarithmic mean temperature difference of condenser and evaporator

Both the condenser and evaporator in a centrifugal chiller are heat exchangers that couple refrigerant with the cooling water and the chilled water, respectively. Therefore, heat transfer relations can describe the performance of these exchangers. Assuming steady-state flow conditions, the relations characterizing the heat transfer process in the condenser are as follows.

$$Q_{cd} = C_{pw} M_{cw} (T_{lcw} - T_{ecw}) \tag{3.1}$$

$$Q_{cd} = M_{ref} (h_3 - h_4) \tag{3.2}$$

$$Q_{cd} = UA_{cd} \Delta T_{cd} \tag{3.3}$$

where Q_{cd} is the load of the condenser, C_{pw} is the specific heat capacity of water, M_{cw} is the condenser water mass flow rate, M_{ref} is the refrigerant mass flow rate, T_{ecw} is the entering condenser water temperature, T_{lcw} is the leaving condenser water temperature, and h_3 and h_4 are the specific enthalpies of the refrigerant at state 3 and state 4 in Figure

2.2, respectively. UA_{cd} is the overall heat transfer coefficient of the condenser and ΔT_{cd} is the average temperature difference along the total effective heat transfer area of the evaporator.

When the logarithmic mean temperature difference approach is applied to Equation (3.3), the heat transfer in the condenser can be modeled using its overall heat transfer coefficient (UA_{cd}) and the logarithmic mean temperature difference ($LMTD_{cd}$) as shown in Equation (3.4).

$$Q_{cd} = UA_{cd} LMTD_{cd} \tag{3.4}$$

where

$$LMTD_{cd} = \frac{T_{lcw} - T_{ecw}}{\ln\left(\frac{T_{lcw} - T_{cd}}{T_{ecw} - T_{cd}}\right)} \tag{3.5}$$

where T_{cd} is the condensing temperature which corresponds to the condensing pressure P_{cd} .

It is worth pointing out that the logarithmic mean temperature difference is originally defined for a single-pass counter-flow heat exchanger without phase change. However, it can be applied to approximate other types of exchangers (McIntosh et al. 2000) without losing much accuracy.

Similarly, the equations for the heat transfer process in the evaporator can be deduced as follows.

$$Q_{ev} = C_{pw} M_{chw} (T_{chwr} - T_{chws}) \tag{3.6}$$

$$Q_{ev} = M_{ref}(h_2 - h_1) \tag{3.7}$$

$$Q_{ev} = UA_{ev} LMTD_{ev} \tag{3.8}$$

$$LMTD_{ev} = \frac{T_{chwr} - T_{chws}}{\ln\left(\frac{T_{chwr} - T_{ev}}{T_{chws} - T_{ev}}\right)} \tag{3.9}$$

where Q_{ev} is the chiller cooling load, M_{chw} is the chilled water mass flow rate, T_{chws} is the chilled water supply temperature, T_{chwr} is the chilled water return temperature, and h_2 and h_1 are specific enthalpies of the refrigerant respectively at state 2 and state 1 in Figure 2.2. UA_{ev} is the overall heat transfer coefficient of the evaporator and T_{ev} is the evaporating temperature which corresponds to the evaporating pressure P_{ev}.

From the above equations, it can be observed that both *UA* and *LMTD* of heat exchangers can reflect the heat transfer efficiency. In this thesis, the *LMTD* is chosen as a performance index to indicate heat transfer side faults, e.g., exchanger fouling, since its calculation is simpler than that of *UA* as the calculation of the latter requires many complicated heat transfer relations.

Mass flow rate of refrigerant

Many centrifugal chillers do not have expansion valves and large-scale centrifugal chillers often use a fixed orifice as the throttling device with no moving part. The conservation of mass for a finite control volume results in a constant refrigerant flow rate along the whole refrigerant circuit at a specific time. Actually, the refrigerant flow rate is to a great extent affected by the pressure difference between the condenser and

evaporator. From Equation (3.6) and Equation (3.7), the refrigerant flow rate can be calculated by Equation (3.10).

$$M_{ref} = \frac{C_{pw} M_{chw} (T_{chwr} - T_{chws})}{h_2 - h_1} \tag{3.10}$$

The refrigerant mass flow rate can be chosen as a performance index to indicate faults which are associated with abnormal pressure difference between the condenser and evaporator, or faults related to refrigerant liquid line.

Polytropic efficiency

As described in ASHRAE (1996), the amount of work required to produce a given pressure rise depends on the efficiency of the compressor and the thermodynamic properties of the refrigerant. For an adiabatic compression process, the work input required, named isentropic work, is a minimum if the compression is isentropic. The ratio of the isentropic work to the actual work is the isentropic efficiency. Due to the thermodynamic properties, a compressor can produce different isentropic results with different refrigerants, and also with the same refrigerant at different suction conditions. Therefore, isentropic efficiency is not consistent enough for the purpose of comparison in FDD. Generally speaking, the compression process in a centrifugal compressor is near a polytropic process (from state 2 to 3 in Figure 2.2), which differs from an adiabatic process (from state 2 to 3′ in Figure 2.2) in that the change of state during it does not take place at constant entropy. Polytropic work is the reversible work required by a polytropic process and is given by Equation (3.11).

$$W_{poly} = \frac{\gamma}{\gamma - 1} P_{ev} v_2 \left[\left(P_{cd} / P_{ev} \right)^{(\gamma-1)/\gamma} - 1 \right] = \left[\frac{P_{cd} v_3 - P_{ev} v_2}{\ln(P_{cd} v_3 / P_{ev} v_2)} \right] \ln\left(P_{cd} / P_{ev}\right) \quad (3.11)$$

where the constant γ is the mean polytropic exponent along the polytropic path. v_2 is the specific volume of refrigerant at the inlet of the compressor and is determined by the compressor suction pressure (approximately P_{ev}) and its corresponding temperature (T_{suc}). v_3 is the specific volume of refrigerant at the outlet of compressor and is determined by the hot gas discharge pressure (approximately P_{cd}) and its corresponding temperature (T_{dis}).

Polytropic efficiency, analogous to the isentropic efficiency, is the ratio of the polytropic work to the actual work consumed, and is given by Equation (3.12).

$$Eff_{poly} = \frac{W_{poly}}{W_{comp}} = \frac{\left[\frac{P_{cd} v_3 - P_{ev} v_2}{\ln(P_{cd} v_3 / P_{ev} v_2)} \right] \ln\left(P_{cd} / P_{ev}\right)}{\left(h_3 - h_2\right)} \quad (3.12)$$

where W_{comp} is the actual power consumed by the compressor.

On the whole, the polytropic work and efficiency are more consistent from one application to another, because a reversible polytropic process duplicates the actual compression between state 2 and 3 in the Figure 2.1 and represents the average stage thermodynamic performance (ASHRAE Handbook, 1996). Therefore, the polytropic efficiency is preferable to isentropic efficiency as a health indicator for the centrifugal compressor. It is sensitive to distortions in the shape of the impeller's blade and base, the shape of vane's blade and base, and any change in surface smoothness during operation.

Drive motor efficiency

As introduced by Jia (2002), the centrifugal compressor is composed of an impeller and inlet vanes. The electric motor in the case of large-scale centrifugal chillers is externally mounted on the compressor. There are two main causes of inefficiencies external to the compressor: electrical degradation (resulting in a lower power factor) and friction losses in the transmission (bearing friction of the shaft, etc.). Other causes of motor degradation include improper motor cooling, inadequate insulation of motor winding, etc. Due to the above causes, just a part of the electricity drawn by the motor is transferred to the compressor and consumed by the compression process there. The ratio of the actual power transferred to and consumed by the compressor to the electric power input to the compressor motor is defined as motor efficiency, as shown in Equation (3.13), and is a good health indicator of the derive motor. It is noteworthy that the motor efficiency is a not constant but is a function of chiller operating conditions, e.g., chiller cooling load.

$$Eff_{motor} = \frac{W_{comp}}{W_{elec}} = \frac{M_{ref}(h_3 - h_2)}{W_{elec}} \tag{3.13}$$

where W_{elec} is the electric power input to the compressor.

Coefficient of performance

The coefficient of performance (*COP*) of a chiller, as shown in Equations (3.14) and (3.15), is often used by chiller manufacturers to provide a chiller's design conditions along with water temperatures and flow rates in their catalogues. The continuously

monitored *COP* provides an overall health indicator that can be sensitive to most component or subsystem faults in chillers.

$$COP = \frac{Q_{ev}}{W_{elec}} \tag{3.14}$$

$$COP = \frac{C_{pw} M_{chw} \left(T_{chwr} - T_{chws} \right)}{W_{elec}} \tag{3.15}$$

For a specific chiller, the *COP* is not a constant during operation but determined by operating conditions of the chillers, e.g., cooling load and entering condenser water temperature.

3.1.2 Rules in Fault Diagnostic Classifier

Once faults are detected according to significantly deviated performance indexes, it is necessary to find the cause of the fault, namely to diagnose the fault. Since different performance indexes are sensitive to different faults, the selection of a certain combination of performance indexes can help identify a particular fault. A fault diagnostic classifier, consisting of a set of rules relating each fault to its impact on each performance index, is constructed for fault diagnosis in this thesis. The set of rules not only can be derived from basic thermophysical principles for chiller systems but also can be examined by using a large number of field and laboratory measurements. As mentioned previously, besides being easily understandable, the fault diagnostic classifier based on the set of rules also has the advantage of being robust because the performance indexes have straightforward physical meaning and can synthesize the information from individual measurements.

Six typical chiller faults (see Table 3.2) are considered in the basic chiller FDD scheme. It is reported that these faults account for a significant part of the service calls made according to the survey conducted by Comstock and Braun (2002). In this regard, selecting these faults is of great practical significance.

Each of the faults results in a different combination of changes in performance indexes. The rules relating the above six faults to their impacts on the six performance indexes are listed in Table 3.2. In the table, "—" indicates that no discernible trend is found in a performance index. The sign "▼" indicates the performance index decreases when the severity of a fault increases. The sign "▲" indicates that the performance index increases when the severity of a fault increases. For instance, condenser fouling generally causes the logarithmic mean temperature difference of the condenser ($LMTD_{cd}$) to increase above its normal value and the refrigerant flow rate (M_{ref}) and chiller efficiency (COP) decrease below their normal values. The signs in the brackets "( )" describe the trends when an expansion valve is stalled and functions well in the chiller. The expansion valve in the centrifugal chiller tends to compensate for the adverse effects of some faults on the performance indexes, and then makes their residuals less noticeable. However, centrifugal chillers using a fixed orifice as the expansion device would exhibit earlier and more significant residuals of performance indexes than those using an expansion valve. Hence, this issue is worth attention when constructing a fault diagnostic classifier for chillers with different expansion devices.

Table 3.2 Rules in fault diagnostic classifier for centrifugal chillers

Fault Types	$LMTD_{ev}$	$LMTD_{cd}$	M_{ref}	Eff_{poly}	Eff_{motor}	COP
Evaporator fouling	▲	—	—	—	—	▼
Refrigerant leakage	—	▼	▼ (—)	—	—	▼ (—)
Excess oil	—	—	—	—	▼	▼
Condenser fouling	—	▲	▲ (—)	—	—	▼
Non-condensables in refrigerant	—	▲	—	—	—	▼
Degradation of compressor	—	—	—	▼	—	▼

The rules in Table 3.2 can be interpreted as follows.

- Evaporator fouling increases the evaporator water temperature difference and therefore increases the logarithmic mean temperature difference of the evaporator, $LMTD_{ev}$. Since the expansion valve attempts to keep evaporator pressure and temperature nearly constant, their decreases are slight. Also, a reduced *COP* is expected for this fault due to the irreversible energy loss resulting from the increased $LMTD_{ev.}$
- Refrigerant leakage is inherently associated with the chiller for its whole service life. Refrigerant leakage results in lower refrigerant flow rate, M_{ref}, and smaller logarithmic mean temperature difference of the condenser, $LMTD_{cd}$, because less refrigerant in the system tends to reduce the condenser pressures and condensing temperatures. Nevertheless, for a chiller with an expansion valve, the valve is able to compensate for the reduction of refrigerant flow by opening further until it cannot compensate any more. Thus, the change in the refrigerant flow rate is very slight

when the expansion valve functions well. Due to the smaller $LMTD_{cd}$ and the decrease of throttling effect on the whole refrigeration cycle, a small increase of *COP* may be observed if the expansion valve is still capable of fulfilling its duty well. A chiller using a fixed orifice as the expansion device would suffer such penalties as reductions of M_{ref} and *COP* earlier than that using an expansion valve.

- Excess oil can not affect the refrigeration system thermodynamically since in the centrifugal chiller the refrigerant cycle is independent from the oil cycle. Therefore, excess oil simply fills up the compressor cavity and submerges some of the gearing. The viscous effects caused by the excess oil lead to increased mechanical losses in the compressor. Consequently the motor efficiency, Eff_{motor}, which is the ratio of the power consumed by the compression process to the electric power consumed by the motor, will decrease. At the same time, *COP* will also decrease due to the increased mechanical losses.
- Condenser fouling is equivalent to having a smaller condenser and larger heat resistance between the water and the refrigerant, resulting in higher condensing temperatures and pressures. The difference between the entering condenser water temperature and the condensing temperature become larger at the inlet, when the entering condenser water temperature holds constant. Therefore, $LMTD_{cd}$ may increase. Such an increase in temperature difference results in more irreversible energy loss and subsequently makes *COP* decrease. For a chiller with a fixed orifice, M_{ref} will increase due to a larger pressure difference between condenser and evaporator. In contrast, an expansion valve in a chiller tends to compensate for the increase of refrigerant flow rate, up to a point where the valve can not open further.
- Non-condensable gases settle in the condenser during operation and make the condenser pressure increase substantially. If the acquisition of condensing

temperature is calculated from measured condenser pressure, the derived condensing temperature is higher than the actual value, thus causing $LMTD_{cd}$ to be extraordinarily overstated. If the condensing temperature is measured by a thermistor, no significant change will be observed in $LMTD_{cd}$ as this fault has little impact on the condensing temperature. As the amount of non-condensables in the system increases, the pressure lift across the compressor becomes higher and requires more electric power input, which inevitably decreases *COP*.

- Degradation of compressor as mentioned before is due to distortions in the shape of the impeller's blade and base, the shape of vane's blade and base, and any change in surface smoothness during operation. It will inevitably lower the polytropic efficiency of the compressor, Eff_{poly}, and the chiller *COP*. This fault does not have any influence on the other performance indexes.

3.1.3 Reference Models of Performance Indexes

Reference models of the six performance indexes are used to characterize the fault-free operation of a chiller system under certain operating conditions, namely to generate benchmark values for the performance indexes. Therefore, the identification of an accurate reference model of chiller performance indexes is a fundamental issue in model-based FDD applications. As mentioned in Chapter 1, in the HVAC&R field, a great amount of effort has been devoted to developing proper chiller models used in optimal control, efficiency monitoring and FDD. Among these models, physical models, e.g., ASHRAE primary toolkit model (Bourdouxhe et al. 1997), only have advantages when detailed information of the target system is available, and therefore is difficult to calibrate. Semi-physical models for centrifugal chillers are among the top priorities. A

chiller model is called semi-physical when that model is derived from a certain amount of physical knowledge and is expressed in terms of one or more regressors (predictor variables) and a set of coefficients.

Assuming constant water flow rate in evaporator and condenser, chiller performance is primarily a function of three variables, i.e., the chiller cooling load, the entering condenser water temperature and chiller water supply temperature (Gordon et al. 1995, Braun 1988 and PG&E 2001). In other words, these three variables are the determinant variables of a chiller system. Moreover, catalogue data of most centrifugal chiller products are usually provided on the basis of the cooling load, the entering condenser water temperature and the chilled water supply temperature. Therefore, polynomial regression models using the three variables as regressors are given great preference and hereby investigated.

In this study, a simple chiller model is presented as shown in Equation (3.16). The mean and variance of the error term, ε, are assumed to be 0 and σ^2 respectively (i.e. $\varepsilon \sim$ N (0, σ^2)) (Montgomery and Runger 1994).

$$\begin{aligned} Y &= f(Q_{ev}, T_{chws}, T_{ecw}) + \varepsilon \\ &= b_0 + b_1 T_{chws} + b_2 T_{ecw} + b_3 Q_{ev} + b_4 T_{chws} T_{ecw} + b_5 T_{chws} Q_{ev} + b_6 T_{ecw} Q_{ev} + b_7 Q_{ev}^2 + \varepsilon \end{aligned} \tag{3.16}$$

The outputs of the polynomial regression models, namely the response variables *Y*, are assigned to the performance indexes (i.e., $LMTD_{ev}$, $LMTD_{cd}$, M_{ref}, Eff_{poly}, Eff_{motor}, COP). The models are expressions for chiller performance indexes as a function of the cooling load (Q_{ev}), the chilled water supply temperature (T_{chws}) and the entering condenser water temperature (T_{ecw}). As for model order, generally speaking, higher order polynomial models provide better fits to the data, but the fit is not smooth between the points used by the regression analysis. Therefore, the primary goal is to find the lowest order model with

satisfactory accuracy. Equation (3.16) is a second order model and the validity this model will be investigated later in Chapter 5.

In particular, such a reference model with only three regressors has a great advantage of being less susceptible to sensor faults as compared with a mechanistic model with many inputs. Since the there are three inputs in the reference model of each performance index, sensor faults, if not affecting these three regressors, will not affect the accuracy of the output of the reference model.

These regressors are important for chiller plant control and monitoring and commonly available on BMSs or chiller control panels. The coefficients ($b_0 \cdots b_7$) are assumed to be constants, which can be found by linear regression techniques using data indicative of chiller normal operation.

3.2 Online Adaptive Estimator of Fault Detection Threshold

Due to unavoidable errors associated with both sensor measurements and model fitting errors, even in the case of fault free operation, there are always residuals between the predicted performance indexes and those which are calculated online. The determination whether the residuals of a performance index deviate from its benchmark value by an allowable amount, called the fault detection threshold in the FDD field, is what FDD decisions rely on. An online adaptive estimator of fault detection threshold is formulated in this section on the basis of evaluating the uncertainty resulting from the fitting errors of the reference models as well as the propagation of measurement errors through the mathematical formulas of the performance indexes shown in Table 3.1.

The fault detection threshold is in practice determined by the calculation uncertainty of a residual at specific operating conditions. Since the residual is the difference between the observed (calculated) value and the model predicted value of a performance index, the residual uncertainty is subject to both the calculation uncertainty of the performance index and the modeling uncertainty of the reference model of the performance index. These two kinds of uncertainty are all affected by operating conditions, such as the cooling load and the chilled water and cooling water temperatures of a chiller system, in addition to measurement errors. Therefore, given a fixed confidence level, thresholds on the residuals of performance indexes will vary with operation conditions.

At a specific operating condition, the modeling uncertainty results from measurement errors associated with the model development data as well as errors arising from an imperfect mapping between the inputs and the outputs (Breuker and Braun 1998). The calculation uncertainty comes from the measurement error propagation. Measurement errors result from sensor faults, i.e., noise errors and bias errors. The threshold for the residual of a performance index can be estimated online by its uncertainty at a certain confidence level, as shown in Equation (3.17).

$$\begin{aligned} Th_{0,i} &= U(\tilde{r}_i) \\ &= t_{\alpha/2,n-p}\tilde{\sigma}_{\tilde{r}_i - r_i} \end{aligned} \tag{3.17}$$

where $Th_{0,i}$ is the threshold of the ith performance index, $\tilde{r}_i$ is the estimator of the residual of the ith performance index. The residual (r_i) is the difference between the observed value and model predicted value of the ith performance index. $U(\tilde{r}_i)$ is the uncertainty of the residual at a certain confidence level. $\tilde{\sigma}^2_{\tilde{r}_i - r}$ is determined by Equation (3.18) and $t_{\alpha/2,n-p}$ is the value of the t distribution with n-p degrees of freedom at a

confidence level of (1-α). n is the number of data points used in the model regression and p is the number of coefficients estimated from the data.

$$\tilde{\sigma}^2_{\tilde{r}_i - r_i} = \underbrace{\sum_j \left[\left(\frac{\partial g_i}{\partial z_j} \right) \sigma_{z_j} \right]^2}_{\textit{Uncertainty 1}} + \underbrace{\tilde{\sigma}^2_{Y_i} [1 + \mathbf{X}_0^T (\mathbf{X}_{reg}^T \mathbf{X}_{reg}) \mathbf{X}_0]}_{\textit{Uncertainty 2}} \tag{3.18}$$

where g_i is the formula for calculating the ith performance index. z_j is the jth element in the vector of measured variables (**z**), which is used to calculate the ith performance index (Y_i). σ_{z_j} is the standard deviation of z_j and $\tilde{\sigma}^2_{Y_i}$ is the estimated variance of the regression error of the ith performance index. $\mathbf{X}_0$ is the vector of regressors for the current prediction and $\mathbf{X}_0^T$ is the transpose of $\mathbf{X}_0$. $\mathbf{X}_{reg}$ is the matrix of regressors associated with the model development data and $\mathbf{X}_{reg}^T$ is the transpose of $\mathbf{X}_{reg}$.

The detailed derivation of Equation (3.17) and Equation (3.18) is given in Appendix A.

In the Equation (3.18), *Uncertainty 1* presents measurement uncertainty and *Uncertainty 2* represents modeling uncertainty. Also, it is very clear from Equation (3.18) that the residual uncertainty of a performance index, at a certain confidence level, varies with operation conditions in addition to magnitudes of random measurement errors.

3.3 Implementation Structure of Basic Chiller FDD Scheme

The implementation structure of the basic chiller FDD scheme, as illustrated in Figure 3.1, includes two groups of tasks, one for reference model development and the other for

online fault detection and diagnosis. The reference model development must be accomplished ahead of the online FDD application.

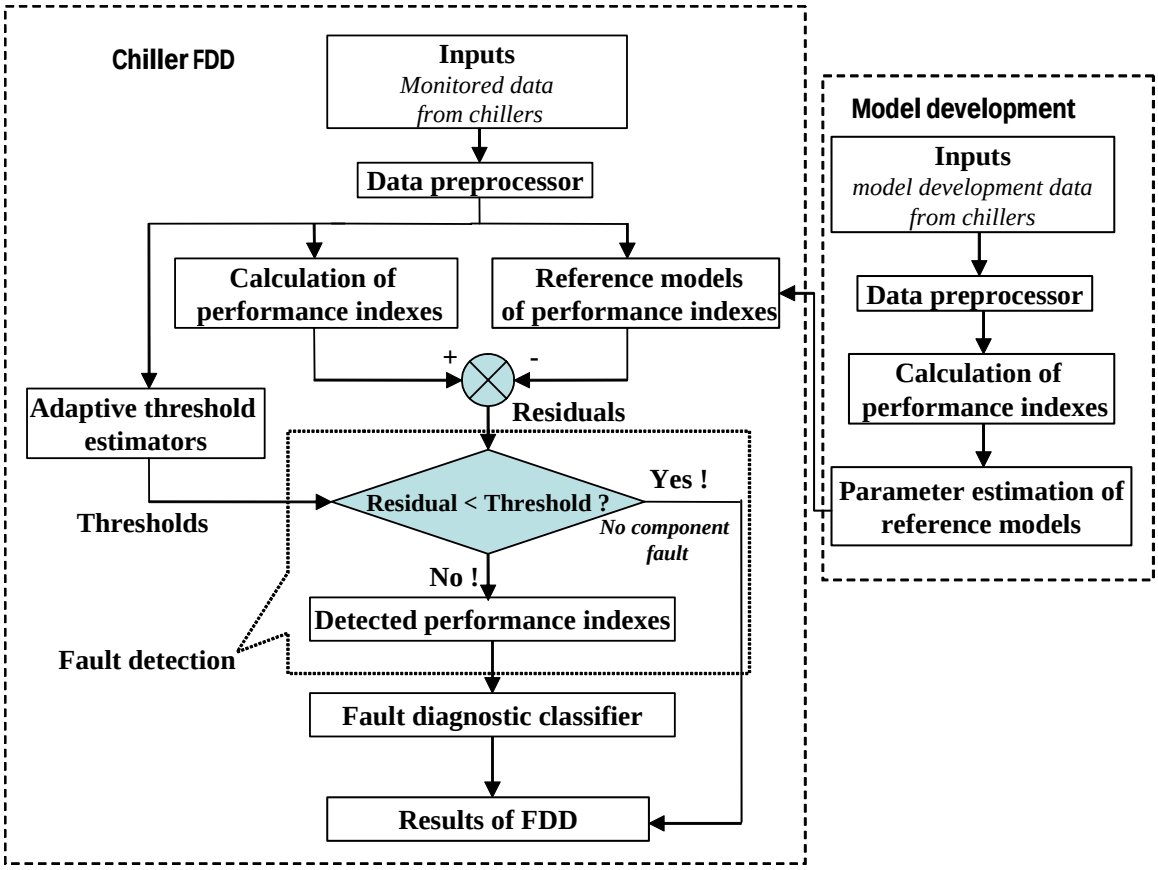

Figure 3.1 Flow chart of the basic chiller FDD scheme

3.3.1 Data Preprocessing

It is evident from Figure 3.1 that there are two sets of data used in the implementation of the developed basic chiller FDD scheme. One set is collected from chillers under normal operation. These data can be regarded as fault free ones and will serve as the model development data of each performance index. The other set is the monitoring data that is processed by the basic chiller FDD scheme to detect and diagnose faults. The quality of both the model development data and the monitored data determines the accuracy and sensitivity of the FDD scheme. Usually data acquisition systems collect one set of data

from every sensor and transducer at an adjustable interval, e.g., ten seconds or two minutes. The collected data, called raw data, contains data representing both transient and steady-state operation, as well as erroneous data. Since the proposed reference models of performance indexes and the fault diagnostic classifier are both based on the steady state operation of centrifugal chillers, a data preprocessor, including three sub-preprocessors, i.e., *a basic validity check, a steady-state filter*, and *an outlier detector*, is needed to ensure that steady-state and reliable data are fed into the FDD system. These three sub-preprocessors perform in parallel, as shown in Figure 3.2.

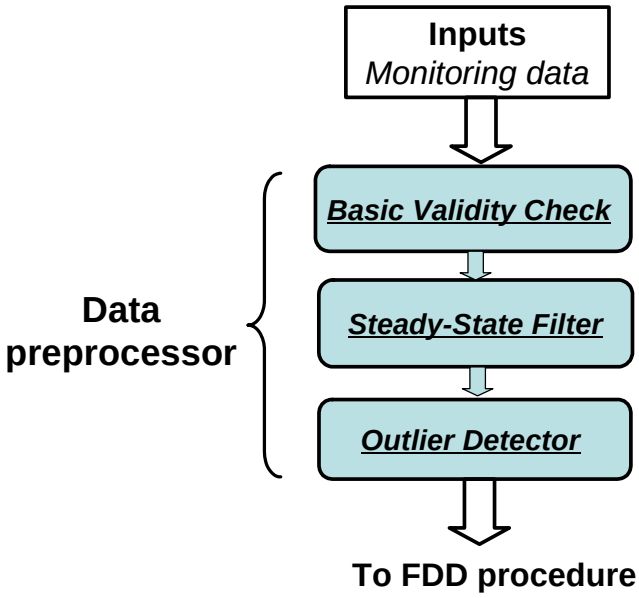

Figure 3.2 Schematic diagram of the data preprocessor

Basic validity check

Basic validity check employs fundamental thermophysical concepts to validate incoming data. In water-cooled centrifugal chillers, magnitudes of each temperature measurement

and pressure measurement should be subject to some physical laws. It is expected that the seven temperatures and the two pressures obey the following two simple relationships respectively:

$$0<T_{ev}< T_{chws} < T_{chwr} < T_{lcw} < T_{ecw} < T_{cd} < T_{dis}$$

$$0<P_{ev}<P_{cd}$$

The two rules were programmed to integrate with the other two data sub-preprocessor programs to floating errors and those associated with sampling timing.

Steady-state filter

As for centrifugal chillers, especially those in large buildings, the fluid flow and heat transfer dynamics are, in general, much faster than the dynamics of the cooling load and ambient conditions which are the main driving forces of the chiller subsystem. This makes the chillers stay in quasi-steady-state operation for large portions of their operating time. Therefore, it is reasonable to consider steady-state operation during FDD. However, during start-up and shut down time periods or when the driving conditions change abruptly, the chillers experience substantial transients and the steady-state assumption does not hold. Thus, all data within a one-hour period after the chillers were started or shut down are excluded from any subsequent analysis. In addition, a steady-state filter is needed to filter out data indicative of transients during operation.

Selecting or defining the quantities capable of indicating existence or occurrence of transients is an important issue for detecting steady-state operation of the chiller. Usually, some thermophysical variables such as temperatures and flow rates are selected as state

characteristics to fulfill the task. There are many classic steady-state filters measuring the change rate of a variable with respect to time. Among them, the method that estimates the variance of samples of a variable over time using a fixed moving time window length is the most popular one. Another method linearly regresses samples of a variable using the OLS (Ordinary Least Squares) method with a fixed moving time window length, and then obtains the slope of the regression line, which can also indicate the change rate of the variable. These two methods and others are summarized by Glass et al. (1996).

The latter was recommended by (Rossi 1995) and is used in this thesis to construct a steady-state filter. Theoretically, only when all variables do not change significantly over a certain period of time, can it be concluded that the chiller is under steady-state operation. However, only three variables, i.e., the chilled water supply temperature (T_{chws}), the chilled water return temperature (T_{chwr}) and the entering condenser water temperature (T_{ecw}) are selected as the state characteristics. The reason behind this is that these three state characteristics, as mentioned in the previous chapter, are the deterministic variables for the performance of a chiller with constant water flow rates. The chiller might be thought to be under steady-state operation if all the linearly regressed slopes of these three variables do not exceed their corresponding threshold values, which are respectively determined by the measurement accuracy of each variable.

Outlier detector

Outliers in measurements are those with abnormal values, such as frozen readings or those significantly deviated from the normal. Existence of outliers has a negative effect on the data analysis in the FDD and monitoring of chillers. Actually, the steady-state filter based on the estimate of moving slopes can help detect and remove part of the

outliers, but the effect is not very desirable. A method based on estimating the mean and variance of samples of a variable over time using a fixed moving time window is adopted in this thesis to detect outliers. After a data point passes the steady-state filter, its value will be compared with the estimated mean value. If its value is more than the estimated mean value by three times of the estimated variance, the data point will be disposed of as an outlier.

3.3.2 Reference Model Development

During reference model development, the data from an actual system under normal operation are used to estimate the model parameters by means of proper statistical techniques. In this thesis, the coefficients of the linear polynomial regression model in Equation (3.16) are estimated by the OLS method using model development data obtained from a centrifugal chiller under normal operation. The OLS method and issues concerning its application to chiller data are described as follows.

Let **X** be the matrix containing the regressors as row vectors. After adopting matrix notation, the linear polynomial regression model in Equation (3.16) can be rewritten as follows.

$$\mathbf{Y} = \mathbf{X}\mathbf{b} + \mathbf{e} \tag{3.19}$$

where **Y** is the vector of response variables, **b** is the vector of regression coefficients ($\mathbf{b}=[b_1,b_2,b_3,b_4]^T$), and **e** is the error term, i.e., the variation in **Y** unexplained by **X** and **b**, which include both measurement errors and model error in both **X** and **Y**(Corcoran and Reddy 2003).

The OLS method is the best estimation technique to use when there is no error in measurement, when there is no collinearity between regressors, when the model residuals have constant variances, and when the errors are normally distributed (Beck, J.V. and K.J. Arnold, 1977). In this case, the coefficient vector is determined such that the sum of the error squares function reaches its minimal value. This results in the system of normal equations on the condition that the matrix ($\mathbf{X}_{reg}$) is not singular (Draper and Smith, 1981), as shown in Equation (3.20).

$$\mathbf{b}_{OLS} = (\mathbf{X}_{reg}^{T}\mathbf{X}_{reg})^{-1}\mathbf{X}_{reg}^{T}\mathbf{Y}_{reg} \tag{3.20}$$

where $\mathbf{b}_{OLS}$ is the OLS estimate of $\mathbf{b}$, $\mathbf{X}_{reg}$ is the matrix of regressors associated with the model development data, and $\mathbf{Y}_{reg}$ is the vector of response variables associated with the model development data.

Problems associated with model under-fitting and over-fitting are usually the result of a failure to identify the nonrandom pattern in time series data (Reddy and Andersen 2002). Under-fitting does not capture enough of the variation in the response variable for the corresponding set of regressors to provide an explanation. Over-fitting means including measurement randomness or some regressors which do not contribute to the variation in the response variables in the model.

Since the data from an actual chiller system are used to carry out parameter estimation using the OLS method, it is favorable that each data set can help reduce the uncertainty in the parameter estimate vector $\mathbf{b}_{OLS}$ given by Equation (3.20). However, collecting more data for parameter estimation does not ensure that the data can result in a more accurate estimate of $\mathbf{b}$. Corcoran and Reddy (2003) recommended that it is best to select regressor

values spread uniformly and over the entire range of variation if the model is only approximately linear.

3.3.3 Online FDD

The procedure of online FDD application comprises a data preprocessor, a set of reference models with three regressors, an online threshold estimator and a fault diagnostic classifier, as shown in Figure 3.1. The data preprocessor handles the monitored data and feeds the processed monitoring data to the next procedure. Calculated residuals of performance indexes are compared with their corresponding thresholds to detect abnormalities in the chiller. Using the deviation pattern of the six performance indexes, the fault diagnostic classifier could determine the existence of a fault and furthermore find out where and what the fault is.

Fault detection

Once a set of data passes through the steady-state filter, all performance indexes at this sampling instance will be calculated. Meanwhile the benchmarks of the performance indexes are also predicted by their corresponding reference models. Thus the residual for each performance index is generated by comparing the measured value with its benchmark. Each residual is compared with its threshold updated online according to the ever-changing operating conditions such as chiller cooling load and water temperatures. When the residuals of one or more performance indexes are larger than their thresholds, the chiller system is considered to be faulty.

Fault diagnosis

Fault diagnosis is performed using a fault diagnostic classifier, which is based on the set of rules (see Table 3.2) and built in the form of a simple expert system. As soon as faulty operation of the chiller is detected, the diagnostic classifier evaluates the probability that each chiller fault applies to the current deviation pattern of the performance indexes. In this thesis, a result of fault diagnosis is only considered valid in the event that the fault probability ratio (Breuker and Braun 1998), namely the ratio of the probability of the most likely chiller fault to that of the second most likely chiller fault, is greater than a specified value. After a chiller fault is identified, a chiller fault alarm will be raised. Furthermore, proper suggestions and recommendations regarding systems maintenance could be provided on the basis of the identified faults.

3.4 Summary

This chapter presents a model-based basic chiller FDD scheme to tackle chiller faults in centrifugal chillers.

The scheme is developed based on six performance indexes that have great physical meaning. These six performance indexes have the capability of describing health conditions of centrifugal chillers and thus accounting for some chiller faults. A set of generic rules relating chiller faults to their impacts on the performance indexes are deduced from theoretical analysis. The fault diagnostic classifier based on the set of rules can help consolidate a great amount of measurement information into a clear and coherent picture of equipment status, and therefore is simpler and more effective than those using impacts of faults on numerical values of individual measurements. The

benchmarks of the performance indexes are provided by a set of simple reference models in the form of polynomial regression equations with only three regressors (i.e., the chiller cooling load, the entering condenser water temperature and the chilled water supply temperature). Fewer regressors in the reference model make it less susceptible to measurement errors as compared with a mechanistic model with many inputs. Moreover, the model parameter estimation is convenient and time-saving because it employs a simple fitting technique, i.e., OLS method.

In particular, an online adaptive estimator of fault detection threshold is developed, by analyzing uncertainty coming from both model-fitting errors and measurement errors (sensor noise errors), to scientifically determine thresholds for detecting abnormal performance indexes. This adaptive FDD threshold estimator has great potential to help operators and engineers identify chiller faults promptly while eliminating as much false alarms as possible. With regard to the online implementation of the basic chiller FDD scheme, a data preprocessor consisting of three subprograms is developed and employed to get rid of undesirable data in the collected data.

However, what needs to be pointed out is that the basic chiller FDD scheme can only tackle faults at the level of chiller components but not sensor faults such as sensor bias errors. All sensors involved in the FDD are assumed to be free from abnormality except noise error. The bias errors associated with sensors in a typical centrifugal chiller will be tackled by the sensor FDD&E scheme which will be developed in Chapter 6. The basic chiller FDD scheme developed in this chapter will be validated in Chapter 5 using both laboratory data provided by an ASHRAE research project and field data collected from the chiller plant in a real building in Hong Kong.

CHAPTER 4 TEST FACILITIES

In this thesis, chiller data from two test facilities are employed to validate the basic chiller FDD scheme, the sensor FDD&E scheme and the robust FDD strategy developed in this study. The two test facilities are a laboratory centrifugal chiller used in a research project sponsored by ASHRAE, and a centrifugal chiller plant in a real building in Hong Kong, respectively. The chapter briefly introduces these two test facilities. The full name of the research project is "Fault Detection and Diagnostic (FDD) Requirements and Evaluation Tools for Chillers" referred to as ASHRAE 1043-RP in this thesis.

Section 4.1 describes the centrifugal chiller test stand which is developed and used in the laboratory study in ASHRAE 1043-RP. The test stand produced a database of laboratory measurements for normal (fault-free) operation and a number of chiller faults at various operating conditions. All chiller faults were tested at different levels of severity to produce a database, which can be used to evaluate the sensitivity and accuracy of FDD methods for chillers. Section 4.2 introduces the centrifugal chiller plant in a real commercial building in Hong Kong. The chiller data retrieved from its BMS over a period of time will be used in the validation tests in this thesis. The summary of this chapter is given in Section 4.3.

4.1 Laboratory Centrifugal Chiller in ASHRAE 1043-RP

ASHRAE 1043-RP is the first phase of a three-phase research project, which was initiated by ASHRAE in 1998 to address the need for a comprehensive study of

automated diagnostics for chillers. During the development of automated FDD for chillers, one of the biggest barriers is the lack of data containing typical chiller faults as it is difficult to find a chiller on which a number of fault tests are allowed to be carried out. The primary objective of ASHRAE 1043-RP is to produce a database of measurements of a chiller under various chiller-fault conditions as well as various operating conditions. Since the laboratory chiller is representative of many chillers in service today, the database can be used in the development and evaluation of FDD methods applied to chillers. According to the report from Comstock and Braun (1999), the laboratory work is a great improvement over previous research efforts in one or more of the categories listed below:

- The faults were introduced at multiple levels of severity as well as at different operating conditions;
- A wide variety of chiller faults were studied;
- A complete suite of sensor data was collected from the chiller at a sampling rate that permits transient analysis;
- The test unit was representative of a typical building chiller installation.

4.1.1 Description of Test Stand

As presented by (Comstock and Braun 1999), a 90-ton (316kW) centrifugal chiller in the test stand is loaded by a hot water loop as a simulated building. The centrifugal chiller is small enough for indoor laboratory test with a nearly constant ambient temperature of 72 ^{o}F (22 ^{o}C) while being representative of centrifugal chillers used in most applications.

The design of the test stand can satisfy the specifications of ARI Standard 550/590 (ARI

2003) for centrifugal and rotary screw water-cooled packages. The refrigerant flow circuit in the chiller is essentially the same as the centrifugal chiller system introduced in Chapter 2. Internal chiller controls, e.g., capacity control and condenser water temperature control, are realized by the onboard chiller controller, namely, a MicroTech controller in the test stand. In addition, power consumption to the compressor can be artificially restricted by the MicroTech controller, which in turn inhibits the opening of the vanes, and can cause the chiller to be unable to meet the chilled water setpoint unless the load is reduced. Figure 4.2 depicts the important equipment contained within the chiller test facility and indicates their approximate relative locations. The abbreviation 'HX' in the figure stands for 'heat exchanger'.

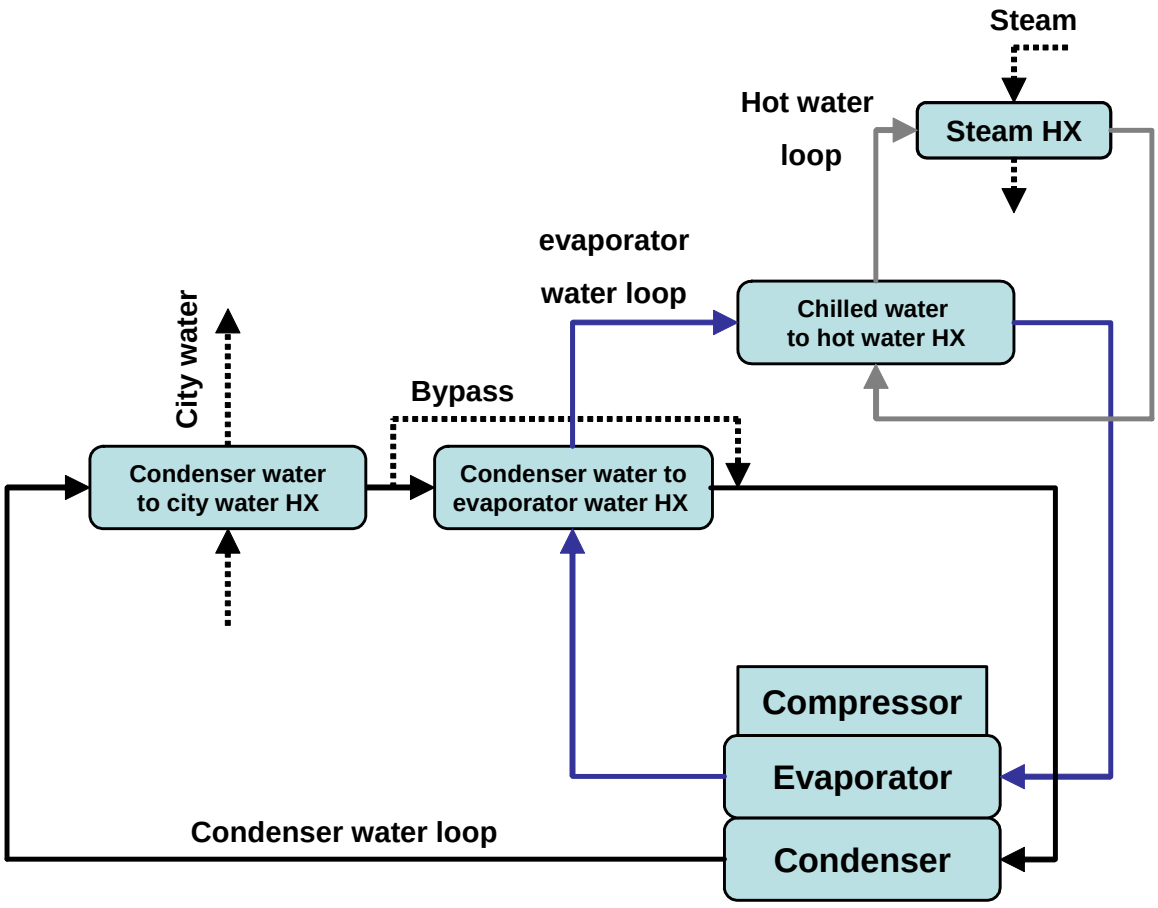

Figure 4.1 Schematic diagram of the laboratory chiller test layout

4.1.2 Instrumentation of Test Stand

A comprehensive suite of sensor information is collected by the MicroTech controller mounted on the chiller as part of its typical installation package. Data are relayed to the PC from the MicroTech controller through a RS-232 connection. The test stand is controlled by a group of three Johnson Controls Inc. Air Handling Unit (JCI AHU) controllers on RS-485 network, which in turn is connected to the PC via a RS-485 to RS-232 converter as shown in Figure 4.2.

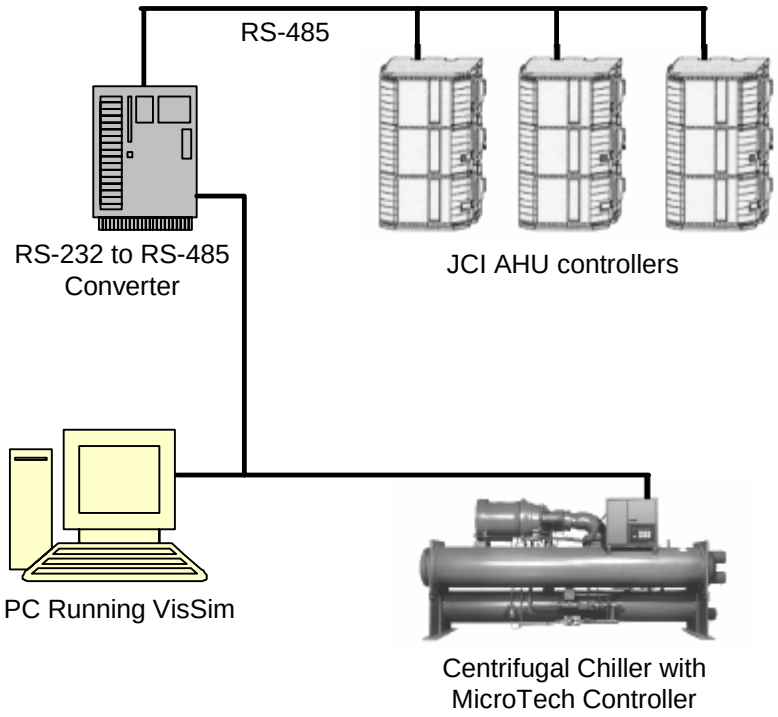

Figure 4.2 Schematic diagram of chiller test stand and its control interface

Both the MicroTech and JCI AHU controllers are interfaced on the PC via VisSim - a visual simulation software package with customizable features that allow various communication protocols to be enabled simultaneously. The program developed within

VisSim collects all the data gathered by the two controllers and exports it to a tab delimited text file. This program also imports data used to automatically control the test sequence and operating conditions. VisSim samples the data at a 10-second interval and makes control adjustments. Table 4.1 gives the consolidated data set of the key variables along with their measurement uncertainties. Detailed information is available in the report presented by Comstock and Braun (1999).

Table 4.1 Listing of key measured and calculated variables with corresponding absolute uncertainties.

Designation	**Source**	**Uncertainty**
$T_{chws,set}$	MicroTech	±0.03 ^{o}C
T_{chwr}	MicroTech	±0.11 ^{o}C
T_{chws}	MicroTech	±0.11 ^{o}C
T_{ecw}	MicroTech	± 0.11 ^{o}C
T_{lcw}	MicroTech	±0.11 ^{o}C
W_{elec}	JCI AHU	±1.8 kW
M_{cw}	JCI AHU	±0.1767 GPM
M_{chw}	JCI AHU	±0.1388 GPM
T_{ev}	MicroTech	± 0.17 ^{o}C
P_{ev}	MicroTech	± 2.067 kPa
T_{cd}	MicroTech	± 0.17 ^{o}C
P_{cd}	MicroTech	±3.445 kPa
T_{sub}	MicroTech	±0.3 ^{o}C
T_{suc}	MicroTech	±0.11 ^{o}C
T_{dis}	MicroTech	± 0.11 ^{o}C

4.1.3 Test Sequence Matrix

Soon after commissioning the chiller test stand, tests were run at various temperature and loading extremes to determine the operating envelope of the chiller. In order to follow ARI Standard 550 and still operate in the safe operating range of the centrifugal chiller, chilled water temperatures were controlled to be 40° F, 45° F, and 50° F (4.4 °C, 7.2 °C and 10 °C), which could be easily achieved. At the same time, the entering condenser water temperatures were controlled between 60° F (15.6 °C) and 85° F (29.4 °C) . The cooling load of the chiller ranged from 25% to 100% of the rated cooling capacity.

Since fault testing relies on comparisons of different test runs, the test sequence was constructed in a manner that was consistent for all the faults tested. That is to say once the test sequence was selected, it was kept unchanged for all the tests performed later. The three control variables chosen were *the chilled water supply temperature (T_{chws}), the entering condenser water temperature (T_{ecw}), and the chiller cooling load (Q_{ev}).* Using these three variables each at three levels resulted in a 3x3x3 test matrix of 27 different tests for each fault level.

A steady state is usually reached within 5 to 15 minutes after a change in operating setpoints. Changes in the chilled water setpoint led to the slowest response to reach steady state; therefore, the test matrix was designed so that this variable was changed the least frequently. Each of the 27 tests was allowed at least 30 minutes to reach steady state, with 45 minutes being allocated to those tests where the chilled water setpoint was changed. This provided between 15 and 25 minutes of steady state operation for each test case. Results of an actual test run at normal (fault free) conditions are shown in Figure 4.3, where the sampling interval is 2 minutes.

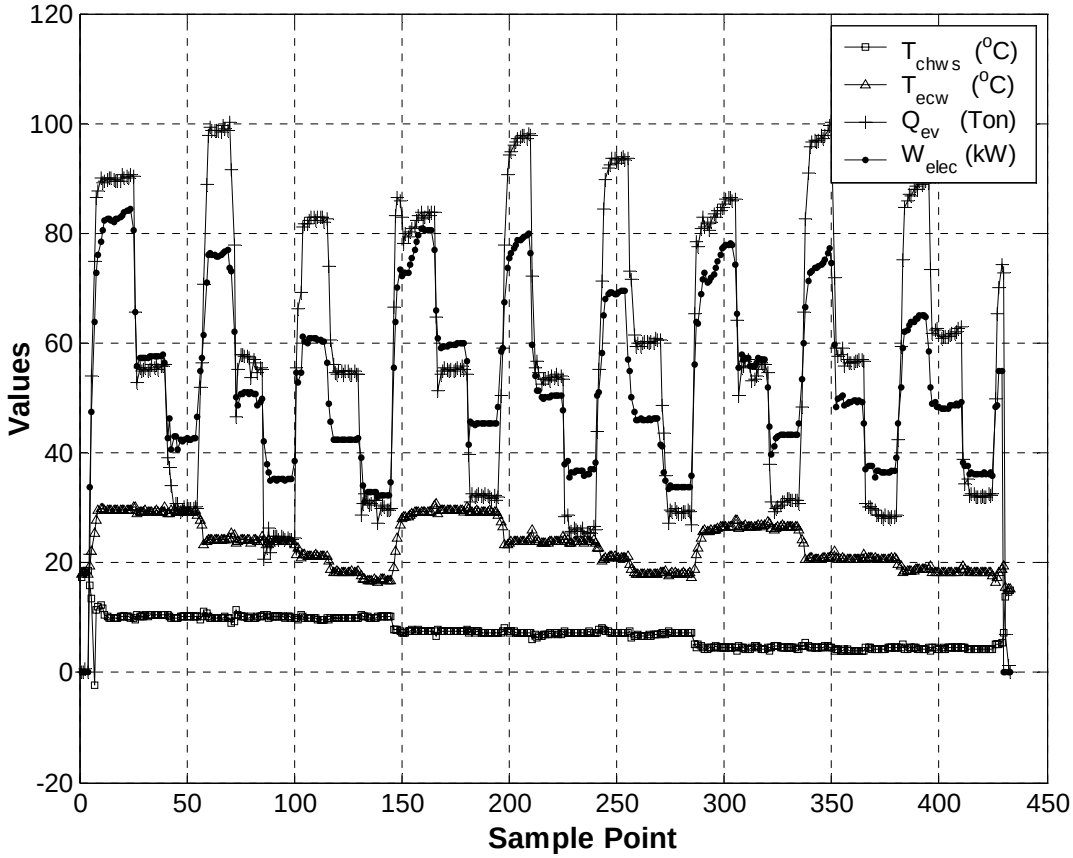

Figure 4.3 Data from an actual test run meeting all 27 operating conditions

4.1.4 Fault Tests

This subsection presents the faults are tested and how they are simulated in the test stand. Table 4.2 gives the different faults tested and the levels of severity of each fault. The tests of the five types of fault which were identified in the fault survey in Chapter 1 are presented in this section, although a total of 8 types of fault were investigated in ASHRAE 1043-RP. Among these faults, refrigerant leakage was simulated by removing known amounts of refrigerant from the refrigerant circuit. Excess oil was simulated by adding known amounts of oil to the centrifugal compressor. Condenser fouling was

obtained by blocking known numbers of tubes in the condenser. Non-condensables in the refrigerant were simulated by adding nitrogen to the refrigerant circuit. The refrigerant overcharge fault was not on the fault survey, but it was tested since it is a fault that can theoretically occur due to improper servicing. In order to compare normal tests with corresponding fault tests, the normal tests were implemented before each group of fault tests. Among these normal tests, the first test, described as the "Normal Test" where all operating conditions were met was selected in the thesis as the benchmark test for comparison. If a fault test did not satisfactorily meet the test conditions, the test would be repeated. It is worth pointing out that the excess oil and non-condensable gases in refrigerant were the only two faults that could not be quantified precisely. Although the excess oil added to the refrigerant circuit could be accurately measured, the nominal amount of oil in the circuit is difficult to quantify since it is impossible to drain all the oil from the compressor. The amount of non-condensables in refrigerant could be calculated. However, the calculation uncertainty was rather high since there was rather small amount of nitrogen existing in the system, e.g., about 0.23 kg nitrogen even at the worst fault level.

4.1.5 Normal Tests

Since fault detection is based on comparison, all the data from each fault test would be meaningless without normal (fault free) data taken from a benchmark test, where no fault was present. In addition, many FDD methods also need normal data for model training. A group of normal tests are recommended in ASHRAE 1043-RP for benchmark tests. Two normal tests, described as "Normal" and "Normal NC" respectively, are selected in this thesis as two benchmark tests for comparison.

Table 4.2 Characterization of Tests of chiller faults

Fault	Simulation approach	Nominal Value	Level 1	Level 2	Level 3	Level 4
Refrigerant leak	Reducing charge	300lb (136kg)	10% reduction in charge (270 lbs)	20% reduction in charge (240 lbs)	30%reduction in charge (210 lbs)	40% reduction in charge (180 lbs)
Refrigerant overcharge	Increasing charge	300lb (136kg)	10% increase in charge	20% increase in charge	30% increase in charge	40% increase in charge
Excess oil	Increasing oil	22lb(10kg)	14% increase in charge (25 lbs)	32% increase in charge (29 lbs)	50% increase in charge(33 lbs)	68% increase in charge (37 lbs)
Condenser fouling	Blocking condenser tubes	164 unblocked tubes	12% reduction in tubes (20 blocked tubes)	20% reduction in tubes (33 blocked tubes)	30% reduction in tubes (49 blocked tubes)	45% reduction in tubes (74 blocked tube)
Non-condensables	Adding nitrogen	No Nitrogen	0.10 pounds (1.0%)	0.16 pounds (1.7%)	0.22 pounds (2.4%)	0.54 pounds (5.7%)

4.2 Centrifugal Chiller Plant in a Real Building in Hong Kong

In order help push the FDD technology closer to field application, chiller data from a chiller plant in a real building is also needed to validate the developed FDD schemes/strategy in this thesis. The second test facility introduced in this chapter is the chiller plant of the central cooling system in a real building in Hong Kong. The building is a twin tower office complex with a total gross floor area of 116,000 square meters in Taikoo Place, a famous grade A office district on Hong Kong island. It consists of Hong Kong Telecom Tower, a 43-storey office tower with a footprint of about 1,500 square meters, and Dorset House, a 40-storey office tower with a similar size floor plate. Four levels of basement provide 400 parking spaces.

4.2.1 Chilled Water System

The central cooling system services the whole building with chilled water produced by a chiller plant consisting of five York water-cooled centrifugal chillers. Among them, three are identical 1540-ton centrifugal chillers (see Figure 4.4) for Day Mode and two are identical 500-ton centrifugal chillers for Night Mode/Holiday Mode. Each of the chillers uses a fixed orifice as the expansion device. The condenser water is provided by 11 identical open cooling towers which are located on the roof level. In this paper, the data collected from a 1540-ton centrifugal chiller will be used as test data to validate FDD schemes developed.

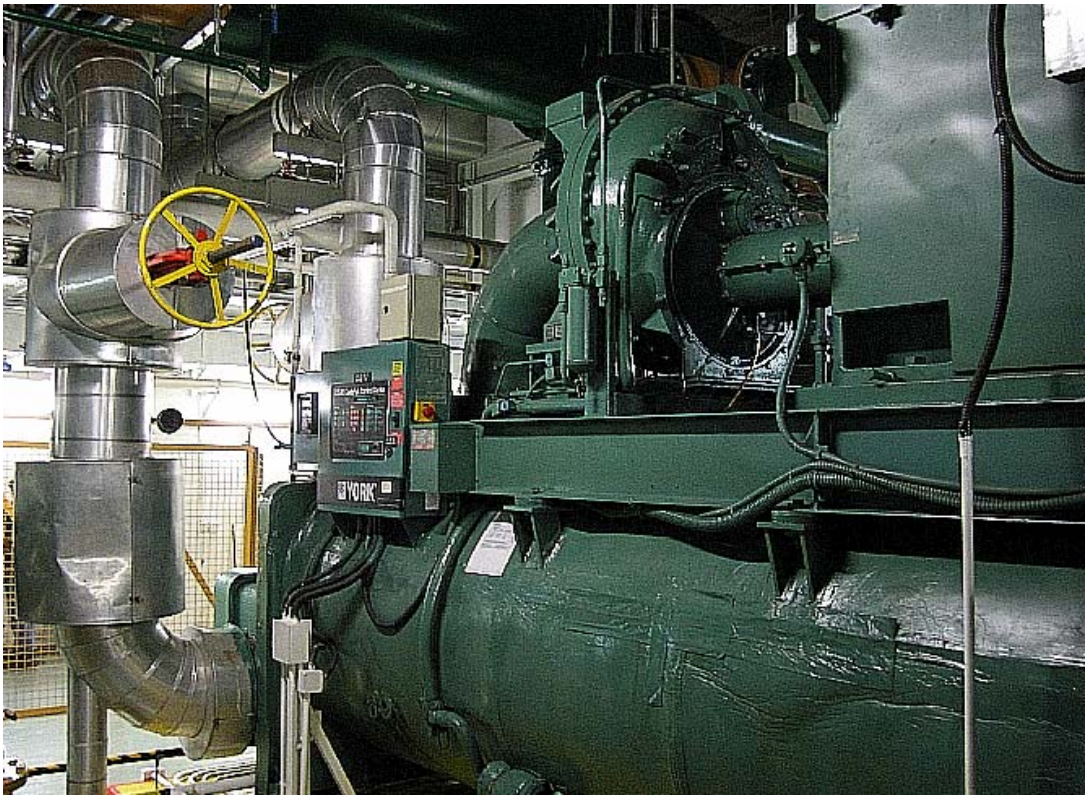

Figure 4.4 A York water-cooled 1540-ton centrifugal chiller in a real building in Hong Kong

The chilled water system can be divided into two loops: the primary system which is also called the production system - the place where chilled water is produced, and the secondary system which is also called the distribution system because its function is to convey the chilled water to the load side. The chilled water in this cooling system is pumped by a typical constant primary – variable secondary pumping system. Figure 4.5 shows the schematic of the chilled water system. The rationale for this configuration is straightforward. On the primary system, chiller manufacturers recommend that the flow through the evaporator of a chiller should be constant, since high flow rates could cause damage to evaporator tubes and low rates could result in unsteady controls. Therefore, each chiller is serviced by a constant-speed primary pump. On the secondary system, variable-speed pumps are preferred in that they can save pumping energy at part load

conditions. Thus, five identical variable-speed pumps are configured in a parallel arrangement in the secondary system. In addition, each chiller is associated with a constant-speed condenser water pump in the condenser water loop. Two identical condenser water pumps and two identical primary chilled water pumps, all constant-speed, are used for standby. The central cooling system operates day and night, including public days.

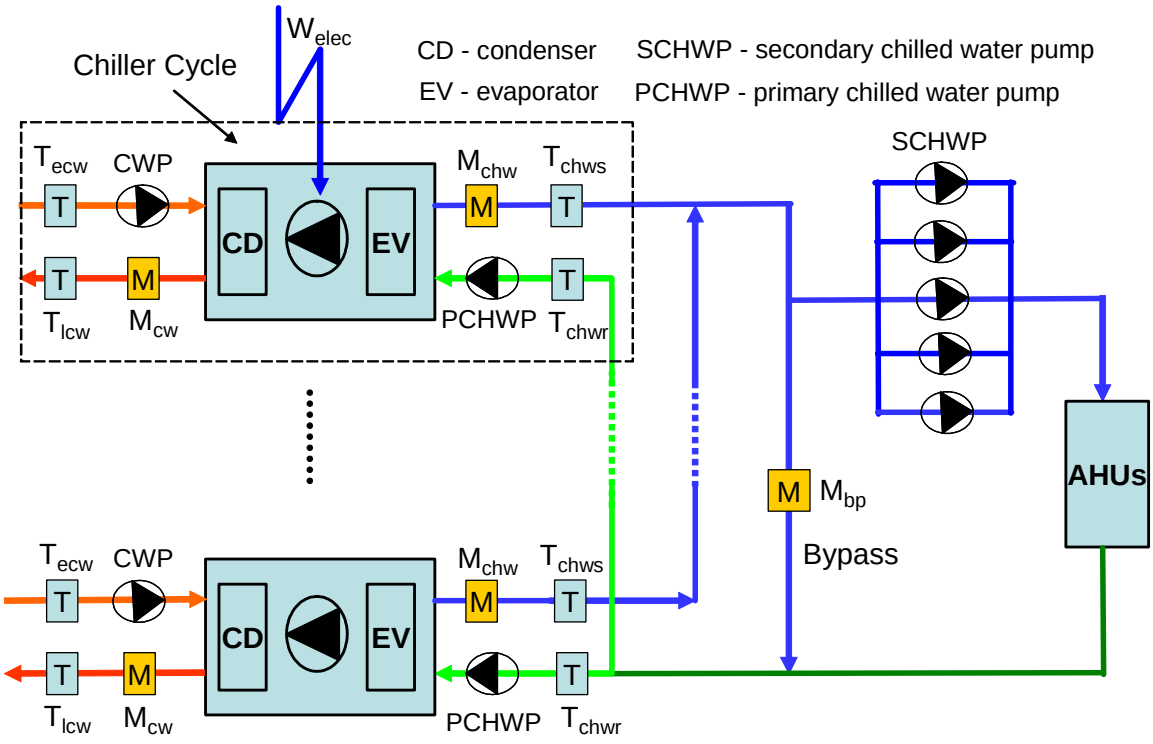

Figure 4.5 Schematic diagram of the chilled water system in a real building in Hong Kong (5 chillers)

4.2.2 Basic System Control

There are two operating modes in the sequencing control. One is Day Mode and the other is Night /Holiday Mode. Each mode is defined by a predetermined time schedule. Chillers and associated pumps should operate under the sequencing control with equal running hours in either of the two modes. Normally, one chiller set, including a chiller, a

condenser water pump and a primary water pump, will be started after the sequencing control is activated for minimum building cooling load. One more chiller set will be started if one of the following conditions occurred in Day Mode:

- The building cooling load is equal to or larger than the total load of the operating chiller(s);
- The return chilled water temperature is higher than 14^{o}C;
- A negative water flow rate larger than 10 liter/second is detected in the bypass pipe.

One chiller set will be stopped if one of the following conditions occur in Day Mode:

- The cooling load of operating chiller(s) exceeds the building cooling load by 110% of the rated capacity of a single chiller;
- A positive water flow rate larger than 110% of the maximum flow rate of a single chiller is detected in the bypass pipe.

As for Night /Holiday Mode, the second chiller set will only be started if the return chilled water temperature is higher than 14^{o}C and stopped if the temperature is less than 13.5^{o}C.

When a control command is sent to start a chiller set, the associated cooling tower will be started first and then the condenser water pump will be started. Subsequently, the primary water pump will be started. After 1 minute, the chiller will be started. The above sequence will be reversed when stopping a chiller set.

The primary concern in the control of secondary pumps is to ensure that the number of pumps put into operation and their speed must have adequate capacity to deliver the required amount of chilled water to the load side, i.e., AHUs. The sequence and the

speed control of the secondary water pumps are carried out according to the differential pressure of the secondary water loop. For conciseness, the details of the control are not provided in this thesis. Each AHU on the load side is equipped with a PID controller, which controls the supply air temperature by adjusting the chilled water flow through the cooling coil. A two-way modulating valve is used.

4.2.3 BMS Monitoring Sensors

The BMS monitoring sensor in the chiller plant are shown in Figure 4.5. Resistance thermometers accurate to ±0.05 °C are installed for the building supply water temperature, the chilled water supply and return temperatures of each chiller. Magnetic flow meters accurate to ±1% of full scale are available for the total building supply water flow rate, the bypass flow rate and the water flow rate of each chiller. Kilowatt meters accurate to ±0.5% of full scale are installed to measure the instantaneous electric power input to each chiller and its associated primary water pump. Condenser water temperature sensors are installed at the inlet and outlet of the condenser of each chiller.

In addition, measurements from internal sensors and transducers in each chiller are available on the BMS as control panels of individual chillers are integrated with the BMS through gateway technologies. On control panels of individual chillers, temperatures were measured by resistance thermometers accurate to ±0.05 °C, water flow rates by magnetic flow meters accurate to ±1% and pressures by pressure transducers accurate to ±0.4% of full scale. Therefore, measurements from all sensors and transducers in the cooling system can be collected from the BMS. The sample interval of the measurements collected from the BMS is one minute.

4.3 Summary

Two test facilities in different environments, namely laboratory and field, were introduced in this chapter. The schemes/strategy developed in this thesis will be tested on these two facilities.

The first test facility is a laboratory centrifugal chiller in an ASHRAE research project whose primary objective is to produce a database which can be used in the development and evaluation of FDD methods applied to centrifugal chillers. In particular, the availability of chiller data from fault tests at different levels of severity can help determine the sensitivity and accuracy of FDD methods in detecting the given fault.

The second test facility represents a typical application of centrifugal chillers in large commercial buildings. Chiller data can be collected from the BMS of the building for a certain period of time and used to validate the schemes/strategy developed in this thesis in terms of field applications.

CHAPTER 5 VALIDATION OF BASIC CHILLER FDD SCHEME

The basic chiller FDD scheme developed in Chapter 3 to identify chiller faults in centrifugal chillers is validated in this chapter using both laboratory data and field data, which were respectively collected from the two test facilities introduced in Chapter 4.

Section 5.1 presents the validation results of the basic chiller FDD scheme using data from the laboratory chiller in ASHRAE 1043-RP. The reference model in the basic FDD scheme was developed by the data collected from a normal test. The data collected from four fault tests under different levels of severity and various operating conditions were employed to evaluate the effectiveness and sensitivity of the basic FDD scheme. In a similar way, Section 5.2 partially validates the basic FDD scheme using the field data collected from the BMS of a real building in Hong Kong. The summary of this chapter is given in Section 5.3.

5.1 Validation Using Laboratory Data from ASHRAE 1043-RP

5.1.1 Test Conditions

The basic chiller FDD scheme was validated using laboratory data from a centrifugal chiller in ASHRAE 1043-RP, which is introduced in Chapter 4. The normal data from the

"Normal" test in ASHRAE 1043-RP were used to estimate the parameters in the reference model of each performance index. The data of the "Normal" test are provided on the CD that is attached as an appendix. After the reference models had been developed, the data from four chiller-fault tests were employed as test data to verify whether the chiller faults could be found by the basic chiller FDD scheme. The selected chiller-fault tests for validation tests in this chapter are listed as follows.

- Refrigerant leakage
- Excess oil
- Condenser fouling
- Non-condensable gases in refrigerant

It is worth noting that all these faults are considered in the set of rules in the fault diagnostic classifier (see Section 3.1.3). However, in this thesis the basic chiller FDD scheme is not validated against another two chiller faults that are considered in the fault diagnostic classifier, i.e., evaporator fouling and degradation of compressor, as the data for these two chiller faults are not available in ASHRAE 1043-RP. For each of the chiller-fault tests used, the fault characterization and fault severity levels are shown in Table 4.2. In addition, the data from the "Normal NC" test were also directly used to verify the basic chiller FDD scheme. Therefore, there are a total of five test cases. Among them, one case represents normal (fault-free) chiller performance, and the other four test cases, each targeting one chiller fault, represent faulty chiller performance.

5.1.2 Reference Model Development and Validation

After going through a well designed data preprocessor developed in Section 3.3.1, 159 out of the original 433 sample points which were collected at a two-minute sampling interval during the "Normal" test remained. The remaining sample points as indicated by "*" in Figure 5.1 could be thought to have the capability to describe the normal (fault-free) and steady-state operation of the chiller. The remaining data were therefore used to regress the reference models of the six performance indexes. The noise errors associated with individual measured data (refer to Table 4.1) were assumed to be a Gaussian distribution with mean zero and standard deviation equal to half of the measurement accuracy specified by instrument manufacturers

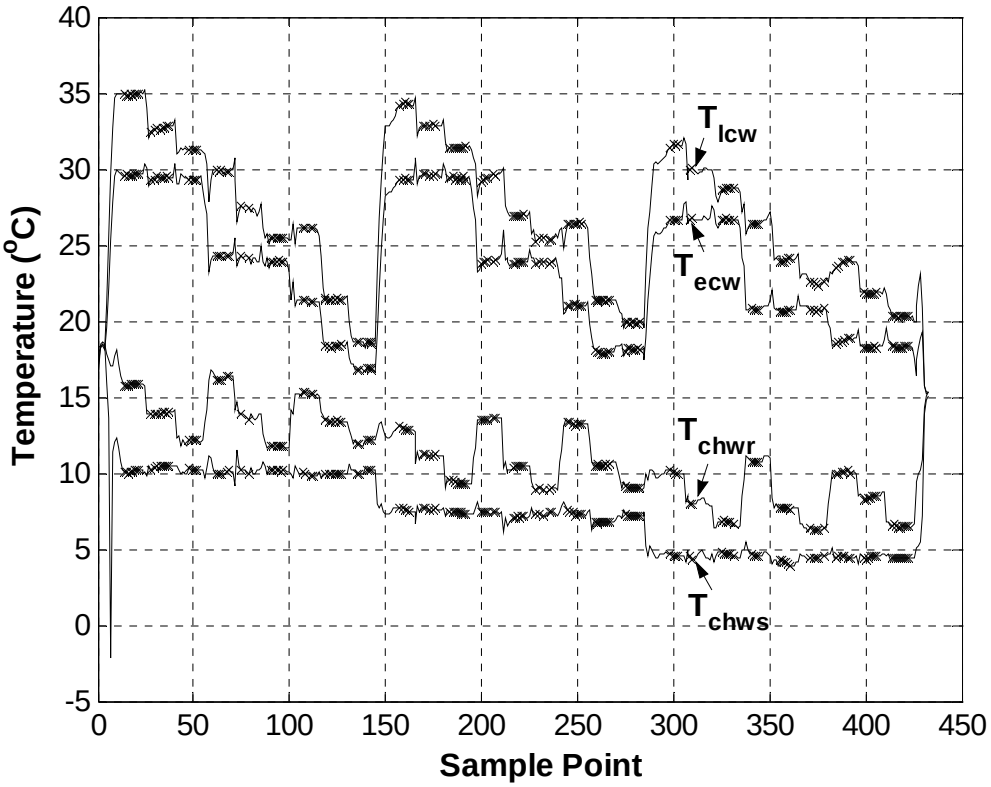

Figure 5.1 Sample points from "Normal" test meeting all 27 operating conditions

It can be seen from Figure 5.1 that the range of variations of the individual variables are rather large and they are reasonably distributed over all typical operating conditions of the chiller. This arrangement of the model development data, just as presented by Corcoran and Reddy (2003), makes it possible to obtain sound reference models of the performance indexes. The OLS method was employed to estimate the coefficients of the reference models in the form of Equation (3.16). The regression statistics are summarized in Table 5.1 and the coefficients in the reference model are summarized in Table 1 in Appendix B.

Table 5.1 Regression statistics of reference models for performance indexes regressed by laboratory data from ASHRAE 1043-RP

(159 sets of steady-state data from "Normal" Test)

	$LMTD_{ev}$	$LMTD_{cd}$	M_{ref}	Eff_{poly}	Eff_{motor}	*COP*
RMSE	0.152K	0.238K	0.002kg/s	0.81%	1.33%	0.05
CV%	3.24%	6.94%	0.17%	1.60%	1.64%	1.32%
R^2	99.06 %	97.07%	99.99%	99.42%	98.07%	99.63%
Adj-R^2	99.05%	97.03%	99.99%	97.41%	98.04%	99.62%

RMSE - Root Mean Square Error; CV% - Coefficient of Variation
R^2 - Coefficient of Determination; Adj-R^2 - Adjusted R^2

The R^2 in Table 5.1 is an indicator of how well the reference model with three regressors fits the model development data. An R^2 close to 1.0 indicates that one has accounted for almost all of the variability with the variables specified in the model. The R^2 would never decrease if one adds more independent variables to a regression model, even when the new variable causes the model to become less efficient (worse). The Adj-R^2 however has the advantage over the R^2 (Montgomery and Runger 1994). It will not always

increase when more variables are added, but only increases if the added variables contribute significantly to the regression model.

From Table 5.1, it can be seen that the adjusted R^2 is a little lower than the R^2, which normally means that no explanatory variable(s) is missing in the regression model (Montgomery and Runger 1994). Furthermore, the maximum CV% of 6.94% and the minimum R^2 of 97.03% for performance indexes are two indicators showing a desirable goodness of fit of the regression models. Comparisons between predicted and calculated performance indexes are shown in Figure 5.2. From the analysis above, it can be concluded that OLS is applicable to the parameter estimation of the reference models though the independent variables here have evidence of collinearity, e.g., the cooling load is correlated with the chilled water supply temperature as the latter is involved in the calculation of the former.

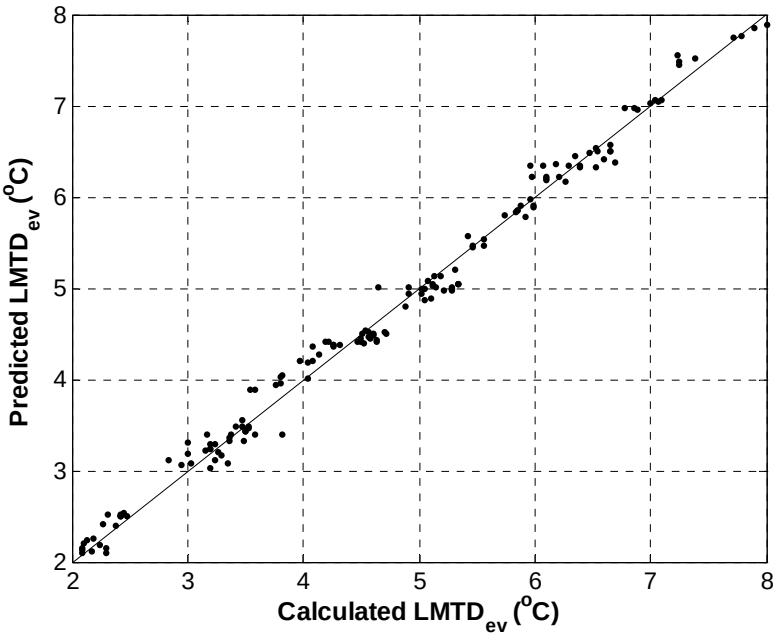

Figure 5.2 – (a) Model predicted $LMTD_{ev}$ and calculated $LMTD_{ev}$

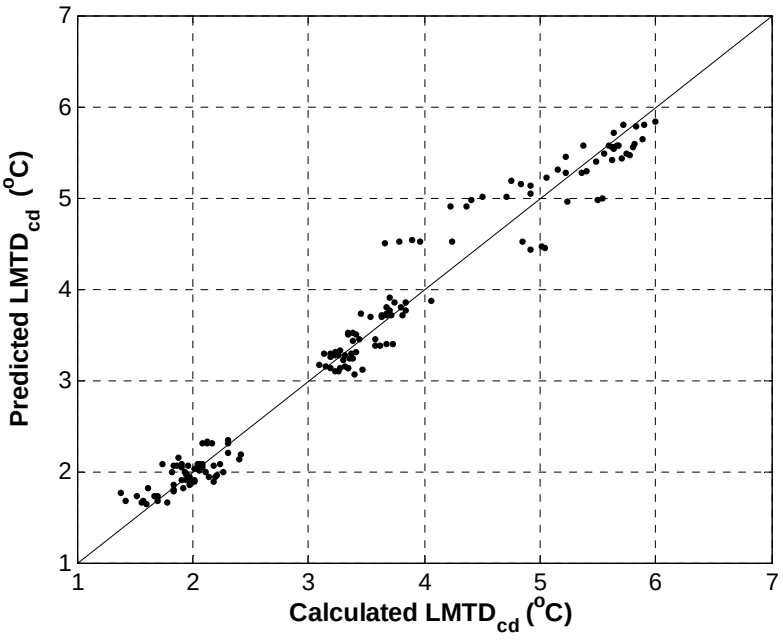

Figure 5.2 - (b) Model predicted $LMTD_{cd}$ and calculated $LMTD_{cd}$

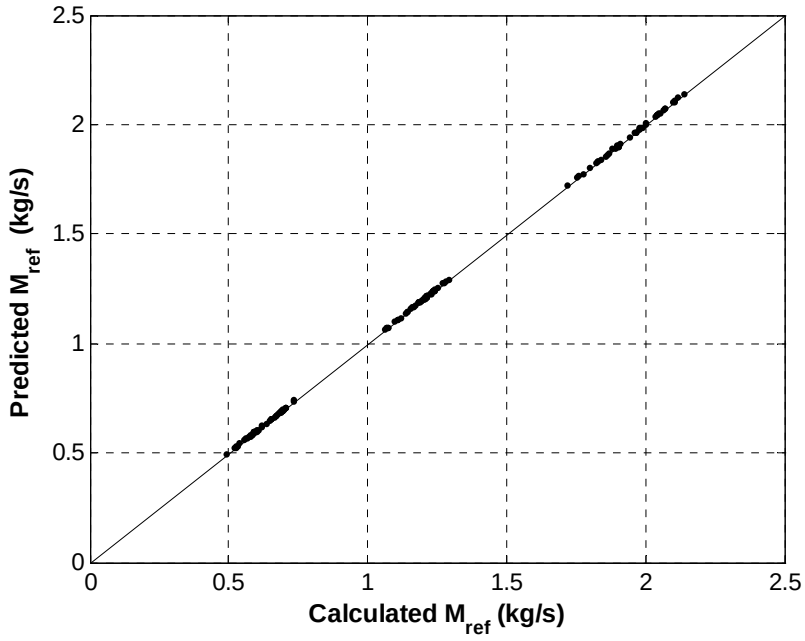

Figure 5.2 -(c) Model predicted M_{ref} and calculated M_{ref}

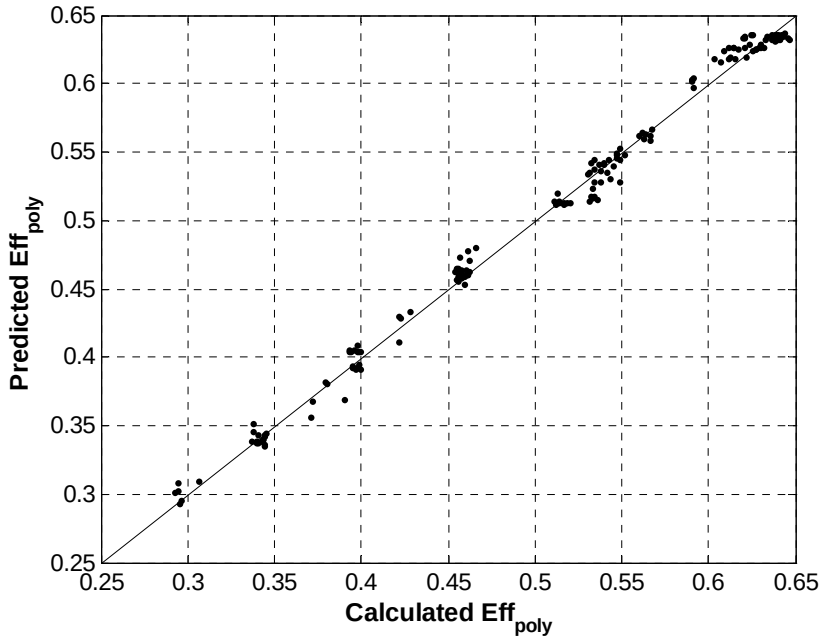

Figure 5.2 - (d) Model predicted Eff_{poly} and calculated Eff_{poly}

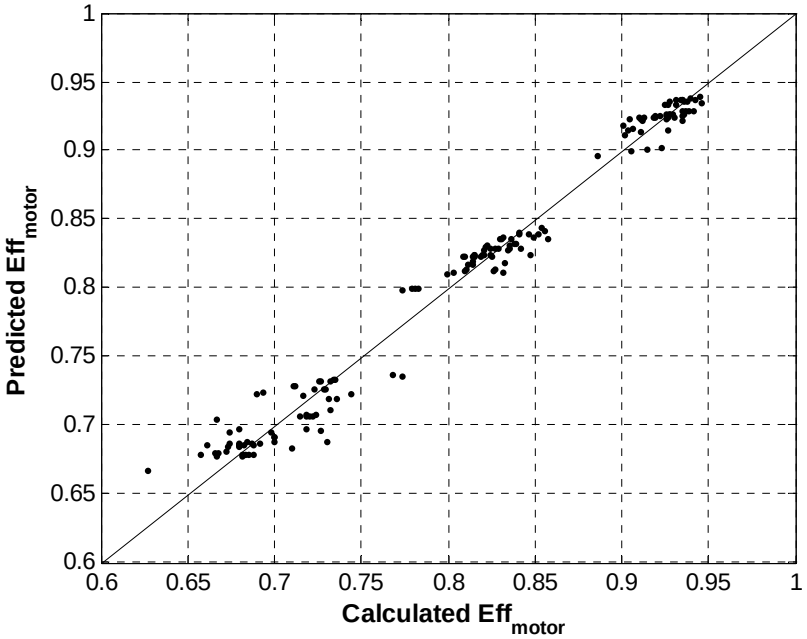

Figure 5.2 - (e) Model predicted Eff_{motor} and calculated Eff_{motor}

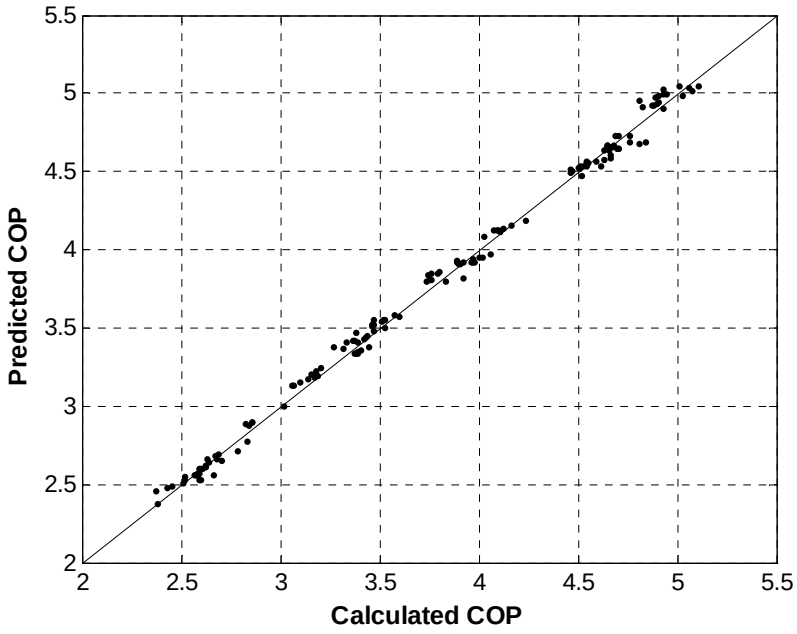

Figure 5.2 - (f) Model predicted *COP* and calculated *COP*

Figure 5.2 Comparison between predicted and calculated values of performance indexes using laboratory data from “Normal” test

5.1.3 Effects of Operating Conditions on Fault Detection Threshold

As analyzed earlier in Chapter 3, the chiller operating conditions affect the uncertainty in the calculation of residuals of performance indexes, and then affect the threshold for fault detection at a certain confidence level. The laboratory data were used to verify the effects of the operation conditions on the fault detection thresholds and check if it is necessary to adopt the online adaptive estimator of fault detection threshold.

The results showed that for each performance index the threshold determined at a certain confidence level changed with operating conditions, i.e., the cooling load, the entering condenser water temperature and chilled supply water temperature. In particular, the

performance indexes, including M_{ref}, Eff_{motor} and COP, changed significantly with the operating conditions, while the performance indexes, including $LMTD_{ev}$, $LMTD_{cd}$ and Eff_{poly}, were less susceptible to the operating conditions. The threshold of the performance index, Eff_{motor}, is chosen in this section to illustrate such effects. As shown in Figure 5.3, the variation of the thresholds of Eff_{motor} is significant when the cooling load (Q_{ev}) and the entering condenser water temperature (T_{ecw}) change under the condition of a constant chilled water supply temperature (T_{chws}).

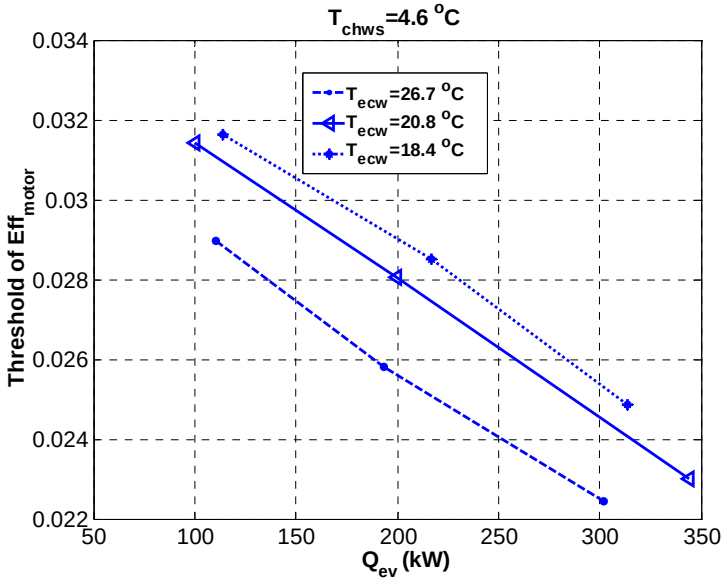

Figure 5.3 Estimated threshold of a performance index (Eff_{motor}) affected by chiller cooling load (Q_{ev}) and entering condenser water temperature (T_{ecw}) under the condition of constant chilled water supply temperature (T_{chws})

5.1.4 Test Results

The basic chiller FDD, as shown in Figure 3.1, was implemented to process the test data from one selected normal test and four chiller- fault tests. The results are provided as follows.

Test case using normal laboratory data from "Normal NC"

The performance indexes were calculated and subtracted from their normal values, which were predicted by the corresponding reference models. That resulted in the residuals of each performance index, which are depicted in Figure 5.4. The dots in the figures represent the residual values. The solid lines in the figures indicate the thresholds, which were ever updated by Equation (3.17) with a confidence level of 95%. Obviously, almost all residuals of each performance index for this normal test were inside its individual threshold band. It is worth pointing out that there were a few residuals of two performance indexes, i.e., $LMTD_{ev}$ and $LMTD_{cd}$, locating outside their thresholds. However, the distribution of the residuals of the two performance indexes was not in one direction and quite random, which meant that these deviations were not due to a specific chiller faults. Therefore, it can be concluded that there was no chiller fault in the chiller system.

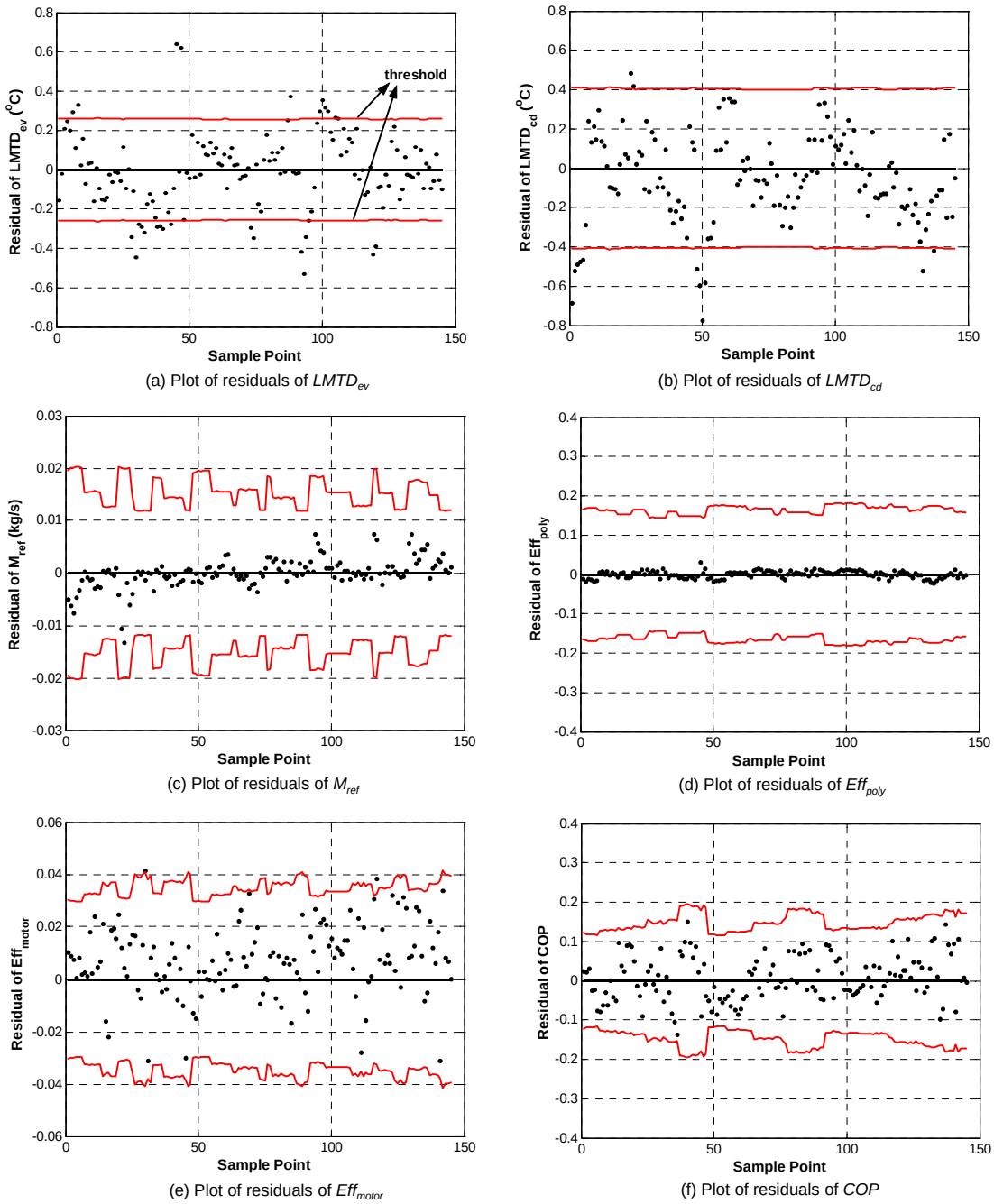

(a) Plot of residuals of $LMTD_{ev}$

(b) Plot of residuals of $LMTD_{cd}$

(c) Plot of residuals of M_{ref}

(d) Plot of residuals of Eff_{poly}

(e) Plot of residuals of Eff_{motor}

(f) Plot of residuals of COP

Figure 5.4 Residuals of performance indexes for "Normal NC" test – no fault detected

Test case using normal laboratory data from chiller-fault tests

The test data were generated by arranging the data from each chiller-fault test in

increasing order of severity (from level 1 to level 4). Residuals and thresholds of each performance index were obtained in the same way mentioned above. In the following figures, the number of steady sample points from each fault level is not exactly the same. Roughly speaking, fault level l includes sample point 1 to 160, fault level 2 includes sample point from 161 to 320, fault level 3 includes sample point 321 to 480 and fault level 4 includes sample point 481 to the last one. The dots in the figures represent the residual values.

With regard to the refrigerant leakage test, the residual of the performance index, $LMTD_{cd}$, began to deviate beyond its upper thresholds at fault level 2 as shown in Figure 5.5-(a). The residual values are illustrated by the solid dots and the fault detection threshold values are indicated by the solid lines. The confidence level of threshold estimation was also 95%. As shown in Figure 5.5-(b), there was almost no residual of M_{ref} locating outside thresholds at low fault levels, but a very few residuals were observed below its lower thresholds. In addition, a slight increase of *COP* was observed at level 2 and level 3, as shown in Figure 5.5-(c). But this increase of *COP* would soon be offset by the ever-increasing negative effects resulting from the fault when the fault severity level reached 4. No discernible residual of the other performance indexes was observed and not presented in this section. The fault diagnostic classifier, according to the rules presented in Table 3.2, identified the existence of refrigerant leakage

As for the excess oil test, only some residuals of Eff_{motor} and *COP* deviated beyond their lower thresholds at higher fault severity levels, as shown in Figure 5.6, while no

discernible residual of the other performance indexes was found. With the aid of continuous monitoring of the trend of residuals of each performance index, the fault diagnostic classifier identified the existence of excess oil when it was at fault severity level 4. Admittedly, the deviations of Eff_{motor} and *COP* were not very obvious. This is because excess oil was slightly introduced to the chiller for protecting the compressor.

Similarly, in the case of condenser fouling, some residuals of two indexes, $LMTD_{cd}$ and *COP* deviated from their corresponding thresholds even when the fault severity level was low, as shown in Figure 5.7. Due to the compensation effect of the expansion valve, few deviated residuals of M_{ref} were observed at low fault levels. However, when the fault level was high, e.g., level 4, the expansion valve could not compensate any more and significantly deviated residuals of M_{ref} appeared. Accordingly, the fault diagnostic classifier identified the existence of condenser fouling.

With regard to the test of non-condensables in refrigerant, the residuals of three indexes, $LMTD_{cd}$ and *COP* began to obviously deviate from their corresponding thresholds at fault level 1, as shown in Figure 5.8. Thus, non-condensables in refrigerant could be identified with the aid of the fault diagnostic classifier.

It can also be seen from Figure 5.5 to Figure 5.8 that the thresholds of the performance indexes, M_{ref}, Eff_{motor}, *COP*, change significantly when the operating conditions change while those of the performance indexes, $LMTD_{ev}$, $LMTD_{cd}$ and Eff_{ploy} are less susceptible to the operating conditions.

To sum up, the four typical chiller faults in the laboratory centrifugal chiller, e.g.,

condenser fouling and excess oil, can be diagnosed by the basic chiller FDD scheme developed in Chapter 3.

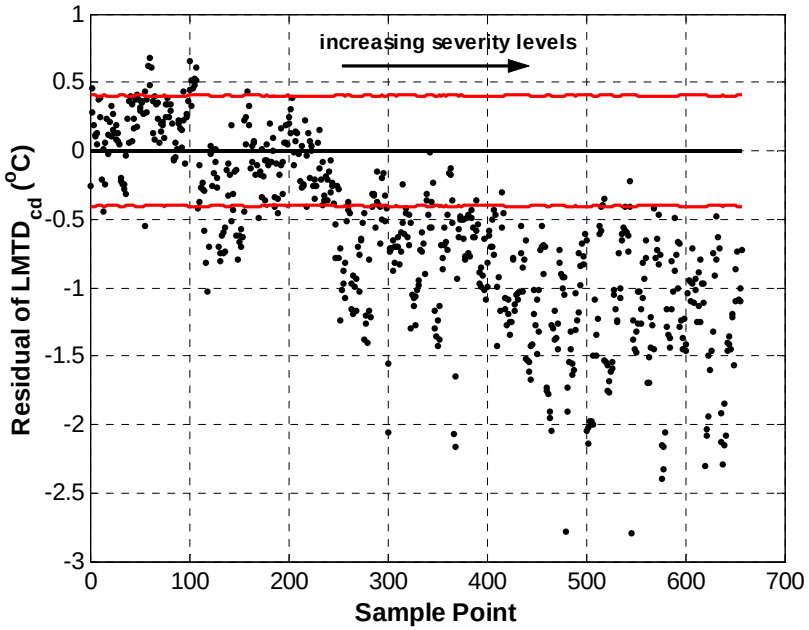

Figure 5.5- (a) Residuals of $LMTD_{cd}$

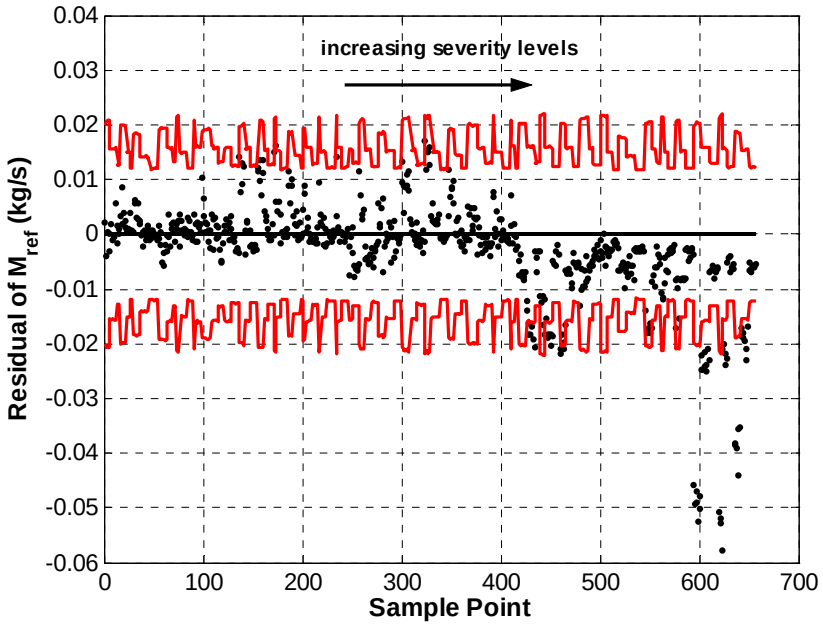

Figure 5.5- (b) Residuals of M_{ref}

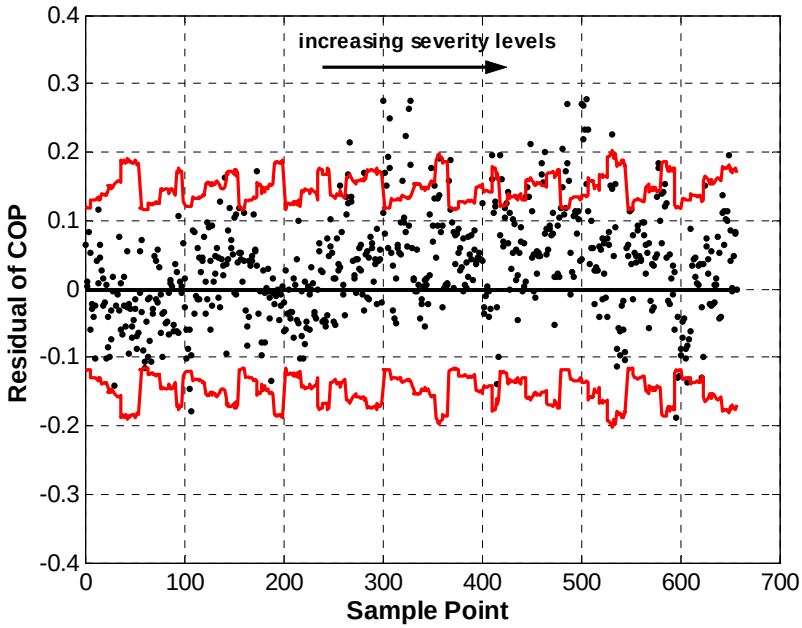

Figure 5.5 - (c) Residuals of *COP*

Figure 5.5 Deviated residuals of performance indexes for refrigerant leakage from fault severity level 1 to level 4

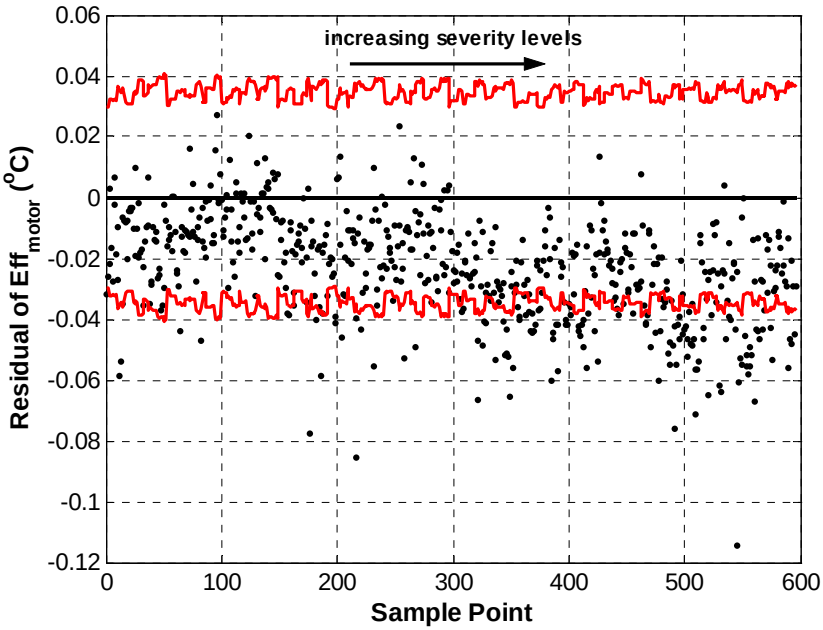

Figure 5.6 - (a) Residuals of Eff_{motor}

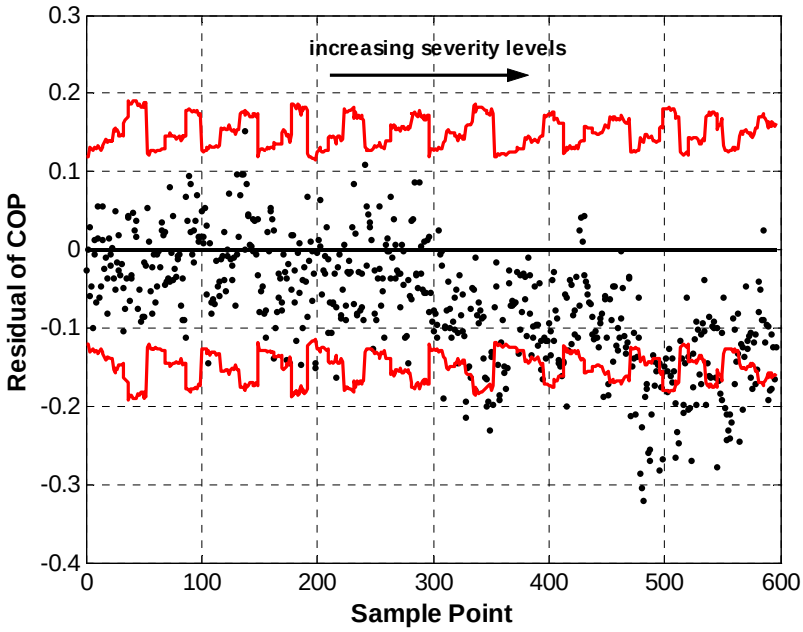

Figure 5.6 - (b) Residuals of *COP*

Figure 5.6 Deviated residuals of performance indexes for excess oil from fault severity level 1 to level 4

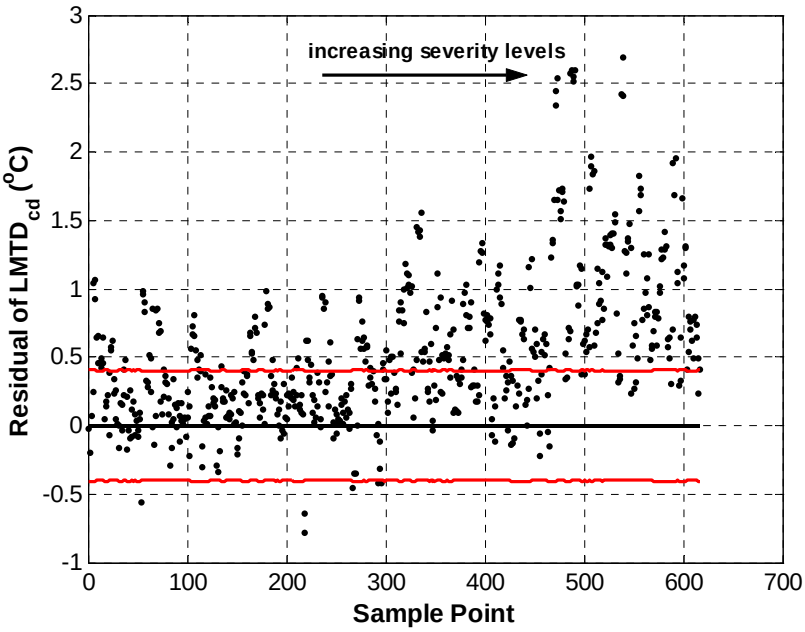

Figure 5.7 - (a) Residuals of $LMTD_{cd}$

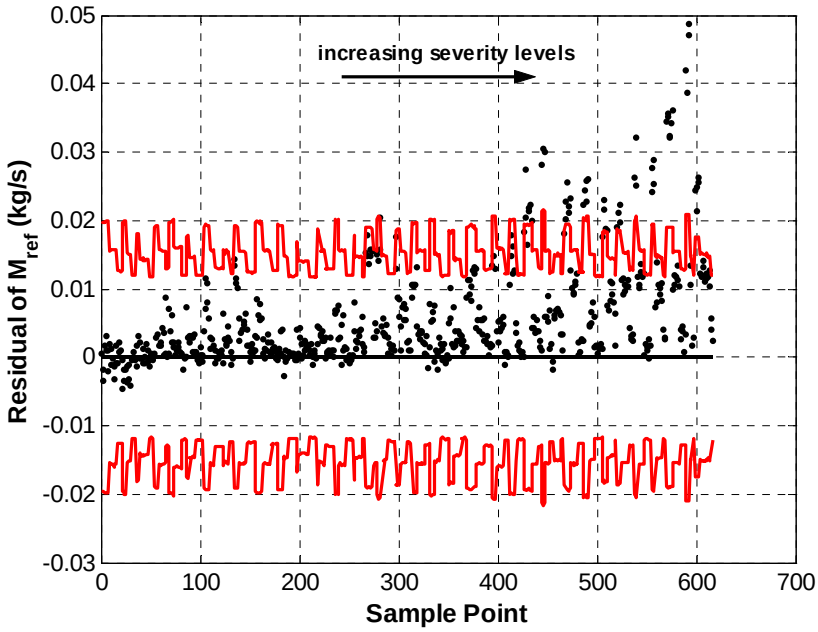

Figure 5.7 - (b) Residuals of M_{ref}

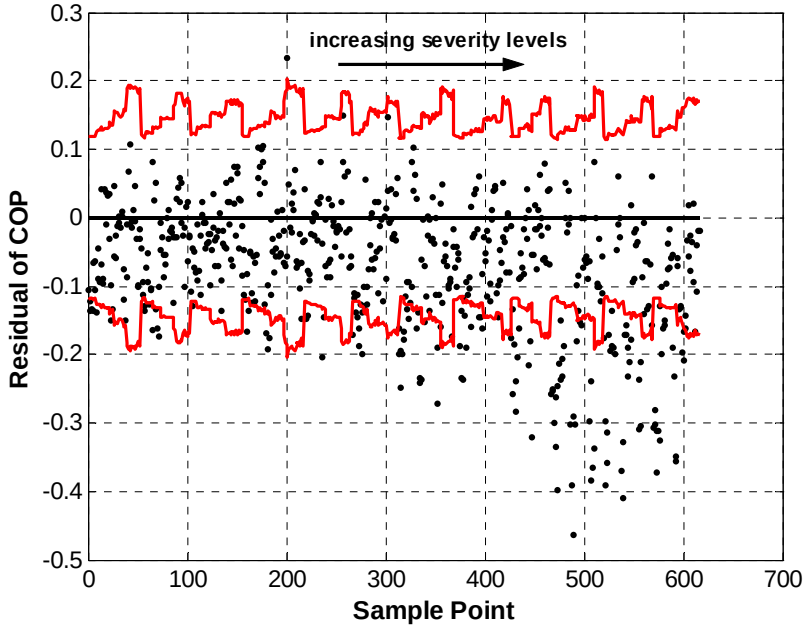

Figure 5.7 - (c) Residuals of *COP*

Figure 5.7 Deviated residuals of performance indexes for condenser fouling from fault severity level l to level 4

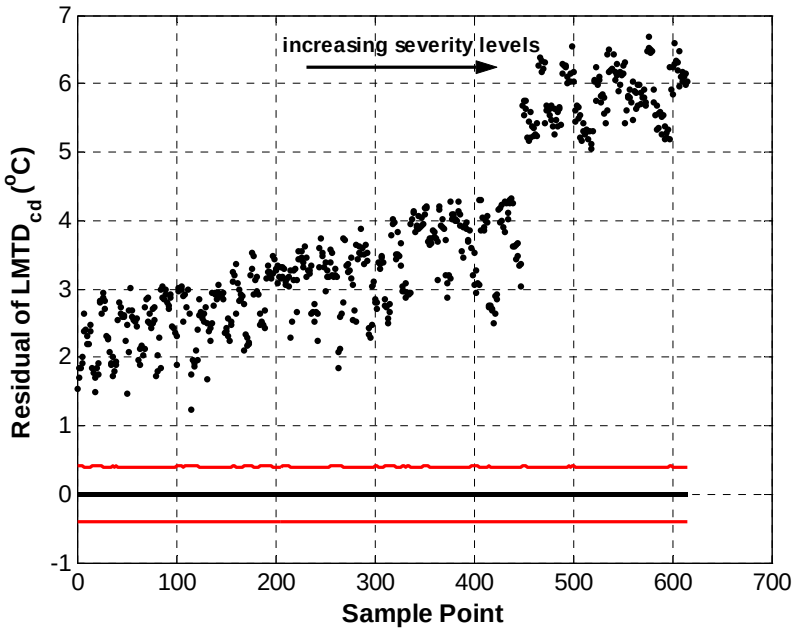

Figure 5.8 - (a) Residuals of $LMTD_{cd}$

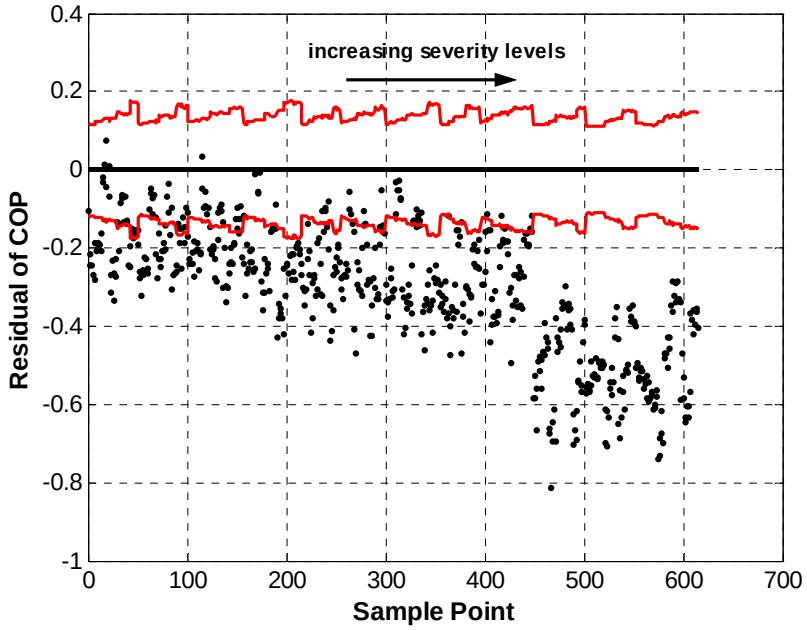

Figure 5.8- (b) Residuals of *COP*

Figure 5.8 Deviated residuals of performance indexes for non-condensables in refrigerant from fault severity level l to level 4

5.2 Validation Using Field Data from a Real Building in Hong Kong

5.2.1 Test Conditions

Apart from the data from chiller-fault tests in ASHARE 1043-RP, the field data collected from a 1540-ton centrifugal chiller in the chiller plant introduced in Section 4.2 were also used to validate the basic chiller FDD scheme. The validation tests using field data can help push the scheme closer to widespread commercialization based on BMS.

The chiller data collected on July 4th, 2001 were used to regress the reference models. The sampling interval was one minute. Since the whole chiller plant just went through a routine process of re-commissioning, healthy and fault-free operations of the components, sensors, controller, actuator, etc., could be ensured. Thus, the collected data sets could be thought to be able to describe the fault-free operation of the centrifugal chillers. The data collected during 30 days after July 4th, 2001 (from July 5th, 2001 to August 3rd, 2001) were used as test data to test the performance of the chiller FDD scheme in identifying chiller faults. Since the condenser water in the system is provided by open cooling towers, continuous contact of the water with air introduces impurities and concentrated materials. Therefore, the fouling of the condenser, without regular purging during the period of 30 days, developed gradually. This fault is expected to be diagnosed by the basic chiller FDD scheme. During the implementation of the scheme, the noise errors associated with individual measurements were assumed to be a Gaussian distribution with mean zero and standard deviation equal to half of the measurement accuracy specified by instrument manufacturers

5.2.2 Reference Model Development and Validation

The data used for reference model development, i.e., for the parameter estimation of the reference models, went through the well-designed data preprocessor first. The data sets were selected prudently from the steady-state data such that the range of variation of the individual variables was as large as possible for identifying sound reference models and they were reasonably distributed over the whole operating range. The OLS method was also employed to estimate the parameters of the reference models in the form of Equation (3.16).

The regression statistics are summarized in Table 5.2. It can be seen from Table 5.2 that the adjusted R^2 is a little lower than R^2, which means that no explanatory variable(s) is likely missing in the regression model (Montgomery and Runger 1994). Furthermore, the maximum CV% of 8.43% and the minimum R^2 of 90.06% are two important indicators showing a strong goodness-of-fit of the regression models. Comparisons between predicted and calculated performance indexes are shown in Figure 5.9. Good agreement found in the comparisons also represents desirable goodness-of-fit of the reference models. The coefficients in the polynomial regression model are given in Table 2 in Appendix B.

Table 5.2 Regression statistics of reference models for performance indexes regressed by field data from a real building in Hong Kong

(301 sets of steady-state data on July 4th, 2001)

	$LMTD_{ev}$	$LMTD_{cd}$	M_{ref}	Eff_{poly}	Eff_{motor}	COP
RMSE	0.256K	0.195K	0.052kg/s	0.32%	1.06%	0.085
CV%	8.43%	4.15%	0.19%	0.44%	1.32%	1.60%
R^2	90.06%	95.44%	99.99%	98.92%	98.62%	94.86%
Adj_R^2	90.03%	95.43%	99.99%	98.91%	98.61%	94.85%

RMSE - Root Mean Square Error; CV% - Coefficient of Variation
R^2 - Coefficient of Determination; Adj-R^2 - Adjusted R^2

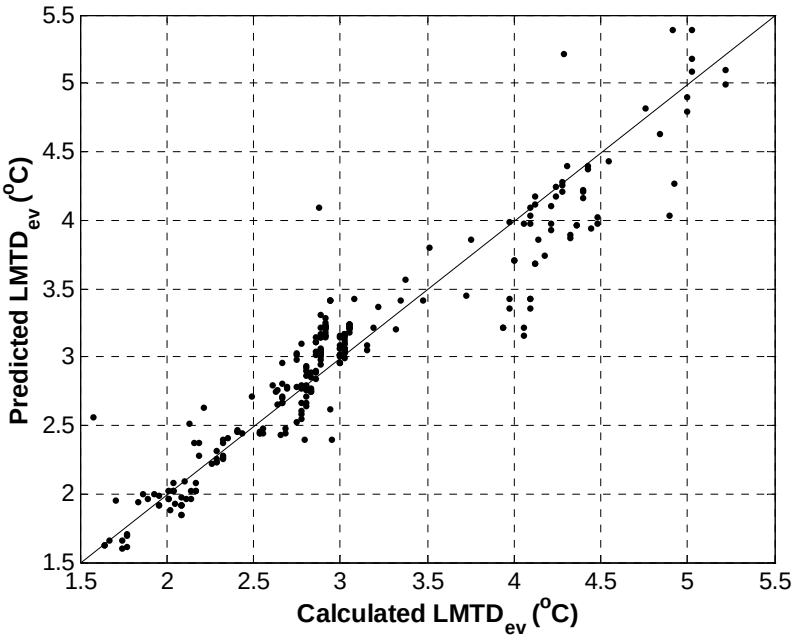

Figure 5.9 - (a) Model predicted $LMTD_{ev}$ and calculated $LMTD_{ev}$

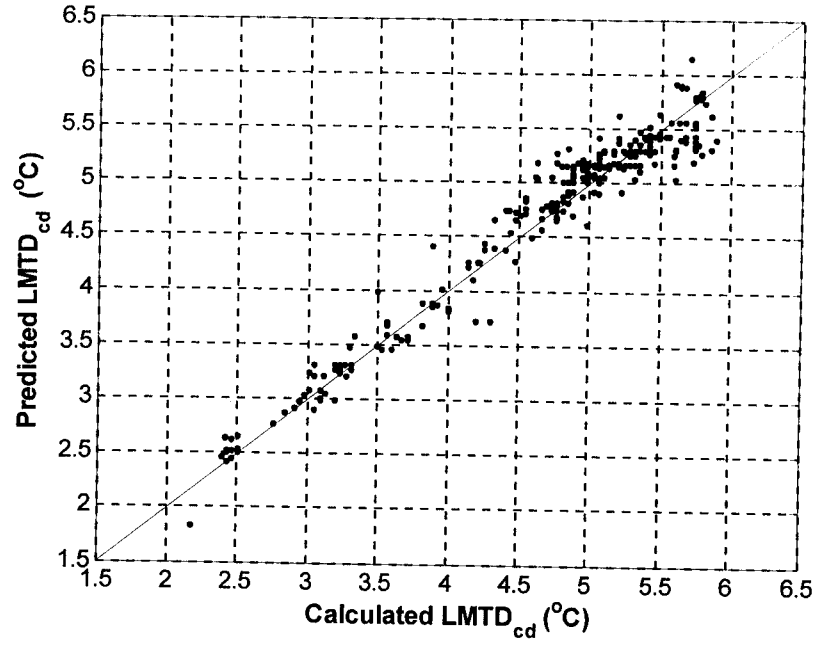

Figure 5.9 - (b) Model predicted $LMTD_{cd}$ and calculated $LMTD_{cd}$

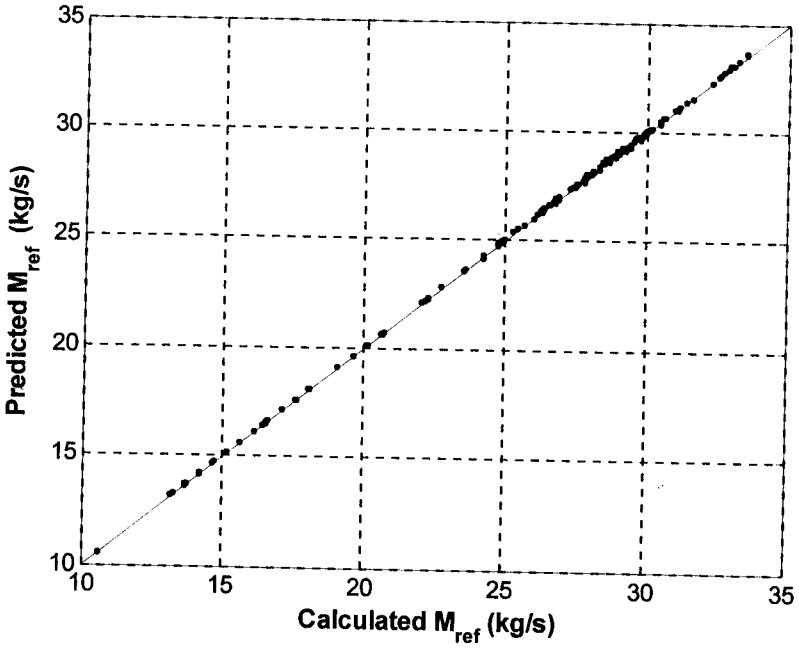

Figure 5.9 - (c) Model predicted M_{ref} and calculated M_{ref}

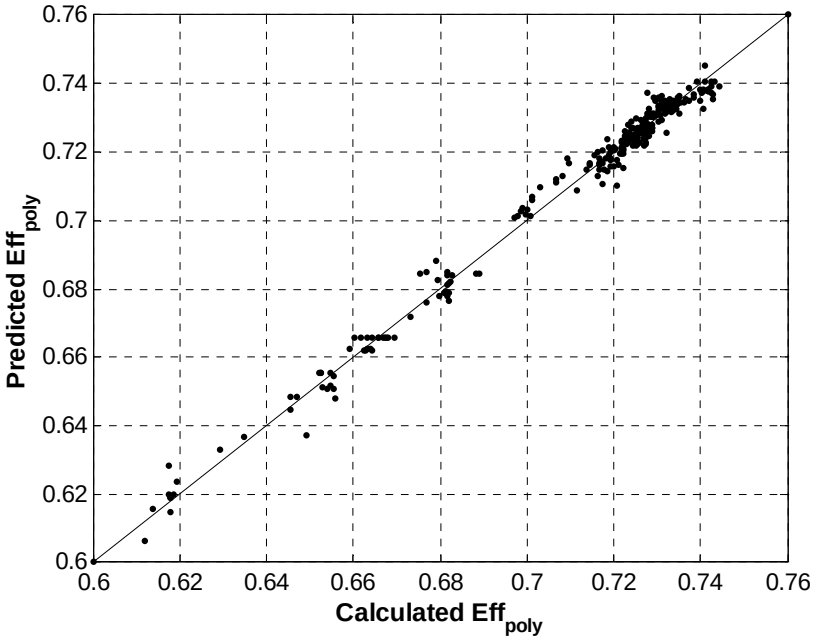

Figure 5.9 - (d) Model predicted Eff_{poly} and calculated Eff_{poly}

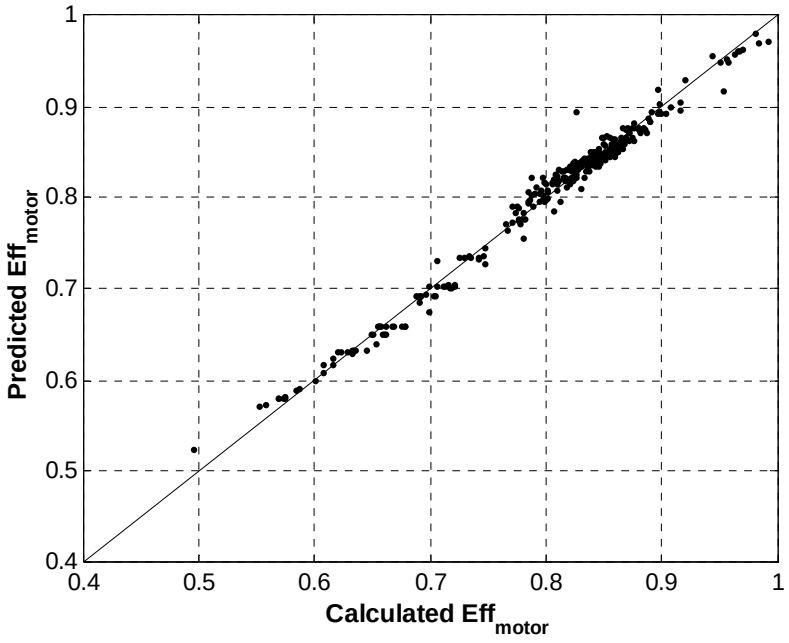

Figure 5.9 - (e) Model predicted Eff_{motor} and calculated Eff_{motor}

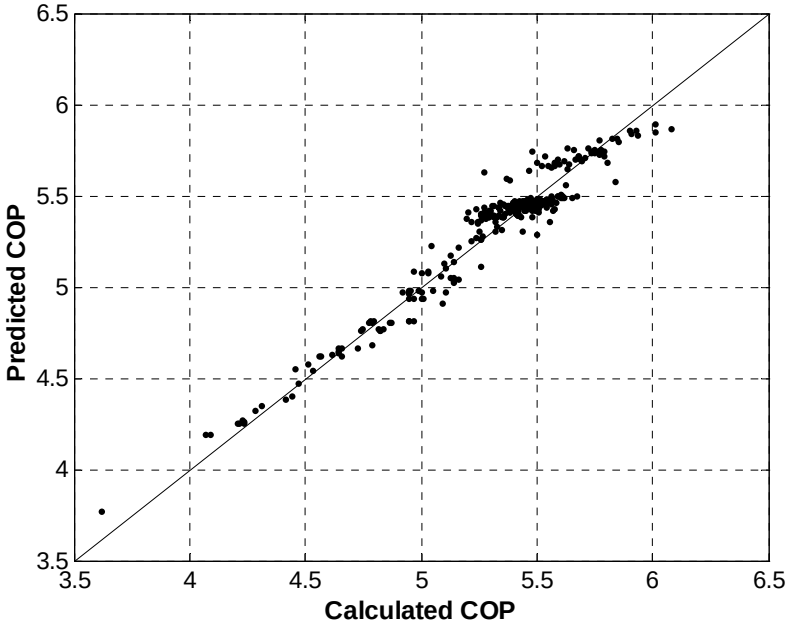

Figure 5.9 - (f) Model predicted *COP* and calculated *COP*

Figure 5.9 Comparisons between predicted and calculated performance indexes using field data collected from a real building on July 4th, 2001

5.2.3 Test Results

The basic chiller FDD, as shown in Figure 3.1, was also implemented to process the data collected after July 4th, 2001. The residuals of the six performance indexes were calculated and then compared with their corresponding fault detection thresholds. The trend and amount of the residuals would be used by the fault diagnostic classifier to diagnose particular chiller faults.

Test cases using field data collected from July 5th to July 24th

In the first 20 days, for each performance index, there were a very few residuals located outside their bands defined by the corresponding thresholds. The residuals of the six performance indexes on July 5th, 2001 are plotted in Figure 5.10 as an example. The dots in the figures represent the residual values. The dots in the figures represent the residual values. The solid lines in the figures indicate the thresholds, which are ever updated by Equation (3.17) with a confidence level of 95%. Since a very small number of residuals go beyond thresholds, the scheme concluded that there was no abnormality in the chiller system on that day.

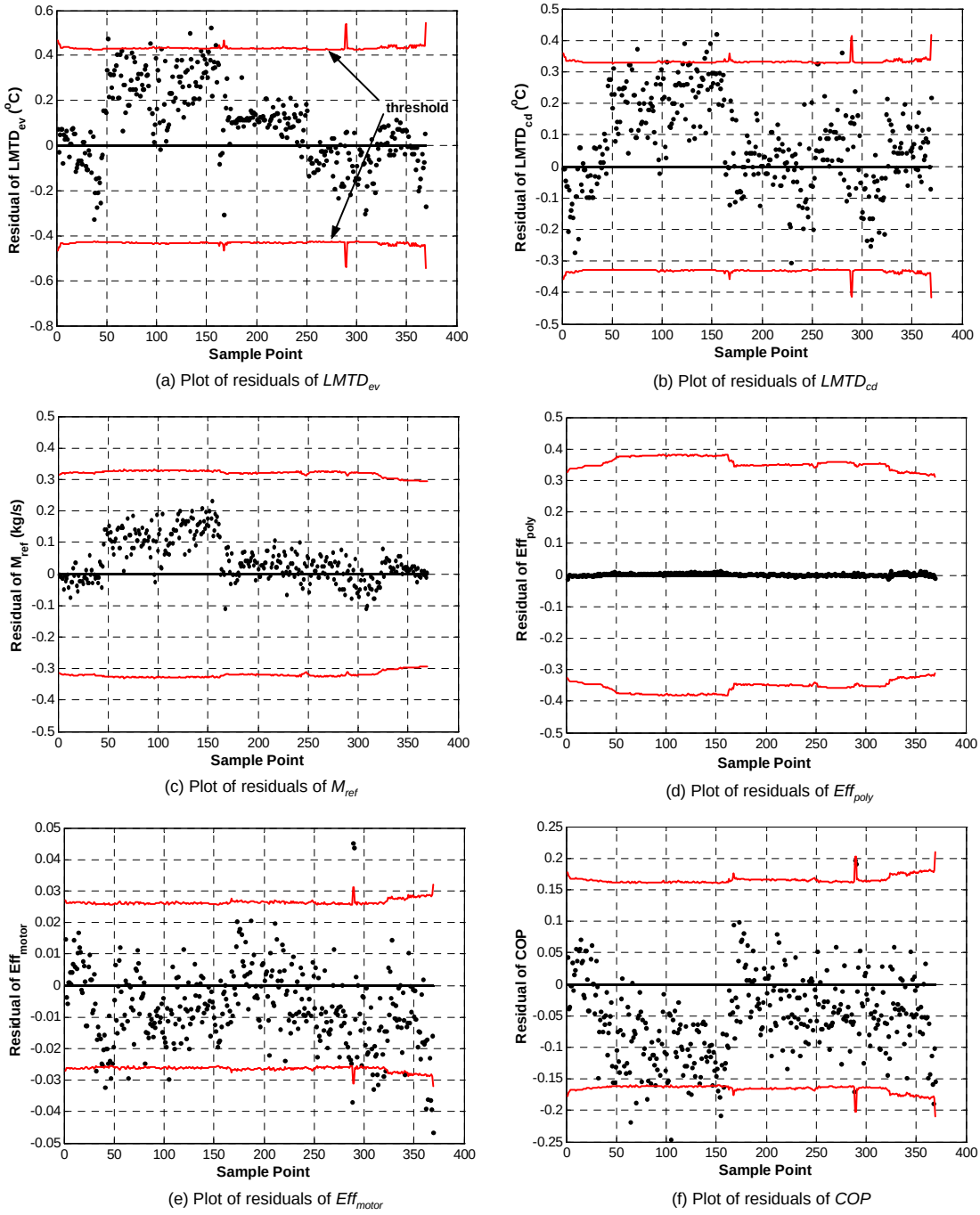

Figure 5.10 Residuals of performance indexes using field data collected from a real building on July 5th, 2001- no fault detected

Test cases using field data collected after July 24th

After July 24th, 2001, the FDD scheme started to find significant residuals in $LMTD_{cd}$

and *COP*, and these residuals became more serious gradually. During the same period, there was no discernible residual in the other four performance indexes. The significantly deviated residuals of the performance indexes on July 31st 2001 (28 days after system commissioning and calibration) are presented in Figure 5.11 to illustrate FDD results of the basic scheme. The thresholds were also ever-updated by Equation (3.17) with a confidence level of 95%. It was clear that the residuals of $LMTD_{cd}$ and M_{ref} increased beyond the thresholds, while the residuals of *COP* decreased below the thresholds. Therefore, the fault diagnostic classifier concluded that the occurred fault was condenser fouling. This conclusion agreed well with the foregoing expectation that the condenser water provided by open cooling towers would foul the condenser gradually. Due to the constraints in operating system, no other faults were artificially introduced into the chiller system to test the basic chiller FDD scheme.

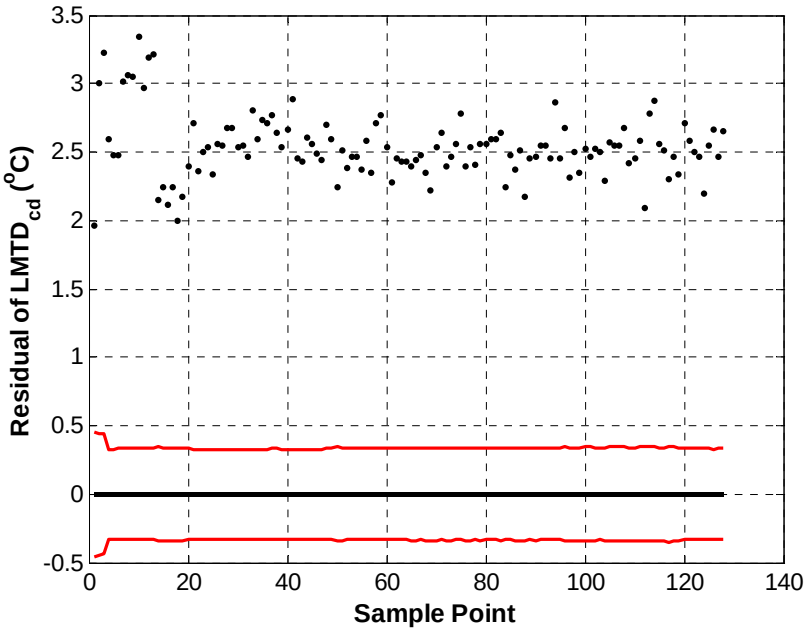

Figure 5.11 - (a) Residuals of $LMTD_{cd}$

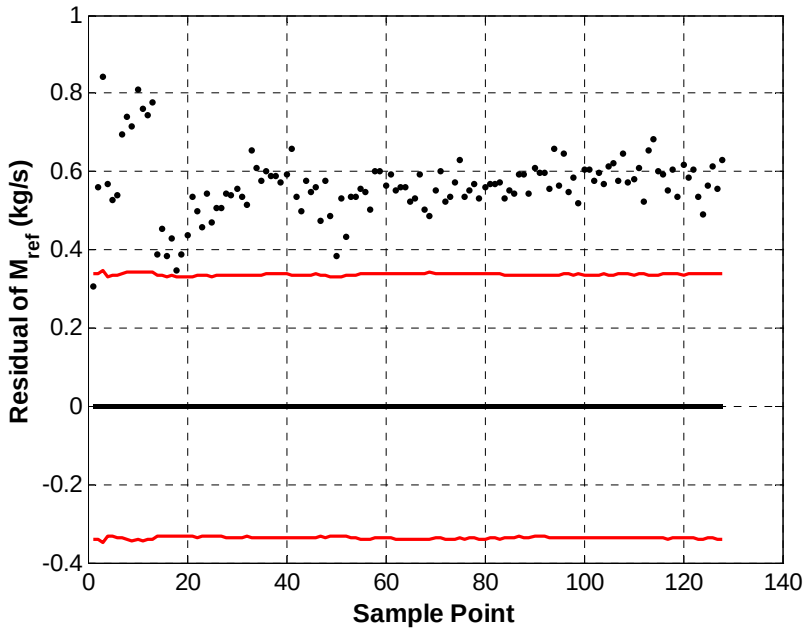

Figure 5.11 - (b) Residuals of M_{ref}

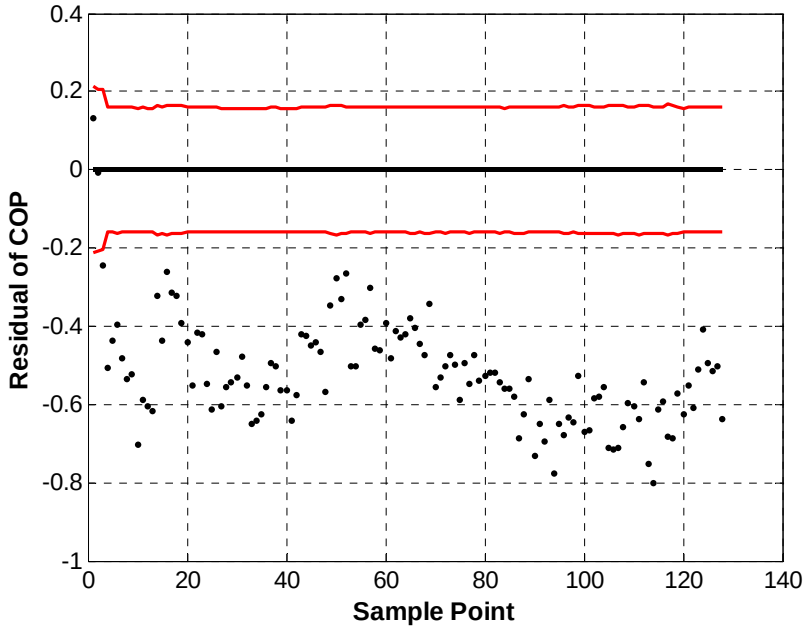

Figure 5.11 - (c) Residuals of *COP*

Figure 5.11 Deviated residuals of performance indexes using field data collected from a real building on July 31st, 2001

5.3 Summary

To sum up, this chapter validated the basic chiller FDD scheme developed in Chapter 3, using both laboratory data from a centrifugal chiller in ASHRAE 1043-RP and field data collected from the BMS of a real building in Hong Kong. The validation results show that it is possible to differentiate between the tested chiller faults using the basic FDD scheme.

First of all, the fitness of the reference models affects the accuracy of the chiller FDD scheme. As for the validation tests using laboratory data, the model development data were collected from a normal test with 27 different operating conditions. Therefore, these data contain rich system information needed to identify sound reference models of the performance indexes. As for the validation tests using field data, chiller data collected over a period of one day immediately after system routine maintenance and commissioning were used to identify reference models of the performance indexes. Although the chiller only experienced a small range of operating conditions during the one-day period, the identified reference model would still be accurate enough for subsequent applications as the operating and control patterns of the chiller remained almost unchanged during the whole period of validation.

In addition, the set of rules in the fault diagnostic classifier that is deduced from basic physical knowledge was proved to be an effective fault diagnosis tool. However, not all chiller faults can lead to significantly deviated performance indexes such as the case of excess oil. Therefore, continuous monitoring of the trend of residuals of each

performance index can help the FDD scheme find existing chiller faults especially in the case that the scheme is not very sensitive to a chiller fault.

More importantly, it is clear from the test results that the threshold estimator can give a reasonable threshold band for each performance index by taking into account the model fitting errors, the chiller operating conditions and the noise errors associated with the sensors. These well defined thresholds can help ensure desirable performance of the basic chiller FDD scheme. The effect of operating conditions on thresholds can be clearly illustrated by comparing the changes of thresholds in Figure 5.4 with those in Figure 5.10. Because the laboratory chiller experienced a wider range of operating conditions during a test than the field chiller did during one-day operation, the thresholds in Figure 5.4 changed much more than those in Figure 5.10.

However, it is worth noting that the basic chiller FDD scheme does not take into account sensor faults and all the chiller data used in the validation tests were thought to be free of sensor faults. In practice, sensor faults may occur to every sensor in centrifugal chillers. In order to enhance the accuracy, effectiveness and robustness of the chiller FDD scheme, a sensor FDD scheme capable of finding the possible existence of sensor faults and correcting faulty sensors is absolutely needed and will be presented in Chapter 6.

CHAPTER 6 SENSOR FDD&E SCHEME

The reliability and quality of measurements in centrifugal chillers play a very important role in the implementation of chiller FDD, efficiency monitoring and optimal control. Therefore, sensor faults need to be detected, diagnosed and corrected/replaced so as to ensure successful implementation of the above tasks. Based on the PCA (principal component analysis) method, a sensor FDD&E (Fault Detection, Diagnosis and Estimation) scheme for centrifugal chillers is developed. This chapter presents the sensor FDD&E scheme to handle sensor faults which might occur to sensors in centrifugal chillers. In the context of this chapter, the sensor fault estimation is an investigation of the deviation magnitude of a sensor fault from its true measurement. The PCA model-based sensor FDD&E is an important and indispensable part of the robust FDD strategy.

Section 6.1 identifies the problems associated with the implementation of the chiller FDD scheme and then proposes the need for a sensor FDD&E scheme. A sensor FDD&E scheme to deal with the problems is thus put forward in Section 6.2, where a PCA method, after a brief literature review of sensor FDD&E, is adopted to detect, diagnose and more importantly estimate sensor errors associated with the key measurements. Considering the thermophysical characteristics of the water-cooled centrifugal chillers, a PCA model is built to capture the correlations among the measurements. Two statistical approaches, i.e., *Q-statistic* plot and *Q-contribution* plot, are used to detect and diagnose sensor faults, respectively. In addition, an iterative approach is employed to estimate true

measurements as well as magnitudes of sensor bias errors.

Based on the methods developed in Section 6.2, the implementation structure of the sensor FDD&E scheme is proposed in Section 6.3. The summary of this chapter is given in Section 6.4.

6.1 The Need for Sensor FDD&E Scheme

At present, there are a great number of sensors installed in centrifugal chillers for various purposes such as efficiency monitoring, local-loop and supervisory control, and chiller FDD.

It can be observed in Chapter 3 and Chapter 5 that the performance of the basic chiller FDD scheme depends heavily on the quality of measurements from sensors. During reference model development, accurate measurements from all relevant sensors can help identify a reference model with desirable goodness-of-fit. In the course of online FDD implementation, accurate measurements also contribute greatly to reducing the uncertainty band of the residual of each performance index, and therefore help identify chiller faults accurately and promptly. Also, the measurements are often utilized by chiller control strategies to maintain chiller operation as expected and optimize it (Wang and Burnett 2001). Moreover, the continuous and accurate measurements of temperature, flow rate, electric power, refrigerant pressure, etc., are also essential to safety interlocks in chillers, quantification of effectiveness of energy-efficiency improvements (Phelan, J.

et al. 1997) and efficiency monitoring (Hartman T. B. 2001) in chillers. More detailed conclusions were presented in the IEA project, Annex 34 (Computer Aided Evaluation of HVAC System Performance).

Unfortunately, sensors in chillers are also subject to degradation and different faults may occur in them. As introduced in Chapter 1, faults associated with a sensor can be divided into two main categories, i.e., hard failures (complete failure) and soft faults. Soft faults can be further divided into the bias error which is the fixed or systematic component of the total error (McIntosh 1999), and the noise error which is the random fluctuating component of the total error. Although hard failures are very harmful to chiller monitoring and control, it is easy to handle them by using the data preprocessor developed in Section 3.3.1. As for noise errors, they can be taken into account and handled by the uncertainty analysis as presented in Chapter 3. However, little research has addressed sensor bias errors, which cannot be handled by the data preprocessor. The existence of sensor biases might result in great deficiency or even malfunctioning of chiller monitoring, control, optimization and FDD. For example, a direct way of measuring chiller cooling load by the product of the differential chilled water temperature and flow rate ($\Delta T \times M_{chw}$) is widely adopted in the calculation of chiller COP and in the chiller sequencing control (namely, determining the time of switching on or off a chiller). In typical chilled water systems in buildings, the differential chilled water temperature, ΔT, is usually small with a design value of around 5K. A bias error of 1K in both supply and return water temperature sensors alone may result in up to 40% error in the total cooling load calculation. Undoubtedly, both calculation of chiller *COP* and

chiller sequencing control will be susceptible to such sensor faults. An example of unfavorable effects of sensor bias errors on the implementation of chiller FDD follows. When $LMTD_{cd}$ is monitored to evaluate the performance of a condenser, the calculated $LMTD_{cd}$ will be unreliable if there is an error associated with the sensor measuring the leaving condenser water temperature. Therefore, the erroneous $LMTD_{cd}$ will make the chiller FDD scheme fail to get the true performance of the condenser and then draw incorrect FDD conclusions.

To sum up, in order to develop a robust FDD strategy, the errors associated with sensors, especially those involved in the basic chiller FDD scheme, should be properly tackled. In order to achieve this goal, a sensor FDD&E scheme needs to be implemented ahead of the implementation of the basic chiller FDD scheme.

6.2 Development of Sensor FDD&E Scheme

6.2.1 Background of Sensor FDD in HVAC&R Applications

To date, there have been relatively few applications of sensor FDD in HVAC&R systems as compared with the applications of component FDD in HVAC&R systems. Stylianou et al. (1996) studied a model-based method to detect soft sensor faults, aiming to make measurements reliable when monitoring the performance of a laboratory chiller. Lee et al. (2004) used general regression neural-network modes to investigate the detection and automatic recovery of a faulty supply air temperature sensor in an AHU (air handling

unit). These methods were designed to detect/diagnose only part of the sensors in the systems. Validating all or most of the sensors in the field is a much heavier and more complicated task. As for sensor faults in building cooling systems, e.g., sensor faults associated with building supply water temperature, building return water temperature and water flow rate in primary/secondary systems, a rule-based diagnosis and validation strategy was studied by Wang et al. (1999, 2002a, 2002b). Although the PCA method has been used in many engineering fields (Lennox et al. 2002, Pranatyasto et al. 2001), it was only recently introduced by Wang and Xiao (2004) into sensor FDD in AHUs (Air Handling Units) and proved to be an efficient means to generate useful residuals for sensor FDD. However, it is noteworthy that up to now there has been little published research directly aimed at sensor FDD for chillers. FDD for sensors in other HVAC&R systems, as mentioned above, has been investigated by many researchers. In centrifugal chiller systems, the measurements of temperature, pressure and electrical power consumption are the variables of greatest concern. Usually the variations of these variables in large water-cooled systems are relatively small when compared with measurements in other HVAC applications such as small chillers and AHUs, which are more susceptible to the ever-changing ambient conditions. Moreover, these variables are strongly correlated with each other through the cycling of refrigerant which interacts with compressor, chilled water and cooling water in the system. It might be expected that PCA's strong capability of capturing the correlations among these variables can make it applicable for sensor fault detection, diagnosis and estimation in chiller systems.

6.2.2 Characteristics and Advantages of PCA Method

The PCA method is one of the popular SPC (Statistical Process Control) methods which can simultaneously deal with the correlations among multiple system variables. In PCA methods, statistics are used to measure normal variance of the correlations among variables in a process. The upper and lower limits define the normal range of the variance of process variables. If the statistics exceed the normal range, it indicates that the correlations among the variables are destroyed and some abnormality has occurred.

The comparison between PCA-based FDD methods and conventional model-based FDD methods is shown in Figure 6.1. The PCA model can be considered as a kind of black box model, to help understand the PCA method without going into details of the PCA method. Since the PCA method uses a pure data-driven model to describe the target system, not much internal information about the system is required. Nevertheless, the PCA method is different from the FDD methods based on the conventional data-driven models like the neural network model. The latter basically has two groups of information, i.e., the inputs and the outputs, and the relationship between the two groups is mapped by the model. Residuals are generated as the differences between the model outputs and the real systems outputs with the same inputs. Significantly deviated residuals from a certain threshold indicate abnormality in the system. As for the PCA method, it regards all variables of concern as the inputs of the PCA model. Instead of simulating the real process, the PCA model captures correlations among the variables by using training data, which are representative of normal operation. The residual vector is generated as the

variances that cannot be captured by the PCA model trained by normal data. Usually, the Square Predicted Error (SPE) of the residual vector is used as a fault index. If the SPE violates a certain threshold which is also determined by the training data beforehand, it might be concluded that some abnormality has occurred.

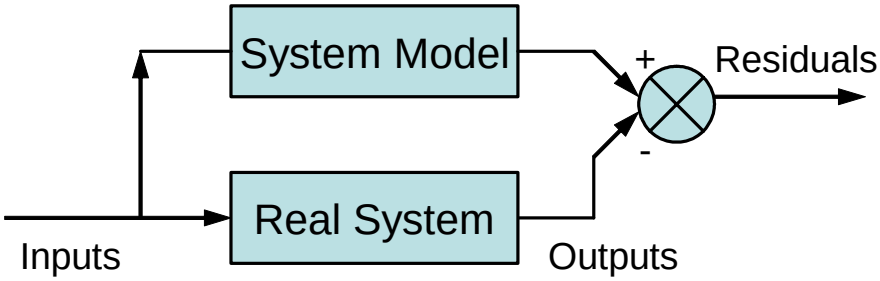

Figure 6.1 - (a) Schematic diagram of a conventional model-based FDD method

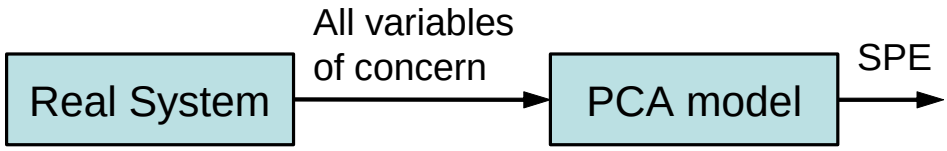

Figure 6.1 - (b) Schematic diagram of the PCA method

Figure 6.1 Comparison between the PCA model and a conventional model-based FDD method

It can be seen from the above comparison analysis that the PCA-based FDD method catches the correlations among system variables in a more straightforward way than conventional model-based FDD methods do. Thanks to this advantage, the time-consuming work associated with building and training complex physical or mathematical models as well as analyzing generated residuals can be avoided.

6.2.3 Outline of PCA Method

PCA is a multivariate statistical analysis technique, in which a group of correlated variables is transformed into a new group of variables which are uncorrelated or orthogonal to each other (Edward 1991 and Jolliffe 1986). By projecting the original correlated data into a lower-dimensional space using linear transformations, PCA is optimal in terms of capturing the variability of the data, and can greatly simplify and improve process monitoring procedures, instead of analyzing all the process variables. PCA can separate the observation space into two subspaces. One captures the systematic variations of the process and the other accounts for the random noise in the process. The applications of PCA in process monitoring, e.g., FDD, is motivated by its characteristic that applying a certain measure to each of the two subspaces can help indicate the sensitivity of the process monitoring method to a fault.

A data set of n observations and m process variables is used to construct a sample matrix $\mathbf{Z}$ ($\mathbf{Z} \in \Re^{n \times m}$), which is assumed in the following context to help illustrate the principle of using the PCA method in sensor FDD applications. Since variables in engineering systems usually have different units, these data need to be transformed into standard units by subtracting from each observation its mean and dividing by its standard deviation. This normalization makes the covariance matrix and the correlation matrix of $\mathbf{Z}$ the same. The mean of the ith variable, M_i, (corresponding to the ith column vector in the training matrix) is calculated by Equation (6.1). The standard deviation of the ith variable, σ_i, is calculated by Equation (6.2). The normalized sample matrix is then

calculated by Equation (6.3) and is denoted by matrix **X** ($\mathbf{X} \in \Re^{n \times m}$).

$$M_i = \frac{1}{n}\sum_{j=1}^{n} z_{j,i} \tag{6.1}$$

$$\sigma_i = \sqrt{\frac{1}{n-1}\sum_{j=1}^{n}(z_{j,i} - M_i)^2} \tag{6.2}$$

$$x_{j,i} = \frac{z_{j,i} - M_i}{\sigma_i} \tag{6.3}$$

where $z_{j,i}$ is an element of matrix **Z** and $x_{j,i}$ is an element of matrix **X.**

The covariance matrix of **X** can be obtained by Equation (6.4).

$$\mathbf{S} = \frac{\mathbf{X}^T\mathbf{X}}{n-1} \tag{6.4}$$

The eigenvalue decomposition of the covariance matrix **S** is obtained by similar transformation of **S**, as shown in Equation (6.5).

$$\mathbf{S} = \mathbf{U}\mathbf{\Lambda}\mathbf{U}^T \tag{6.5}$$

where the **Λ,** as shown in Equation (6.6), is a diagonal matrix of non-negative real eigenvalues with decreasing magnitude ($\lambda_1 > \lambda_2 > \ldots > \lambda_m$). **U** ($\mathbf{U} \in \Re^{m \times m}$) is a matrix whose columns are the corresponding eigenvectors. Where, $\mathbf{U}\mathbf{U}^T = \mathbf{I}$ and **I** is a *m*-dimensional unit matrix.

$$\mathbf{\Lambda} = \begin{bmatrix} \lambda_1 & & & \\ & \lambda_2 & & \\ & & \cdots & \\ & & & \lambda_m \end{bmatrix} \tag{6.6}$$

In order to effectively capture the system variations while minimizing the effect of random noise corrupting the PCA representation, only those eigenvectors in **U** associated with the first a ($a<m$) largest eigenvalues, are retained in the PCA model. In the PCA method, the retained eigenvectors and the number of the retained eigenvectors are called the loading vectors and the number of retained PCs (Principal Components), respectively. There are many ways to determine an optimal number of PCs, such as the proportion of trace explained method and the SCREE test (Jolliffe 1986).

The proportion of trace explained method chooses the number of a, i.e., the number of the loading vectors when the *CPV* (Cumulative Percent Variance*)* of the first a largest eigenvalues reaches a predetermined limit, CPV_α, e.g.,95%, as shown in Equation (6.7)

$$CPV(a) = \frac{\sum_{j=1}^{a} \lambda_j}{\sum_{j=1}^{m} \lambda_j} \times 100\% = \frac{\sum_{j=1}^{a} \lambda_j}{tr(\mathbf{S})} \times 100\% \geq CPV_\alpha \tag{6.7}$$

where $\sum_{j=1}^{m} \lambda_j$ is the sum of the eigenvalues and is equal to the trace of covariance matrix, $tr(\mathbf{S})$, which indicates the total system variance. $\sum_{j=1}^{a} \lambda_j$ is the sum of sample variance of the a PCs corresponding to the first a largest eigenvalues.

The SCREE test is a graphical technique plotting all of the eigenvalues in one graph in

decreasing order. The value of the eigenvalue is the ordinate and the number is the abscissa. There will be a break or knee between the first *a* largest values and the remaining ones. That is an effective clue for choosing the optimal number of *a*.

After the optimal number of retained vectors in **U** (also the number of retained PCs in the PCA method) is determined, e.g., to be *a*, a loading matrix, **P** ($\mathbf{P} \in \Re^{m \times a}$) can be obtained with its columns corresponding to the retained loading vectors in **U.** Therefore, the projections of the observations in **X** into the lower-dimensional space **Y** ($\mathbf{Y} \in \Re^{m \times a}$) are shown as follows.

$$\mathbf{Y} = \mathbf{XP} \tag{6.8}$$

For the *i*th loading vector $\mathbf{p}_i$

$$\mathbf{y}_i = \mathbf{X}\mathbf{p}_i \tag{6.9}$$

where the transformed variable $\mathbf{y}_i$ is called the *i*th principal component of **X.**

The projection of **Y** back into the *m*-dimensional observation space, $\hat{\mathbf{X}}$, which is called the score subspace, is shown by Equation (6.10). It is commonly accepted with certain assumptions that the portion of the score subspace corresponding to the first *a* largest eigenvalues describes most of the system variations occurring in the process (Wise et al. 1990). In this regard, $\hat{\mathbf{X}}$ is an accurate representation of the process under normal operation (Chiang et. al 2001).

$$\hat{\mathbf{X}} = \mathbf{YP}^T = \mathbf{XPP}^T \tag{6.10}$$

The difference between **X** and $\hat{\mathbf{X}}$ is indicated by the residual matrix **E**, which is called the residual subspace where abnormal variation and noise may occur.

$$\mathbf{E} = \mathbf{X} - \hat{\mathbf{X}} = \mathbf{X} - \mathbf{X}\mathbf{P}\mathbf{P}^T = \mathbf{X}(\mathbf{I} - \mathbf{P}\mathbf{P}^T) \tag{6.11}$$

For a new observation (row vector) after normalized into **x**, the difference between **x** and its estimate, $\hat{\mathbf{x}}$ (shown in Equation (6.12)), is the residual vector **e**, as shown in Equation (6.13). The difference, **e**, is also a projection of **x** into its residual subspace. Therefore, **x** can be decomposed into two orthogonal vectors, i.e., **x** and **e**, as shown in Figure 6.2.

$$\hat{\mathbf{x}} = \mathbf{x}\mathbf{P}\mathbf{P}^T = \mathbf{x}\mathbf{C} \tag{6.12}$$

where **C** is equal to $\mathbf{P}\mathbf{P}^T$ and is called identity matrix.

$$\mathbf{e} = \mathbf{x} - \hat{\mathbf{x}} = \mathbf{x}(\mathbf{I} - \mathbf{P}\mathbf{P}^T) = \mathbf{x}(\mathbf{I} - \mathbf{C}) \tag{6.13}$$

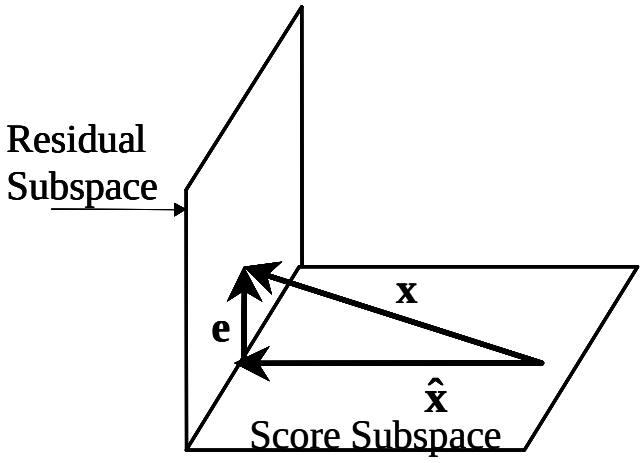

Figure 6.2 Decomposition of new sampled vector **x**

The PCA method implicitly assumes that the observation at one time instant is statistically independent of observations at past time instants. For most typical industrial

and engineering processes, this assumption is valid only for long sampling intervals. Kourti and MacGregor (1996) pointed out that in practice the presence of serial correlations in the data does not compromise the effectiveness of the static PCA method when there are sufficient data representing all the normal variations of the system.

6.2.4 PCA Method in Sensor FDD Applications

With respect to the applications of PCA to FDD, either the T^2-*statistic* (Hotelling 1947 and Kresta et al. 1991) or the *Q-statistic* (Edward and Mudholkar 1979), also known as the Squared Prediction Errors (SPE), can be used as an index of faulty conditions.

Statistic I: Q-statistic

As shown in Equation (6.14), the *Q-statistic* is defined as the squared sum of the residual vector which is actually the difference between an observation vector (**x**) and its PCA estimate ($\hat{\mathbf{x}}$).

$$Q-statistic = SPE = \mathbf{e}^T\mathbf{e} = \left\|\mathbf{x}-\hat{\mathbf{x}}\right\|^2 = \left\|\mathbf{x}\left(\mathbf{I}-\mathbf{P}\mathbf{P}^T\right)\right\|^2 \qquad (6.14)$$

When there is no fault in the new observation vector (**x**), the correlations among measurements in the new observation vector will still remain unchanged from those captured in the PCA model. Therefore, the *Q-statistic* will be less than its threshold, Q_α, as shown in Equation (6.15). However, when faults exist in the new observation vector,

the correlations among measurements will be destroyed and the *Q-statistic* will go beyond Q_α.

$$Q - statistic \le Q_\alpha \tag{6.15}$$

where Q_α is the threshold determined by Equation (6.16) (Edward 1991**)**..

$$Q_\alpha = \theta_1 \left[\frac{c_\alpha \sqrt{2\theta_2 h_0^2}}{\theta_1} + 1 + \frac{\theta_2 h_0 (h_0 - 1)}{\theta_1^2} \right]^{\frac{1}{h_0}} \tag{6.16}$$

where,

$$\theta_i = \sum_{j=a+1}^{m} \lambda_j^i \quad (i = 1,\ 2,\ 3) \tag{6.17}$$

$$h_0 = 1 - \frac{2\theta_1 \theta_3}{3\theta_2^2} \tag{6.18}$$

c_α is the confidence limit for the $1-\alpha$ percentage in a normal distribution; *a* is the number of principal components; *m* is the number of variables and λ_j are the eigenvalues of the covariance matrix. Given a certain level of confidence, α, the threshold for *Q-statistic*, Q_α, can be computed using Equation (6.16).

Statistic II: Hotelling T^2

The Hotelling T^2*-statistic* is the earliest multivariate statistic, which is a quantity indicating the overall conformance of an individual sample vector to its mean or an

established standard or reference.

Supposing **X** is the matrix of n samples (rows) of the m original variables (columns) after normalization, the T^2 *-statistic* can be given by Equation (6.19) (Tracy et al 1992).

$$T^2 = \mathbf{X}^T \mathbf{S}^{-1} \mathbf{X} \tag{6.19}$$

where **S** is the covariance matrix of **X** as shown in Equation (6.5).

Assuming the observations are randomly sampled from a multivariate normally distributed process, an upper control limit on the T^2 is given by Equation (6.20).

$$T^2_{UCL} = \frac{m(n-1)(n+1)}{n(n-m)} F_\alpha(m, n-m) \tag{6.20}$$

where $F_\alpha(m, n-m)$ is the upper 1-α percentage critical point of the F distribution with m and n-m degrees of freedom. A new multivariate sample that produces a T^2*-statistic* greater than the upper control limit will indicate that the process is out of control and faults exist in the process.

Substituting the similar transformation equation of **S** in Equation (6.19) for Equation (6.5) yields:

$$\begin{aligned} T^2 &= \mathbf{X}(\mathbf{U}\mathbf{\Lambda}\mathbf{U}^T)^{-1}\mathbf{X}^T \\ &= \mathbf{X}\mathbf{U}\mathbf{\Lambda}^{-1}\mathbf{U}^T\mathbf{X}^T \\ &= (\mathbf{X}\mathbf{U}\mathbf{\Lambda}^{-1/2})(\mathbf{X}\mathbf{U}\mathbf{\Lambda}^{-1/2})^T \end{aligned} \tag{6.21}$$

If only the loading vectors corresponding to the first a largest eigenvalues are used in the Equation (6.21), the equation will be rewritten as Equation (6.22).

$$T^2 = (\mathbf{XP\Lambda}_a^{-1/2})(\mathbf{XP\Lambda}_a^{-1/2})^T \quad (6.22)$$

where $\mathbf{\Lambda}_a$ is the diagonal matrix whose diagonal elements are corresponding to the first *a* largest eigenvalues retained in the PCA method. The upper limit of the T^2-*statistic* can also be determined by Equation (6.20), while substituting *a* for *m*.

The Hotelling T^2-*statistic* also assumes that the observation at one time instant is statistically independent of observations at other time instants. This can be a bad assumption for a short sampling interval in most engineering processes. However, if there are enough data in the training set to capture the normal system variations, the T^2-*statistic* will be an effective tool for process monitoring even if there are deviations from normality or the statistical independence assumption (Russell et al. 2000).

From the above introduction of the two popular statistics which can be used as indexes of faulty conditions, it is obvious that faults in the process can cause both the *Q-statistic* and the T^2- *statistic* to increase. An increase in T^2-*statistic* alone indicates that the change is consistent with the model; it may be just a shift of operating region (Dunia R. and Qin S.J. 1998). For example, when a chiller plant begins to run or stop, the change of water flow rate, which is actually not a fault, will increase T^2-*statistic* but not the *Q-statistic*. Considering the ambiguity of the T^2-*statistic* in discriminating faults from normal operation changes, the *Q-statistic* is used as the index for fault detection in this study.

Once a fault is detected using the *Q-statistic*, the next step is to identify the cause behind the fault. The aim of sensor fault diagnosis is to determine which process variable is most relevant to the fault and therefore to focus the operators and engineers on the place

where the fault occurred. Admittedly, the process of diagnosing a fault is rather complicated and challenging when the number of process variables is large.

Up to now, a PCA model used in FDD applications is constructed. It is not represented by some equations or logical descriptions as most conventional models introduced in Chapter 1. Actually, a PCA model involves several basic elements, including the loading vectors of the PCs which are used to decompose the observation space, the mean and standard deviation vectors which define a statistical average operation condition, and the threshold of the *Q-statistic* which is used to detect faults.

6.2.5 Sensitivity Analysis of PCA-based FDD&E Scheme

It is not always right to say that a sensitive sensor FDD method is preferable to a less sensitive one. If a sensor FDD method is very sensitive to faults, it will be at the same time very sensitive to normal system disturbances and measurement noise errors, which might result in many false alarms during applications of the sensor FDD method. On the other hand, if the method is too insensitive to faults, slight faults will not be detected promptly, let alone the need for preventative maintenance. Therefore, there is always a tradeoff between the sensitivity and the effectiveness of sensor FDD methods.

The factor which affects the sensitivity of the PCA-based FDD method most is the number of retained PCs in the PCA model. The more PCs are retained, the more

information about the correlations among concerned variables that is retained. However, it is worth pointing out that retaining more PCs also means more trivial and unstable correlations retained in the model. In this regard, the PCA model will be less sensitive. Therefore, there is an optimal number of retained PCs which can effectively capture the system variations while minimizing the effect of random noise on the PCA representation. Methods such as the proportion of trace explained method and the SCREE test are applicable to get the optimal number of the retained PCs (see Section 6.2.3). In addition, for a certain number of retained PCs, the smaller the confidence level at which the threshold of the *Q-statistic* is calculated, the lower the threshold will be and more sensitive the PCA model will be to faults. The confidence level of 95% or 97.5 % is an acceptable one for most engineering applications.

Moreover, the sensitivity of the PCA-based FDD method is also affected by the quality of the training data. A sufficient amount of training data is required to effectively capture the correlations among variables and to satisfy the requirements for defining the *Q-statistic*.

In order to improve the quality of training data and consequently obtain favorable sensitivity of the PCA model, training data need to be carefully selected. Data under steady state are used because under such a state the governing laws and rules are correctly reflected and the correlations among variables are more stable and consistent. Admittedly, there is seldom an optimal rule regarding the selecting of the training data. Some practical experience can help make such a choice. For example, the training data

should just cover as much typical operating conditions of centrifugal chillers as possible.

6.2.6 PCA Model of Centrifugal Chillers

As mentioned in Chapter 2, there are a lot of variables measured in a typical centrifugal chiller, and some of these measurements are closely correlated. However, it is very difficult and unnecessary to validate all the measurements because not all of them are crucial to basic chiller FDD, performance monitoring and optimal control. With reference to Table 2.1 in Chapter 2, the 13 variables, i.e., T_{chws}, T_{chwr}, T_{ev}, P_{ev}, T_{lcw}, T_{ecw}, T_{cd}, P_{cd}, T_{suc}, T_{dis}, M_{chw}, $M_{cw,}$, W_{elec}, are those of main concern in the basic chiller FDD, performance monitoring and optimal control. Therefore, these variables need to be considered in the sensor FDD&E. Among these variables, both M_{chw} and $M_{cw,}$ i.e., the chilled water flow rate and the cooling water flow rate, are usually maintained constant in a centrifugal chiller. Using the average of the historical measurements of these two variables is a simple and effective way to detect and diagnose faults associated with the flow meters. Therefore, the chilled water flow rate and condenser water flow rate are not considered in the PCA-based sensor FDD&E scheme in this thesis. The PCA model in this thesis includes the other 11 variables only. After various combinations of these variables were tested, it was found that including all the 11 variables in a single PCA model could produce satisfactory performance in the sensor fault detection, diagnosis and estimation. Matrix **A** represents the original matrix with *n* samples of the variables.

$$\mathbf{A} = \begin{bmatrix} T_{chws}^1 & T_{chwr}^1 & T_{ev}^1 & P_{ev}^1 & T_{lcw}^1 & T_{ecw}^1 & T_{cd}^1 & P_{cd}^1 & T_{suc}^1 & T_{dis}^1 & W_{elec}^1 \\ T_{chws}^2 & T_{chwr}^2 & T_{ev}^2 & P_{ev}^2 & T_{lcw}^2 & T_{ecw}^2 & T_{cd}^2 & P_{cd}^2 & T_{suc}^2 & T_{dis}^2 & W_{elec}^2 \\ \cdot & \cdot & \cdot & \cdot & \cdot & \cdot & \cdot & \cdot & \cdot & \cdot & \cdot \\ T_{chws}^n & T_{chwr}^n & T_{ev}^n & P_{ev}^n & T_{lcw}^n & T_{ecw}^n & T_{cd}^n & P_{cd}^n & T_{suc}^n & T_{dis}^n & W_{elec}^n \end{bmatrix}$$

The strong correlations among the variables in matrix **A** can be explained as follows. For a specific chiller system with constant chilled water and cooling water flow rates, the temperatures of chilled water (T_{chws} , T_{chwr}) as well as the entering condenser water temperature (T_{ecw}) are the determinant variables for operating conditions and performance of a centrifugal chiller with constant water flows (Braun 1988 and PG&E 2001). Clearly, these three deterministic variables, i.e., T_{chws} , T_{chwr} and T_{ecw}, are included in matrix **A**. At the same time, the 11 variable in matrix **A** are involved in the calculation of the performance indexes which indicate the chiller performance (see Table 3.1 in Chapter 3).

In addition, due to energy balance of the chiller under steady state, there are strong correlations among these 7 variables: W_{elec} , M_{chw} , T_{chws} , T_{chwr} , M_{cw} , T_{ecw} and T_{lcw}, ,as shown in Equation (6.24) and (6.25).

$$W_{comp} + Q_{evap} - Q_{cond} = 0 \tag{6.24}$$

$$W_{elec} + M_{chw} C_{pw} (T_{chwr} - T_{chws}) - M_{cw} C_{pw} (T_{lcw} - T_{ecw}) \approx 0 \tag{6.25}$$

According to the above analysis, it might be concluded that all the variables in matrix **A** are strongly correlated with each other from a perspective of thermophysics, and the correlations might be captured by the PCA method.

6.3 Implementation Structure of PCA-based Sensor FDD&E Scheme

The implementation structure of the PCA-based sensor FDD&E scheme is shown in Figure 6.3. It basically consists of two major groups of tasks, i.e., the training of PCA

models, and the online sensor FDD&E scheme. The PCA models should be obtained prior to the online application. After the online sensor FDD&E scheme is carried out, conclusions about the performance of the sensors can be made. Also, corresponding suggestions can be given in relation to sensor recalibration or replacement.

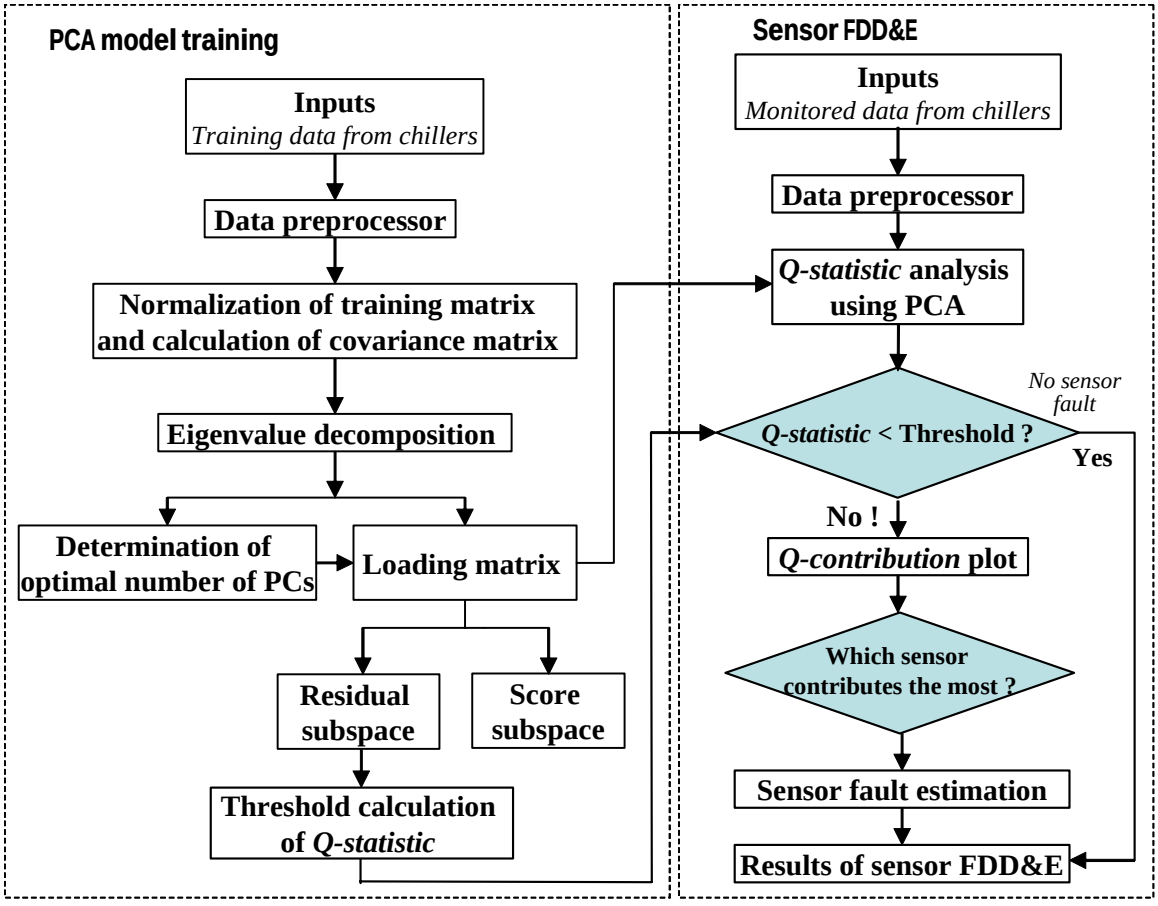

Figure 6.3 Flow chart of the sensor FDD&E scheme

6.3.1 Data Preprocessing

Two kinds of data are used in the implementation of the PCA-based sensor FDD&E scheme. One is the training data and the other is the monitored data. Their quality

determines the sensitivity and accuracy of the PCA method. Different methods are used to improve the equality of these two kinds of data.

The training data should be collected under normal operation of chillers without either sensor faults or chiller component faults. Therefore, commissioning and maintenance are needed before sampling training data. Moreover, in order to remove transient data and outliers, both the training data and the monitored data must go through the data preprocessor developed in Section 3.3.1.

6.3.2 PCA model Training

The original training matrix in the form of matrix **A** is constructed using measurements when the sensors and chiller system are all in normal condition. The training of the PCA model includes three main steps: *(i) decomposing of the covariance matrix of normalized training data; (ii) retaining loading vectors; (iii) determining the threshold of the Q-statistic*. The mean of the *i*th variable (corresponding to the *i*th column in the original training matrix) is calculated using Equation (6.1), and the variance of the variable is calculated using Equation (6.2). Because different variables in chiller systems have different units, columns of the training matrix need to be normalized by the calculated means and standard deviations into zero mean and unit variance. The purpose for this is to set all variables to a comparable magnitude so as to prevent a variable of larger numerical value from dominating the *Q-statistic*. Subsequently, the general procedures of the PCA method introduced previously are carried out as shown in the left part of

Figure 6.2. The eigenvalues and eigenvectors of the covariance matrixes of the normalized training matrix **X** can be obtained through its eigenvalue decompositions.

It is commonly accepted with certain assumptions that the loading vectors corresponding to the larger eigenvalues describe most of the system variations in the process, and the loading vectors corresponding to the smaller eigenvalues describe the random noise (Wise et al. 1990). In order to decouple the system variations from the random noise effectively, the optimal number of loading vectors should be retained in the PCA model. In this thesis, the number of loading vectors retained is determined by the proportion of trace explained method. The threshold of the *Q-statistic* is calculated by Equation (6.16) with a certain confidence level.

6.3.3 Online sensor FDD&E

The sensor FDD and the subsequent sensor fault estimation for centrifugal chillers can not only detect and diagnose faulty sensors but also obtain correct measurements and resume chiller FDD and optimal control there. The sensor fault FDD&E involves five main steps: *(i) preprocessing of incoming data; (ii) calculation of the Q-statistic of the model; (iii) sensor fault detection by comparing Q-statistic against its threshold; (iv) sensor fault diagnosis by the Q-contribution plot; (v) sensor fault estimation using an iterative approach.*

Fault detection

The sensor fault detection is made straightforward and understandable when the *Q-statistic* introduced previously is employed. After the monitored data pass through the data preprocessor, the remaining data are normalized by the means and standard deviations obtained during the PCA model training. The *Q-statistic* for each normalized sample will be calculated using the PCA model trained beforehand. When the *Q-statistic* is below its threshold calculated at a certain confidence level, it can be concluded that there is no faulty sensor in the chiller system. A faulty sensor condition is detected when the *Q-statistic* goes beyond the threshold, and a fault report/warning will be generated after a certain number of consecutive samples have been detected to contain abnormal measurements.

Fault diagnosis

Once a faulty sensor condition is detected, the contribution of individual variables to the *Q-statistic* is estimated as shown in Equation (6.26).

$$\eta_i = \frac{\|e_i\|^2}{Q - statistic} \tag{6.26}$$

where e_i presents the *i*th element of the residual vector **e** and η_i is the contribution of the *i*th variable to the squared sum of the residual vector, i.e., the *Q-statistic*. In principle, the larger the contribution a variable makes to the *Q-statistic*, the higher the possibility of a

fault in the variable. The *Q-contribution* plot is therefore generated and used to reduce the possible fault sources and thus focus on the most probable faulty sensor. The sensor is diagnosed to be faulty one when its *Q-contribution* value is the largest in the *Q-contributio*n plot.

Fault estimation

The objective of sensor fault estimation is to estimate the magnitude of the bias error and to acquire the true measurement value ($\mathbf{x}^*$) of the observation vector ($\mathbf{x}$), by using the remaining measurements in the observation vector, the constructed PCA model and the detected fault direction. If this procedure can be successfully implemented, the chiller FDD and control will be put back into normal operation even in the presence of sensor faults.

Three methods have been presented for the correction of a faulty sensor, namely the estimate of the true measurement value of the sensor. They are the iterative approach (Dunia et. al 1996), the missing data replacement approach (Martens and Naes, 1989) and the optimization approach (Wise and Ricker 1991). Actually, the three reconstruction methods give almost identical reconstructed results. In this study, the iterative approach is employed and explained as follows.

As introduced in the outline of PCA, the Equation (6.12) can be used to estimate the *i*th variable (x_i) from the observation vector (**x**). The estimated *i*th variable ($\hat{x}_i$) is used as the reconstruction of x_i, which can be expressed by Equation (6.27).

$$\begin{aligned}\hat{x}_i &= \mathbf{x}\mathbf{c}_i \\ &= \begin{bmatrix} x_1 & x_2 & \cdots & x_i & \cdots & x_m \end{bmatrix} \begin{bmatrix} c_{1i} & c_{2i} & \cdots & c_{ii} & \cdots & c_{mi} \end{bmatrix}^T \\ &= \mathbf{x}\begin{bmatrix} \mathbf{c}_{-i} & 0 & \mathbf{c}_{+i} \end{bmatrix}^T + x_i c_{ii}\end{aligned} \tag{6.27}$$

where,

$$\mathbf{C} = \mathbf{P}\mathbf{P}^T = \begin{bmatrix} \mathbf{c}_1 & \mathbf{c}_2 & \cdots & \mathbf{c}_m \end{bmatrix} \tag{6.28}$$

$$\mathbf{c}_i = \begin{bmatrix} c_{1i} & c_{2i} & \cdots & c_{ii} & \cdots & c_{mi} \end{bmatrix}^T = \begin{bmatrix} \mathbf{c}_{-i} & c_{ii} & \mathbf{c}_{+i} \end{bmatrix}^T \tag{6.29}$$

The subscripts *-i* and *+i* in Equation (6.29) denote a shorter row vector formed by the first *i*-1 and the last *m*-*i* elements of the original vector, respectively. The drawback of this approach is that the faulty sensor contained in **x** is used in the estimate. Therefore, the estimate is somewhat contaminated by the fault. To eliminate the effect of the faulty sensor, the estimate of the *i*th variable (x_i) is fed back again to the input and iterated until it converges to a value (x_i^*).

The iteration can be represented by Equation (6.30).

$$\hat{x}_i^{new} = \mathbf{x}\begin{bmatrix} \mathbf{c}_{-i} & 0 & \mathbf{c}_{+i} \end{bmatrix}^T + \hat{x}_i^{old} c_{ii} \tag{6.30}$$

As addressed by Dunia et al. (1996, 1998), the iteration in Equation (6.30) always converges. The converged value (x_i^*), regardless of the initial condition, for $c_{ii} < 1$ is

$$x_i^* = \frac{\mathbf{x}\begin{bmatrix}\mathbf{c}_{-i} & 0 & \mathbf{c}_{+i}\end{bmatrix}^T}{1 - c_{ii}} \tag{6.31}$$

and, $x_i^* = x_i$ for $c_{ii} = 1$. In this case,

$$\mathbf{c}_i = \begin{bmatrix}0 & 0 & \cdots & 1 & \cdots & 0\end{bmatrix}^T \tag{6.32}$$

is the *i*th column of the identity matrix (**C)**. This is the case where x_i is not correlated to the other sensors, but only to itself. In this case, the true measurement of this sensor cannot be reconstructed from the measurements from the other sensors. In this case, the sensor should not be included in the PCA model.

6.4 Summary

Besides chiller faults, sensor faults may also exist in centrifugal chillers. The existence of the sensor faults will not only lead to incorrect monitoring and unreliable control but also affect the reliability and accuracy of the implementation of chiller FDD schemes.

This chapter presents the sensor FDD&E scheme using the PCA method for a typical centrifugal chiller. The PCA method provides a good means of generating useful residuals for sensor fault detection and diagnosis. Another advantage of the PCA method in sensor FDD application is that the thresholds for fault detection can be easily calculated, at a specified confidence level, rather than empirically designated.

The PCA method demands that all variables in the PCA model should be closely correlated. Fortunately, the key variables in typical centrifugal chillers are closely

correlated with each other due to the cycling of refrigerant there. Therefore, these variables can be grouped into a PCA model which is capable of capturing the correlations among them. Moreover, since the PCA method is based on steady-state operation of the chiller, a data preprocessor is needed to eliminate transient data and outlier in the training and new monitoring data. The *Q-statistic*, the *Q-contribution* plot and an iterative approach are respectively used as tools for fault detection, diagnosis and estimation. The sensor FDD&E scheme will be validated in the following chapter using laboratory data from a centrifugal chiller in ASHRE 1043-RP.

CHAPTER 7 VALIDATION OF SENSOR FDD&E SCHEME

The PCA-based sensor FDD&E scheme presented in Chapter 6 is validated in this chapter using both laboratory data and field data respectively from the two test facilities introduced in Chapter 4. The validation results show that the sensor FDD&E scheme has great potential to enhance the accuracy of measurements from sensors in chillers, and therefore can provide a reliable premise for the implementation of the basic chiller FDD scheme.

Section 7.1 presents the validation tests of the sensor FDD&E scheme in the case where there are no chiller faults. The data from the one normal test in ASHRAE 1043-RP are used to train the PCA model and the data from another normal test were added with bias errors to generate data containing sensor faults. The generated data are used to evaluate the performance of the sensor FDD&E scheme in the case of no chiller fault. Similarly, the validation tests using field data from the chiller plant in a real building in Hong Kong are given in Section 7.2.

Section 7.3 examines the sensitivity of the sensor FDD&E scheme to typical chiller faults. In order to investigate whether simultaneous chiller faults could disturb the implementation of the sensor FDD&E scheme, the chiller data from different chiller-fault tests at various severity levels in ASHRAE 1043-RP were employed to test the sensitivity of the scheme to typical chiller faults, including excess oil, refrigerant leakage, refrigerant overcharge, condenser fouling and non-condensables in refrigerant Section

7.4 provides the validation of the sensor FDD&E scheme in the presence of chiller faults. The chiller data from each chiller-fault test at various severity levels were artificially corrupted with predetermined sensor bias errors to generate test data containing both chiller faults and sensor faults. The generated test data were then used to test the sensor FDD&E scheme. The summary of this chapter is given in section 7.5.

7.1 Validation Using Laboratory Data from ASHRAE 1043-RP

The validation tests on the PCA-based sensor FDD&E scheme are presented in this section. The tests were conducted using chiller data from the laboratory chiller in ASHRAE 1043-RP under the condition that there was no chiller fault but only sensor faults in the chiller.

7.1.1 Test Conditions

The chiller data from a normal operation test, called the “Normal” test in ASHRAE 1043-RP, which provides normal data for the parameter estimation of the reference models in Section 5.1.1, were also used in this section to train the PCA model. After the PCA model was trained, chiller data representative of sensor fault conditions were needed to validate the sensor FDD&E scheme. Many validation tests were conducted by adding various bias errors to the chiller data collected from normal tests provided in ASHRAE 1043-RP. As for the validation tests presented in this section, the chiller data

from a normal test, called “Normal NC”, were used to generate test data. The generated test data were then used to test the accuracy and sensitivity of the sensor FDD&E scheme in the case of no chiller fault.

7.1.2 PCA model Training

Using the normal data for the “Normal” test, the model training procedure in the sensor FDD&E scheme, as shown in Figure 6.2, was carried out to obtain the PCA model. Since the PCA-based FDD&E scheme is based on steady-state operation of the chiller system, both the PCA model training and the implementation of the scheme should use steady-state data. The data preprocessor developed in Section 3.3.1.is also employed in this chapter to preprocess data.

The number of original samples collected from the “Normal” test was 433. After the original samples passed through the data preprocessor, 159 samples remained. These samples were then used to construct a training matrix with a size of 159×11. Subsequently, the mean and standard deviation of each of the 11 variables were calculated. The variables in the matrix were afterwards transformed into standard units by subtracting from each observation its mean and dividing by its standard deviation. The loading vectors and their corresponding eigenvalues were then obtained by solving an eigenvalue decomposition of the covariance matrix of the normalized training matrix.

To determine the optimal number of maintained loading vectors, namely the number of

principal components, the proportion of trace explained method was adopted. This method is easy to understand and manipulate. The proportion of trace explained by the principal components is shown in Table 7.1. It is clear that the first three PCs explain 99.2356％of the total variance of the system. Therefore the first three largest PCs are retained in the PCA model. The threshold of *Q-statistic* at the confidence level of 95% is calculated to be 0.2985. Figure 7.1 shows the *Q-statistic* plot of the “Normal” test under normal sensor and component conditions. The *Q-statistics* of all samples are below the threshold value and no sample is detected to be abnormal. This shows that the PCA model is capable of capturing the major correlation and variance among the concerned 11 variables.

Table 7.1 Proportion of trace explained by PCs

The *i*th principal component	**Eigenvalues**	**Variance explained (%)**	**Cumulative variance explained (%)**
1	**6.0351**	**54.8645**	**54.8645**
2	**3.3370**	**30.3363**	**85.2008**
3	**1.5438**	**14.0348**	**99.2356**
4	0.0521	0.4733	99.7089
5	0.0239	0.2172	99.9261
6	0.0045	0.0405	99.9666
7	0.0015	0.0133	99.9799
8	0.0012	0.0108	99.9907
9	0.0006	0.0053	99.996
10	0.00025	0.0023	99.9983
11	0.00019	0.0018	100

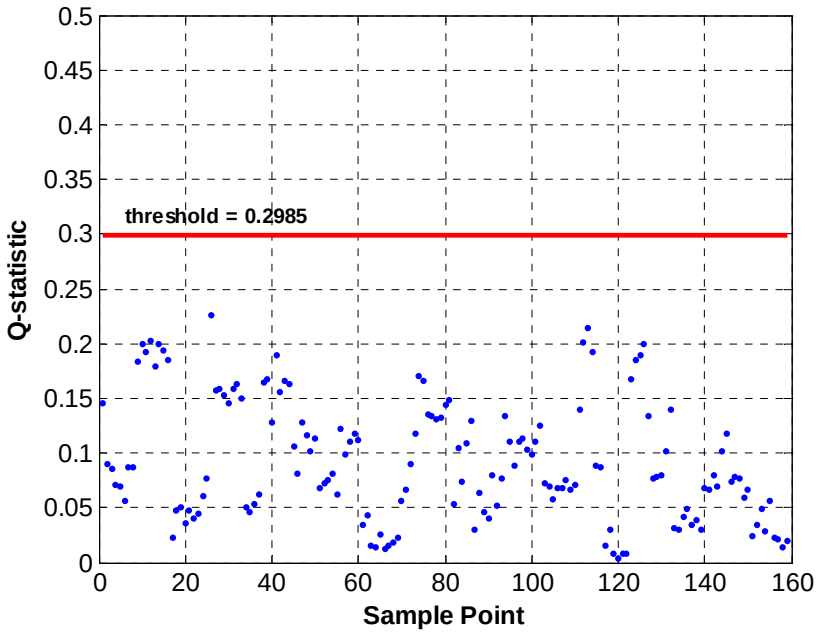

Figure 7.1 *Q-statistic* plot of training data from "Normal" test in ASHRAE 1043-RP

7.1.3 Generation of Test Data

Various predetermined bias errors were added to the corresponding measurements from the "Normal NC" test to generate test data containing sensor faults. The magnitudes of the bias errors added to these measurements are described in Table 7.2. Only one sensor was set to be biased at a time as the chance of simultaneous multiple sensor faults is low. Also, only the sensors which are not involved in any feedback control of the chiller were added with biases. The reason for this arrangement is clear: it is impossible to simulate the real operation of the chiller system by simply adding a bias to a variable used in a feedback control loop without simulating its effects on other variables. Since the chilled water supply water temperature (T_{chws}) and the entering condenser water temperature

(T_{ecw}) are usually involved in chiller control, only one of the rest nine sensors, i.e., T_{chwr}, T_{ev}, P_{ev}, T_{lcw}, T_{cd}, P_{cd}, T_{suc}, T_{dis} and W_{elec} , was added with a bias error in each test. In addition, the data from the "Normal NC" test were also directly used to test the sensor FDD&E scheme. Therefore, there are a total of ten test cases. Among them, one case has only normal sensor condition, and the other nine cases, each targeting one selected sensor, test faulty sensor conditions.

7.1.4 Test Results

The sensor FDD&E procedure, as shown in Figure 6.2, was implemented to process the generated test data.

Test case using normal laboratory data from the "Normal NC"

The *Q-statistic* plot of the test data directly from the "Normal NC" test is shown in Figure 7.2. Clearly, almost all *Q-statistic* values in this normal test were below the threshold. Therefore, it can be concluded that no sensor fault existed in any sensor.

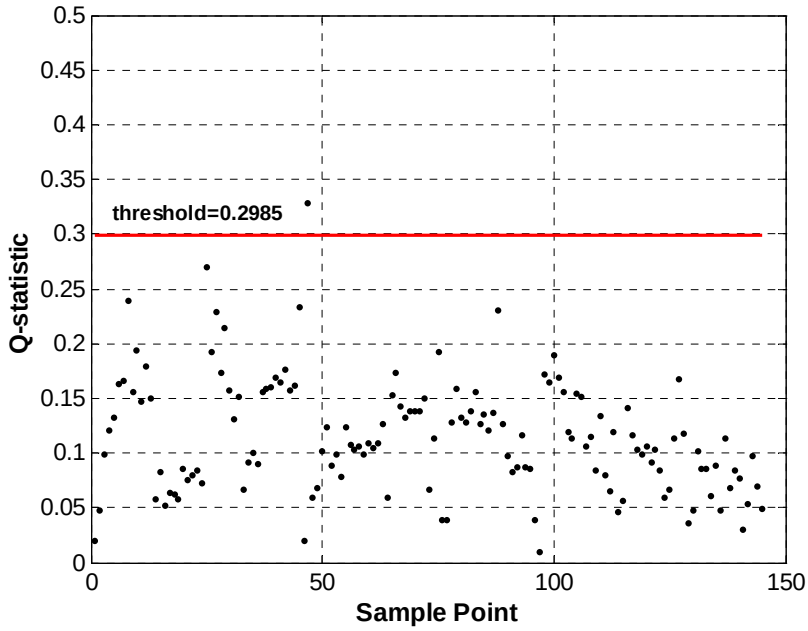

Figure 7.2 *Q-statistic* plot of test data directly from "Normal NC" test in ASHRAE 1043-RP – no sensor was biased

Test cases using test data containing sensor faults

The general test results of the nine test cases using test data containing sensor faults are given in Table 7.2. In this table, the "Detection ratio" is the ratio of the number of samples whose, *Q-statistic* values go beyond the threshold, to the total number of samples used in the test. The "Diagnosis ratio" is the ratio of the number of samples which are successfully diagnosed to the number of samples which are detected to contain a fault. The "Relative estimation error" is the ratio of the absolute difference between the estimated bias error and the added bias error to the added bias error. The "Estimated bias" is the average value of the estimated biases of all the samples which are successfully diagnosed.

Table 7.2 General results of validation tests using test data generated from "Normal NC" test in ASHRAE 1043-RP

	Added bias	**Detection ratio**	**Diagnosis ratio**	**Estimated bias**	**Relative estimation error**
T_{chwr}	+2.2°C	100%	95.97%	+2.37°C	7.64%
T_{ev}	+1.2°C	99.32%	98.64%	+1.06°C	11.90%
P_{ev}	+20kPa	100%	100%	+18.42kPa	7.88%
T_{lcw}	+3.5°C	100%	100%	+3.64°C	3.90%
T_{cd}	+3.5°C	91.90%	100%	+3.56°C	1.58%
P_{cd}	+75kPa	100%	100%	+74.30kPa	0.93%
T_{suc}	+1.5°C	95.27%	100%	+1.61°C	7.11%
T_{dis}	+7°C	93.92%	100%	+7.21°C	3.00%
W_{elec}	+12kW	48.28%	100%	+13.17kW	9.71%

The added bias error to each sensor is around 15% of the average of the measurements from the sensor. It can be found from Table 7.2 that most of the added biases can be estimated accurately with all "Relative estimation error" values not more than 11.90%. Also, almost all added bias errors were detected and diagnosed with all "Detection ratio" values not less than 91.90% and diagnosed with all "Diagnosis ratio" not less than 95.97%, except the one added to the electrical power input whose "Detection ratio" values is 48.28%. This might be explained as follows. The electrical power input is more affected by the determinant variables such as the chilled water temperature and cooling load than other measurements. Since the determinant variables (also the control variables in the laboratory chiller) experienced significant changes during the tests, the electrical power input tended to experience a wider range of variation, which is difficult for the PCA model to allow for. Therefore, if there is a bias error with the measurement of the electrical power input, it is relatively difficult for the PCA-based sensor FDD&E scheme

to tackle the fault. However, in practical applications, the measurement of electrical power is much more accurate and more reliable than temperature and pressure measurements.

The *Q-statistic* and *Q-contribution* plots in the test cases for three sensors, T_{chwr}, P_{ev} and W_{elec}, are presented respectively in this section to illustrate the results of the validation tests. The test cases for the other sensors are given in the attached CD and similar conclusions can also be drawn from them.

Figure 7.3 gives the *Q-statistic* plot of the test data generated by adding a bias error of +2.2^{o}C to T_{chwr} in the data from the "Normal NC" test. Clearly, most *Q-statistic* values in this test were above the threshold when +2.2^{o}C bias error was added to the sensor of T_{chwr}. Figure 7.4 shows the results of sensor fault diagnosis using the *Q-contribution* plot of the test data. It should be pointed out that each column in the figure represents a mean of the contribution values of five samples which were consecutively detected to be faulty. The purpose of this handling was to eliminate as much as possible the effect of system noise on the fault diagnosis. It can be observed in Figure 7.4 that the *Q-contribution* of T_{chwr} , signified by " ◪ " , was much higher than that of other sensors when a bias error of +2.2°C existed in T_{chwr}. Therefore, the biased sensor, T_{chwr}, was identified correctly. The bias of the faulty sensor was also estimated accurately by the fault estimation approach with a relative error of 7.64%, and the results are shown in Table 7.2.

Similarly, the *Q-statistic* plots in the test cases with bias errors of +20kPa and +12kW respectively added to P_{ev} and W_{elec} are shown in Figure 7.5 and Figure 7.7, and the corresponding *Q-contribution* plots are given in Figure 7.6 and Figure 7.8, respectively.

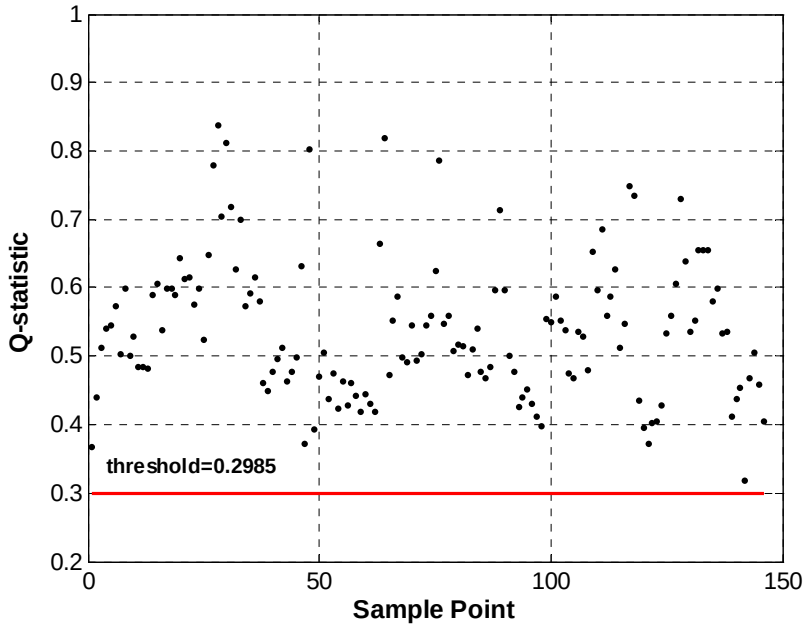

Figure 7.3 *Q-statistic* plot of test data from "Normal NC" test in ASHRAE 1043-RP – T_{chwr} was biased with +2.2°C

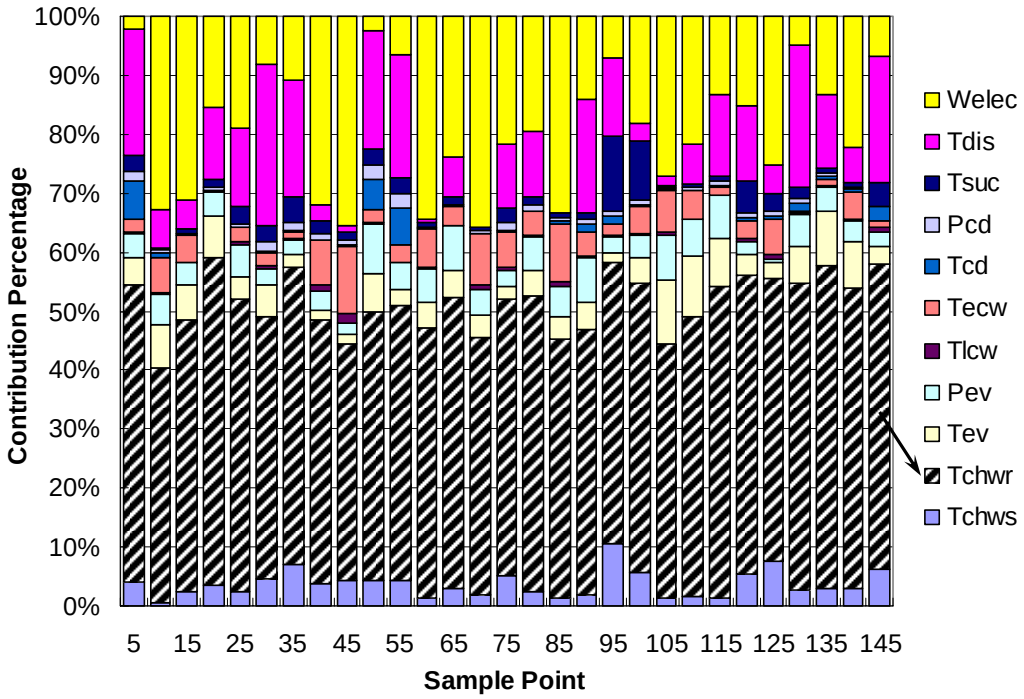

Figure 7.4 *Q-contribution* plot of test data from "Normal NC" test in ASHRAE 1043-RP – T_{chwr} was biased with +2.2°C

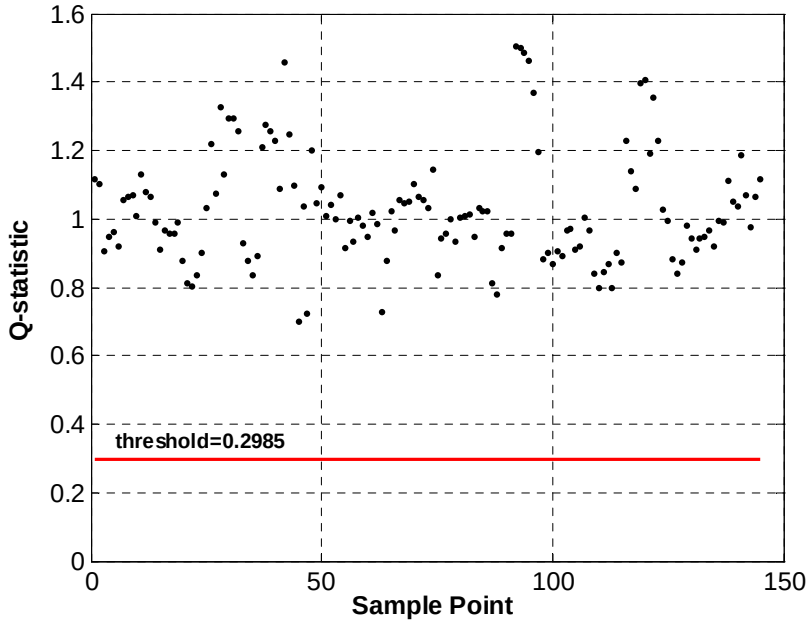

Figure 7.5 *Q-statistic* plot of test data from "Normal NC" test in ASHRAE 1043-RP – P_{ev} was biased with +20kPa

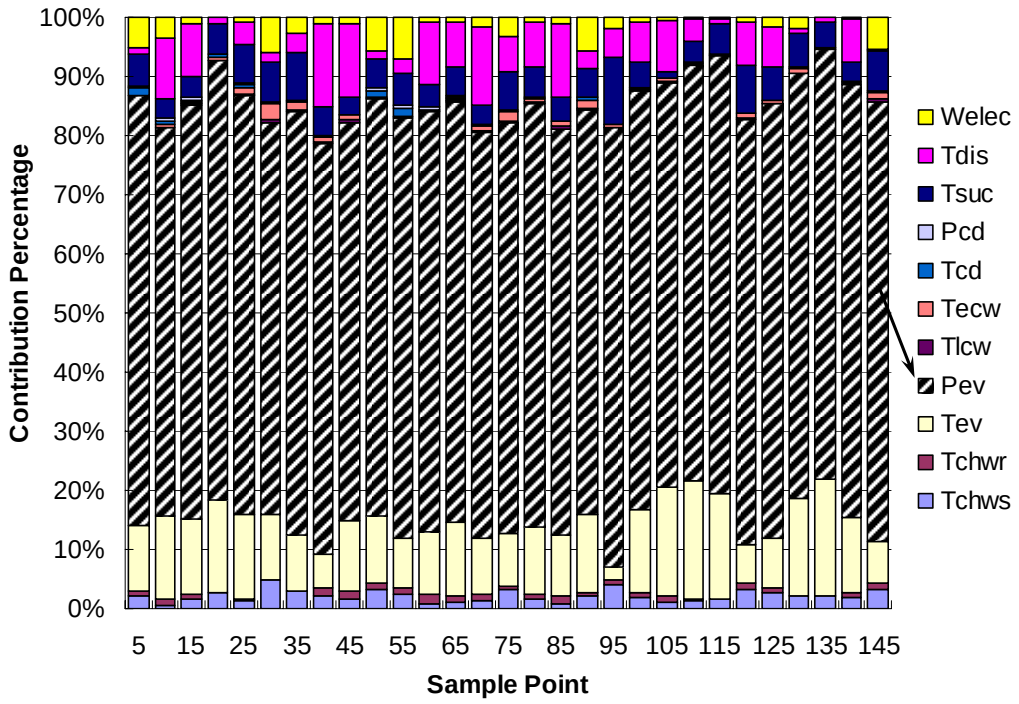

Figure 7.6 *Q-contribution* plot of test data from "Normal NC" test in ASHRAE 1043-RP – P_{ev} was biased with +20kPa

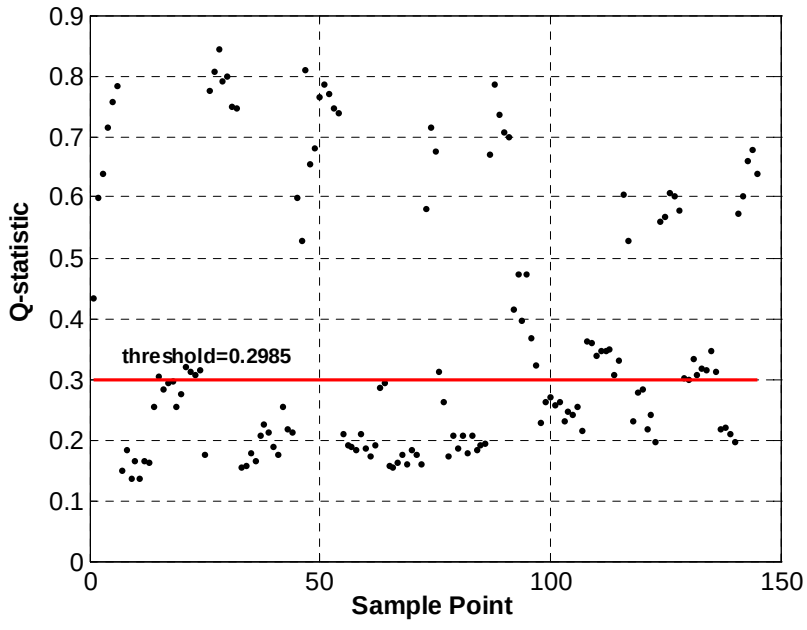

Figure 7.7 *Q-statistic* plot of test data from "Normal NC" test in ASHRAE 1043-RP – W_{elec} was biased with +12kW

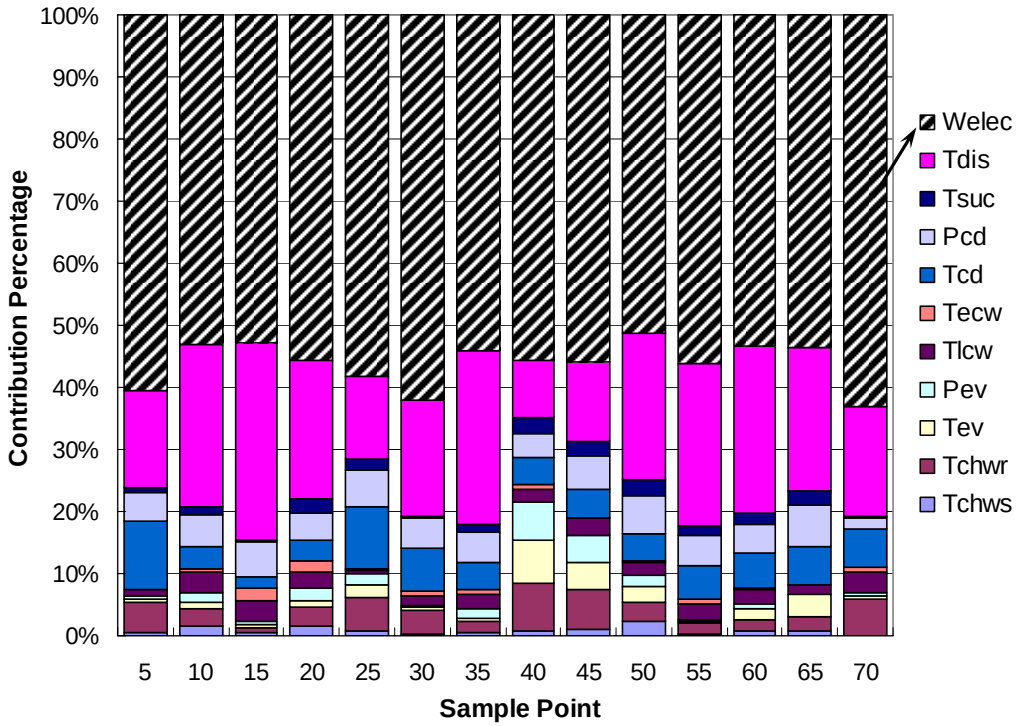

Figure 7.8 *Q-contribution* plot of test data from "Normal NC" test in ASHRAE 1043-RP – W_{elec} was biased with +12kW

7.2 Validation Using Field Data from a Real Building Chiller System

7.2.1 Test Conditions

The PCA-based sensor FDD&E scheme was also validated using field data from the real building chiller plant introduced in Chapter 4, as part of efforts to push the scheme closer to field application. The chiller plant of the building operates all day. The data collected from the BMS on July4th, 2001 were used to train the PCA model. The operation of the whole chiller plant could be guaranteed to be normal and fault-free as it had just gone through routine maintenance services before. Data three days, i.e., July 5th, 10th and 13th **,** were used to generate test data. Totally, 24 (8 sensors/day×3 days) validations tests

were conducted using the generated test data to test the fault detectability and isolability of the sensor FDD&E scheme. For conciseness, only the test results using the data collected on July 5th, 2001 are presented in this thesis. For results of other test cases, please refer to the attached CD. During such a short operating period of one day, the determinant variables of centrifugal chillers, e.g., the chilled water supply temperature and the entering condenser water temperature, varied within a small range due to the internal control of the chillers and the slowly changing ambient conditions. The PCA method could easily capture the systems trend because the determinant variables did not vary significantly.

7.2.2 PCA model Training

Using the data from July 4th, 2001, the PCA model training procedure in the sensor FDD&E scheme, as shown in Figure 6.2, was implemented to train the PCA model. The number of original samples used for model training was 894. After passing through the data preprocessor, 301 samples remained. These samples were used to train the PCA model. Note, since the measurement from T_{suc} was not available in the BMS of the building, this variable was not included in the training matrix **A** and the number of sensors investigated in this validation was 10.

The number of principal components (a=3) and the *Q-statistic* threshold of 95% confidence level (Q_α=0.58341) were determined in the same way as described in Section 7.1.2. The three principal components corresponding to the first three largest eigenvalues

explain 98.1846％of the total variance of the system. Figure 7.9 shows the *Q-statistic* values of 92.03 % samples were below the threshold. The total number of samples detected to be abnormal was 24 (7.97 %). That means that the PCA model can also capture the major correlations among these key variables in the field centrifugal chiller.

Table 7.3 Proportion of trace explained by PCs

The *i*th principal component	**Eigenvalue**	**Variance explained (%)**	**Cumulative variance explained (%)**
1	**7.1727**	**71.727**	**71.727**
2	**2.3245**	**23.245**	**94.972**
3	**0.32126**	**3.2126**	**98.1846**
4	0.13481	1.3481	99.5327
5	0.020754	0.20754	99.74024
6	0.011327	0.11327	99.85351
7	0.0074549	0.074549	99.92806
8	0.0039825	0.039825	99.96788
9	0.002594	0.02594	99.99382
10	0.00053718	0.0053718	100

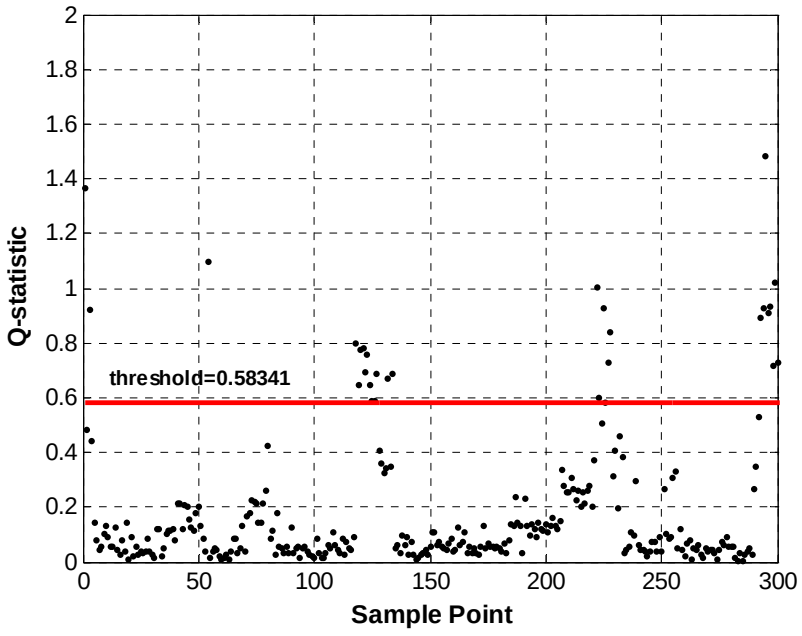

Figure 7.9 *Q-statistic* plot of training data from a real building in Hong Kong on July 4th, 2001

7.2.3 Generation of Test Data

Various predetermined bias errors were added to the corresponding measurements collected from the BMS on July 5th, 2001 so as to generate test data containing sensor faults. The magnitudes of the bias errors are described in Table 7.2. For the same reason given in section 7.1.3, only one sensor was set biased at a time and only readings from the sensors not used for feedback control were added with bias errors. That is to say, the measurements from one of T_{chwr}, T_{ev}, P_{ev}, T_{lcw}, T_{cd}, P_{cd}, T_{dis} and W_{elec} were respectively added with a bias error in each test. Moreover, the data collected on July 5th, 2001 were also directly used to test the sensor FDD&E scheme. Therefore, there are a total of 9 test cases. Among them, one case tested normal sensor condition, and 8 cases, each targeting one selected sensor, tested faulty sensor conditions.

7.2.4 Test Results

The sensor FDD&E procedure in the sensor FDD&E scheme was implemented to process the test data after the training of the PCA model, as shown in Figure 6.2.

Test case using field data collected on July 5th

The *Q-statistic* plot of the test data directly collected on July 5th, 2001 is shown in Figure 7.10. Obviously, almost all the *Q-statistic* values in this test were below the threshold

and that means no sensor fault existed in any sensor. The explanation is that the test data used were free from faults as they were collected immediately after routine maintenance.

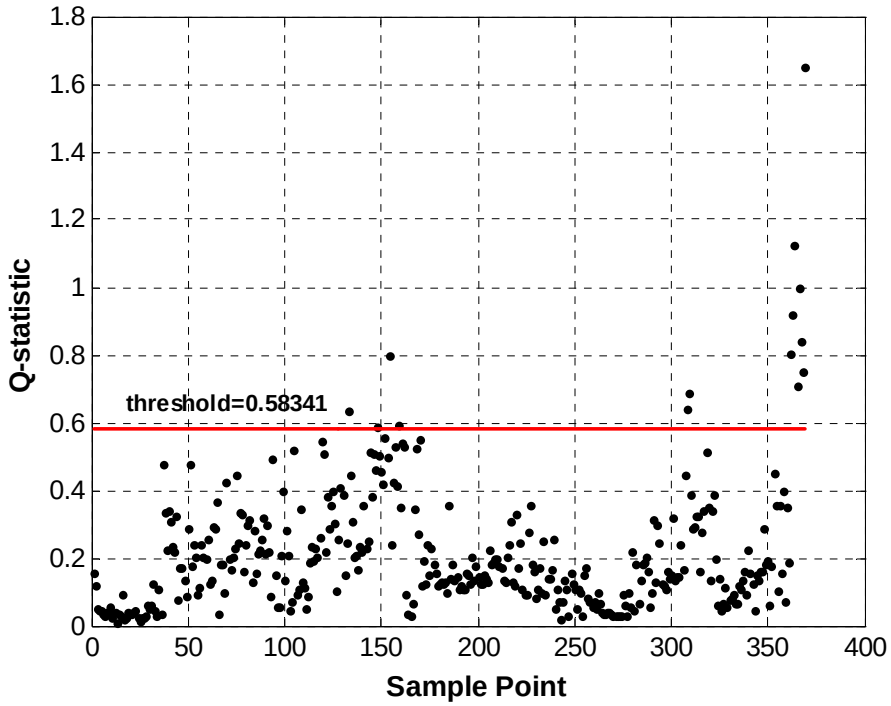

Figure 7.10 *Q-statistic* plot of test data directly from a real building on July 5th, 2001 – no sensor was biased

Test cases using test data containing sensor faults

General results of the validation tests are provided in Table 7.4. The added bias error to each sensor is around 15% or less of the average of measurements from the sensor. It is clear from Table 7.4 that most of the added sensor biases could be estimated accurately with all "Relative estimation error" values not more than 10.03%. Moreover, almost all added bias errors were detected and diagnosed with all "Detection ratio" values not less than 82.93% and all "Diagnosis ratio" value not less than 94.82%. Obviously, the test

results shown in Table7.4 are better than those shown in Table 7.2. The reason for this is that the slowly changing ambient conditions of the field chiller allow better performance of the PCA-based sensor FDD&E scheme.

Just as in Section 7.1, only the *Q-statistic* and *Q-contribution* plots of the test cases concerning the three sensors, T_{chwr}, P_{ev} and W_{elec}, are presented in this section to illustrate the results of the validation tests, and those in relation to the other sensors are presented in the attached CD.

Table 7.4 General results of validation tests using test data generated from field data collected from a real building in Hong Kong on July 5th, 2001

	Added bias	**Detection ratio**	**Diagnosis ratio**	**Estimated bias**	**Relative estimation error**
T_{chwr}	+1.8°C	100%	99.73%	+1.62°C	10.03 %
T_{ev}	+0.8°C	99.46%	94.82%	+0.75°C	6.48%
P_{ev}	+50kPa	100%	100%	+49.14kPa	1.72%
T_{lcw}	+3°C	100%	100%	+3.00°C	0.15%
T_{cd}	+3°C	100%	100%	+3.00°C	0.01%
P_{cd}	+100kPa	100%	100%	+100.19kPa	1.90%
T_{dis}	+7°C	100%	100%	+7.15°C	2.17%
W_{elec}	+90kW	82.93%	95.75%	+97.32kW	8.14%

Figure 7.11 shows the *Q-statistic* plot of test data, which were generated by adding a bias error of +1.8°C to T_{chwr} in the field data collected on July 5th. It can be observed that nearly all the *Q-statistics* values were above the threshold. The sensor faults were successfully detected. Figure 7.12 shows the results of sensor fault diagnosis using the *Q-contribution* plot of the PCA model. When a bias error existed in T_{chwr}, the *Q-*

contribution of it was much higher than those of other sensors at the same time. In order to avoid the effects of systems noise, each column in the figure was designed to represents a mean of the contribution values of ten samples which are consecutively detected to be faulty. The biases of the faulty sensors were also estimated correctly and the results are shown in Table 7.4.

Similarly, the *Q-statistic* plots in the test cases that bias errors of +20kPa and +12kW were respectively added to P_{ev} and W_{elec} are shown in Figure 7.13 and Figure 7.15, and their corresponding *Q-contribution* plots are given in Figure 7.14 and Figure 7.16, respectively.

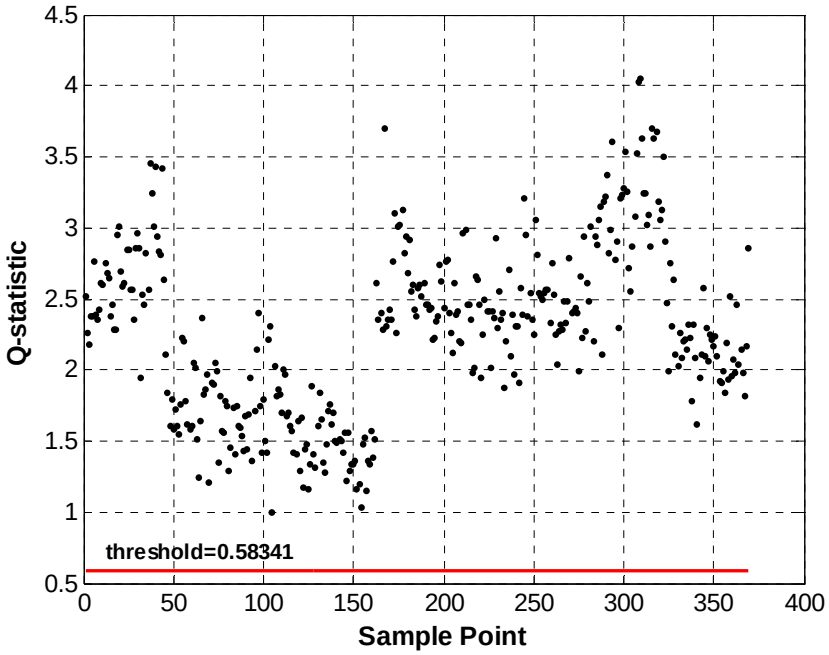

Figure 7.11 *Q-statistic* plot of test data from a real building on July 5th, 2001 – T_{chwr} was biased with +1.8°C

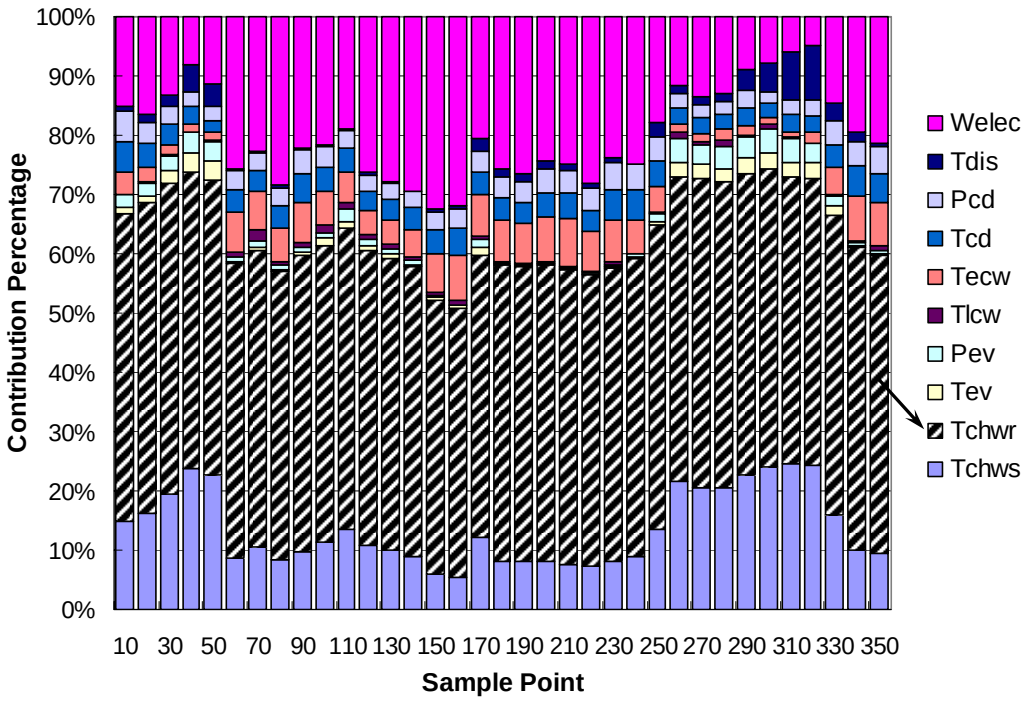

Figure 7.12 *Q-contribution* plot of test data from a real building on July 5th, 2001 – T_{chwr} was biased with +1.8°C

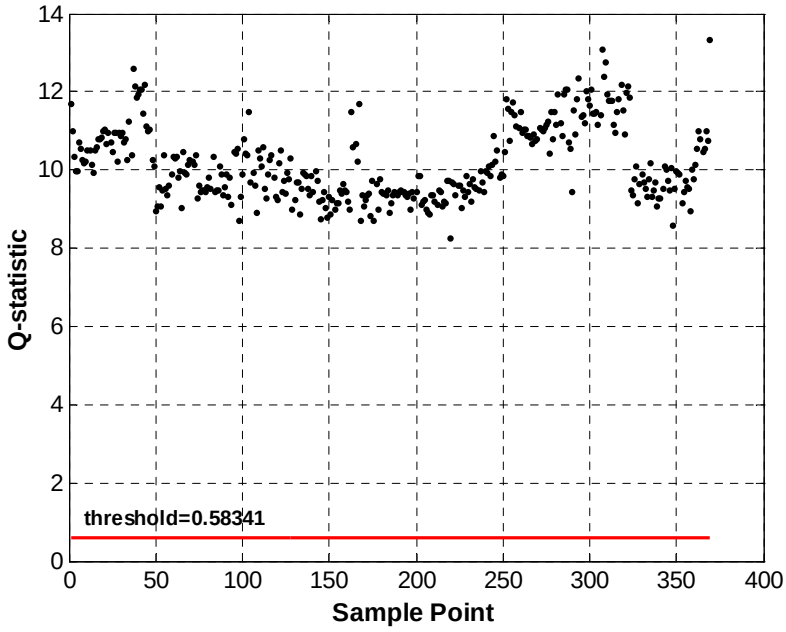

Figure 7.13 *Q-statistic* plot of test data from a real building on July 5th, 2001 – P_{ev} was biased with +50kPa

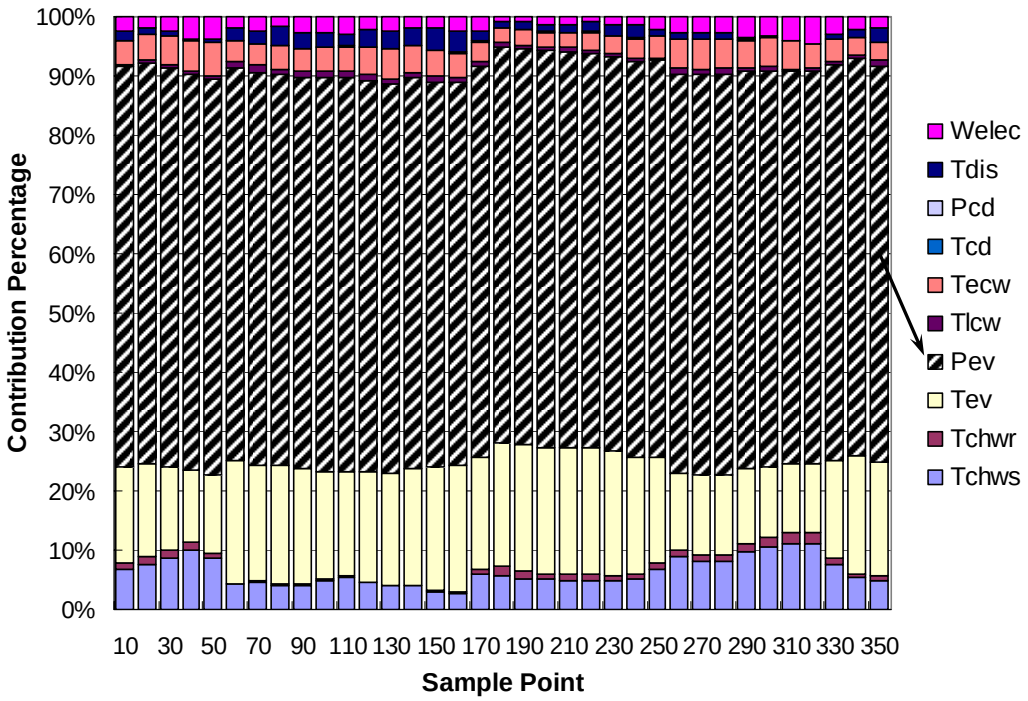

Figure 7.14 *Q-contribution* plot of test data from a real building on July 5th, 2001 – P_{ev} was biased with +50kPa

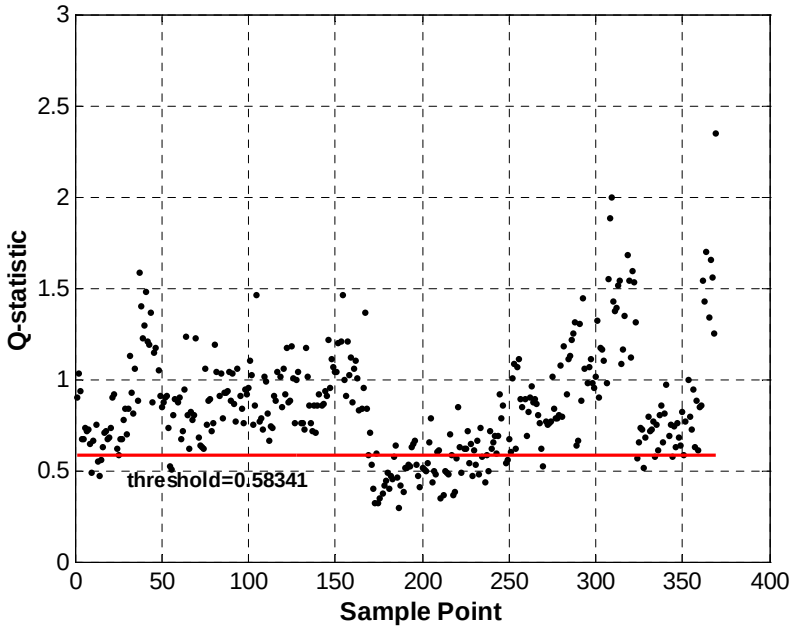

Figure 7.15 *Q-statistic* plot of test data from a real building on July 5th, 2001 – W_{elec} was biased with +90kW

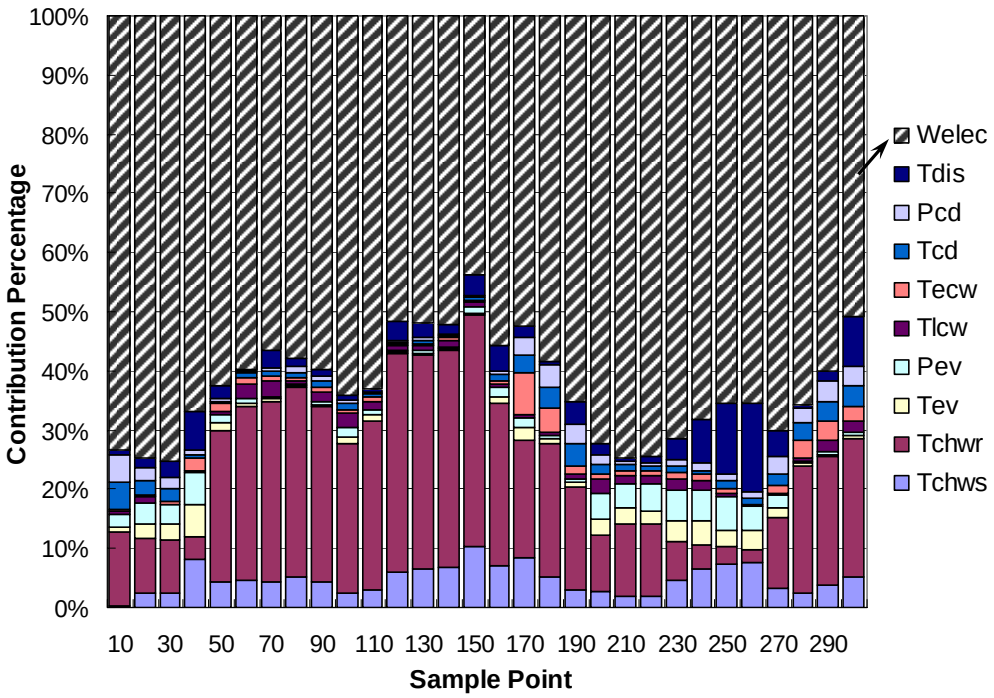

Figure 7.16 *Q-contribution* plot of test data from a real building on July 5th, 2001 - W_{elec} was biased with +90kW

7.3 Sensitivity of the Output of PCA Model to Chiller Faults

As mentioned in Chapter 1, both sensor faults and chiller faults can occur simultaneously in chillers. The sensor FDD&E scheme based on the PCA model is proposed with the aim to ensure measurement quality of the variables, which are crucial to chiller FDD and optimal control. Naturally, a series of questions rise as follows. Does the existence of chiller faults affect the output (i.e, the *Q-statistic*) of the PCA model and the implementation of the sensor FDD&E scheme? If the answer is affirmative, then what is the extent of the effect? To guarantee favorable reliability and accuracy of the sensor FDD&E and the subsequent chiller FDD, it is essential to answer these questions. And, the kernel of the problem is to find out whether and to what extent the *Q-statistics* of the

PCA model are sensitive to chiller faults. If the *Q-statistics* is immune to the chiller faults, it would be expected that the implementation of the PCA-based sensor FDD&E scheme would be immune from the chiller faults. Therefore, the sensor FDD&E scheme would be capable of successfully fulfilling its duty regardless of the existence of chiller faults. Otherwise, a supplementary approach is needed to differentiate sensor faults from chiller faults.

The chiller data containing various typical chiller faults are absolutely needed for the sensitivity test. In this thesis, the chiller data from various fault tests in ASHRAE 1043-RP were employed to study the sensitivity of the *Q-statistics* to typical chiller faults, which include refrigerant leakage, refrigerant overcharge, excess oil, condenser fouling, and non-condensables in refrigerant. Please note that a fault, namely refrigerant overcharge, was not selected for investigation in the basic chiller FDD scheme in Chapter 3. Including this additional chiller fault in the sensitivity analyses can help us find out whether this chiller fault would have some unexpected effects on the *Q-statistic*. For each chiller fault, the laboratory data from 4 different levels of fault severity were used to study the sensitivity of the *Q-statistic* to the chiller fault as well as the impact of fault severity levels on the sensitivity.

During the sensitivity tests, the PCA model used was trained by the same training data used in Section 7.1.2. The number of principal components (a=3) and the *Q-statistic* threshold of 95% confidence level (Q_α=0.2985) were determined in the same way as described in Section 7.1.2.

Figures 7.15 to 7.19 show the *Q-statistic* plots of test data from the five chiller-fault tests each at 4 different levels of fault severity. It is very clear from these figures that most *Q-statistic* values under the conditions of most chiller faults, at different levels of severity, are below the threshold. There are two exceptions in the tests. One is the non-condensables in refrigerant and the other is refrigerant overcharge at higher levels of severity. However, it is unusual to see refrigerant overcharge at higher severity levels, say greater than 30% overcharge. The strong sensitivity of the *Q-statistic* to non-condensables in the refrigerant can be explained as follows. The condensing pressure is increased substantially when non-condensable gases settle in the condenser during operation, but the actual temperature increases by only a small amount. The collected condensing temperature is derived from condensing pressure using saturation tables. Therefore, the collected condensing temperature is higher than its actual value, and from this perspective, this fault is in fact a kind of sensor fault to which the PCA model is sensitive.

Chiller faults are pertinent to performance degradations that are physically explainable and belong to systems variations captured by the PCA model. Therefore, the output of the PCA model, i.e., *Q-statistic*, is insensitive to these chiller faults. Therefore, it can be concluded that when there is no sensor fault, the *Q-statistic* will remain below the threshold even in the case of typical chiller faults. That is to say, the output of the PCA model on which the sensor FDD scheme is based is insensitive to most typical chiller faults but sensitive to sensor faults only. Thanks to this fact, the *Q-statistic* can be used as an index to differentiate sensor faults from chiller faults.

Based on the above test results, it might be expected that the PCA-based sensor FDD&E scheme would still be capable of detecting and diagnosing sensor faults even in the presence of chiller faults. This tentative conclusion will be validated by tests in the following section.

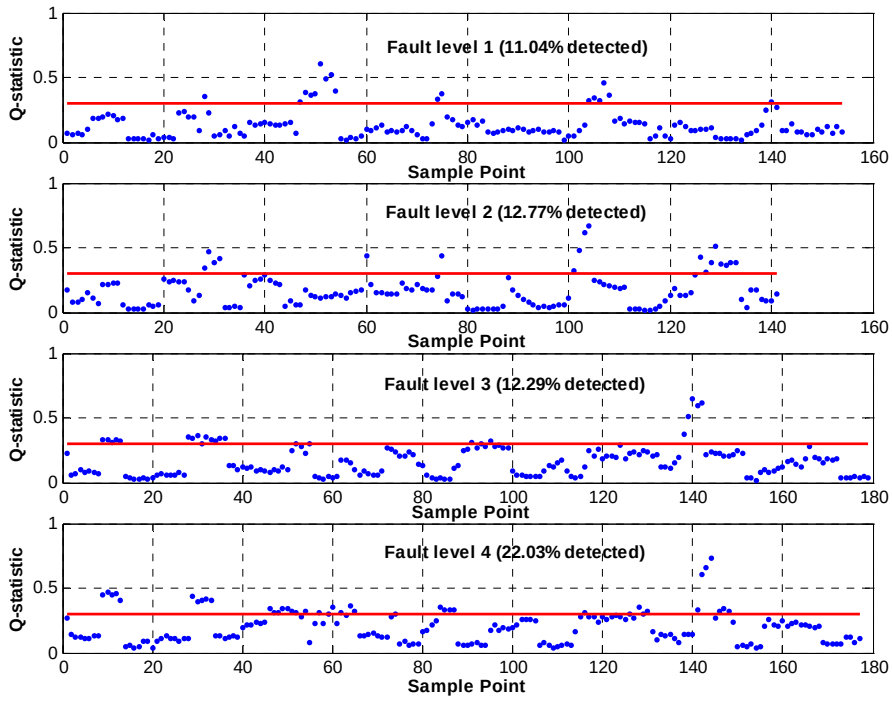

Figure 7.17 *Q-statistic* plots of test data from refrigerant leakage test at different levels of fault severity

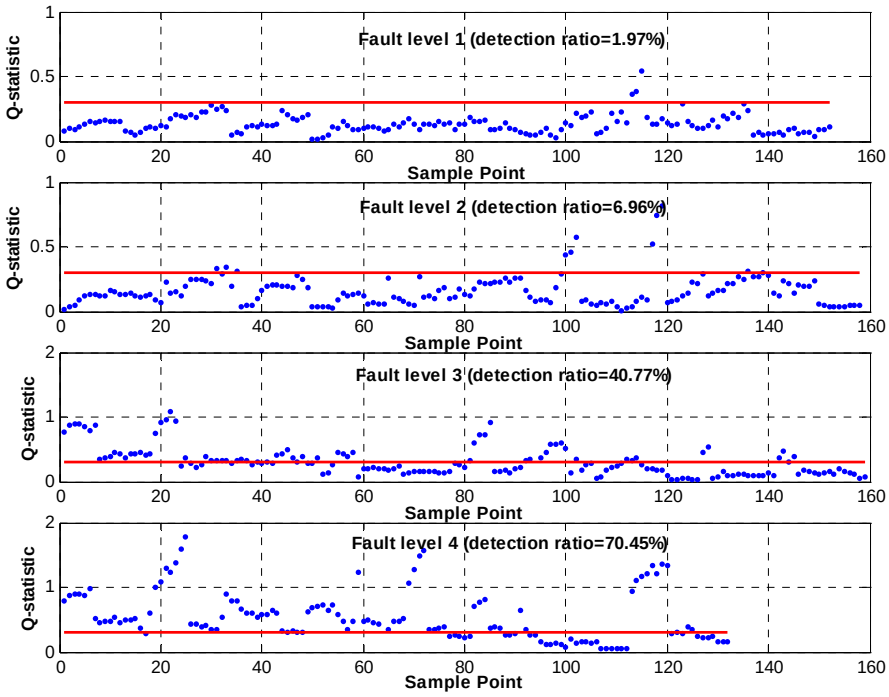

Figure 7.18 *Q-statistic* plots of test data form refrigerant overcharge test at different levels of fault severity

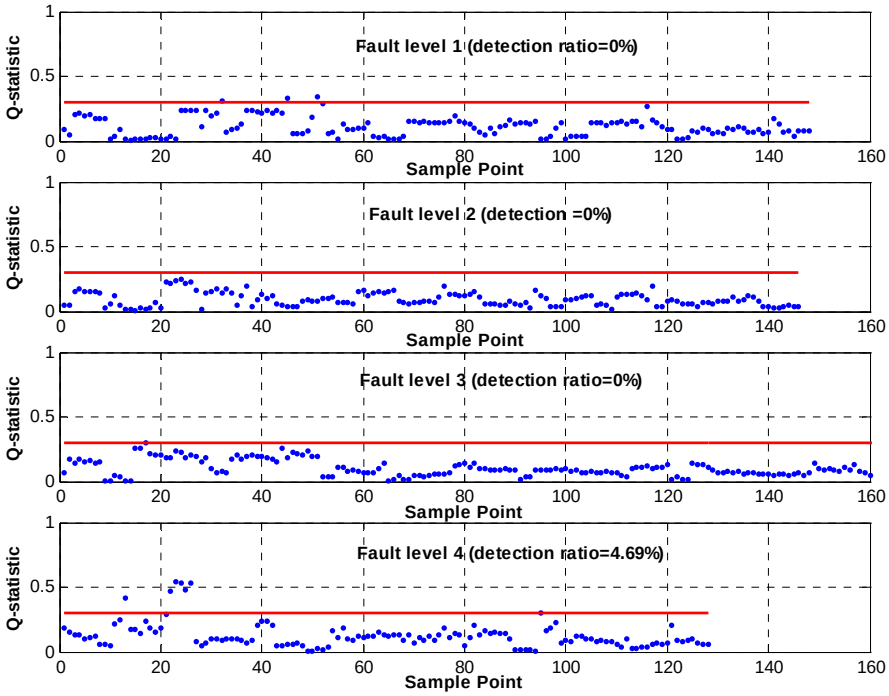

Figure 7.19 *Q-statistic* plots of test data from excess oil test at different levels of fault severity

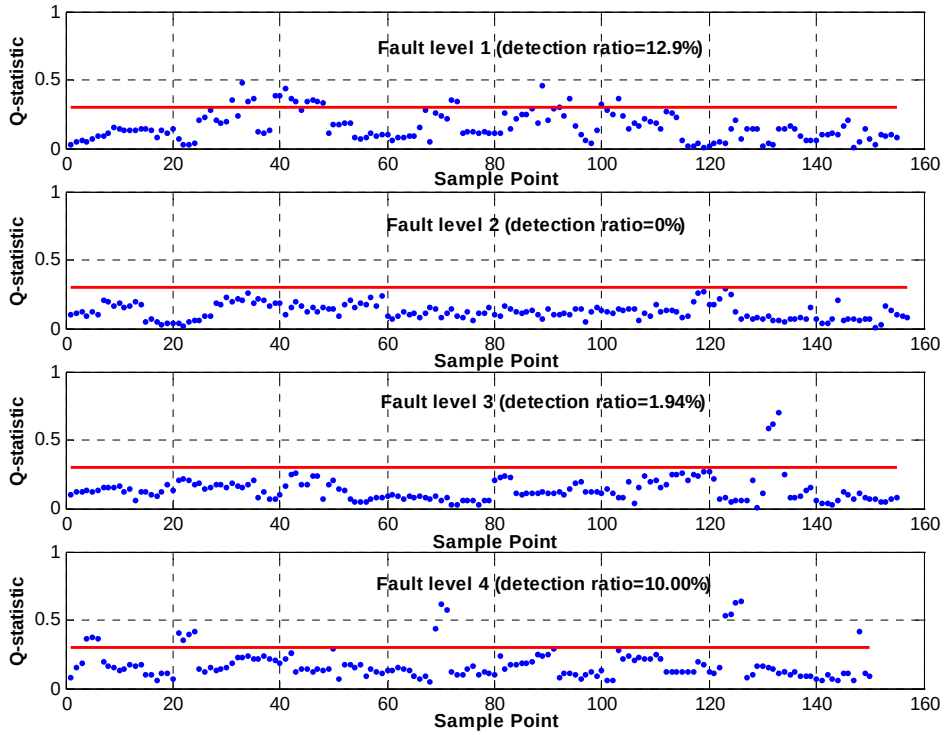

Figure 7.20 *Q-statistic* plots of test data from condenser fouling test at different levels of fault severity

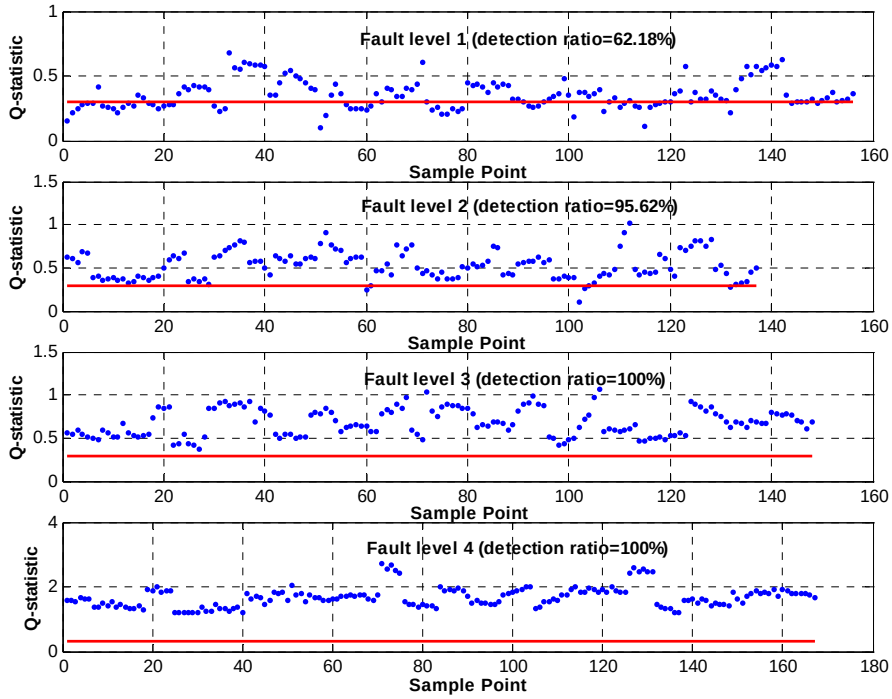

Figure 7.21 *Q-statistic* plots of test data from non-condensables in refrigerant test at different levels of fault severity

7.4 Validation Using Laboratory Data from ASHRAE 1043-RP under Conditions of Chiller Faults

Although it was proved in the previous section that the PCA model used by the sensor FDD&E scheme is not sensitive to most typical chiller faults of concern in this thesis, it does not necessarily ensure that sensor faults can be successfully found by the scheme when both sensor faults and chiller faults occur simultaneously. This section provides the validation tests of the sensor FDD&E scheme using test data containing both a chiller fault and a sensor fault. The test data were generated using chiller data from chiller-fault tests in ASHRAE 1043-RP.

7.4.1 Test Conditions

The PCA model trained in Section 7.1.2 was also employed in the tests. The chiller data from four chiller-fault tests, i.e., refrigerant leakage, refrigerant overcharge, excess oil, and condenser fouling, at different fault severity levels (from level 1 to level 4), were used to generate test data that contain both sensor faults and chiller faults. The test of non-condensables in refrigerant is not used here as the *Q-statistic* is sensitive to this fault. Considering that chiller faults at high fault severity levels would seldom happen if the robust FDD strategy presented in this thesis could be successfully implemented in time, only results of tests in relation to chiller-fault tests at severity level 2 are presented in this thesis and results of other tests are given in the attached CD.

7.4.2 Generation of Test Data

Similar to the generation of test data in previous validation tests, various predetermined bias errors were added to the corresponding measurements from the four chiller-fault tests, each at fault severity level 2, to generate test data. For the same reason given in section 7.1.3, only the sensors not used for feedback control had biases added. Thus, the involved sensors are T_{chwr}, T_{ev}, P_{ev}, T_{lcw}, T_{cd}, P_{cd}, T_{suc}, T_{dis} and W_{elec}. The bias error added to each sensor, as described in Table 7.5, is around 15% of the average of measurements from the sensor. Since all 9 sensors each had a bias error added for each of the four chiller-fault tests, there were a total of 36 sets of test data.

7.4.3 Test Results

The sensor FDD&E scheme was applied to the generated test data, and produced test results for 36 test cases accordingly. Table 7.5 gives the general results of the 36 test cases. Table 7.5 shows that all the test cases were detected as faulty in the case of chiller faults. More importantly, for all the test cases, most of the introduced sensor biases were accurately diagnosed and estimated with all “Diagnosis ratio” values not less than 74.83% and all “Relative estimation error” values not more than13.45%.

Only the *Q-statistic* and *Q-contribution* plots for the four test cases where a known bias error was added to the measurements of T_{chwr} are presented in this section to illustrate the results. From Figures 7.22, 7.24, 7.26 and 7.28, it is apparent that, for each test case, the

Q-statistic values increased significantly and exceeded the threshold determined at a confidence level of 95%. At the same time, the *Q-contribution* plots in Figures 7.23, 7.25, 7.27 and 7.29 and 7.31 all suggest that the measurement of T_{chwr} provided the largest contribution to the *Q-statistic* and T_{chwr} was the most probably faulty sensor. Similar to the *Q-contribution* plots in Section 7.1.4, each column in a *Q-contribution* plot represents a mean of the contribution values of five samples which were consecutively detected to be faulty.

From the test results, it can be concluded that the proposed PCA-based sensor FDD&E scheme for centrifugal chillers is capable of detecting and diagnosing faulty sensors as well as estimating the magnitudes of the bias errors regardless of the existence of a typical chiller fault including refrigerant leakage, refrigerant overcharge, excess oil, condenser fouling. Since non-condensables in the refrigerant overstates the measurement of condensing temperature and then result in a kind of sensor fault, the sensor FDD&E can not diagnosis sensor faults in the case of this chiller fault. Except for non-condensable in refrigerant, the hypothesis made in the previous chapter has been verified, namely, the successful implementation of the sensor FDD&E scheme based on the PCA model is immune to the existence of a chiller fault.

Table 7.5 General results of validation tests using test data generated from four fault tests each at severity level 2 in ASHRAE 1043-RP

(*Q-statistic* values are determined with a confidence level of 95%)

Sensor and added bias	Results	Refrigerant leakage	Refrigerant overcharge	Excess oil	Condenser fouling
T_{chwr} +2.2°C	Detection ratio	98.60%	99.39%	93.46%	98.15%
	Diagnosis ratio	89.36%	93.25%	93.71%	90.57%
	Estimated bias	+2.38°C	+2.34°C	+2.21°C	+2.27°C
	Relative estimation error	7.97%	6.14%	0.61%	3.20%
T_{ev} +1.2°C	Detection ratio	100%	100%	100%	100%
	Diagnosis ratio	80.58%	76.69%	99.35%	99.39%
	Estimated bias	+1.05°C	+0.96°C	+1.09°C	+1.11°C
	Relative estimation error	12.53%	19.74%	9.38%	7.60%
P_{ev} +20K	Detection ratio	100%	100%	100%	100%
	Diagnosis ratio	99.30%	98.77%	100%	100%
	Estimated bias	18.14kPa	17.36kPa	19.43kPa	19.67kPa
	Relative estimation error	9.28%	13.21%	2.86%	1.66%
T_{lcw} +3.5°C	Detection ratio	100%	100%	100%	100%
	Diagnosis ratio	100%	98.15%	100%	100%
	Estimated bias	+3.75°C	+3.21°C	+3.5 °C	+3.44°C
	Relative estimation error	7.12%	8.41%	2.59%	1.64%
T_{cd} +3.5°C	Detection ratio	92.31%	100%	96.69%	99.38%
	Diagnosis ratio	98.848%	100%	100%	100%
	Estimated bias	+3.38°C	+3.87°C	+3.46°C	+3.67°C
	Relative estimation error	3.19%	10.69%	1.19%	4.98%
P_{cd} +75kPa	Detection ratio	96.50%	100%	100%	100%
	Diagnosis ratio	97.10%	98.77%	100%	100%
	Estimated bias	+71.92kPa	+83.00kPa	+73.72kPa	+77.75kPa
	Relative estimation error	4.10%	10.68%	1.70%	3.67%
T_{suc} 1.5°C	Detection ratio	97.90%	100%	99.34%	87.50%
	Diagnosis ratio	100%	100%	100%	100%
	Estimated bias	+1.67°C	+1.71°C	+1.60°C	+1.5^{4o}C
	Relative estimation error	11.66%	14.11%	6.75%	2.63%
T_{dis} +7°C	Detection ratio	84.62%	99.38%	74.83%	79.37%
	Diagnosis ratio	100%	100%	100%	100%
	Estimated bias	+7.72°C	+8.09°C	+7.67°C	+7.94°C
	Relative estimation error	10.33%	15.69%	9.57%	13.45%
W_{elec} +12kW	Detection ratio	66.43%	59.26%	67.55%	60.62%
	Diagnosis ratio	87.37%	87.50%	100%	100%
	Estimated bias	+12.63kW	+12.83kW	+13.38kW	+13.59kW
	Relative estimation error	5.29%	6.92%	11.505	13.28%

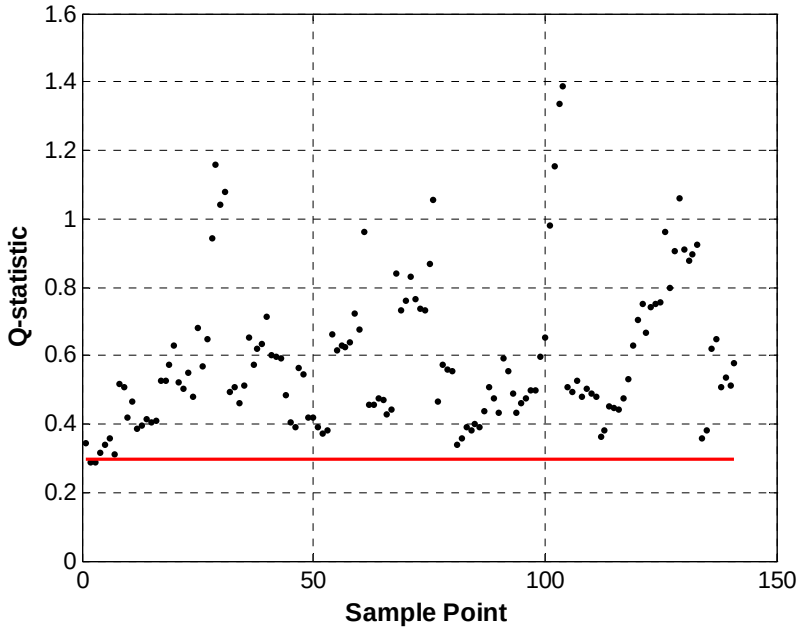

Figure 7.22 *Q-statistic* plot of test data from refrigerant leakage test at fault severity level 2 – T_{chwr} was biased with +2.2°C

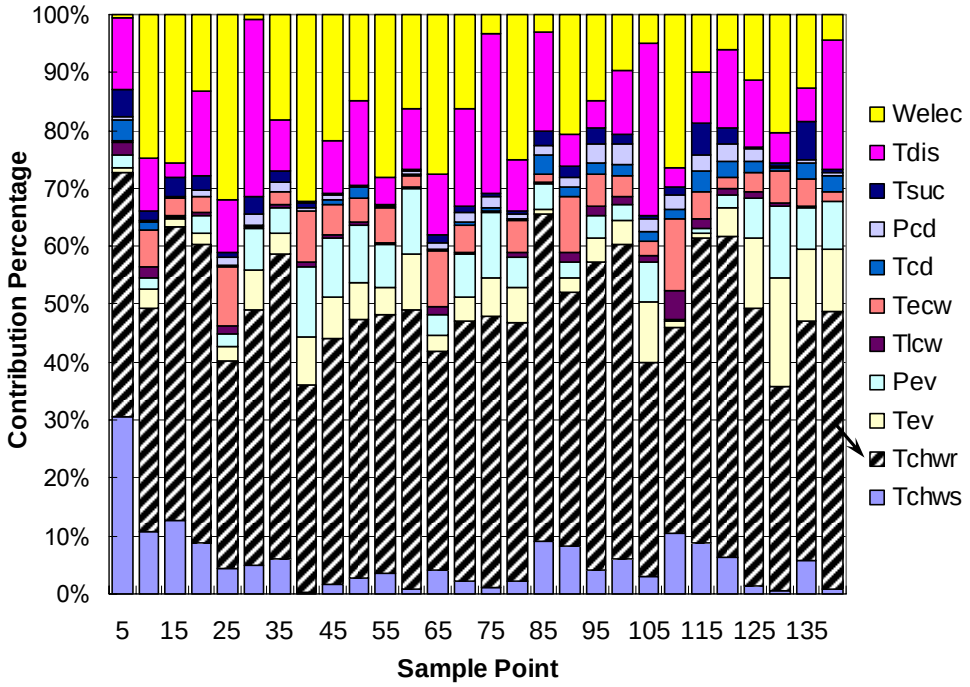

Figure 7.23 *Q-contribution* plot of test data from refrigerant leakage test at fault severity level 2 – T_{chwr} was biased with +2.2°C

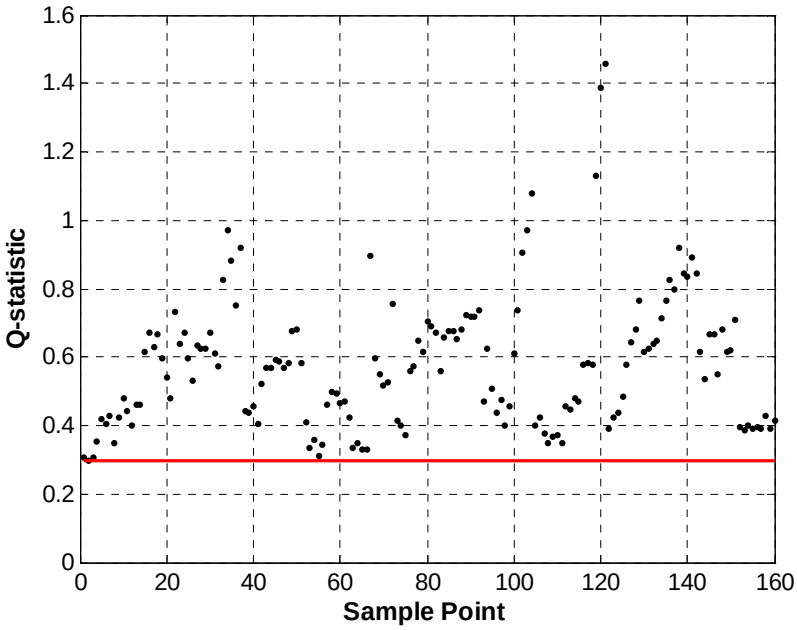

Figure 7.24 *Q-statistic* plot of test data from refrigerant overcharge test at fault severity level 2 – T_{chwr} was biased with +2.2°C

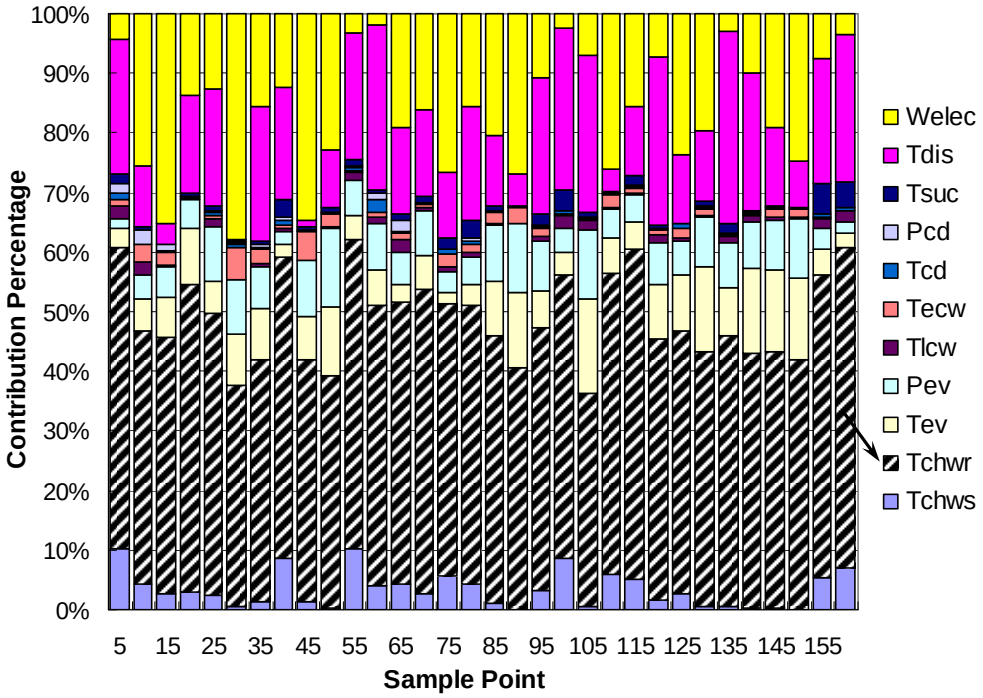

Figure 7.25 *Q-contribution* plot of test data from refrigerant overcharge test at fault severity level 2 – T_{chwr} was biased with +2.2°C

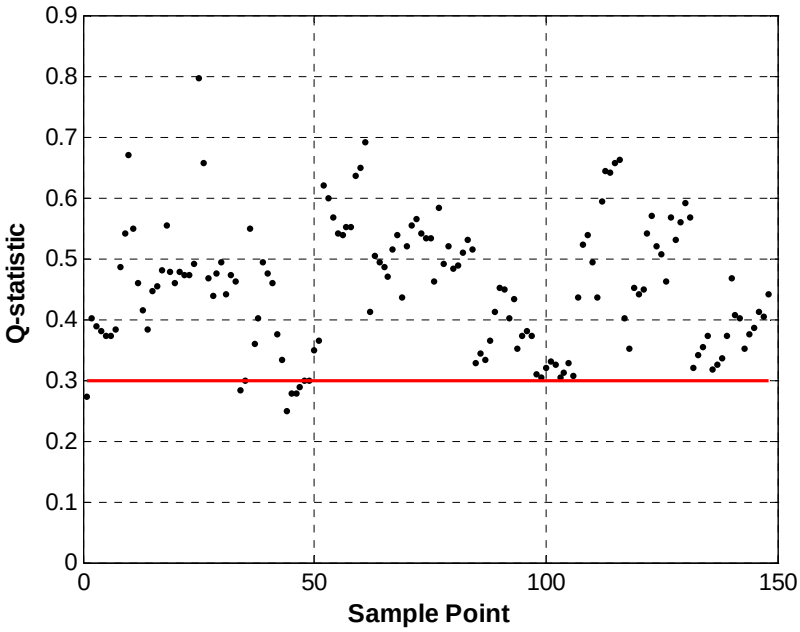

Figure 7.26 *Q-statistic* plot of test data from excess oil test at fault severity level 2 – T_{chwr} was biased with +2.2°C

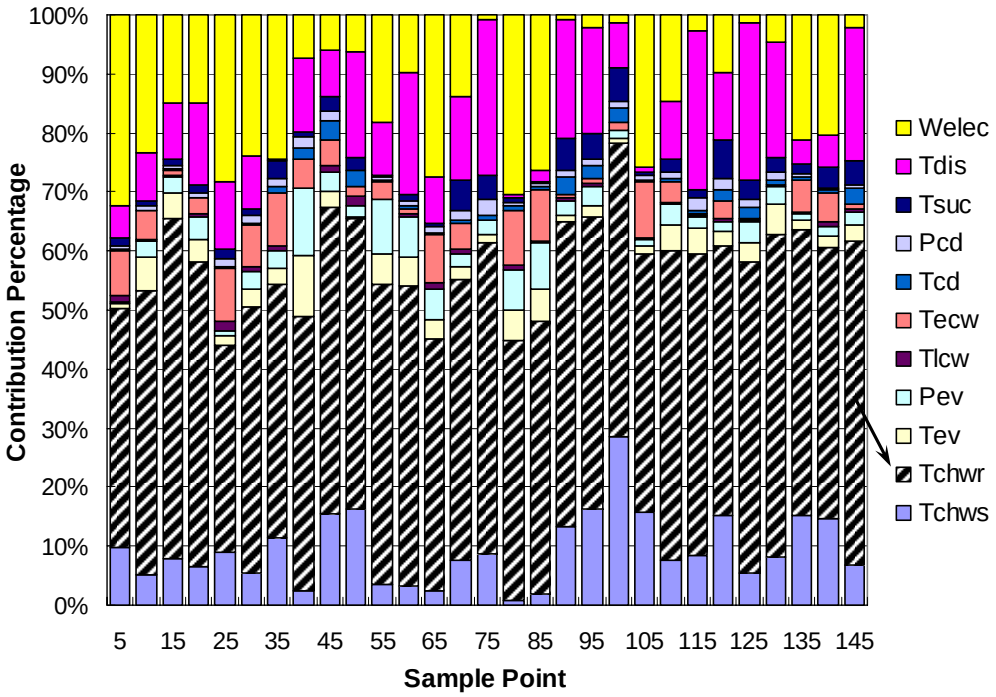

Figure 7.27 *Q-contribution* plot of test data from excess oil test at fault severity level 2 – T_{chwr} was biased with +2.2°C

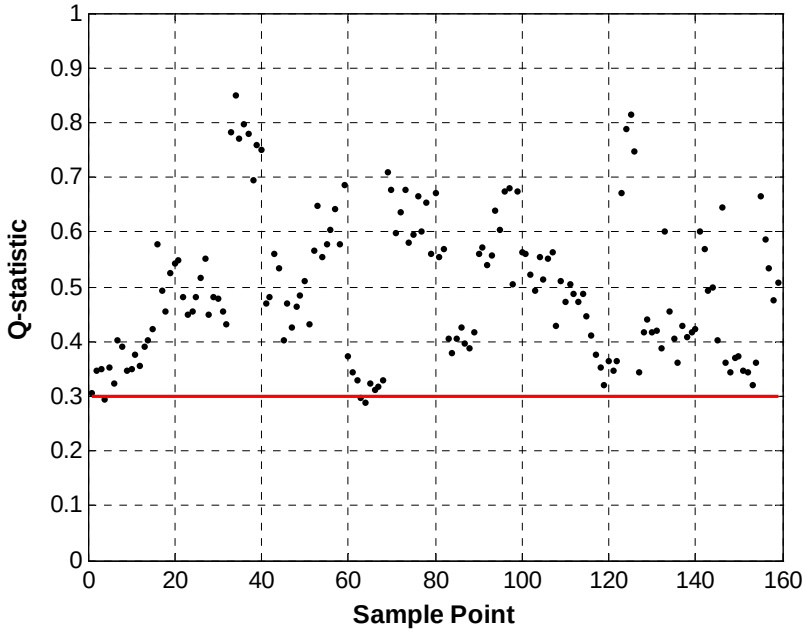

Figure 7.28 *Q-statistic* plot of test data from condenser fouling test at fault severity level 2 – T_{chwr} was biased with +2.2°C

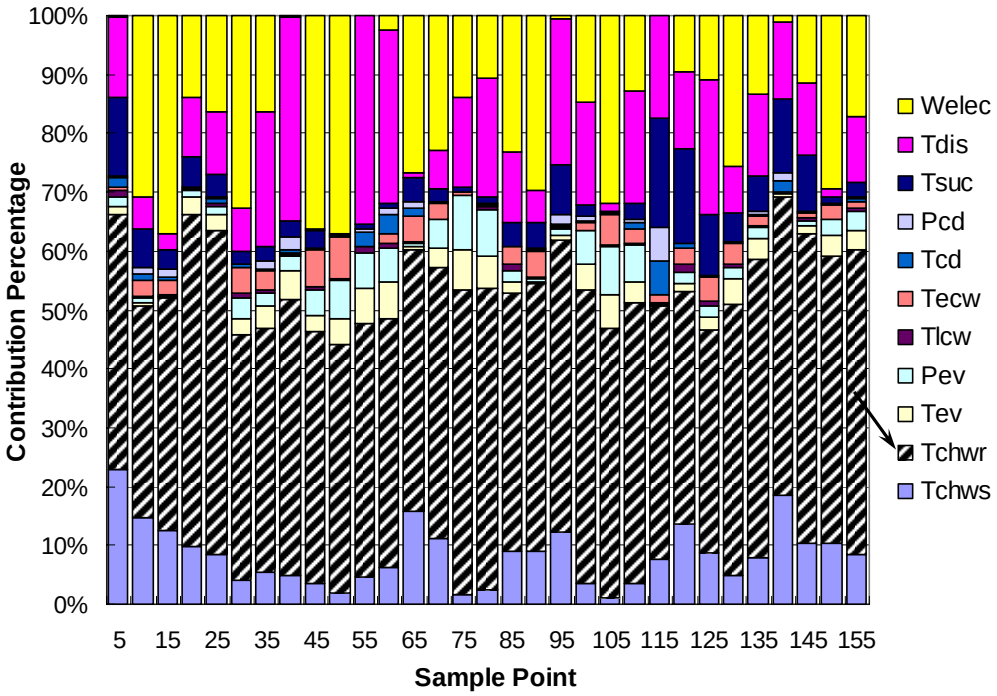

Figure 7.29 *Q-contribution* plot of test data from condenser fouling test at fault severity level 2 - T_{chwr} was biased with +2.2°C

7.6 Summary

First of all, the results of validation using laboratory chiller data from ASHRAE 1043-RP as well as field chiller data from a real building in Hong Kong confirmed that the sensor FDD&E scheme can successfully detect, diagnose and estimate a single sensor fault in a centrifugal chiller when the chiller is free of chiller faults. Except for sensor faults in connection with the chilled water supply temperature (T_{chws}) and the entering condenser water temperature (T_{ecw}), sensor faults in connection with all the rest variables were tested by using the field and the laboratory data. In particular, the PCA model consisting of a set of key variables in a centrifugal chiller was proved capable of capturing the correlations among the variables and effectively decoupling the systematic variations of centrifugal chillers from random noises. The uses of the *Q-statistic* plot, the *Q-contribution* plot and the iterative approach, respectively, as tools of fault detection, diagnosis and estimation, respectively, were tested to be effective in dealing with sensors in chillers.

More importantly, the validation tests also show that the PCA model is insensitive to typical chiller faults, including refrigerant leakage, refrigerant overcharge, excess oil and condenser fouling. The presence of any one of these chiller faults does not compromise the effectiveness and capability of the sensor FDD&E scheme. However, there is an exception, namely non-condensable gases in refrigerant. This fault makes the scheme fail to fulfill its duty as it can extraordinarily overstate the condensing temperature. In this regard, it is recommended to collect the condensing and evaporating temperatures by

temperature sensors rather than by deriving from condensing pressure using refrigerant saturation tables.

Since the sensor FDD&E scheme is proved to be able to fulfill its duty regardless of the existence of some typical chiller faults, the implementation of the scheme can ensure accurate and reliable measurements on which other BMS-based diagnosis and control tools hinge. Therefore, it can be expected that the joint use of the sensor FDD&E scheme and the basic chiller FDD scheme, efficiency monitoring and optimal control tools would significantly improve the reliability of BMS as well as enhance the overall energy efficiency of chiller plants.

CHAPTER 8 ROBUST CHILLER FDD STRATEGY AND ITS VALIDATION AND APPLICATION SOFTWARE PACKAGE

In the previous chapters, this thesis presents the development and validation of a basic chiller FDD scheme targeting chiller faults as well as those of a sensor FDD&E scheme targeting sensor faults in centrifugal chillers. The second scheme can ensure reliable and accurate sensor measurements that are prerequisite to the successful implementation of the first scheme. Therefore, it is feasible to construct a chiller FDD strategy that is capable of tackling both chiller faults and sensor faults. This chapter presents the implementation structure of such a robust FDD strategy for centrifugal chillers. This strategy distinguishes itself from the basic chiller FDD scheme developed in Chapter 3 by taking into account sensor faults and employing a PCA-based sensor FDD&E scheme to tackle sensor faults. More importantly, the performance of the robust FDD strategy is verified by the laboratory data from ASHRAE 1043-RP. On the platform of MATLAB 6.1, the software package of the robust FDD strategy is built up. When this software package is integrated with BMS, online FDD for centrifugal chillers can be carried out.

Section 8.1 gives the implementation structure of the robust FDD strategy for centrifugal chillers and the issues concerning its online applications. Section 8.2 validates the robust FDD strategy using test data from the laboratory centrifugal chiller in ASHRAE 1043-RP. Section 8.3 describes a software package of the robust strategy

on the platform of MATLAB 6.1 and its integration with an intelligent building management platform. The software package is built up according to the corresponding schemes and approaches in the robust FDD strategy as well as its implementation structure. Section 8.4 summarizes this chapter.

8.1 Implementation Structure of Robust Chiller FDD Strategy

Figure 8.1 gives the implementation structure of the robust chiller FDD strategy. The inputs to the robust FDD strategy are measurements obtained from the BMS or chiller control panels.

After passing through the data preprocessor, the measurements are fed into the sensor FDD&E scheme where the sensor faults will be detected, diagnosed and estimated by a series of approaches, respectively. Note, in order to avoid false alarms, an alarm regarding a sensor fault is sent out only after a sensor is diagnosed to be faulty for a certain number of consecutive samples, e.g., 5 consecutive samples. Once a sensor is diagnosed to be faulty, the faulty sensor will be corrected by using the fault estimation approach to get the true measurement from the sensor. Subsequently, the corrected measurements are fed into the chiller FDD scheme, where all performance indexes at each sampling instant are calculated. Meanwhile, benchmarks of the performance indexes are also predicted by their corresponding reference models. Thus the residual for each performance index is generated by comparing the measured value with its benchmark. Each residual is compared with the corresponding fault detection threshold.

When the residuals of one or more performance indexes are larger than their fault detection thresholds, the chiller system is considered to be faulty. Furthermore, specific chiller faults are diagnosed by a fault diagnostic classifier according to the amount and direction of the deviation of the performance indexes, and a chiller fault alarm will be raised.

If the sensor FDD&E scheme does not find any sensor fault, no change will be made to the measurements and they are directly fed into the chiller FDD scheme for analysis. In the end, proper suggestions and recommendations concerning sensor calibration or system maintenance will be generated by analyzing the implementation results of the robust FDD strategy.

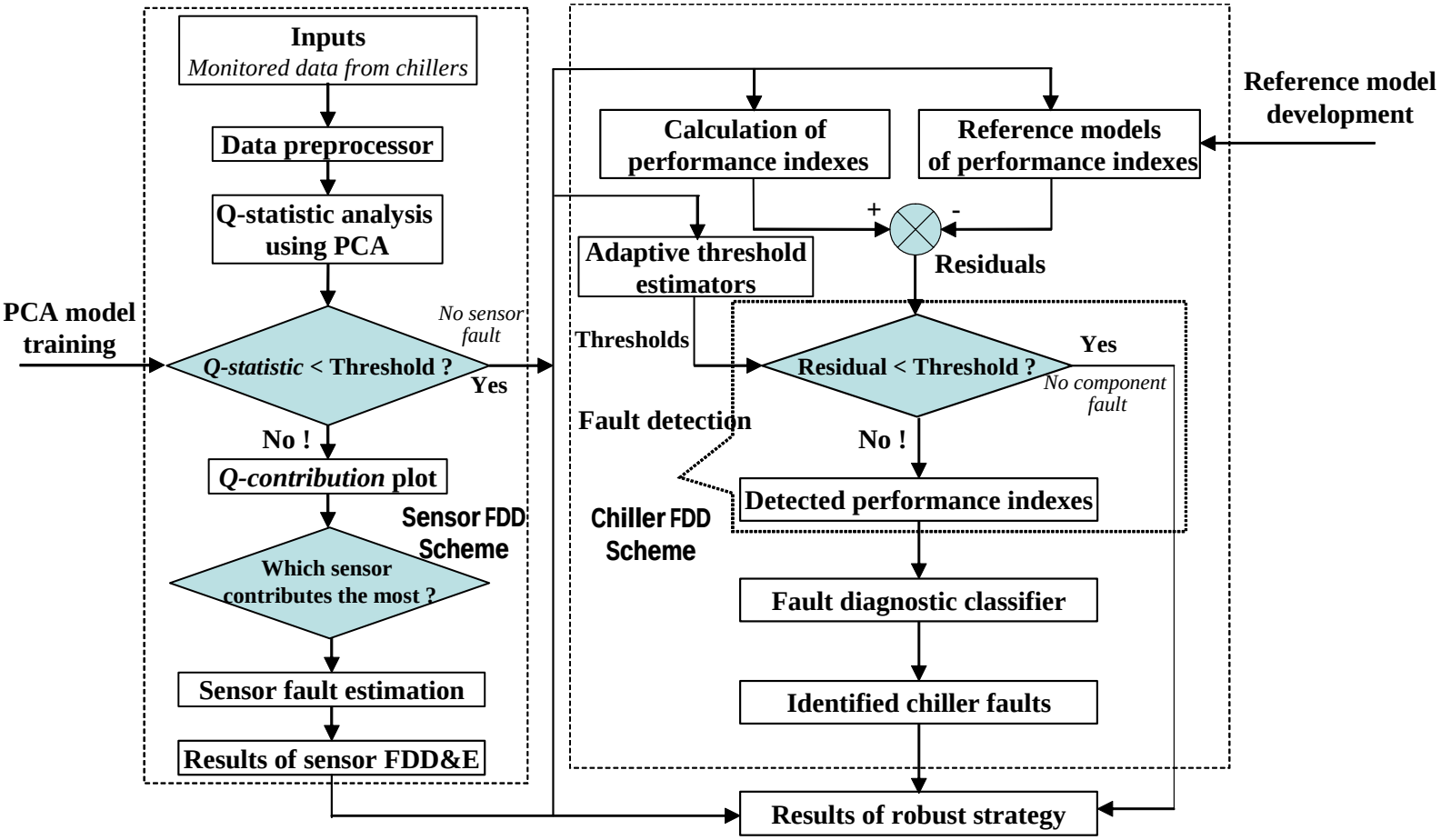

Figure 8.1 Flow chart of the robust chiller FDD strategy

8.2 Validation of Robust Chiller FDD Strategy Using Laboratory Data from ASHRAE 1043-RP

Each of the two FDD schemes in the robust strategy has been validated in the previous chapters. But an important question still remains: Can the robust chiller FDD strategy effectively detect and diagnose occurred chiller faults in the presence of sensor faults? This is the ultimate problem this research is dedicated to solving. Therefore, the emphasis of the validation tests here is to evaluate the performance of the robust strategy in detecting and diagnosing chiller faults after correcting faults associated with the key sensors.

8.2.1 Test Conditions

The "Normal" test in ASHRAE 1043-RP, were used for the reference model development in the chiller FDD scheme and the PCA model training in the sensor FDD&E scheme, respectively. Similar to the validation tests in the previous chapter, the laboratory data from a normal operation test, called "Normal NC", and three other chiller-fault tests in ASHRAE 1043-RP were employed to generate test data. The three chiller-fault tests include refrigerant leakage, excess oil, condenser fouling, all considered in the basic chiller FDD scheme. Two chiller faults, including degradation of the compressor and non-condensables in the refrigerant, were not tested in this chapter though these two chiller faults are considered in the basic chiller FDD scheme. The reason is that the data concerning degradation of the compressor are not available in ASHRAE 1034-RP, and the sensor FDD&E scheme can not tackle sensor faults in the event of non-condensables in refrigerant as the *Q-statistic* is sensitive to this chiller fault.

8.2.2 Generation of Test Data

In order to validate the robust FDD strategy as comprehensively as possible, the test data should include the data free of faults, the data containing sensor faults only, the data containing chiller faults only, and the data containing both chiller faults and sensor faults.

Accordingly, four groups of such test data, called groups A, B, C and D, respectively, were generated using laboratory data from ASHRAE 1043-RP. Group A comprises the data directly from “Normal NC” test and can be regarded as the data free of faults. Group B was generated by adding various bias errors to the corresponding measurements from “Normal NC” and thus can be regarded as the data containing sensor faults only. Group C comprises the data directly from the three chiller fault tests and thus can be regarded as the data containing chiller faults only. As for group D, it was generated by adding various bias errors to the measurements from the three chiller-fault tests, each of them arranged in an increasing order of severity (from level 1 to level 4). Thus, the group can be regarded as the data containing both chiller faults and sensor faults at the same time. The magnitudes of the bias error added to each measurement are the same as described in Table 7.2. For the same reason given in the previous chapter, nine sensors, i.e, T_{chwr}, T_{ev}, P_{ev}, T_{lcw}, T_{cd}, P_{cd}, T_{suc}, T_{dis} and W_{elec}, were added with a bias error to generate sensor faults. T_{chws} and T_{ecw} are usually involved in any feedback control of the chiller, so bias error was not added to them.

After the test data were generated, the robust chiller FDD strategy was applied to the four data groups, i.e., group A, group B, group C and group D, to find out whether the strategy could successfully detect and diagnose the chiller faults after correcting sensor faults associated with the key sensors in chillers. That results in 4 groups of test results, accordingly.

8.2.3 Results of Tests Using Fault-free Test Data

When the robust FDD strategy was applied to data group A, the *Q-statistic* values of the test data were first calculated and compared with the corresponding threshold. The *Q-statistic* plot of this group of test data was the same as shown in Figure 7.2. The plot clearly indicated that all *Q-statistic* values were below the threshold. That means all sensors in the chiller are free of sensor faults. Subsequently, the test data, without any change, were directed into the next procedure, i.e., the chiller FDD scheme. As expected, no significantly deviated residual of any performance index was observed. The plots of residuals of the six performance indexes were the same as shown in Figure 5.4. Therefore, it can be concluded that there are no chiller faults or sensor faults within the chiller, which coincides well with what is anticipated.

8.2.4 Results of Tests Using Test Data Containing Sensor Faults Only

Since each of the 9 sensors was added with a bias error individually, there were 9 sets of data in group B. The robust FDD strategy was applied to each data set in data group B, resulting in 9 test cases. For each test case, most *Q-statistic* values of the test data were above the corresponding threshold, indicating the existence of a sensor fault in the chiller. The *Q-contribution* plot and iterative approach were then activated to find faulty sensors and estimate the magnitudes of sensor faults, respectively. Since the test data in group B are the same as those used in Section 7.1, the general results of the sensor FDD&E procedure are the same as given in Table 7. 4. After that, the test data were fed into the chiller FDD scheme, where no significantly deviated residuals of performance indexes were observed. Hence the conclusion that the chiller is free of chiller faults but suffers from sensor faults, tallies with what was anticipated.

8.2.5 Results of Tests Using Test Data Containing Chiller Faults Only

There were three sets of data in group C and each of them came from one chiller fault. The robust FDD strategy was applied to each of the three data sets, resulting in 3 test cases. For each test case, most *Q-statistic* values of the test data were below the threshold, as shown in Figure 8.2, Figure 8.3 and Figure 8.4. The *Q-statistic* values of 85.08% of the samples from refrigerant leakage test were below the threshold, and this figure was 98.32% for excess oil and 93.68% for condenser fouling. All these means that there is no sensor fault within the chiller. Without any change to the test data, they were subsequently fed into the chiller FDD scheme for further analysis. Because the test data are the same as those used in Section 5.1, the results of the chiller FDD procedure for the three test cases are the same as given in Figure 5.5, Figure 5.6 and Figure 5.7.

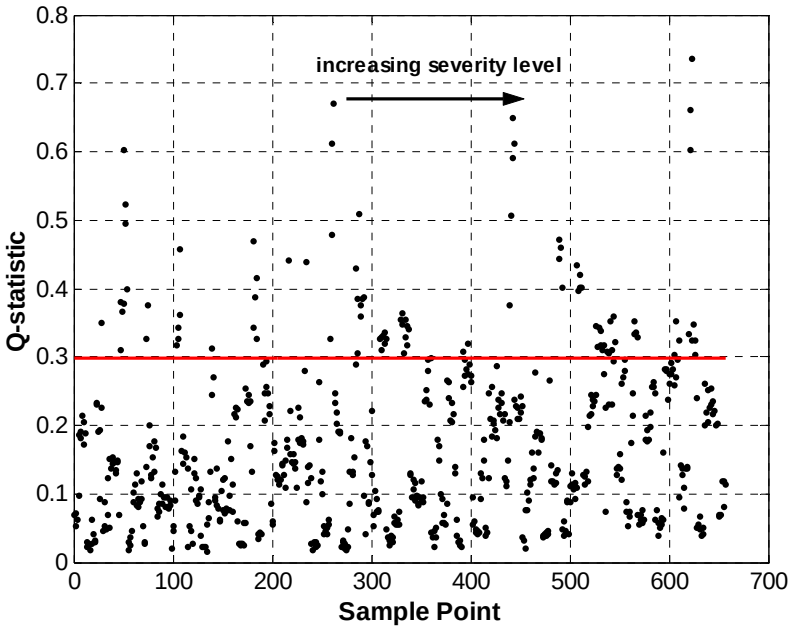

Figure 8.2 *Q-statistic* plot of test data group C- Refrigerant leakage test from fault severity level 1 to 4

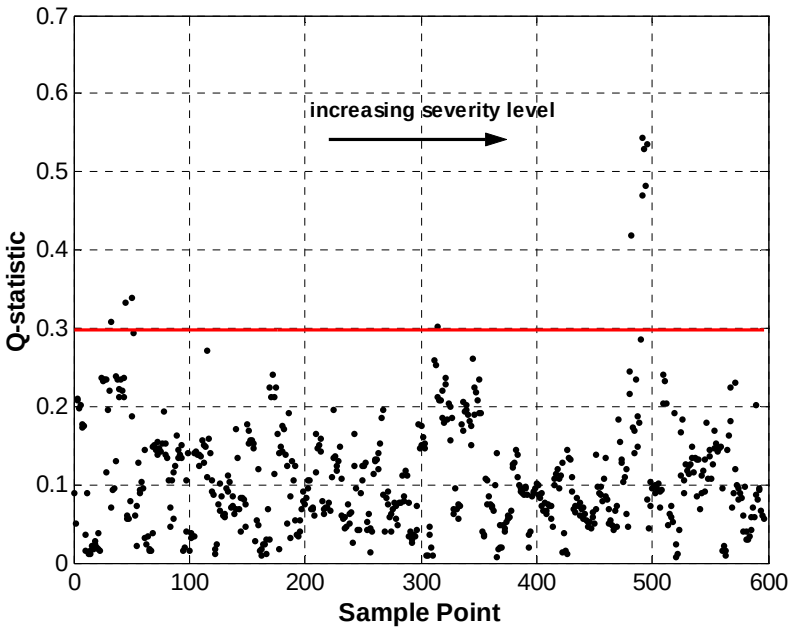

Figure 8.3 *Q-statistic* plot of test data group C- Excess oil test from fault severity level 1 to 4

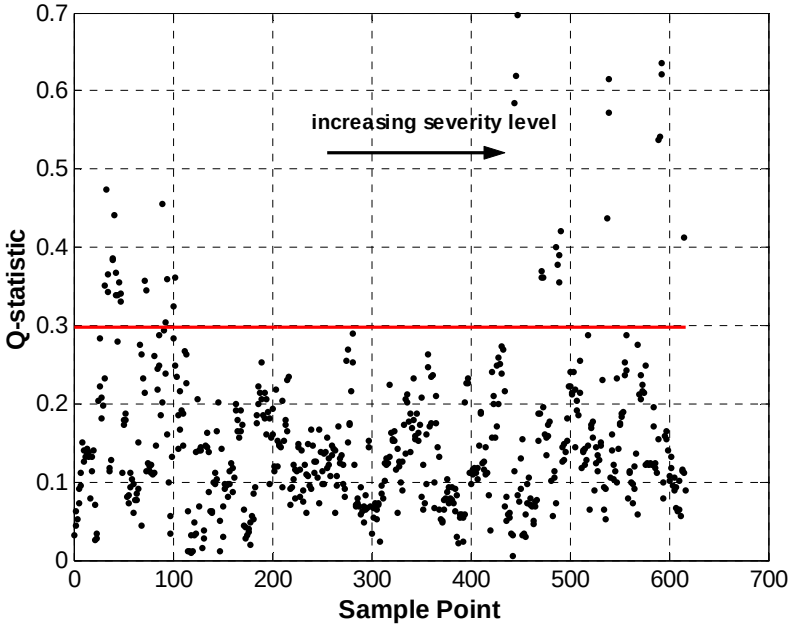

Figure 8.4 *Q-statistic* plot of test data group C- Condenser fouling test from severity level 1 to 4

8.2.6 Results of Tests Using Test Data Containing Both Sensor Faults and Chiller Faults

Since each of the 9 sensors was added with a bias error for each of the three fault tests, there were a total of 27 sets of data in group D. The robust FDD strategy was applied to each data set, resulting in 27 test cases, respectively. Most *Q-statistic* values in each test case were above the *Q-statistic* threshold, indicating that the chiller suffered from sensor faults. Accordingly, the *Q-contribution* plot and iterative approach were activated to identify faulty sensors and estimate the magnitudes of sensor faults, respectively. Results of sensor FDD&E for the 27 test cases are summarized in Table 8.1. It can be observed from the table that in each test case, bias errors were accurately detected, diagnosed and estimated by the sensor FDD&E scheme with no “Diagnosis ratio” values less than 89.04% and no “Relative estimation error” values higher than 14.79%.

Table 8.1 General results of validation tests using test data generated from three fault tests each from severity level 1 to 4 in ASHRAE 1043-RP

(*Q-statistic* values are determined with a confidence level of 95%)

Sensor and added bias	Results	Refrigerant leakage	Excess oil	Condenser fouling
T_{chwr} +2.2°C	**Detection ratio**	98.78%	95.97%	99.04%
	Diagnosis ratio	89.04%	94.92%	89.95%
	Estimated bias	+2.32°C	+2.21°C	+2.29°C
	Relative estimation error	5.35%	0.61%	3.93%
T_{ev} +1.2°C	**Detection ratio**	99.85%	99.83%	99.84%
	Diagnosis ratio	93.75%	98.32%	96.10%
	Estimated bias	+1.11°C	+1.13°C	+1.11°C
	Relative estimation error	7.58%	5.76%	7.87%
P_{ev} +20kPa	**Detection ratio**	100%	99.84%	100%
	Diagnosis ratio	99.39%	96.10%	100%
	Estimated bias	+18.70kPa	+19.09kPa	+18.71kPa
	Relative estimation error	6.52%	4.55%	6.47%
T_{lcw} +3.5°C	**Detection ratio**	100%	100%	99.84%
	Diagnosis ratio	100%	100%	96.59%
	Estimated bias	+3.96°C	+3.61°C	+3.33 °C
	Relative estimation error	13.17%	3.17%	4.82%
T_{cd} +3.5°C	**Detection ratio**	83.56%	98.83%	99.35%
	Diagnosis ratio	96.17%	100%	100%
	Estimated bias	+3.30°C	+3.45°C	+3.80°C
	Relative estimation error	5.81	1.52%	8.52%
P_{cd} +7.5kPa	**Detection ratio**	91.63%	99.83%	100%
	Diagnosis ratio	94.52%	99.16%	99.84%
	Estimated bias	+69.10kPa	+72.93kPa	+81.20kPa
	Relative estimation error	7.87%	2.76%	8.26%
T_{suc} +1.5°C	**Detection ratio**	99.09%	99.66%	96.11%
	Diagnosis ratio	99.85%	100%	98.31%
	Estimated bias	+1.43°C	+1.6°C	+1.59°C
	Relative estimation error	9.53%	7.13%	6.03%
T_{dis} +7°C	**Detection ratio**	81.58%	80.37%	93.35%
	Diagnosis ratio	100%	100%	100%
	Estimated bias	+7.40°C	+7.58°C	+7.00°C
	Relative estimation error	5.71%	8.33%	12.87%
W_{elec} +12kW	**Detection ratio**	70.02%	65.77%	60.62%
	Diagnosis ratio	92.83%	99.23%	95.89%
	Estimated bias	+12.81kW	+13.14 kW	+13.77 kW
	Relative estimation error	6.77%	9.53%	14.79%

The corrected measurements were then fed into the chiller FDD scheme of the robust strategy, where chiller faults were successfully detected and diagnosed. For the sake of conciseness, only the chiller FDD results for the three test cases related to T_{chwr} are presented in this section to illustrate the details. The chilled water return temperature is involved in the calculation of three performance indexes: $LMTD_{ev}$ and M_{ref} and COP. The bias error added to the sensor was +2.2^{o}C. During each test case, chiller faults were identified by the chiller FDD scheme after the FDD&E scheme had identified the faulty sensor and corrected it. All the test results coincide with our anticipation.

Test case 1: Refrigerant leakage with biased chilled water return temperature sensor

In this test case, most *Q-statistic* values went beyond the threshold of a confidence level of 95% when T_{chwr} was biased with +2.2 ^{o}C, as shown in Figure 8.5-(a). Thus, the sensor FDD&E scheme was activated to tackle sensor faults. The biased T_{chwr} was successfully identified with a "Detection ratio" value of 98.78% and a "Diagnosis ratio" value of 89.04%, and the biased error was estimated to be +2.32^{o}C with a "Relative estimation error" value of 5.35%, as shown in Table 8.1. After measurements from T_{chwr} in the test data were corrected, each performance index would be calculated and compared with its threshold which was determined online with a confidence level of 95%. Figure 8.5-(b) shows that the residuals of $LMTD_{cd}$, deviated from its low thresholds with increasing fault severity levels, while only a few residuals of M_{ref} , as shown in Figure 8.5-(c), under its lower thresholds at fault level 4. Figure 8.5-(d) shows there are a very few residuals of *COP* under its lower thresholds. In these figures, the residual values are indicated by the solid dots and threshold values are indicated by the solid lines in the figures. The explanation for the slightly degraded *COP* is that the T_{chwr} was overcorrected with an

estimated bias of +2.32°C instead of a true value of +2.2 °C, which resulted in lower calculated cooling load and lower calculated *COP*. No discernible residuals of the rest performance indexes were found and therefore they are not presented in this section. Considering the fact that an expansion valve was used in the chiller, the fault diagnostic classifier identified the existence of refrigerant leakage.

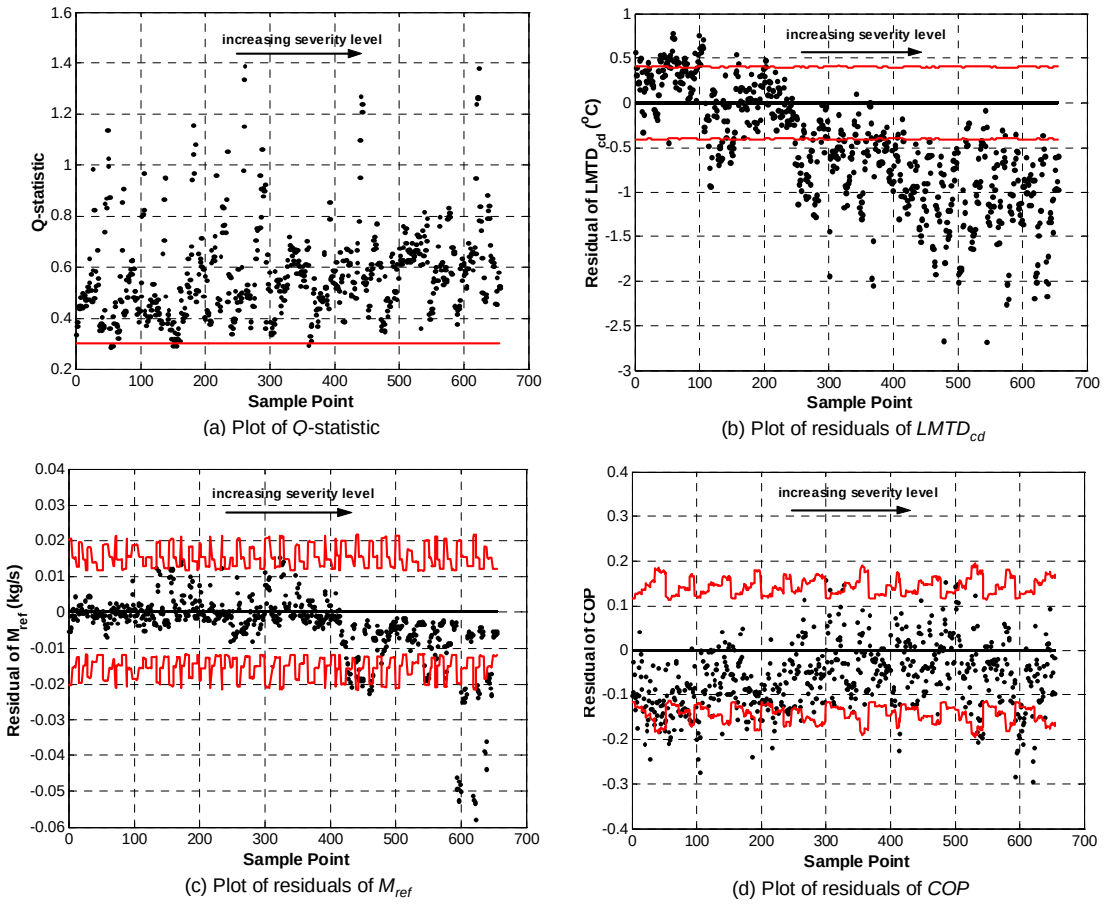

(a) Plot of *Q*-statistic

(b) Plot of residuals of $LMTD_{cd}$

(c) Plot of residuals of M_{ref}

(d) Plot of residuals of *COP*

Figure 8.5 Plots of *Q-statistic* and deviated residuals of performance index using test data group D - Refrigerant leakage test from fault severity level 1 to 4 with biased T_{chwr}

Test case 2: Excess oil with biased chilled water return temperature sensor

Similarly, most *Q-statistic* values went beyond the threshold, as shown in Figure 8.6-(a). Subsequently, the sensor FDD&E scheme was activated to tackle sensor faults. The

biased T_{chwr} was successfully identified with a "Detection ratio" value of 95.97% and a "Diagnosis ratio" value of 94.92%, and the biased error was estimated to be 2.21°C with a "Relative estimation error" value of 0.61%, as shown in Table 8.1. During the implementation of the chiller FDD scheme, only the residuals of Eff_{motor} and *COP* deviated from their corresponding thresholds with the increasing fault severity levels, as shown in Figure 8.6-(b) and (c), while no discernible residual of the other performance indexes was found. The fault diagnostic classifier identified the existence of excess oil.

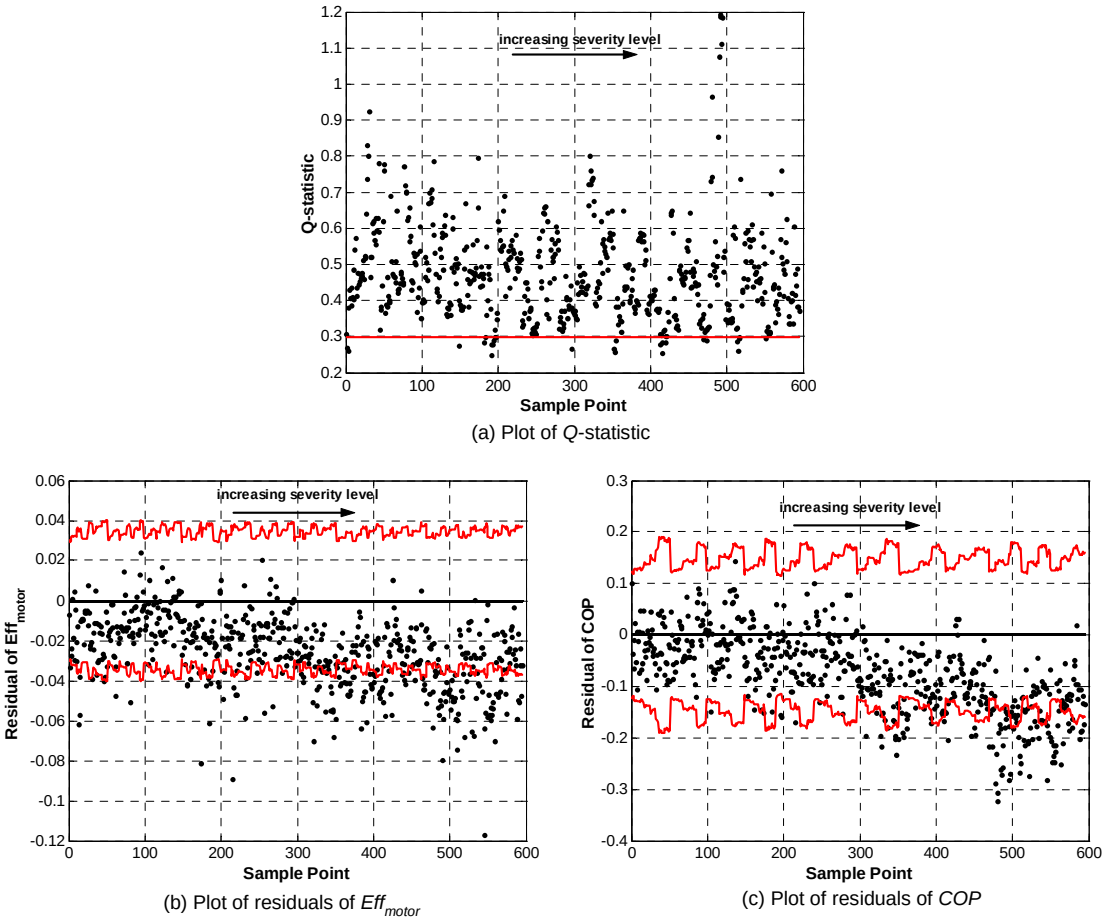

(a) Plot of *Q*-statistic

(b) Plot of residuals of Eff_{motor}

(c) Plot of residuals of *COP*

Figure 8.6 Plots of *Q-statistic* and deviated residuals of performance index using test data group D- Excess oil from fault severity level 1 to 4 with biased T_{chwr}

Test case 3: Condenser fouling with biased chilled water return temperature sensor

In the case of condenser fouling, the sensor FDD&E procedure was accordingly activated to tackle sensor faults as most *Q-statistic* values also went beyond the threshold, as shown in Figure 8.7-(a). The biased T_{chwr} was successfully identified with a "Detection ratio" value of 99.04% and a "Diagnosis ratio" value of 89.95%, and the biased error was estimated to be 2.29 ^{o}C with a "Relative estimation error" value of 3.93%, as shown in Table 8.1. As for the chiller FDD procedure, the residuals of three indexes, $LMTD_{cd}$,, M_{ref}, and *COP* deviated from their corresponding thresholds with the increasing fault severity levels, as shown in Figure 8.7-(b), (c) and (d). Therefore, the fault diagnostic classifier identified the existing fault as condenser fouling.

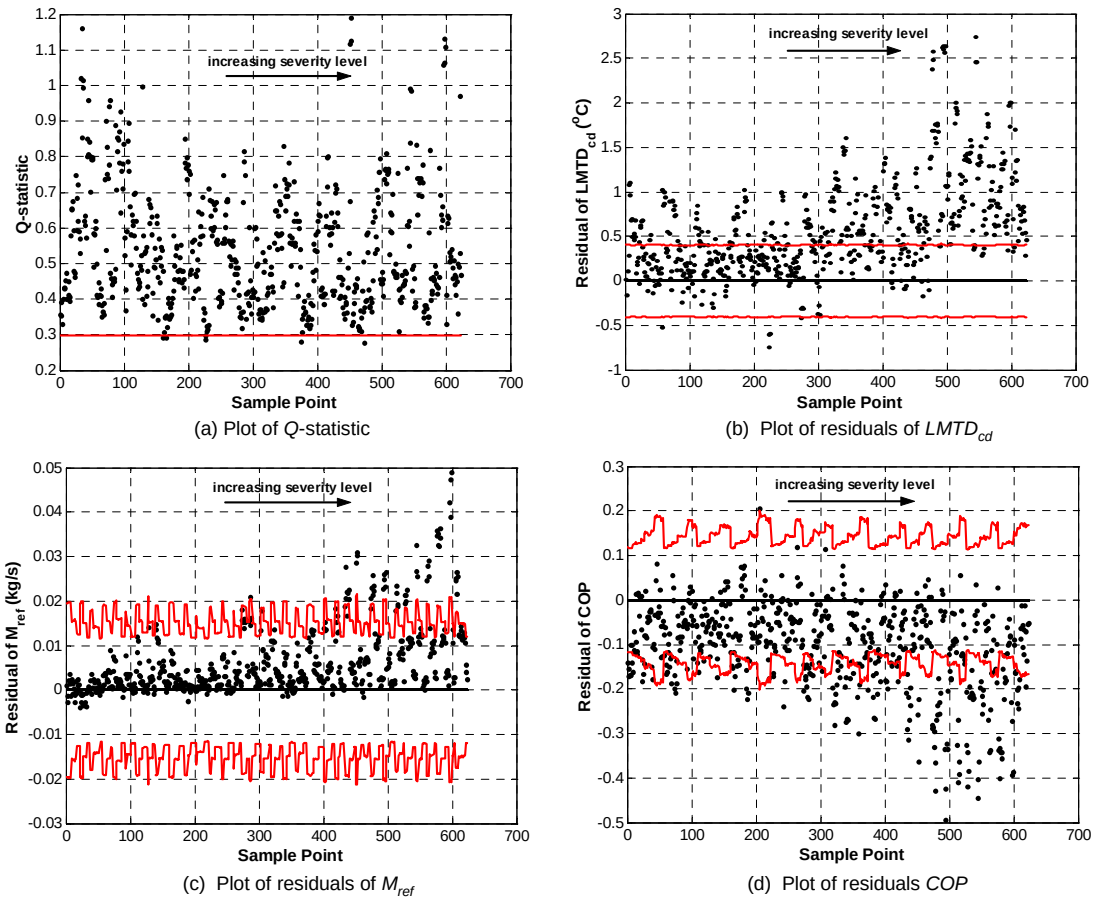

(a) Plot of *Q*-statistic

(b) Plot of residuals of $LMTD_{cd}$

(c) Plot of residuals of M_{ref}

(d) Plot of residuals *COP*

Figure 8.7 Plots of *Q-statistic* and deviated residuals of performance index using test data group D - Condenser fouling from fault severity level 1to 4 with biased T_{chwr}

8.3 Application Software Package of Robust Chiller FDD Strategy

8.3.1 Formation of FDD Application Software Package

The application software package of the robust FDD strategy was developed on the platform of MATLAB 6.1, which is a high-level technical computing language and interactive environment for algorithm development, data visualization, data analysis, and numerical computation. The application software package mainly comprises an initialization subprogram and a FDD main program incorporating three subprograms, including a data preprocessor subprogram, a sensor FDD&E subprogram and a chiller FDD subprogram, as shown in Figure 8.8. All subprograms are built up on the basis of the corresponding schemes and approaches which have already been developed and validated in the previous chapters. It is worth pointing out that this application software package is, to a great extent, a prototype application of the robust FDD strategy proposed in this thesis. Both normal (fault-free) data and monitored data are saved in the working directory as the binary "MAT" files with a suffix of ".mat". These data may be retrieved using a simple MATLAB function "LOAD".

The initialization subprogram is responsible for building up the PCA model and the reference model of each performance index. System configuration information, including the sensor configuration and component configuration, is contained in the program. The sensor configuration defines the accuracy of sensors and which sensors are considered in the PCA model as well as their measurement sequence. The sensor configuration may be different for different applications, but, for a specific application, the sequence of measurements in the training matrix and in the new samples (new monitored data) must be the same. Component configuration defines information concerning system component and subsystem, e.g., refrigerant and water properties. Normal data are

prepared in a "*.mat" file beforehand. If they are not prepared, the data from the first day after system commissioning will be used as normal data. The data preprocessor (see Section 3.3.1) is embedded in the initialization subprogram to eliminate undesirable data as much as possible. Certainly, the initialization subprogram should be implemented before starting the main program.

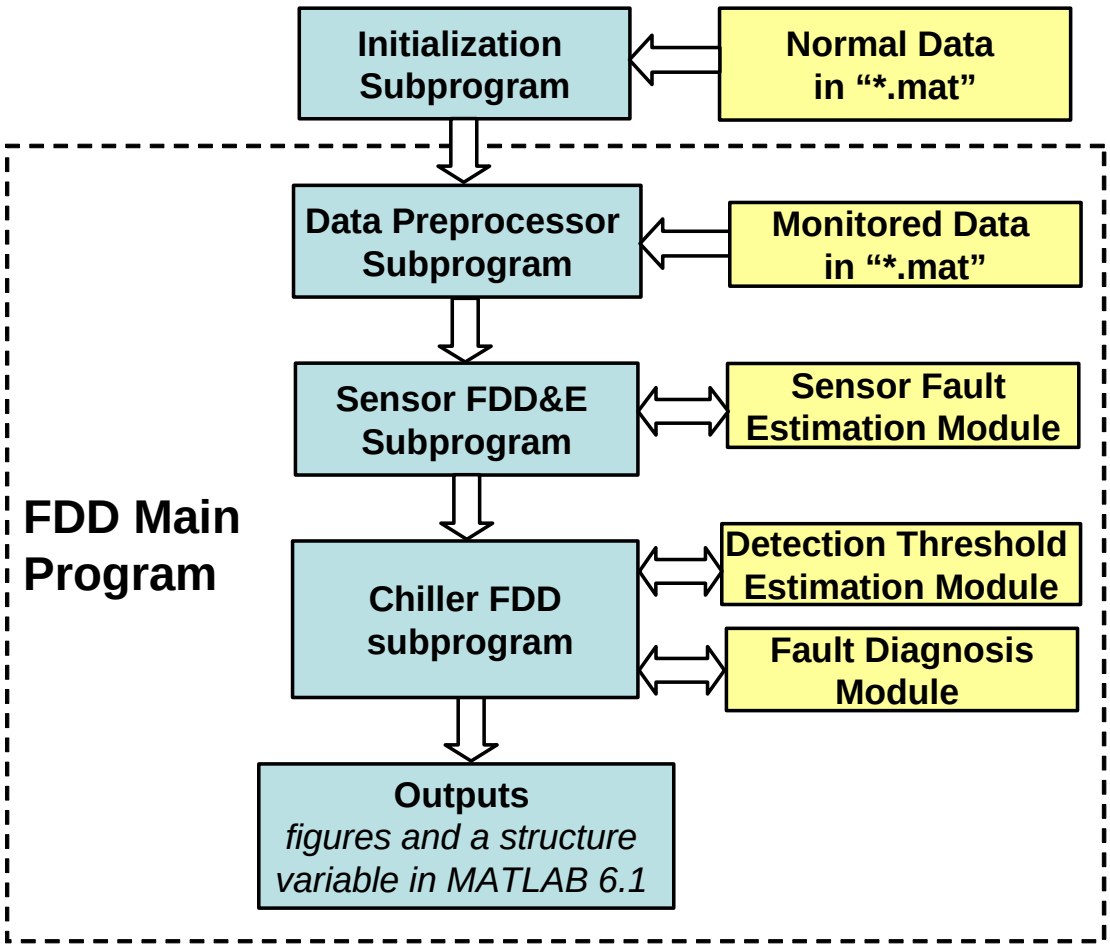

Figure 8.8 Schematic diagram of the structure of the FDD application software package in MATLAB 6.1

The main FDD program organizes the implementation sequence of three subprograms and calls them in a specified order when a certain number of samples from the monitored data are available.

The data preprocessor subprogram is called first of all to preprocess the incoming samples. Subsequently, using the trained PCA model from the initialization subprogram, the sensor FDD&E subprogram carries out PCA modeling, e.g., calculation of the *Q-statistic* and *Q-contributio*n. Sensor faults, if present, can be detected and diagnosed. Moreover, the sensor fault estimation module is called to correct identified sensor faults.

The chiller FDD subprogram will be called by the main FDD program after the samples are validated. The subprogram not only uses the corrected sample measurements to calculate the current performance indexes, but also employs the regressed reference models from the initialization subprogram to predict benchmark values of the performance indexes. Meanwhile, the chiller FDD subprogram calls a functional module, i.e., fault detection threshold estimation module, to update the fault detection threshold for each sample. Both residuals and fault detection thresholds of each performance index are outputted accordingly. The residuals are compared with corresponding thresholds to find out whether there is a chiller fault within the chiller system. Once a chiller fault is detected, the fault diagnosis module in the form of a simple expert system will be called to diagnose particular chiller faults. The simple expert system compares the current deviation pattern of the performance indexes against the fault diagnostic rules (see Table 3.2) and tries to find a match among them.

The implementation results, including the *Q-statistics*/threshold, the *Q-contribution* of each sensor measurement, and the residuals/thresholds are plotted on figures and saved along with diagnosed faults in a structure variable in MATLAB 6.1. In addition, the estimated magnitudes of sensor bias errors are also outputted and saved in the structure variable, and those can be used to further assess the severity of sensor faults as well as determine which measure, e.g., sensor recalibration or replacement, should be taken to tackle them.

8.3.2 Integration of FDD Application Software Package with IBmanager

The FDD application software package is integrated with an Intelligent Building management platform, namely IBmanager, as an application example of its integration with BMSs.

The IBmanager is an open IB (Intelligent Building) management platform based on middleware technologies. It can communicate with various BA (Building Automation) systems like LonMark and BACnet, and inter-operate with BMS (Building Management System) and FDD application software package with IP (Internet Protocol) integration. IBmanager server (as shown in Fig. 8.9) can be implemented on Intranet and Internet.

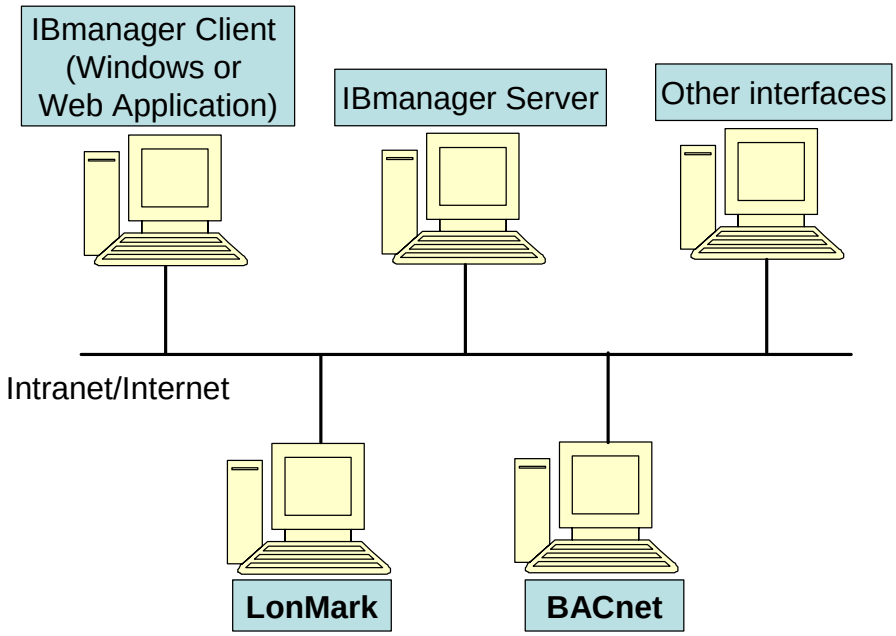

Figure 8.9 Schematics of IBmanager server

Figure 8.10 shows the schematic diagram of the integration of the FDD application software package with the IBmanager. Computer and network technologies are employed to build various standard interfaces between the IBmanager, the FDD

application software package, remote clients as well as the simulated building system. Except for the virtually simulated building system, the other components are real. Just like BMSs, the IBmanager server samples chiller data at a fixed interval from the simulated building system and monitors its operation.

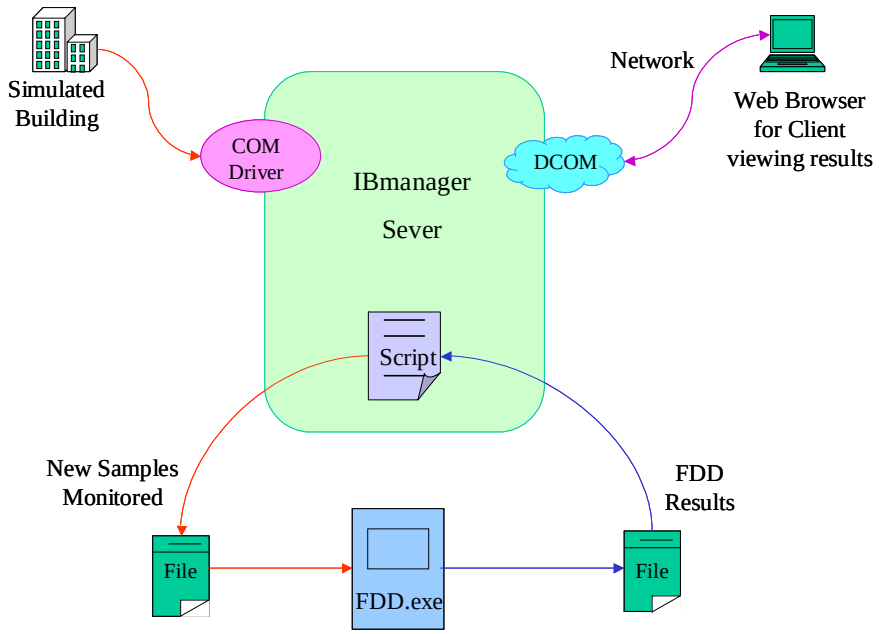

Figure 8.10 Schematic diagram of integration of the FDD application software package with the IBmanager sever

A script is coded and added to the IBmanager server to customize the chiller FDD application. The script mainly assumes functions of scheduling and communication. It sends variables to the FDD application software package in the format as it demands, and then the FDD application software package is executed by the IBmanager server. The FDD results are saved to the IBmanager server automatically. The local and remote user/clients can use network tools, e.g., Internet Explorer, to view FDD results on the IB manager server.

8.4 Summary

During chiller operation, two kinds of faults, i.e., sensor faults and chiller faults, may exist simultaneously. The implementation structure of the robust chiller FDD strategy, organically combining the basic chiller FDD scheme with the sensor FDD&E scheme, is presented in this chapter, aiming to carry out overall chiller fault detection and diagnosis. With the aid of real-life chiller data from ASHRAE 1043-RP, this chapter presents results of validation tests of the robust chiller FDD strategy on the platform. The test results prove that the robust strategy has the capability to detect and diagnose typical chiller faults after correcting sensor faults.

In addition, the robust FDD strategy was also tested using the field data from the real building introduced in Chapter 4. However, these tests are not presented in this thesis due to the following facts. Firstly the results of the tests using laboratory data have strong evidence to make the favorable conclusion on the performance of the robust FDD strategy. Secondly and more importantly, there is a lack of data containing known chiller faults (only the data containing condenser fouling are available), which however are needed to carry out tests and draw the conclusion at the same level of confidence as the laboratory data do. In fact, during the validation tests using the field data, the PCA model in the sensor FDD&E scheme was trained by more normal data, say the data from July 4th, 2001 to July 6th, 2001 instead of those from July 4th, 2001 only as in Section 7.2.2, so as to obtain a PCA model which can account for as many normal system variations as possible. Bias errors were added to the data collected on July 31st, 2001 to generate test data containing both sensor faults and a chiller fault (condenser fouling). As expected, the robust FDD strategy successfully tackled these two kinds of fault.

Besides validation tests of the robust FDD strategy using real life chiller data, the

application software package of the strategy developed on the platform of MATLAB 6.1 is presented in this chapter. As an application example of its integration with BMSs, the software package is integrated with the IBmanager, which is a versatile intelligent building management platform.

CHAPTER 9 SUMMARIES AND RECOMMENDATIONS

This final chapter summarizes the key features of the robust FDD strategy for centrifugal chillers and the main findings of this research work. Recommendations are also provided for utilizing the strategy as well as for future work in FDD within the HVAC&R industry.

A chiller involves many subsystems, components and sensors, all of which might be susceptible to faults. Chiller faults, i.e., faults associated with subsystems or components of chillers, if not detected or corrected, would result in increased operating costs and poor indoor environment quality. In addition, sensor faults, i.e., faults associated with sensors could lead to unreliable control, inaccurate efficiency monitoring as well as the failure of chiller FDD for chillers. To achieve efficient and effective operation and maintenance of chiller systems, a chiller FDD strategy capable of handling sensor faults and chiller faults simultaneously is highly desirable.

This thesis presents a basic chiller FDD scheme, a sensor FDD&E scheme, as well as a robust chiller FDD strategy organically incorporating the two schemes together. The basic chiller FDD scheme can effectively tackle six typical chiller faults, including evaporator fouling, condenser fouling, refrigerant leakage, excess oil, non-condensables in refrigerant and compressor degradation. The sensor FDD&E scheme can handle bias errors associated with temperature sensors, pressure sensors, and electric power meters in centrifugal chillers. After the two schemes were respectively validated by both laboratory data and field data, the robust chiller strategy organically incorporating the two schemes was developed. The strategy is called a robust one in that it is capable of

both diagnosing a chiller fault in the presence of a sensor fault, and diagnosing and estimating a sensor fault in the presence of a chiller fault. The robust strategy was tested and validated using laboratory data from ASHRAE 1043-RP.

9.1 Conclusions on Main Contributions

The primary contribution of this thesis is that a robust FDD strategy was developed to tackle two kinds of faults, i.e., sensor faults and chiller faults, which may simultaneously exist in a typical centrifugal chiller. Applicable algorithms for implementing the strategy were also formulated, which can be easily integrated with current BMSs. The developed strategy was validated using laboratory data from an ASHRAE research project whose main objective is to provide a database for the development and evaluation of FDD methods. In order to evaluate the applicability of the strategy in relation to on-line implementation, both schemes in the robust strategy were validated using field data collected from the BMS of a real building in Hong Kong.

Firstly, a basic chiller FDD scheme was developed based on six performance indexes indicative of chiller health conditions. The performance indexes have straightforward and strong thermophysical meaning and can synthesize information provided by individual measurements from a number of sensors in chillers. The fault diagnostic classifier in the basic chiller FDD scheme is constructed on the basis of a set of rules that relates each chiller fault to its impact on the performance indexes. Therefore, the fault diagnostic classifier is more understandable during construction and more effective during implementation, as compared with those based on rules relating each chiller fault to its impact on numerical measurements from sensors. More importantly, an online adaptive estimator of fault detection threshold has been developed. The estimator can

update the fault detection threshold according to the chiller operating conditions as well as the degree of sensor noise and the magnitude of fitting error of the reference model.

It is worth pointing out that the basic chiller FDD scheme fails to fulfill its duty when sensor faults occur in chillers. In order to cope with this shortcoming, a PCA-based FDD&E scheme was developed for the fault detection, diagnosis, and estimation of soft sensor faults. The PCA method is capable of capturing system variations of centrifugal chillers. Thanks to the fact that most chiller faults belong to system variations which can be captured by the PCA model whereas sensor faults do not, the output of PCA method, namely *Q-statistic*, is sensitive to sensor faults but insensitive to most chiller faults. Therefore, the sensor FDD&E scheme based on the PCA method can still successfully fulfill its duty even in the presence of these chiller faults.

9.2 Summary on Performance of the Basic Chiller FDD scheme

The major function of the basic chiller FDD scheme developed in this study is to consolidate the information from chillers into a clear and coherent picture of chiller status, which can help building operators detect existing faults and identify the cause. Various FDD methods were analyzed and compared after an extensive literature review. A model-based FDD method was finally chosen because it is suitable for fault detection and diagnosis for centrifugal chillers.

9.2.1 Performance Indexes

Six performance indexes, namely, logarithmic mean temperature difference of the evaporator and condenser ($LMTD_{ev}$ and $LMTD_{cd}$), refrigerant mass flow rate (M_{ref}), compressor polytropic efficiency (Eff_{poly}), drive motor efficiency (Eff_{motor}) and coefficient of performance (COP), were selected to indicate the health of a typical centrifugal chiller. In a thermophysical perspective, these performance indexes give a more comprehensive picture of the chiller than a great number of measurements from sensors do.

9.2.2 Reference Model and Its Identification

A reference model in the form of a polynomial with only three regressors (independent variables) is used in this study to predict benchmark values for each performance index of a centrifugal chiller. The reference model, after trained by normal data, can effectively capture the relationship between determinant variables and the performance indexes. In this way, the reference model is able to describe the baseline behavior of the chiller.

The reference model has the following advantages. The few regressors in the polynomial regression model not only make the model structurally simple but also make it less vulnerable to measurement errors associated with the variables. Furthermore, the identification of the reference model can be accomplished by a simple parameter estimation method, e.g., OLS, with the aid of a mount of normal data.

With regard to the normal data used in the model identification, it is recommended to select regressor values spreading uniformly over their whole range of variation.

9.2.3 Fault Diagnostic Classifier

The fault diagnostic classifier is based on a set of rules that relates each fault to the direction in which each performance index changes when the fault occurs. Such rules are deduced from theoretical analyses based on thermophysical principles. However, it should be mentioned that there is no universal fault diagnostic classifier and it needs to be carefully tailored to specific applications. For example, chillers using an expansion valve have a different fault diagnostic classifier from that of chillers using a fixed orifice, as shown in Table 3.2. In addition, since the set of rules in the fault diagnostic classifier defines qualitatively but not quantitatively the changing trends of the performance indexes when a fault occurs, continuous monitoring of chiller operation is highly recommended so as to help find such trends during the implementation basic chiller FDD.

9.2.4 Fault Detection Threshold

It is now generally accepted that setting an appropriate threshold for fault detection is a fundamental issue in FDD applications. A lower fault detection threshold can benefit the earlier detection of major faults but tends to produce false alarms, and vice versa. The adaptive estimator of fault detection threshold developed in this thesis takes into account essential influencing factors, e.g., chiller operating conditions on fault detection threshold, and can set reasonable thresholds accordingly. Therefore, the robustness of FDD can be enhanced.

9.2.5 Fault Detection and Diagnosis

The detection and diagnosis of faults involves comparison of online performance indexes with the corresponding benchmark values at the same operating conditions. Residuals for each performance index are generated from the comparison and then compared with the ever-updated fault detection threshold. When a specific portion of the residuals of one or more performance indexes are larger than their thresholds, the chiller system is considered to be faulty. Specific faults can be diagnosed by the fault diagnostic classifier according to deviation patterns of the performance indexes.

9.2.6 Validation Tests

The basic chiller FDD scheme was validated using both laboratory data and field data. Since the laboratory data come from an ASHRAE research project which is specifically designed to generate data for the development and evaluation of FDD methods, the validation tests based on such data should give us great confidence in the FDD scheme although not all the chiller faults considered in the scheme were tested. In addition, the validation test using the field data from the BMS in a real building convinced us of the feasibility of implementing the scheme on BMSs.

9.3 Summary on Performance of the Sensor FDD&E Scheme

The primary objective of the sensor FDD&E scheme is to tackle bias errors associated with key sensors whose measurements are crucial to chiller FDD, efficiency monitoring

and optimal control. The sensor FDD&E scheme includes three major function groups: sensor fault detection, sensor fault diagnosis and sensor fault estimation. These three groups enable the sensor FDD&E scheme not only to find abnormal sensor conditions and identify faulty sensors but also to estimate bias errors in the faulty sensor and correct them. Therefore, the chiller data after being processed by the sensor FDD&E scheme can be thought of as free of sensor faults. It should be mentioned that the scheme can detect a fault condition when one or more sensors is faulty, but the scheme is invalid for fault diagnosis and estimation when more than one sensor is faulty at the same time. In the case of multiple sensor faults, using PCA models comprising fewer variables would narrow the fault-searching range and help insolate faulty sensors. In addition, since the chance of more than one sensor going faulty simultaneously is slim, the scheme proposed in this thesis is still of significance in most engineering applications.

9.3.1 PCA Model

The basic method employed in the sensor FDD&E scheme is the PCA method. The PCA method was chosen on the one hand because it is insensitive to chiller faults at the component or system level, and on the other hand, because of its strong capability in capturing the correlations among a number of variables, which is particularly suitable for sensor FDD in chillers. Measurements in large-scale chillers such as a centrifugal chiller are heavily correlated with one another due to the cycling of refrigerant that interacts with compressor, chilled and cooling water in the system. However it is difficult to represent all these correlations precisely using mechanistic models because of complex thermodynamic processes. Moreover, the variations in measurements from sensors in a centrifugal chiller are relatively small as compared with those in other HVAC&R

systems, some of which, such as AHUs, are more susceptible to ever-changing environmental conditions. Therefore, it is easy for the PCA method to catch correlations among the number of variables.

The PCA method uses the correlation matrix to depict correlations among variables in a process. It does not require complex physical models of the dynamic and nonlinear air-conditioning system and its components, nor does it need to construct and train complex mathematic models such as black-box models. Problems caused by model uncertainty and training complexity can be avoided.

In order to apply the PCA method to centrifugal chillers, a PCA model including variables that are crucial to chiller FDD, performance monitoring and control was built. These measurements include the chilled water supply water temperature (T_{chws}), the chilled water return temperature (T_{chwr}), the evaporating temperature (T_{ev}), the evaporating pressure (P_{ev}) the leaving condenser water temperature (T_{lcw}), the entering condenser water temperature (T_{ecw}), the condensing temperature (T_{cd}), the condensing pressure (P_{cd}), the compressor suction temperature (T_{suc}), the compressor discharge temperature (T_{dis}), and the electrical power input to the compressor (W_{elec}).

9.3.2 Fault Detection, Diagnosis and Estimation

Sensor faults were detected using the *Q-statistic*, in the form of squared prediction error, which measures the magnitude of the projection of a measurement vector onto the residual subspace. An abnormal condition can be detected when the calculated *Q-statistic* is larger than its threshold, which is determined at a certain confidence level.

The *Q-contribution* plot can be used to identify the faulty sensor after the *Q-statistic* detects an abnormality. It can help reduce the possible fault sources and thus focus on a narrower fault-search range. Since determining the true measurements of the sensor is crucial to providing reliable data for the subsequent chiller FDD, the procedure of sensor fault estimation is of great importance in the scheme and the robust FDD strategy. The estimation is realized using an iterative approach, which always converges if only each variable in the PCA model is correlated with others.

9.3.3 Validation Tests

The sensitivity of the output of the PCA model, i.e., the *Q-statistic* to typical chiller faults was tested using laboratory chiller data from ASHRAE 1043-RP. The results of the sensitivity test shows that the *Q-statistic* is insensitive to the typical chiller faults including refrigerant leakage, refrigerant overcharge, excess oil, and condenser fouling. Furthermore the sensor FDD&E scheme was roundly validated by test data containing sensor faults as well as those containing both a sensor fault and a chiller fault. Validation results show the scheme can tackle a bias error as low as or even less than 15% of the average of sensor measurements. It is the first time in the HVAC&R field that a sensor FDD method has been tested using test data generated from real-life data to evaluate its performance while taking into consideration the possible effects of typical chiller faults. Moreover, the validation tests using field data from the BMS in a real building show that the sensor FDD&E scheme is also promising for future integration with BMSs.

9.4 Summary on Performance of Robust FDD Strategy

The robust FDD strategy for centrifugal chillers has been developed on the basis of incorporating the basic chiller FDD scheme with the sensor FDD&E scheme. Thus, the summaries of the basic chiller FDD scheme and the sensor FDD&E also apply to the robust FDD strategy. The validation tests of the robust strategy were implemented using different groups of test data generated from various tests in ASHRAE 1043-RP. These groups of test data respectively represent chiller normal operation conditions, sensor-fault conditions, chiller-fault conditions, as well as both sensor-faults and chiller-fault conditions. The test results show that the robust strategy is capable of identifying a chiller fault, after identifying and correcting a sensor fault.

Moreover, the data preprocessor that was first developed in Section 3.3.1 and widely used in all validation tests plays an important role in the implementation of the robust FDD strategy. The scope of the research work in this thesis focuses on the steady-state operation centrifugal chillers which are widely used in larger buildings. Since the dynamics of the fluid flow and heat transfer in centrifugal chillers are generally much faster than those of the chiller load and ambient conditions such as ambient temperatures, the steady-state operation can be assumed. In order to obtain data representative of steady-state operation, a steady-state filter, an outlier detector and a basic validity check were respectively designed to remove the transients, outliers and abnormalities in the data for both model development/training and online implementation. Undoubtedly, a well-designed data preprocessor consisting of these three tools is a prerequisite to the successful implementation of the basic chiller FDD scheme, the sensor FDD&E scheme and the robust FDD strategy.

9.5 Expandability and Transportability

The proposed robust FDD strategy is expandable in that it is able to accommodate more complicated abnormalities in chillers, no matter whether they belong to chiller faults or sensor faults. Additional performance indexes representative of an extra process or component that may need to be investigated can be added easily. Also, the PCA model can be expanded to include a larger number of sensors or shrunk to contain a smaller number of sensors according to practical applications. Moreover, the robust FDD strategy is transportable in the sense that it uses fundamental thermophysical principles to process data in the basic chiller FDD scheme and utilizes a pure data-driven PCA method to process data in the sensor FDD scheme. This characteristic allows the robust strategy to be applied to a variety of chillers, e.g., reciprocating chillers and rotary screw chillers, with a little modification if necessary.

9.6 Recommendations and Further Work

Research efforts made as part of this thesis have primarily concentrated on the development of robust chiller FDD strategy conceptually. It would be very desirable and valuable to make further efforts on a few aspects related to the research presented in this thesis.

1. Although the prototype schemes and strategy have been verified predominantly with laboratory data and field data, extensive field test of them on centrifugal chillers must still be carried out to secure greater confidence in the conclusions and recommendations made on the basis of this research work, and to promote their application in BMSs in real buildings.

2. The proposed schemes are expandable and transportable in the sense of being able to accommodate other chiller faults or sensor faults and may be applied to other vapor compression equipment. Additional performance indexes representative of chiller operation can be added. Also, additional sensors such as flow meters can be added to the PCA model so as to have a more comprehensive sensor FDD scheme.
3. An overall FDD system should be able to evaluate the impact of the faults and afterwards recommend a course of action. If a fault has been identified but the current operation is not adversely affecting the equipment life, the energy efficiency, or the environment, then the best decision should come from a tradeoff between costs associated with maintenance service and energy costs associated with the fault. Maintenance service costs money but reduces energy costs. Therefore, a method involving optimal maintenance scheduling is also needed in the future. That, of course, would require more knowledge beyond the HVAC&R technology itself.
4. In this paper, either the fault detection sensitivity of the chiller FDD scheme to chiller faults or the sensitivity of the sensor FDD&E scheme to sensor faults is discussed and evaluated qualitatively only but not quantitatively. Therefore, the investigation of the fault detection sensitivity of the schemes would be an important research topic in the future, which might involve an improved fault classifier and test data indicative of more faulty operating conditions.

REFERENCES

1. 1996 ASHRAE Handbook. HVAC System and Equipment. *ASHRAE, Inc*.
2. ARI 550/590. 2003. Standard for Performance Rating of Water – Chilling Packages Using the Vapor Compression Cycle. *The Air-Conditioning and Refrigeration Institute (ARI)*
3. Bailey M.B. 1998. *The Design and Viability of a Probabilistic Fault Detection and Diagnosis Method for Vapor Compression Cycle Equipment*. Ph.D. Thesis, School of Civil Engineering, University of Colorado.
4. Beck J.V. and K.J. Arnold. 1977. Parameter Estimation in Engineering and Science. New York: John Wiley & Sons.
5. Bourdouxhe J.P., M. Grodent, and J.J. Lebrun. 1997. HVAC1 Toolkit: Algorithms and Subroutines for Primary HVAC System Energy Calculations. *The American Society of Heating, Refrigerating and Air Conditioning Engineers*.
6. Braun J.E. 1988. *Methodologies for the Design and Control of Central Cooling Plant.* Ph.D. Thesis, University of Wisconsin – Madison.
7. Braun J.E. 1999. Automated Fault Detection and Diagnostics for the HVAC&R Industry. *HVAC&R Research*, Atlanta, Vol. 5(2):85-98.
8. Braun J.E. 2003. Automated Fault Detection and Diagnostics for Vapor Compression Cooling Equipment. *Journal of Solar Energy Engineering*, Vol. 125(3):266-274.
9. Breuker M.S. 1997. *Evaluation of a Statistical, Rule-Based Fault Detection and Diagnostics Method for Vapor Compression Air Conditioners*, Master Thesis, School of Mechanical Engineering, Purdue University.

10. Breuker M.S. and J.E. Braun. 1998. Evaluating the Performance of a Fault Detection and Diagnostic System for Vapor Compression Equipment," *International Journal of Heating, Ventilating, and Air Conditioning and Refrigerating Research*, Vol. 4(4): 401-425.
11. Chan K.T. and F.W. Yik. 2002. Part Load Efficiency of Air-Cooled Multiple-Chiller Plants. *Building Service Engineering Research and Technology*, Vol. 23(1):31–41.
12. Chiang L.H., Russell E.L. and R.D. Braatz. 2001. *Fault Detection and Diagnosis in Industrial Systems*. Heidelberg: Springer.
13. Comstock, M.C. and J.E. Braun. 1999. Literature Review for Application of Fault Detection and Diagnostic Methods to Vapor Compression Cooling Equipment. Ray W. Herrick Laboratories, Purdue University, HL99-19, Report #4036-2, *ASHRAE Research Project 1043.*
14. Comstock M.C. and J.E. Braun. 1999. Development of Analysis Tools for The Evaluation of Fault Detection and Diagnostics for Chillers. HL 99-20, Report #4036-3. *ASHRAE Research Project 1043*
15. Comstock M.C. and J.E. Braun. 2001. The Sensitivity of Chiller Performance to Common Faults. *HVAC&R Research***,** Atlanta, Vol. 7(3):263-279.
16. Corcoran Joseph P. and T. Agami Reddy. 2003. Improving the Process of Certified and Witnessed Factory Test for Chiller Procurement. *ASHRAE Transaction*, Career and Technical Education, Vol. 109:193-201
17. Dexter Arthur L. and Jouko Pakanen. Fault Detection and Diagnosis Methods in Real Buildings. *International Energy Agency, Energy conservation in Buildings and Community Systems, Annex 34*: *Computer-aided evaluation of HVAC system performance*, 2001.
18. Dexter Arthur L. 2001. Fault Diagnosis in Air-Conditioning Systems: A Multi-

Step Fuzzy Model-Based Approach. *HVAC&R Research*, Atlanta, Vol. 7(1): 83-102

19. Dorr R., F. Kratz, J. Ragot, F. Loisy, and J.L. Germain. 1997. Detection, Isolation, and Identification of Sensor Faults in Nuclear Power Plants. *IEEE Trans. on Control System Technology*, Vol. 5(1):42-60.
20. Draper N. and H. Smith. 1981. *Applied Regression Analysis*, 2nd edition. New York: John Wiley & Sons.
21. Dunia R. and S.J. Qin. 1998. Joint Diagnosis Of Process And Sensor Faults Using Principal Component Analysis. *Control Engineering Practice*, Vol. 6:457-469.
22. Dunia R., S.J. Qin, T.F. Edgar, and T.J. McAvoy. 1996. Identification of Faulty Sensors Using Principal Component Analysis. *AIChE Journal*. Vol. 42: 2797-2812.
23. Frank P.M. 1990. Fault Diagnosis in Dynamic Systems Using Analytical and Knowledge-Based Redundancy – A Survey and Some New Results. *Automatica*, Vol. 26(3):459-474
24. Glass A. and P. Gruber. 1996. Steady State Detection. *IEA Annex 25, Building Optimization and Fault Diagnosis Source Book*, Technical Research Center of Finland, 265-267.
25. Gordon J.M., K.C. Ng, and H.T. Chua. 1995. Centrifugal chillers: thermodynamic modeling and a diagnostic case study. *International Journal of Refrigeration*, Vol. 18(4):253-257.
26. Grimmelius H.T., J.K. Woud, and G. Been. 1995. On-line Failure Diagnosis for Compression Refrigeration Plants. *International Journal of Refrigeration*, Vol. 18, No. 1, pp. 31-41.
27. Han C.Y., Y. Xiao and C.J. Ruther. 1999. Fault Detection and Diagnosis of HVAC Systems. *ASHRAE Transactions*, Atlanta; Vol. 105:568-578.

28. Hartman Thomas B. 2000. Chiller-Plant Control Using Gateway Technologies. *HPAC Engineering*, Vol. 72(1):81-85
29. Hartman Thomas B. 2001. Instrumentation Issues for Monitoring Chiller Plant Efficiency. *ASHRAE Transactions*, Vol. 107 (1):407-414.
30. Haves P. 1999. Overview of Diagnostic Methods. *Proceedings of Diagnostics for Commercial Buildings: From Research to Practice*, San Francisco, CA.
31. Huang J., H. Akbari, L. Reiner, and R. Ritschard. 1991. 481 Prototypical Commercial Buildings for 20 Urban Market Areas. *GRI Report GRI-90/0326*.Chicago: Gas Research Institute.
32. IEA Annex 25, 1996, *Building Optimization and Fault Diagnosis Source Book*, Eds. J. Hyvärinen and S. Kärki, Technical Research Centre of Finland.
33. Inatsu H., H. Matsuo, K. Fujiwara, K. Yamada, and K. Nishizawa. 1992. Development of Refrigerant Monitoring Systems for Automotive Air-Conditioning Systems. *Society of Automotive Engineers*, SAE Paper, No. 920212.
34. Jackson J. Edward and Govinod S. Mudholkar. 1979. Control Procedures for Residual Associated with Principal Component Analysis. *Technometrics*, Vol. 21(3):341-349
35. Jackson J. Edward. 1991. *A User's Guide to Principal Components*. New York: John Wiley & Sons.
36. Janos J. Gertler. 1998. *Fault Detection and Diagnosis in Engineering Systems*. New York : Marcel Dekker.
37. Jia Yongzhong. 2002. *Model-Based Generic Approaches for Automated Fault Detection, Diagnosis, Evaluation (FDDE) and for Accurate Control of Field Operated Centrifugal Chillers*. Ph.D. Thesis. Drexel University.
38. Jolliffe I.T. 1986. *Principal Component Analysis*. New York: Springer-Verlag.
39. Kourti T. and F.F. MacGregor. 1996. Multivariate SPC Methods for Process and

Product Monitoring. *Journal of Quality Technology*, Vol. 28:409-428.

40. Kresta J., MacGregor, J.F., and T.E. Marlin. 1991. Multivariable Statistical Monitoring Of Process Operating Performance. *Can. J. Chem. Eng.* Vol. 69:35-47.
41. Lee Won-Yong, House John M. and Kyong Nam-Ho. 2004. Subsystem Level Fault Diagnosis of A Building's Air-Handling Unit Using General Regression Neural Networks. *Applied Energy*, Vol. 77(2):153-170.
42. Lee W.Y., L.M. House and D.R. Shin. 1997. Fault Diagnosis and Temperature Sensor Recovery for an Air Handling Unit. *ASHRAE Transactions*, Vol. 103(1):621-633
43. Lennox J. and C. Rosen. 2002. Adaptive Multi-Scale Principal Components Analysis for Online Monitoring of Wastewater Treatment. *Water Science and Technology*, Vol. 45(4-5):227-235.
44. Li Haorong and James E. Braun. 2003. An Improved Method for Fault Detection and Diagnosis Applied to Packaged Air Conditioners. *ASHRAE Transactions*, Vol. 109(2):683-692
45. Martens H. and T. Naes. 1989. *Multivariate Calibration*. New York: John Wiley & Sons.
46. Menzer Mark. 1997. Studies Show How Air-Conditioning Equipment Efficiency Has Increased. *Proceedings of International Climate Change Conference*. Baltimore.
47. McIntosh Ian B.D. 1999. *A Model-Based Fault Detection and Diagnosis Methodology for HVAC Subsystems*. Ph.D. Thesis, University of Wisconsin, Madison.
48. McIntosh Ian B.D., John W. Mitchell, and William A. Beckman. 2000. Fault Detection and Diagnosis in Chillers--Part I: Model Development and Application / Discussion. *ASHRAE Transactions*. Atlanta, Vol. 106(2):268-282

49. Montgomery Douglas C. and George C. Runger. 1994. *Applied Statistics and Probability for Engineers.* New York: John Wiley & Sons

50. Ogaji S.O.T., Singh R. and S.D. Probert. 2002. Multiple-Sensor Fault-Diagnoses for a 2-Shaft Stationary Gas-Turbine. *Applied Energy*, Vol. 71(4):321-339

51. Pacific Gas and Electric. 2001. *CoolTools: A Toolkit to Optimize Chilled Water Plants*. San Francisco, CA. http://www.hvacexchange.com/cooltools/

52. Patton R.J. and J. Chen. 1991. Parity Space Approach to Model-based Fault Diagnosis – A Tutorial Survey and Some New Results. *IFAC/IMACS Symposium on Fault Detection, Supervision and Safety for Technical Proce*ss, Baden-Baden.

53. Peitsman H. and V. Bakker. 1996. Application of Black-Box Models to HVAC Systems for Fault Detection. *ASHRAE Transactions*, Vol. 102(1):628-640

54. Phelan J., Brandemuehl M., and M. Krarti. 1997. In-Situ Performance Test of Chillers for Energy Analysis. *ASHRAE Transactions*, Vol. 103(1):290-302.

55. Pranatyasto T.N., S.J. Qin. 2001. Sensor Validation And Process Fault Diagnosis For FCC Units Under MPC Feedback. *Control Engineering Practice*, Vol. 9(8):877-888.

56. Reddy T.A. Niebur D., Gordon J., Seem J., Cabrera G., Jia Y., Andersen K. K., and P. Pericolo. 2001. Development and Comparison of On-line Model Training Techniques for Model-Based FDD Methods Applied to Vapor Compression Chillers: Evaluation of Mathematical Models and Training Techniques. Final Report, *ASHRAE Research Project 1139*

57. Reddy T. Agami, Klaus K. Andersen. 2002. An Evaluation of Classical Steady-State Off-Line Linear Parameter Estimation Methods Applied to Chiller Performance Data. *HVAC&R Research Journal*, Vol. 8(1):101-124.

58. Reddy T. Agami, Klaus K. Andersen, and Dagmar Niebur. 2003. Information Content of Incoming Data during Field Monitoring: Application to Chiller

Modeling (RP-1139). *HVAC&R Research*, Vol. 9(4):365-384.

59. Rossi T.M. 1995. *Detection, Diagnosis, and Evaluation of Fault in Vapor Compressor Cycle Equipment.* Ph.D. Thesis, Purdue University
60. Rossi T.M. and J.E. Braun. 1997. A Statistical, Rule-Based Fault Detection and Diagnostic Method for Vapor Compression Air Conditioners. *International Journal of HVAC&R Research*, Vol. 3(1):19-37.
61. Russell E.L., L.H. Chiang and D.B. Richard. 2000. *Data-Driven Techniques for Fault Detection and Diagnosis in Chemical Process*. London: Hong Kong, Springer.
62. Stallard L.A. 1989. *Model Based Expert System for Failure Detection and Identification of Household Refrigerators,* Master Thesis, School of Mechanical Engineering, Purdue University.
63. Stylianou M.P. and D. Nikanpour. 1996. Performance Monitoring, Fault Detection, and Diagnosis of Reciprocating Chillers. *ASHRAE Transactions*, Vol. 102(1):615-627.
64. Stylianou M.P. 1997. Application of Classification Functions to Chiller Fault Detection and Diagnosis. *ASHRAE Transactions*, Vol. 103(1): 645-656.
65. Tracy N.D., J.C. Yung, and R.L. Mason. 1992. Multivariate Control Charts for Individual Observations. *Journal of Quality Technology*, Vol. 24 (2): 88-95.
66. Tsutsui H. and K. Kamimura. 1996. Chiller Condition Monitoring Using Topological Case-Based Modeling. *ASHRAE Transactions*, Vol. 102(1):641-648.
67. Tzafestas S. 1991. Second Generation Expert Systems: Requirements, Architectures and Prospects. *IFAC/IMACS Symposium on Fault Detection, Supervision and Safety for Technical Process*, Baden-Baden, Vol. 2:1-6.
68. Usoro P.B., L.C. Schick, and S. Negahdaripour. 1985. An Innovation-Based Methodology for HVAC System Fault Detection. *Journal of Dynamics Systems,*

Measurement, and Control, Transactions of the ASME. Vol.107:284-285.

69. Vachekov G. and H. Matsuyama. 1992. Identification of Fuzzy Rule Based System for Fault Diagnosis in Chemical Plants. *IFAC Symposium on On-line Fault Detection and Supervision in the Chemical Process Industries*, Newark.
70. Wagner J. and R. Shoureshi. 1992. Failure Detection Diagnostics for Thermofluid Systems. *Journal of Dynamic Systems, Measurement, and Control*, Vol. 114(4):699-706.
71. Wang S.W. and J. Burnett. 2001. Online Adaptive Control for Optimizing Variable-Speed Pumps of Indirect Water-cooled Chilling Systems. *Applied Thermal Engineering*, Vol. 21(11):1083-1103.
72. Wang S.W. and J.B. Wang. 1999. Law-Based Sensor Fault Diagnosis and Validation for Building Air-conditioning Systems, *International Journal of HVAC&R Research*, Vol. 5(4):353-378.
73. Wang S.W. and J.B. Wang. 2002a. Automatic Sensor Evaluation in BMS Commissioning of Building Refrigeration Systems. *Automation in Construction*, Vol. 11(1):59-73.
74. Wang S.W. and J.B. Wang. 2002b. Robust Sensor Fault Diagnosis and Validation in HVAC Systems. *Transactions of the Institute of Measurement and Control*, Vol. 24(3):231-262.
75. Wang S.W. and F. Xiao. 2004. AHU Sensor Fault Diagnosis Using Principal Component Analysis Method. *Energy and Buildings*, Vol. 36 (2):147-160.
76. Wise B. M. and N. L. Ricker. 1991. Recent Advances in Multivariate Statistical Process Control: Improving Robustness and Sensitivity. *Proceedings of the IFAC Symposium on Advanced Control of Chemical Processes*, France, 125-130.
77. Wise B.M., Ricker N.L., and Velkamp D.J., and B.R. Kowalski. 1990. A Theoretical Basis for the Use of Principal Component Models for Monitoring

Multivariate Processes. *Process control and Quality*, Vol.1:41-51.

78. Yoshimura M. and N. Ito. 1989. Effective Diagnosis Methods for Air-Conditioning Equipment in Telecommunications Buildings. *Proceedings of IEEE INTELEC 89: The Eleventh International Telecommunications Energy Conference*, October 15-18, Centro dei Congressi, Firenze, Vol. 2(21) (1):1-7.
79. Yung S.K. and D.K. Clarke. 1989. Local Sensor Validation. *Measurement and Control,* Vol. 22:132-150.

APPENDIX A

Derivation of Equation (3.17) and Equation (3.18) - Estimating Variance of the Residual of a Performance Index

According to the principle of OLS, the observed value of the ith performance index (Y_i) corresponding to a specific observed regressor vector should satisfy Equation (1).

$$Y_i = f_i(\hat{Q}_{ev}, \hat{T}_{ecw}, \hat{T}_{chws}) + \varepsilon_i \quad (1)$$

where $\hat{Q}_{ev}, \hat{T}_{ecw}$ and $\hat{T}_{chws}$ represent the observed (measured) values of Q_{ev}, T_{ecw} and T_{chws}, respectively. ε_i is normally distributed error with a mean of zero and a variance of $\sigma_{Y_i}^2$. $\sigma_{Y_i}^2$ is the variance of the regression error of *i*th performance index, namely the square of the SEE (Standard Error of Estimate) of Y_i. $f_i(\ )$ represents the polynomial regression model of the *i*th performance index.

Therefore, the normal distribution of Y_i has a mean value of $f(\hat{Q}, \hat{T}_{ecw}, \hat{T}_{chws})$ and a variance of $\sigma_{Y_i}^2$, as illustrated by Equation (2).

$$Y_i \sim N(f(\hat{Q}, \hat{T}_{ecw}, \hat{T}_{chws}), \sigma_{Y_i}^2) \quad (2)$$

Also, the output of the corresponding reference model ($\tilde{Y}_i$) at the same observed regressor vector is normally distributed with a mean value of $f(\hat{Q}, \hat{T}_{ecw}, \hat{T}_{chws})$ and a variance of $\sigma_{Y_i}^2 \mathbf{X}_0^T (\mathbf{X}_{reg}^T \mathbf{X}_{reg}) \mathbf{X}_0$ (Montgomery and Runger 1994). That can be illustrated by Equation (3).

$$\tilde{Y}_i \sim N(f(\hat{Q}, \hat{T}_{ecw}, \hat{T}_{chws}), \sigma_{Y_i}^2 \mathbf{X}_0^T (\mathbf{X}_{reg}^T \mathbf{X}_{reg}) \mathbf{X}_0) \quad (3)$$

The true value of the residual of the *i*th performance index, r_i, can be given by Equation (4).

$$r_i = g_i(\mathbf{z}) - Y_i \tag{4}$$

where $g_i(\cdot)$ presents the calculation formula of the *i*th performance index (see Table 3.1) and $\mathbf{z}$ is the vector of true values of relevant variables.

However, due to measurement and modeling uncertainty, the residual of the *i*th performance index is estimated as shown in Equation (5).

$$\tilde{r}_i = g_i(\hat{\mathbf{z}}) - \tilde{Y}_i \tag{5}$$

where $\tilde{r}_i$ is the estimate of r_i and $\hat{\mathbf{z}}$ is the vector of measured values of variables concerned. $g_i(\hat{\mathbf{z}})$ is the *i*th performance index calculated using $\hat{\mathbf{z}}$. By replacing $g_i(\hat{\mathbf{z}})$ with $g_i(\mathbf{z})$ plus the first-order item in its Taylor expansion while neglecting the second and higher order, Equation (5) can be further deduced as shown in Equation (6).

$$\tilde{r}_i \approx g_i(\mathbf{z}) + \sum_j \left(\frac{\partial g_i}{\partial z_j}\delta z_j\right) - \tilde{Y}_i \tag{6}$$

where z_j is the *j*th element in $\mathbf{z}$, δz_j is zero mean Gaussian noise associated with z_j and its standard deviations are σ_{z_j}.

By subtracting Equation (4) from Equation (6), Equation (7) is derived.

$$\tilde{r}_i - r_i = \sum_j \left(\frac{\partial g_i}{\partial z_j}\delta z_j\right) - (\tilde{Y}_i - Y_i) \tag{7}$$

Since δz_j, $\tilde{Y}_i$ and Y_i are independent of each other (Montgomery and Runger 1994), the mean and variance of $\tilde{r}_i - r_i$ can be respectively given by Equation (8) and Equation(9) while referring to Equation (2) and Equation (3).

$$E(\tilde{r}_i - r_i) = 0 \tag{8}$$

$$D(\tilde{r}_i - r_i) = \sigma^2_{\tilde{r}_i - r_i} = \sum_j \left[\left(\frac{\partial g_i}{\partial z_j} \right) \sigma_{z_j} \right]^2 + \sigma^2_{Y_i} [1 + \mathbf{X}_0^T (\mathbf{X}_{reg}^T \mathbf{X}_{reg}) \mathbf{X}_0] \quad (9)$$

Therefore, $\tilde{r}_i - r_i$ is can been assumed to be normally distributed with mean zero and variance $\sigma_{\tilde{r}_i - r_i}$ as shown in Equation (10).

$$\tilde{r}_i - r_i \sim N(0, \sigma^2_{\tilde{r}_i - r_i}) \quad (10)$$

or,

$$\frac{\tilde{r}_i - r_i}{\sigma_{\tilde{r}_i - r_i}} \sim N(0,1) \quad (11)$$

When $\sigma^2_{Y_i}$ in Equation (9) is replaced with its unbiased estimate, $\tilde{\sigma}^2_{Y_i}$, which is given by Equation (12), the unbiased estimate of $\tilde{\sigma}^2_{\tilde{r}_i - r_i}$ can be obtained by Equation (13).

$$\tilde{\sigma}^2_{Y_i} = \sum_{k=1}^{n} (Y_k - \tilde{Y}_k)^2 \Big/ n - p \quad (12)$$

$$\tilde{\sigma}^2_{\tilde{r}_i - r_i} = \sum_j \left[\left(\frac{\partial g_i}{\partial z_j} \right) \sigma_{z_j} \right]^2 + \tilde{\sigma}^2_{Y_i} [1 + \mathbf{X}_0^T (\mathbf{X}_{reg}^T \mathbf{X}_{reg}) \mathbf{X}_0] \quad (13)$$

where Y_k is the *k*th response variable in the model development data and $\tilde{Y}_k$ is the output of the reference model. *n* is the number of observations in the model regression and *p* is the number of coefficients estimated from the model development data.

Now, it can be concluded that $\frac{\tilde{r}_i - r_i}{\tilde{\sigma}_{\tilde{r}_i - r_i}}$ has a *t* distribution with *n-p* degree of freedom (Montgomery and Runger 1994) as shown in Equation (14).

$$\frac{\tilde{r}_i - r_i}{\tilde{\sigma}_{\tilde{r}_i - r_i}} \sim t_{n-p} \quad (14)$$

This leads to a (1-α) confidence interval for the predictor of the residual of the *i*th performance index (r_i), which is shown in Equation (15).

$$\left(\tilde{r}_i - t_{\alpha/2,n-p}\tilde{\sigma}_{\tilde{r}_i - r_i}\right) \le r_i \le \left(\tilde{r}_i + t_{\alpha/2,n-p}\tilde{\sigma}_{\tilde{r}_i - r_i}\right) \quad (15)$$

During implementation of FDD, the uncertainty of the predictor of r_i with a (1-α) confidence level is given in Equation (16).

$$U(\tilde{r}_i) = \pm t_{\alpha/2,n-p}\tilde{\sigma}_{\tilde{r}_i - r_i} \quad (16)$$

APPENDIX B

Coefficients of reference models

Table 1 Coefficients of reference models for performance indexes regressed by laboratory data from ASHRAE 1043-RP

	$LMTD_{ev}$	$LMTD_{cd}$	M_{ref}	Eff_{poly}	Eff_{motor}	COP
b_0	-1.1434e+0	8.2319e-1	-1.4914e-3	1.0136e-2	3.9392e-1	1.2979e+0
b_1	3.8130e-1	-1.8205e-1	1.1724e-3	-2.1175e-2	6.3934e-3	2.8785e-2
b_2	-1.6299e-2	1.1000e-3	8.5315e-5	1.0832e-2	4.5674e-3	-2.3601e-2
b_3	2.3194e-2	1.9652e-2	4.8725e-3	2.8316e-3	2.1561e-3	2.9253e-2
b_4	1.2399e-3	5.3341e-3	-5.9017e-5	2.7584e-4	-1.9924e-4	-1.3106e-3
b_5	3.9263e-4	3.7342e-4	-2.5335e-5	4.2543e-5	-1.7412e-5	2.3538e-4
b_6	-2.9814e-4	-3.6158e-4	4.3487e-5	-3.5885e-5	-1.8657e-6	-3.2290e-4
b_7	-1.4647e-5	1.9673e-6	6.4895e-7	-2.8723e-6	-2.2315e-6	-3.5574e-5

Table 2 Coefficients of reference models for performance indexes regressed by field data from a real building in Hong Kong

	$LMTD_{ev}$	$LMTD_{cd}$	M_{ref}	Eff_{poly}	Eff_{motor}	COP
b_0	-3.0609e+1	2.4870e+1	-3.3868e+0	2.0176e+0	5.3509e+0	5.3675e+1
b_1	2.9431e+0	4.3414e-1	1.0836e+0	-1.9718e-1	-7.1897e-1	-6.6236e+0
b_2	7.4667e-1	-7.8776e-1	1.2969e-01	-3.8817e-2	-2.1438e-1	-2.0318e+0
b_3	3.0375e+1	-2.4330e+1	1.6969e+1	-4.3845e-1	1.3349e+0	5.0349e+0
b_4	-3.3003e-2	-4.3876e-2	-4.0575e-2	4.5395e-3	3.0749e-2	2.5830e-1
b_5	-2.4401e+0	7.7810e-1	-8.7548e-2	5.3131e-2	-1.9582e-1	-8.1082e-1
b_6	-7.2190e-1	9.9646e-1	2.8513e-1	1.6583e-2	1.9602e-2	2.8446e-1
b_7	5.1804e+0	-1.6415e+0	1.4434e+0	-1.3641e-1	-9.5938e-2	-3.0818e+0

PUBLICATIONS DURING PHD STUDY

Journal Papers

2005 Cui J.T. and Wang S.W. "An Overall FDD Strategy for Centrifugal Chillers", submitted to <*International Journal of HVAC&R Research*>

2005 Cui J.T. and Wang S.W. "A Robust Sensor Fault Detection, Diagnosis and Estimation Strategy for Centrifugal Chillers", submitted to <*Building and Environment*>

2005 Cui J.T. and Wang S.W. "A Model-Based Online Fault Detection and Diagnosis Strategy for Centrifugal Chiller Systems", *International Journal of Thermal Sciences*, Vol. 44 (10): 986-999 (2005)

2005 Wang S.W. and Cui J.T. "Sensor Fault Detection, Diagnosis and Estimation in Centrifugal Chiller Systems Using Principal Component Analysis Method", *Applied Energy*, Vol. 82 (3):197-213 (2005)

2004 Cui J.T. and Wang S.W. "Application Of CFD In Evaluation and Energy-Efficient Design of Air Curtains for Horizontal Refrigerated Display Cases", *International Journal of Thermal Sciences*, Vol. 43 (10): 993–1002 (2004),

Conference Papers

2004 Cui J.T. and Wang S.W. "Health Monitoring and Continuous Commissioning Of Centrifugal Chiller Systems", *The 4th International Conference for Enhanced Building Operation (ICEBO 2004)*, Paris, France

2003 Wang S.W. and Cui J.T. "A Robust Control Strategy of Centrifugal Chiller Systems in Centralized Cooling Plants", *The 6th national cryogenics and refrigeration engineering conference, Xi'an* (2003)

2003 Wang S.W. and Cui J.T. "Automatic Diagnosis and Commissioning Of Central Chilling Systems", *Annual symposium on the new technologies in refrigeration and air-conditioning, Shanghai* (2003)